Fakultät für Mathematik und Naturwissenschaften | RWTH AACHEN UNIVERSITY

Environmental Fate of Microplastics, with a Focus on Polymer Microcapsule Formulations Used in Pesticide Applications

Von der Fakultät für Mathematik und Naturwissenschaften der RWTH Aachen University
zur Erlangung des akademischen Grades einer Doktorin
der Naturwissenschaften genehmigte Dissertation

vorgelegt von

Eva-Maria Teggers

Master of Science

aus

Troisdorf

Berichter: Prof. Dr. Andreas Schäffer

Prof. Dr. Annika Jahnke

Tag der mündlichen Prüfung: 23.01.2026

I. Eidesstattliche Erklärung

Ich, Eva-Maria Teggers

erkläre hiermit, dass diese Dissertation und die darin dargelegten Inhalte die eigenen sind und selbstständig, als Ergebnis der eigenen originären Forschung, generiert wurden.

Hiermit erkläre ich an Eides statt

1. Diese Arbeit wurde vollständig oder grösstenteils in der Phase als Doktorandin dieser Fakultät und Universität angefertigt;
2. Sofern irgendein Bestandteil dieser Dissertation zuvor für einen akademischen Abschluss oder eine andere Qualifikation an dieser oder einer anderen Institution verwendet wurde, wurde dies klar angezeigt;
3. Wenn immer andere eigene-oder Veröffentlichungen Dritter herangezogen wurden, wurden diese klar benannt;
4. Wenn aus anderen eigenen-oder Veröffentlichungen Dritter zitiert wurde, wurde stets die Quelle hierfür angegeben. Diese Dissertation ist vollständig meine eigene Arbeit, mit der Ausnahme solcher Zitate;
5. Alle wesentlichen Quellen von Unterstützung wurden benannt;
6. Wenn immer ein Teil dieser Dissertation auf der Zusammenarbeit mit anderen basiert, wurde von mir klar gekennzeichnet, was von anderen und was von mir selbst erarbeitet wurde;
7. Ein Teil oder Teile dieser Arbeit wurden zuvor veröffentlicht und zwar in…

…den folgenden Publikationen:

1) Teggers, E.-M., Hardebusch, J., Meisterjahn, B., Simon, M., Hennecke, D., Heumann, R., Egger, H., Dalkmann, P., Schäffer, A., Jahnke, A., 2025a. Diversifying endpoints in biodegradation testing of microplastics. Environ Sci Eur 37, 65. https://doi.org/10.1186/s12302-025-01096-8
2) Teggers, E.-M., Winterhoff, S., Heck, S., Hardebusch, J., Meisterjahn, B., Simon, M., Hennecke, D., Heumann, R., Egger, H., Dalkmann, P., Schäffer, A., Jahnke, A., 2025. Simulated Sunlight Exposure can be a Prerequisite for the Biodegradation of Persistent Microplastics. Journal of Hazardous Materials. Under Review.
3) Teggers, E.-M., Heck, S., Meisterjahn, B., Simon, M., Hennecke, D., Heumann, R., Egger, H., Dalkmann, P., Jahnke, A., Schäffer, A., 2025b. Modified oil extraction of pristine and weathered synthetic polyurea microcapsules and polyethylene microplastics from soil. Microplastics and Nanoplastics. https://doi.org/10.1186/s43591-025-00121-0

… und im Rahmen der folgenden Konferenzvorträge sowie eines Workshops vorgestellt:

1) 2024 - MICRO - Plastic Pollution from Macro to Nano, Arrecife, Spain, 5th Edition
   - “Towards a Comprehensive Microplastic Fate Assessment: Integrating Size Analyses and Abiotic Degradation into Regulatory Testing”
2) 2024 - Society of Environmental Toxicology and Chemistry (SETAC) Europe Sevilla, Spain, 34th Annual Meeting
   - “Towards an improved fate assessment of microplastics: Inclusion of specific analyses and abiotic degradation in regulatory tests”
   - “Photolysis on soil surface makes persistent microplastic biodegradable”
3) 2024 - SETAC Young Environmental Scientists (YES) meeting, Landau, Germany, 12th Annual Meeting
   - “The inclusion of supplementary analysis within a standardized biodegradability testing framework has the potential to provide enhanced comprehension of microplastic degradation”
2) 2023 – Microplastics Workshop for Early Career Researchers, Ascona, Switzerland.
   - “Improving the understanding of microplastic capsules degradation in a standard test setup”
4) 2023 - Society of Environmental Toxicology and Chemistry (SETAC) Europe, Dublin, Irland, 33th Annual Meeting
   - “The integration of further analysis in a standardized biodegradability test system can lead to better insights into microplastic degradation.”

Ort, Datum

Unterschrift

II. Foreword

This doctoral project was initiated by Bayer AG with the objective to gain insights into the environmental fate and biodegradability of the polymeric shell material of polyurea microcapsules used in plant protection products (PPPs). The project was launched in the context of the proposed restriction of intentionally added synthetic polymeric microparticles (commonly known as microplastics (MPs)) under the European REACH regulation and the associated guidelines for demonstrating biodegradability of MPs.

The work was supervised and hosted by INVITE GmbH, a cross-industry research organization with 50% ownership by Bayer AG and 50% by academic institutions. I, Eva-Maria Teggers, was employed at INVITE GmbH throughout the course of the project. The experimental work was conducted at Fraunhofer Institute for Molecular Biology and Applied Ecology (IME) in Schmallenberg, Germany. Fraunhofer IME was selected due to its long-standing expertise in environmental fate and bioaccumulation studies, regulatory knowledge, and its specialized laboratories for investigating radiolabeled substances. The Fraunhofer IME in Schmallenberg offered the required infrastructure and expertise for performing biodegradation and extraction experiments using ^{14}C-labeled polymers under controlled and environmentally relevant conditions.

The scientific supervision was provided by Prof. Dr. Andreas Schäffer and Prof. Dr. Annika Jahnke from RWTH Aachen University, with Annika Jahnke also being affiliated with the Helmholtz Centre for Environmental Research (UFZ) in Leipzig. Their expertise in environmental chemistry, environmental fate and regulatory assessment was highly valuable.

This project aimed to contribute to the development of reliable and regulatory-relevant test methods for evaluating the environmental fate of MPs. A particular focus was placed on polyurea microcapsules, which represent a special challenge for assessing the polymer biodegradation due to their complex composition. The work addressed key methodological aspects in biodegradation testing, the influence of irradiation of the MPs with simulated sunlight, and their extraction from soil matrices.

III. Danksagung

Zuallererst möchte ich meiner betreuenden Professorin Prof. Dr. Annika Jahnke und meinem betreuenden Professor Prof. Dr. Andreas Schäffer, für ihre außerordentliche fachliche und menschliche Unterstützung danken. Es ist, wie ich finde, eine besondere Ausnahme, dass Rückmeldungen, selbst zu umfangreichen Revisionen, nie länger als zwei bis drei Tage auf sich warten ließen. Beide hatten jederzeit ein offenes Ohr für meine Anliegen und halfen mir mit großem Verständnis, insbesondere in herausfordernden Phasen, den Fokus für das Wesentliche zu behalten und meinen Weg konsequent zu verfolgen. Für Euren klaren Blick, das beständige Vertrauen und Eure verlässliche Betreuung danke ich Euch herzlich.

Mein ausdrücklicher Dank gilt auch Dr. Boris Meisterjahn, Dr. Markus Simon und Dr. Dieter Hennecke für ihre engagierte und konstruktive Begleitung meines Promotionsprojekts. Ich bin sehr dankbar, dass ich meine Dissertation an einem so spannenden und hervorragend ausgestatteten Institut wie dem Fraunhofer IME realisieren durfte. Die hohe fachliche Kompetenz, die wertschätzende Arbeitsatmosphäre sowie die technisch exzellente Ausstattung haben mein wissenschaftliches Arbeiten nachhaltig geprägt.

Dankbar bin ich ebenso den Projektpartnern Dr. Philipp Dalkmann, Dr. Holger Egger, Dr. Werner Hoheisel und Dr. Roman Heumann von der Bayer AG und der INVITE GmbH. Die fachlichen Gespräche auf Augenhöhe, das mir entgegengebrachte Vertrauen und die offene, konstruktive Haltung haben maßgeblich dazu beigetragen, dass ich mich inhaltlich wie persönlich weiterentwickeln konnte. Dieses Projekt und insbesondere die regelmäßigen Status-Meetings haben mich in vielerlei Hinsicht wachsen lassen. Für Euer großes Interesse und die konstruktive Unterstützung bin ich Euch sehr dankbar.

Mein besonderer Dank gilt außerdem allen Mitarbeitenden des Fraunhofer-Instituts, die mir den Einstieg ins Labor durch ihre Erfahrung, Geduld und Hilfsbereitschaft erheblich erleichtert haben. Zu nennen sind hier insbesondere Thomas Hennecke, Jonas Hardebusch, Christoph Eggenstein-Deimel sowie das gesamte Laborteam. Vor allem aber möchte ich Julia Peters danken, mit der ich nicht nur ein Büro, sondern auch die Herausforderungen und Erfolge des Promotionsalltags geteilt habe, danke ich sehr herzlich. Ich bin dankbar für jedes offene Gespräch, für die gegenseitige Unterstützung und für das vertrauensvolle und freundliche Miteinander, das wir über die Jahre gepflegt haben. Ein großes Dankeschön geht auch an die Laufgruppe H!Hills!, die mir mit vielen schönen Laufrunden im Sauerland und anregenden Gesprächen einen wertvollen Ausgleich zum wissenschaftlichen Arbeiten geboten hat.

Zu guter Letzt möchte ich meinem Freund Christian Marcks von Herzen danken, der mir in dieser Zeit stets Halt und Kraft gegeben hat. Außerdem möchte ich meiner Familie und meinen Freunden für ihren starken Rückhalt danken. Ohne Euch hätte mir der Boden unter den Füßen gefehlt.

IV. Summary

This thesis investigates the biodegradability and environmental fate of microplastics (MPs), with a particular focus on intentionally added polyurea (PUA) microcapsules in plant protection products (PPPs) to the terrestrial environment. Despite growing attention to plastic pollution in soils, this compartment has received comparatively little attention in both scientific and regulatory discussions. The work was initiated based on the proposed restriction under the REACH regulation on intentionally added MPs and was aimed to contribute to the development of reliable and regulatory-relevant test methods. MPs can be derogated if their biodegradability is demonstrated using proposed standardized testing methods (e.g., OECD or ISO), with a primary focus on complete mineralization to CO_2 or the corresponding oxygen consumption.

To assess the biodegradation of microplastics, the following main objectives were addressed, each investigated in a separate section of this thesis: (i) the development of analytical methods to assess alternative endpoints of biodegradation besides mineralization as the main endpoint of the regulation, e.g., physical or chemical changes of the MP; (ii) the investigation of the influence of abiotic factors, such as simulated sunlight exposure on MP biodegradation; (iii) the development of an appropriate extraction method applying the analytical methods developed in (i) and ideally identify transformation products within a biodegradation test in soil. In total two polymer types were investigated: PUA microcapsules, representing industrially applied encapsulants in PPP formulations and linear low-density polyethylene (LLDPE) microparticles, representing rather persistent commodity plastics. Radiolabeling with ^{14}C enabled mass balance investigations and allowed for exact tracking of polymer degradation and development of transformation products under controlled laboratory conditions.

The major outcomes of this thesis are threefold: (1) This thesis highlights the importance of purification and thorough characterization, or where feasible, the separation of complex materials into their constituent fractions to better understand which components are mineralized and which persist in the environment, thereby avoiding misleading results caused by carbonaceous co-constituents. This was exemplified in the first part of the thesis, where radiolabeled low-molecular-weight synthesis residues caused increased mineralization results that did not reflect actual polymer biodegradation. In this context, the applied purification approach proved effective in sufficiently isolating microcapsules from these formulation residues through filtration and resuspension, which could also be applied to regular testing without radiolabeling.

(2) Simulated sunlight irradiation influenced the degradability of MPs, particularly for PUA in the second part of this thesis. Irradiated PUA microcapsules released aminocaproic acid, a compound readily mineralized under test conditions, resulting in elevated $^{14}CO_2$ evolution. The LLDPE particles were disintegrated only to a minor degree and did not show elevated mineralization after irradiation on the soil surface. While ^{14}C-fragments from aqueous irradiation of LLDPE were detected, biodegradation

of this suspension remains untested. These results highlight the importance of considering photo-oxidative effects when evaluating MP degradation, especially if the respective products may exhibit exposure scenarios involving sunlight.

(3) In the last part of this thesis, a modified oil extraction protocol was developed which proved to recover ^{14}C-labeled PUA and LLDPE MPs from two different types of agricultural reference soils. The method was effective for both pristine and simulated sunlight-exposed particles and showed potential for extracting the most challenging small MPs (<500 µm). Radiolabeling also proved beneficial here since it enabled quantification of recovery and identification of losses.

Taken together, this work leads to three main conclusions and recommendations. First, thorough characterization or, where feasible, fractionation of test materials by properties such as particle size or composition is essential for accurately interpreting biodegradation data and avoiding misclassification of microplastic degradability. Such efforts are recommended for future studies to improve the reliability and clarity of biodegradation assessments. Second, simulated sunlight was shown to influence microplastic degradation and should be considered in environmental fate evaluations. Lastly, it may be beneficial to integrate microplastic extraction methods, such as the modified oil extraction method described in this thesis, into soil biodegradation testing to investigate physicochemical changes and transformation products. This could support more robust biodegradation testing under simulated environmental conditions.

Since sunlight exposure in realistic application scenarios remains uncertain, the environmental relevance of simulated sunlight effects on PUA microcapsules must be validated. Controlled lysimeter or field studies are essential to determine whether the photodegradation observed under laboratory conditions also occurs in agricultural environments. This is crucial for assessing the transferability of experimental results to real-world settings.

V. Zusammenfassung

Diese Dissertation untersucht die biologische Abbaubarkeit und das Umweltverhalten von Mikroplastik (MP), mit besonderem Fokus auf gezielt zugesetzte Polyharnstoff- (PUA-) Mikrokapseln in Pflanzenschutzmitteln (PPP) im terrestrischen Umfeld. Trotz zunehmender Aufmerksamkeit für Kunststoffverschmutzung in Böden wurde dieses Kompartiment bislang in wissenschaftlichen und regulatorischen Diskussionen vergleichsweise wenig berücksichtigt. Die Arbeit wurde im Kontext des vorgeschlagenen Beschränkungsvorhabens gemäß der REACH-Verordnung für absichtlich zugesetzte MPs initiiert und zielte darauf ab, zur Entwicklung verlässlicher und regulatorisch relevanter Testmethoden beizutragen. MPs können von der Beschränkung ausgenommen werden, wenn ihre biologische Abbaubarkeit durch vorgeschlagene standardisierte Prüfmethoden (z. B. OECD oder ISO) nachgewiesen wird, wobei der vollständige Abbau zu CO_2 oder der entsprechende Sauerstoffverbrauch im Mittelpunkt steht.

Zur Bewertung der biologischen Abbaubarkeit von Mikroplastik wurden folgende Hauptziele verfolgt, die jeweils in einem eigenen Kapitel dieser Dissertation behandelt werden: (i) die Entwicklung analytischer Methoden zur Bewertung alternativer Endpunkte des biologischen Abbaus neben der Mineralisierung als Hauptendpunkt der Regulierung, z. B. physikalische oder chemische Veränderungen des MP; (ii) die Untersuchung des Einflusses abiotischer Faktoren wie z. B. der Exposition gegenüber simuliertem Sonnenlicht auf den MP-Abbau; (iii) die Entwicklung einer geeigneten Extraktionsmethode, welche die unter (i) entwickelten Analysen anwendet und idealerweise Transformationsprodukte in einem Bodenabbaustest identifiziert. Insgesamt wurden drei Polymertypen untersucht: PUA-Mikrokapseln, die als industriell eingesetzte Verkapselungssysteme in PPP-Formulierungen dienen, sowie Mikropartikel aus linearem Polyethylen niedriger Dichte (LLDPE), die eher persistente Massenkunststoffe repräsentieren. Die Radiomarkierung mit ^{14}C ermöglichte Massenbilanzen und erlaubte die exakte Nachverfolgung des Polymerabbaus und der Bildung von Transformationsprodukten unter kontrollierten Laborbedingungen.

Die wichtigsten Ergebnisse dieser Arbeit lassen sich wie folgt zusammenfassen: (1) Diese Arbeit unterstreicht die Bedeutung der Reinigung und gründlichen Charakterisierung oder, wo möglich, der Auftrennung komplexer Materialien in ihre Einzelbestandteile, um besser zu verstehen, welche Komponenten mineralisiert werden und welche in der Umwelt verbleiben, und um irreführende Ergebnisse durch kohlenstoffhaltige Koverbindungen zu vermeiden. Dies wurde im ersten Teil der Arbeit gezeigt, in dem radiomarkierte, niedermolekulare Syntheserückstände zu erhöhten Mineralisierungswerten führten, die nicht den tatsächlichen Polymerabbau widerspiegelten. In diesem Zusammenhang erwies sich der angewandte Reinigungsansatz, bei dem die Mikrokapseln durch Filtration und Resuspendierung ausreichend von Formulierungsrückständen isoliert wurden, als effektiv und könnte auch ohne Radiomarkierung in Routineprüfungen angewendet werden.

(2) Die Bestrahlung mit simuliertem Sonnenlicht beeinflusste die Abbaubarkeit von MPs, insbesondere von PUA, im zweiten Teil dieser Arbeit. Bestrahlte PUA-Mikrokapseln setzten Aminocapronsäure frei, eine Verbindung, die unter den Testbedingungen leicht mineralisiert wurde und zu einer erhöhten $^{14}CO_2$-Freisetzung führte. Die LLDPE-Partikel wurden nur in geringem Maße zersetzt und zeigten nach Bestrahlung auf der Bodenoberfläche keine erhöhte Mineralisierung. Zwar wurden ^{14}C-haltige Fragmente aus der wässrigen Bestrahlung von LLDPE detektiert, deren biologische Abbaubarkeit wurde jedoch nicht getestet. Diese Ergebnisse verdeutlichen die Bedeutung der Berücksichtigung photooxidativer Effekte bei der Bewertung des MP-Abbaus, insbesondere wenn die jeweiligen Produkte potenziell Sonnenlicht ausgesetzt sind.

(3) Im letzten Teil dieser Arbeit wurde ein modifiziertes Öl-Extraktionsprotokoll entwickelt, das in der Lage war, ^{14}C-markierte PUA- und LLDPE-MPs aus zwei unterschiedlichen landwirtschaftlichen Referenzböden zurückzugewinnen. Die Methode war sowohl bei unbehandelten als auch bei simuliertem Sonnenlicht ausgesetzten Partikeln wirksam und zeigte Potenzial für die Extraktion besonders kleiner MPs (< 500 µm). Die Radiomarkierung erwies sich auch hier als vorteilhaft, da sie die Quantifizierung der Rückgewinnung und die Identifikation von Verlusten ermöglichte.

Zusammenfassend führt diese Arbeit zu drei zentralen Schlussfolgerungen und Empfehlungen: Erstens ist eine gründliche Charakterisierung oder, wo möglich, Fraktionierung von Prüfmaterialien nach Eigenschaften wie Partikelgröße oder Zusammensetzung unerlässlich, um Abbaudaten korrekt zu interpretieren und Fehleinschätzungen zur MP-Abbaubarkeit zu vermeiden. Solche Bemühungen werden für zukünftige Studien empfohlen, um die Verlässlichkeit und Aussagekraft von Abbauprüfungen zu verbessern. Zweitens zeigte sich, dass simuliertes Sonnenlicht den Abbau von Mikroplastik beeinflussen kann und bei der Bewertung des Umweltverhaltens berücksichtigt werden sollte. Drittens könnte es sinnvoll sein, Mikroplastik-Extraktionsmethoden wie das in dieser Arbeit beschriebene modifizierte Öl-Extraktionsverfahren in Bodenabbaustudien zu integrieren, um physikochemische Veränderungen und Transformationsprodukte zu erfassen. Dies könnte robustere Abbaubewertungen unter simulierten Umweltbedingungen ermöglichen.

Da die Sonnenlichtexposition unter realistischen Anwendungsszenarien ungewiss ist, muss die Umweltrelevanz der im Labor beobachteten Effekte durch simuliertes Sonnenlicht auf PUA-Mikrokapseln validiert werden. Kontrollierte Lysimeter- oder Feldstudien sind notwendig, um zu bestimmen, ob die im Labor beobachtete Photodegradation auch unter landwirtschaftlichen Bedingungen auftritt. Dies ist entscheidend, um die Übertragbarkeit experimenteller Ergebnisse auf reale Anwendungsszenarien zu bewerten

VI. Contents

I. Eidesstattliche Erklärung ... III
II. Foreword ... V
III. Danksagung ... VII
IV. Summary ... IX
V. Zusammenfassung ... XI
VI. Contents ... XIII
VII. List of Tables ... XV
VIII. List of Figures ... XVI
IX. List of Abbreviations ... XVIII
1 Introduction ... 1
1.1 Microplastic Pollution ... 1
1.2 REACH Restriction on the Use of Intentionally Added Microplastics in Products ... 2
1.3 Biodegradation of Polymers ... 4
1.4 Photodegradation of Polymers ... 5
1.5 Extraction of MPs from Soils ... 7
1.6 Synthetic Polymer Microcapsules used for Pesticide Applications ... 8
1.7 Background and Motivation of this Thesis ... 10
1.8 Scope and Aims of this Thesis ... 12
1.9 Structure of this Thesis ... 12
2 Material and Methods ... 15
2.1 General Materials and Methods ... 15
2.1.1 Microcapsule Suspension ... 15
2.1.2 LLDPE Particles ... 16
2.1.3 Utilized Soil Material ... 16
2.1.4 Quantification of Radioactivity in Different Compartments ... 17
2.1.5 Data Analysis ... 17
2.2 Part 1 – Broadening the Framework in Biodegradation Testing of Microplastics ... 18
2.2.1 Overview of the Screening Biodegradation Test (OECD TG 301B) ... 18
2.2.2 Preparation of the Test Inoculum ... 19
2.2.3 Biodegradation of the Bulk PUA_{mod} CS (T1) ... 19
2.2.4 Sequential Filtration Integrated into the First Biodegradation Test (T1) ... 21
2.2.5 Biodegradation of the Different Size Fractions of the PUA_{mod} Bulk CS (T2) ... 22
2.2.6 Ultra-High Performance Liquid Chromatography with High Resolution Mass Spectrometry (UHPLC-HRMS) ... 23
2.3 Part 2 – The Influence of Simulated Sunlight on the Biodegradation of Persistent Microplastics ... 24
2.3.1 Simulated Sunlight Irradiation Settings ... 24
2.3.1 Biodegradation after Simulated Sunlight Exposure ... 29
2.3.2 Sequential Filtration of the MPs Suspensions ... 29
2.4 Part 3 – Extraction of Pristine and Weathered Microplastics from Soil Using a Modified Oil-Based Method ... 30
2.4.1 Overview of the Microplastic Extraction Procedures ... 30
2.4.2 Experiment I) - Modified Oil Extraction Using Octanol ... 31
2.4.3 Experiment II) - Density Extraction Using $ZnCl_2$ ... 33
2.4.4 Experiment III) - Repeated KOH Extraction ... 33
2.4.5 pH Dependence of Microplastic Extraction Efficiency ... 34
3 Results 35
3.1 Part 1 – Broadening the Framework in Biodegradation Testing of Microplastics ... 35
3.1.1 Biodegradation of the Bulk PUA_{mod} CS (T1) ... 35
3.1.1 Sequential Filtration Integrated into the First Biodegradation Test (T1) ... 37
3.1.2 Biodegradation of the Different Size Fractions of the PUA_{mod} Bulk CS (T2) ... 38

3.1.3 Ultra-High Performance Liquid Chromatography with High Resolution Mass Spectrometry (UHPLC-HRMS) 39
3.2 Part 2 – The Influence of Simulated Sunlight on the Biodegradation of Persistent Microplastics 42
3.2.1 Simulated Sunlight Irradiation 42
3.2.2 Alterations of Size Distribution and Release of ^{14}C-Compounds 43
3.2.3 Biodegradation after Simulated Sunlight Exposure 47
3.3 Part 3 – Extraction of Pristine and Weathered Microplastics from Soil Using a Modified Oil-Based Method 49
3.3.1 Extraction Efficiencies of the Different Extraction Experiments 49
3.3.2 Impact of Soil Types on the Extraction Efficiency 52
3.3.3 Impact of Sunlight Irradiation on the Extraction Efficiency 53
3.3.4 pH Dependence of Microplastic Extraction Efficiency 53
4 Discussion 55
4.1 Part 1 – Broadening the Framework in Biodegradation Testing of Microplastics 55
4.1.1 Biodegradation of Bulk PUA_{mod} CS (T1) 55
4.1.2 Sequential Filtration Integrated into the First Biodegradation Test (T1) 56
4.1.3 Biodegradation of the Different Size Fractions of the PUA_{mod} Bulk CS (T2) 57
4.1.4 Ultra-High Performance Liquid Chromatography with High Resolution Mass Spectrometry (UHPLC-HRMS) 58
4.2 Part 2 – The Influence of Simulated Sunlight on the Biodegradation of Persistent Microplastics 59
4.2.1 Simulated Sunlight Irradiation 59
4.2.2 Alterations of Size Distribution and Release of ^{14}C-Compounds 60
4.2.1 Biodegradation after Simulated Sunlight Exposure 61
4.3 Part 3 – Extraction of Pristine and Weathered Microplastics from Soil Using Modified Oil-Based Method 63
4.3.1 Extraction Efficiencies of the Different Extraction Experiments 63
4.3.1 Impact of Soil Types on the Extraction Efficiency 65
4.3.2 Impact of Sunlight Irradiation on the Extraction Efficiency 65
4.3.3 pH Dependence of Microplastic Extraction Efficiency 66
4.4 General Discussion 67
5 Conclusion 70
6 Future Implications and Outlook 71
7 Contributions in Publications and Chapters 73
X. References 77
XI. Appendix – General 90
XII. Appendix - Part 1 96
XIII. Appendix – Part 2 100
XIV. Appendix – Part 3 110
XV. Appendix - Curriculum Vitae 112
XVI. Appendix – Publications 115
1.1 Diversifying endpoints in biodegradation testing of microplastics 115
1.2 Simulated Sunlight Exposure as a Prerequisite for the Biodegradation of Persistent Microplastics 115
1.3 Modified oil extraction of pristine and weathered synthetic polyurea microcapsules and polyethylene microplastics from soil 115

VII. List of Tables

Table 1. Irradiation duration and irradiation energy of the performed irradiation procedures 26

Table 2. Overview of the procedures used to assess the effect of simulated sunlight exposure on polymer biodegradation and fragmentation. 28

Table 3. Overview of the performed experiments. Not executed experiments are abbreviated by “N/A”. LLDPE was only tested in experiment I). Reproduced from Teggers et al. (2025b). 31

Table 4. Overview of the different irradiation procedures under 75 W/m² irradiation intensity within the 300–400 nm wavelength range. 43

Table 5. Mineralization and recovery of the biodegradation test in soil (OECD TG 307). 49

Table 6. Overview of the total extraction recoveries (referring to the total applied radioactivity (AR)) and extraction efficiencies (excluding the AR recovered from the soil) of all performed extraction experiments (I-III), given in percentage of AR. 50

VIII. List of Figures

Figure 1. Illustration of the four steps involved in polymer biodegradation:....4

Figure 2. Graphical abstract of Teggers et al. (2025a) representing the employed methods, idea and key outcomes of the first part of the thesis.....13

Figure 3. Graphical abstract of the second part of this thesis (Teggers et al., 2025c, under review), illustrating the performed methods and the general findings. 14

Figure 4. Graphical abstract of the third part of this thesis representing the materials and methods employed (reproduced from Teggers et al. (2025b).....14

Figure 5. Incubation schedule of the bulk capsule suspension (CS) samples and process control samples supplied with sodium benzoate tested in the OECD TG 301B.....20

Figure 6. Preparation of the last process control at 161 d.....21

Figure 7. Preparation of the test samples for testing the separated size fractions of the bulk CS in an OECD TG 301B biodegradation test.....23

Figure 8. Procedures (P) to investigate the influence of simulated sunlight exposure of MPs by implementing two different irradiation methods (MI and MII) on the biodegradation and fragmentation of the MPs. 25

Figure 9. Images of the simulated sunlight irradiation set-up.....27

Figure 10. Protocol of the extraction experiment I). The modified oil extraction using octanol as an alternative to the density extraction (experiment II)).....33

Figure 11. Biodegradation ability of the filtered supernatant opposed to the standard inoculum (30 mg/L dry weight (dw) sewage sludge particles) in the OECD TG 301F test.....35

Figure 12. Biodegradation performance of the process controls (PC) within the two OECD TG 301B tests testing the bulk PUA_{mod} suspension (T1) and the separated size fractions of the PUA_{mod} suspension (T2).....36

Figure 13. Biodegradation test results of the fist OECD TG 301B (T1) assessing the bulk PUA_{mod} capsule suspension (bulk PUA_{mod} CS).....37

Figure 14. Results of the sequential filtration integrated in the first biodegradation test (T1), which was performed based on OECD TG 301B.....38

Figure 15. Biodegradation test results of the second OECD TG 301B (T2).....39

Figure 16. High-Resolution Mass Spectrometry (HRMS) analysis of the PUA_{mod} capsule suspension (CS) (<0.2 µm filtrate).....40

Figure 17. Ultra-high performance liquid chromatography (UHPLC) column recovery of the <0.2 µm filtrate from the bulk PUA_{mod} capsule suspension (CS). 41

Figure 18. Isotopic pattern analysis of the PUA_{mod} capsule suspension (CS) filtrate (<0.2 µm) using UHPLC-HRMS analysis. 42

Figure 19. Proportion of applied radioactivity (AR) recovered in the different fractions obtained by sequential filtration.....44

Figure 20. Ultra-High Performance Liquid Chromatography - High-Resolution Mass Spectrometry (HRMS) analysis for the investigation of the irradiated PUA_{mod} filtrate (<0.2µm). 45

Figure 21. Ultra-High Performance Liquid Chromatography - High-Resolution Mass Spectrometry (HRMS) analysis for distinctive identification of aminocaproic acid in the filtrate (<0.2µm) of the irradiated PUA_{mod} with the addition of the reference compound aminocaproic acid.....46

Figure 22. Isotopic pattern analysis of the irradiated PUA_{mod} microcapsule suspension (filtrate <0.2 µm; 100 µL) of the radio-UHPLC-HRMS analysis. 46

Figure 23.Results of the column recovery separating the irradiated capsule suspension's filtrate of <0.2 µm with the UHPLC. Eluates were collected for the following retention time intervals: 0 to 4 min; 4 to 7 min; 7.5 to 15 min and from 15 to 60 minutes in 7.5 min intervals. The radioactivity of the eluates was quantified by LSC. Means of *n*=3. 47

Figure 24. Biodegradation in soil following OECD TG 307. 48

Figure 25. Microscopic image of the polyurea capsules (roundish shapes which look similar as bubbles. Some microcapsules were always found to be deformed) in (A) water and in KOH (pH 14) after (B) one hour and (C) after five days of incubation. 51

Figure 26. Recoveries of applied radioactivity (%AR) from various extraction experiments (I, II, III; see Table 3). 52

Figure 27. Proportion of the applied radioactivity (AR) recovered by four extraction solutions comprising different pHs. 54

Figure 28. Turbidity of the different extraction solutions comprising different pHs. 54

Figure 29. Overview of the main methods and ideas involved in this thesis. 68

IX. List of Abbreviations

Abbreviation	Definition
AR	Applied radioactivity
ATR–FTIR	Attenuated Total Reflectance – Fourier Transform Infrared Spectroscopy
BTDA	3,3′,4,4′-Benzophenonetetracarboxylic Dianhydride
CS	Capsule Suspension
ECHA	European Chemicals Agency
EPA	Environmental Protection Agency (USA)
FAO	Food and Agriculture Organization (UN)
FTIR	Fourier-transform infrared spectroscopy
GC	Gas Chromatography
HMDA	Hexamethylenediamine (sometimes specifically [1,6-14C] labeled)
HRMS	High resolution mass spectrometry
kBq	Kilobecquerel
LC	Liquid chromatography
LC50	Median Lethal Concentration
LLDPE	Linear Low-Density Polyethylene
LSC	Liquid Scintillation Counting
MBq	Megabecquerel
MP	Microplastic
NaOH	Sodium Hydroxide
OC	Organic carbon (content)
OECD	Organisation for Economic Co-operation and Development
PE	Polyethylene
PET	Polyethylene terephthalate
PPP	Plant Protection Product
PSA	Particle Size Analysis
PUA	Polyurea
PUAmod	Modified Polyurea
REACH	Registration, Evaluation, Authorisation and Restriction of Chemicals
RH	Relative Humidity
ROS	Reactive Oxygen Species
RT	Retention Time
SEM	Scanning Electron Microscopy
SOM	Soil organic matter
TC	Total carbon (content)
TG	Test Guideline
ThoD	Theoretical Oxygen Demand
TRR	Total recovered radioactivity
UHPLC	Ultra-High Performance Liquid Chromatography
HRMS	High Resolution Mass Spectrometry
UHQ	Ultra-High Quality (water)
UNEP	United Nations Environment Programme
WHC	Water holding capacity

1 Introduction

1.1 Microplastic Pollution

The extensive production and uncontrolled release of plastics, including synthetic polymeric microparticles commonly known as microplastics (MPs), raise major concerns due to their persistence, widespread dispersion, and potential adverse effects on both human health and ecosystems (Anbumani and Kakkar, 2018; Bravo Rebolledo et al., 2013; Cui et al., 2022; Dissanayake et al., 2022; Gregory, 2009; Imhof et al., 2013; Lusher et al., 2013). Plastics contribute to greenhouse gas emissions throughout their life cycle and, owing to their durability and complex chemical composition, are linked to biodiversity loss and the erosion of biosphere integrity. Consequently, plastic pollution is recognized as a key factor in transgressing planetary boundaries that safeguard Earth's stability and resilience (Bachmann et al., 2023; MacLeod et al., 2021; Persson et al., 2022; Richardson et al., 2023; Schmidt et al., 2024; Villarrubia-Gómez et al., 2024). Addressing this crisis requires a substantial reduction in plastic production and pollution, as well as the development of international frameworks for sustainable plastic life cycle management (UNEP, 2022).

MP pollution is now recognized as a global issue, reaching from mountaintops to the deepest oceans and permeating air, water, soil, and living organisms. Despite its ubiquity, the environmental pathways and cycling of MPs remain insufficiently understood (Bank et al., 2022; Horton and Dixon, 2018). While research has long focused on aquatic contamination, the presence and potential impacts of MPs in agricultural soils have only recently gained broader attention. Sources of MPs to agricultural soils include the use of mulch films, which is the main source, but it varies depending on the country or land use (e.g., acc. to a review of Büks and Kaupenjohann (2020)) with 4.5 mg/kg). Other major sources are surface runoff (66 to 199 particles/L found in stormwater run-off (Piñon-Colin et al., 2020), sewage irrigation (1 particle/L after treatment; Lares et al., 2018)), and sewage sludge application, which contributes an estimated 0.63–4.3 million tons annually in Europe (Ng et al., 2018). Atmospheric deposition is also remarkable, with remote areas such as the French Pyrenees receiving up to 249 fragments, 73 films, and 44 fibers per m² per day (Allen et al., 2019). Further sources include the use of fertilizers (Fan et al., 2023) and pesticide formulations containing MPs. Given their persistence in the environment, it is critical to minimize MP emissions through effective and wide-ranging mitigation strategies (Borrelle et al., 2020; Lau et al., 2020).

Understanding of MP sources and behavior is further complicated by inconsistent size classifications, which differ widely across studies and regulatory bodies (European Commission, 2023; GESAMP, 2016; Gigault et al., 2018; International Organization for Standardization., 2023). Hartmann et al. (2019) called for a standardized definition of MPs, proposing a size range of 1 µm to 1 mm. MPs may enter the environment directly as "primary MPs" or form through degradation of larger plastics as "secondary

MPs" (Cole et al., 2014; Manshoven et al., 2022). However, quantifying their release remains difficult due to methodological variability, inconsistent data, and the complex behavior of MPs across environmental matrices (Galafassi et al. 2019). The European Chemicals Agency (ECHA, 2021), based on Hann et al. (2018), estimated that 176,300 tons of secondary MPs are released into surface waters annually within the European environment. For primary MPs, global releases to the oceans are estimated at 1.5 million tons per year, though Boucher and Friot (2017) advise caution in interpreting these figures. According to their breakdown, major sources include synthetic textiles (35%), car tyres (28%), city dust (24%), and smaller contributions from road markings, marine coatings, personal care products, and plastic pellet losses. Secondary MPs are typically derived from mismanaged plastic waste, such as littered packaging or abandoned fishing gear (Manshoven et al., 2022). Several reviews have examined MP emissions to terrestrial systems, analytical detection methods, and potential effects on soil biota and human health (Bläsing and Amelung, 2018; Hoang et al., 2024; Seo et al., 2024; Surendran et al., 2023). These studies emphasize the difficulties in source attribution due to analytical limitations, varying degradation states, diverse input routes, and spatial heterogeneity of soils. Sa'adu and Farsang (2023) estimate that plastic mulch accounts for the largest share of agricultural MP inputs (39%), noting that of the 100,000 tons applied annually, only 32% is collected post-harvest. Other identified sources include sewage sludge (16%), compost (15%), and coated fertilizers (3%). Encapsulated plant protection products are also a contributor, though they are rarely considered in existing studies.

1.2 REACH Restriction on the Use of Intentionally Added Microplastics in Products

The European Union recently adopted a restriction on intentionally added MPs to products under the REACH regulation, representing a major regulatory effort to limit plastic emissions to the environment (European Commission, 2023). The restriction entered into force on 17 October 2023, with transitional periods applying depending on product category and availability of alternatives. In the context of the restriction, MPs are defined as solid synthetic polymer particles ranging from 0.1 to 5 mm in size, including particles that comprise at least 1% of a material by weight or that form a continuous surface coating on other particles. The scope of the restriction covers intentionally added MPs in products such as cosmetics, detergents, fertilizers, paints, and plant protection products, which are commonly used to enhance product performance but are likely to be released into the environment during application and use. As of October 2023, the placing on the European market of products with a risk of MP release is restricted, with certain exemptions.

Polymers are exempted from the restriction if they (i) have a water solubility greater than 2 g/L, (ii) do not contain carbon atoms in their chemical structure, (iii) are of natural origin and have not been chemically modified, or (iv) can be demonstrated to meet biodegradability criteria using the accepted test methods specified in Appendix 15 (Entry 78) of Annex XVII of Regulation (EC) No 1907/2006.

These methods, developed by international standard-setting bodies such as the Organisation for Economic Co-operation and Development (OECD) and the International Organization for Standardization (ISO), are essential in regulatory contexts as they provide harmonized, scientifically validated protocols to ensure comparability and reliability of results across regulatory domains. The accepted test methods for demonstrating MP biodegradability, summarized in Table A1, are organized into five groups. Groups 1 to 3 consist of standard screening and inherent biodegradability tests (e.g., OECD TG 301 and 302) and are sufficient for demonstrating compliance if pass criteria, typically ≥60% mineralization within 28–60 days, are met. Groups 4 and 5 comprise more advanced screening and environmental simulation tests designed for complex or mixed materials, requiring polymer-specific evidence that the observed degradation applies directly to the tested substance.

The regulatory framework predominantly defines biodegradability through mineralization, the process by which synthetic polymers are biologically broken down into carbon dioxide (CO_2), water, and biomass through microbial activity. Complete or "ultimate" biodegradation implies no residual transformation products remain. A common regulatory benchmark is achieving ≥60% mineralization of the test material within a test period of 28 to 60 days, such as those defined in OECD Test Guidelines 301 B, C, D, F and TG 310, applicable to Group 1 and 2 test methods.

However, the suitability of these methods for solid, high-molecular-weight polymer particles such as MPs has been questioned. Most of the proposed methods are originally designed for soluble and low molecular weight (LMW) chemicals. These tests are at risk to overlook important intermediate degradation processes and the complexity of plastic materials (Carmichael, 2014; Hahn and Hennecke, 2023; Haider et al., 2019; Mitrano and Wohlleben, 2020; Silva et al., 2023). Plastics often consist of diverse molecular structures, including additives, and their degradation typically proceeds through multiple stages (see next chapter 1.3). Therefore, relying mostly on mineralization as a proof for biodegradability may be misleading for complex solid polymers. These materials may leave behind residual fragments or generate transformation products that may persist in the environment or may have toxic properties, even after meeting mineralization thresholds.

In addition, abiotic weathering processes such as photooxidation, mechanical abrasion, hydrolysis, and thermal degradation play a substantial role in altering the structure and environmental behavior of MPs. However, to date such processes are not considered in biodegradation assessments. Among these, photooxidation and mechanical stress often cause the most rapid transformation, while hydrolysis and thermal degradation proceed more slowly (Chamas et al., 2020; Gewert et al., 2015; Mekaru, 2020; Wohlleben et al., 2024; Xu et al., 2024). Integrating these environmental influences into future assessment frameworks would provide a more realistic understanding of the potential fate of MP in the environment and help address current regulatory gaps.

1.3 Biodegradation of Polymers

From a scientific perspective, the biodegradation of polymers is divided into four steps: biodeterioration, depolymerization, bioassimilation and mineralization (Haider et al., 2019; Lucas et al., 2008), which are illustrated in Figure 1. During this process, Albright and Chai (2021) defined the loss of one key property of the polymer, such as mass fragmentation or tensile strength, as primary degradation. Within the second step, depolymerization, the polymer is disintegrated to low-molecular weight compounds, which can be assimilated by microorganisms. In the final step, these degradation products may undergo catabolic degradation, where they are fully oxidized into simple molecules such as carbon dioxide (CO_2) or nitrate, or reduced (like methane, ammonium) for energy generation; or they may be subjected to anabolic assimilation, where they are incorporated into microbial biomass (Haider et al., 2019; Lucas et al., 2008; Silva et al., 2023).

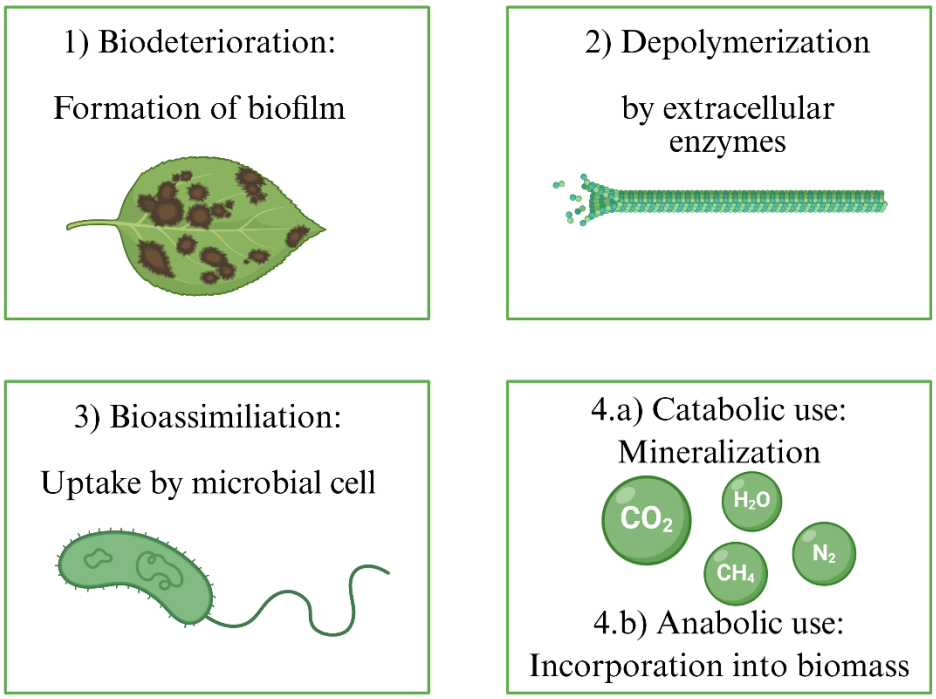

Figure 1. Illustration of the four steps involved in polymer biodegradation: Biodeterioration (1), depolymerization (2), bioassimilation (3), and mineralization (4), adapted from Haider et al. (2019) and Lucas et al. (2008), with distinction between catabolic (4.a) and anabolic (4.b) pathways in the final step.

However, the microbial assimilation of polymer-derived compounds is challenging to trace. Although some degradation products are incorporated into microbial biomass, the metabolic pathways involved are often unclear, particularly under environmental conditions. Stable isotope labeling approaches have been proposed to follow the fate of polymer carbon into biomass or mineralized products, but these methods are still rarely used due to their complexity (Zumstein et al., 2018).

Material properties influence these degradation steps substantially. Crystallinity, for example, determines how accessible a polymer is to microbial attack. Highly crystalline regions tend to be tightly

packed and ordered, which limits the interaction with water and enzymes, while amorphous regions are more disordered and accessible, facilitating earlier stages of biodegradation. Consequently, polymers with low crystallinity are generally more susceptible to biodeterioration and enzymatic depolymerization than their highly crystalline counterparts (Benedict et al., 1983; Eldsater et al., 2000; Nishida and Tokiwa, 1992; Tokiwa et al., 2009). In addition to crystallinity, molecular weight plays a crucial role in determining the biodegradability of a polymer (Benedict et al., 1983; Fields et al., 1974). Polymers with high molecular weight are less bioavailable and often require abiotic pre-fragmentation, for example through UV radiation or oxidation, before microbial degradation becomes possible. In contrast, lower molecular weight polymers are more readily metabolized by microbial enzymes (Gewert et al., 2015; Kale et al., 2007). Another important factor is hydrophobicity, which affects microbial adhesion to the polymer surface. Hydrophobic materials, such as polyethylene (PE), repel water and hinder microbial colonization, thereby slowing down degradation (Gewert et al., 2015; Wang et al., 2022). Moreover, additives and plasticizers within polymer formulations can either inhibit or enhance degradation. While stabilizers and flame retardants may reduce the rate of biodegradation by interfering with enzymatic activity, pro-oxidant additives can accelerate abiotic breakdown, facilitating subsequent microbial assimilation (Chiellini et al., 2003; Sridharan et al., 2022). In addition, surface area and particle morphology influence the rate of microbial degradation; polymers forms with high surface-to-volume ratios, such as films or fibers, allow for greater microbial access and enzymatic interaction than dense pellets or larger fragments (Wang et al., 2022). The presence of hydrolysable functional groups, such as esters or amides, also plays a decisive role in the susceptibility of polymers to enzymatic attack, as these chemical moieties are more easily cleaved by microbial enzymes (Wang et al., 2022).

Environmental conditions such as temperature, oxygen availability, pH, and moisture also affect the rate and extent of polymer biodegradation. For example, aerobic conditions generally promote oxidation and faster microbial metabolism, while anaerobic conditions tend to slow down these processes or lead to different by-products, such as methane instead of carbon dioxide. Soil type, nutrient availability, and microbial diversity further influence how and whether degradation progresses occur in a given environment (Haider et al., 2019; Koh and Khor, 2023; Lucas et al., 2008; Rujnić-Sokele and Pilipović, 2017).

Overall, the interplay between material properties and environmental conditions determines whether a polymer will undergo full biodegradation or merely fragment into smaller, persistent pieces.

1.4 Photodegradation of Polymers

Photooxidation processes are considered to be the main cause for polymer aging (Feldman, 2002; Hamid, 2000; Lemaire et al., 1988; Mao et al., 2020). In this process, light initiates a cascade of reactions, beginning with the formation of free radicals in the polymer matrix, which then propagate oxidation and result in chain scission, cross-linking, and eventual structural degradation. These

transformations can lead to embrittlement, yellowing, and a decline in mechanical strength of the plastic material. The susceptibility of polymers to photooxidation is influenced by intrinsic factors such as polymer composition, presence of chromophores, and additives like UV stabilizers or flame retardants, which can either inhibit or enhance degradation (Fritscher, 1994; Gewert et al., 2015; Singh and Sharma, 2008).

The Earth's atmosphere filters solar radiation below approximately 290 nm; however, around 6% of the radiation that reaches the Earth's surface remains in the ultraviolet (UV) range (Feldman, 2002). Although this fraction is energetic enough to trigger photochemical reactions, most polymers lack inherent chromophore groups in their backbone structures and therefore do not strongly absorb UV-visible light. As a result, they are generally photostable unless modified by specific structural features or the presence of additives and impurities that act as chromophores. In many cases, photooxidative degradation is initiated by such constituents, impurities, processing residues, or additives, which absorb light and generate reactive species. Additionally, pollutants that are absorbed in or adsorbed onto the polymer can further accelerate photo-oxidation or induce indirect photolysis via the formation of reactive oxygen species (ROS), including hydroxyl radicals (•OH), singlet oxygen ($^1O_2$), and superoxide anions ($O_2^{\bullet-}$) (Duan et al., 2022; Xu et al., 2024). In surface waters and soil environments photooxidation may be accelerated by dissolved substances such as cations, anions, dissolved organic matter (DOM) and minerals, which can act as photosensitizer to which the polymers are often exposed to (Chen et al., 2019; Ding et al., 2022; Yu et al., 2022; Zhu et al., 2022). Components of DOM, including quinones and aromatic ketones, have been shown to generate ROS upon solar irradiation and thereby facilitate the degradation of polymers (Bai et al., 2021; McNeill and Canonica, 2016; Rabek and Rånby, 1974; Wang et al., 2019; Zhang et al., 2022).

However, the influence of environmental constituents on photooxidation is not universally accelerating. Some compounds may exert protective or inhibitory effects. For instance, dichloride radical anions ($Cl_2^{\bullet-}$) can quench hydroperoxyl radicals ($HO_2^{\bullet}$), potentially slowing the rate of oxidative degradation. Similarly, iron red pigments and complex mixtures such as humic and fulvic acids have been reported to shield polymers from UV radiation or neutralize ROS, although these effects are controversially discussed (Liu et al., 2021; Wu et al., 2021a, 2021b). Moreover, the spectral quality and intensity of sunlight, seasonal variation, and geographic latitude also influence the extent and rate of photooxidation, adding further complexity to understanding its environmental relevance.

Photo-oxidation can induce a range of physicochemical alterations in plastic materials, including surface cracking, reduction in molecular weight, increased hydrophilicity, and the formation of oxygenated functional groups (Alimi et al., 2022; Duan et al., 2022). These changes often result in the fragmentation of larger plastic items into smaller micro- or nanoplastic particles, which may exhibit higher bioavailability. Furthermore, these alterations can enhance the susceptibility of the degraded polymers to microbial colonization and enzymatic breakdown, thus acting as a crucial pre-conditioning step for

subsequent biodegradation (Albertsson and Karlsson, 1990; Arnaud et al., 1994; Jakubowicz et al., 2011; Sadi et al., 2013).

1.5 Extraction of MPs from Soils

MPs are increasingly recognized as contaminants of concern in terrestrial environments, with soils acting as major sinks due to various input pathways such as agricultural activities, atmospheric deposition, and wastewater application. The extraction of MPs from soil is a critical step for their subsequent detection, identification, and quantification. However, the heterogeneous nature of soil matrices, the diversity of MP types, and their interactions with organic matter and mineral particles pose significant methodological challenges. As a result, the development and refinement of efficient and reliable extraction techniques remain key objectives in current research.

Most established methods for extracting MPs from soils rely on either density separation or oil-based approaches (Crichton et al., 2017; Mani et al., 2019; Prosenc et al., 2021a; Radford et al., 2021; Scopetani et al., 2020a). Less frequently applied techniques include electrostatic separation, magnetic extraction, or froth flotation (He et al., 2021; Möller et al., 2020; Wenzel et al., 2022). In general, the removal of soil organic matter (SOM) can substantially improve the extraction efficiency of MPs from soil matrices (Hurley et al., 2018; Radford et al., 2021).

Commonly used reagents for SOM removal include acids, potassium hydroxide (KOH), hydrogen peroxide, and Fenton's reagent (Möller et al., 2020; Schwaferts et al., 2019). Despite their frequent application, the influence of these chemical solutions and the associated physical and chemical mechanisms involved in MP extraction remain poorly understood (Nuelle et al., 2014; Prosenc et al., 2021a). A study by Nava and Leoni (2021a) demonstrated efficient recovery of nylon and polyethylene terephthalate (PET) MPs in three particle size classes (250–500 µm, 500–2000 µm, 2–5 mm) using a 10% KOH solution at 60 °C with constant agitation for 30 minutes, followed by sieving through a 250 µm mesh. Recovery rates ranged from 60–100% for nylon and 67–100% for PET particles >250 µm. However, smaller particle sizes were associated with lower extraction efficiency, which remained an ongoing challenge. Additional difficulties in MP analysis were reported by Möller et al.(2020) and da Costa and Duarte (2022), particularly for small particles, where error rates up to 70% have been observed for visual identification, alongside matrix-related issues in spectroscopic analysis (e.g., Fourier-transform infrared spectroscopy (FTIR)) and other methodological constraints.

Further limitations in the extraction process arise from alterations in MP properties caused by reagent exposure (Dehaut et al., 2016; Hurley et al., 2018; Kühn et al., 2017; Scheurer and Bigalke, 2018) as well as environmental degradation processes. As mentioned in the previous chapter (1.4), photo-oxidation processes can alter the polymer structure and lead to polymer chain cleavage, formation of free radicals, and the introduction of oxygen-rich functional groups such as hydroxyl and carboxyl

groups on the MP surface (Alimi et al., 2022). Changes, which increase surface hydrophilicity, reduce material stability, making particles more prone to fragmentation (Alimi et al., 2022; Duan et al., 2022). Subsequently, these physical and chemical alterations of MPs can also affect their interaction with soil components and influence aggregation behavior, which may impact extraction efficiency (Duan et al., 2022).

1.6 Synthetic Polymer Microcapsules used for Pesticide Applications

A less frequently discussed source of MP pollution in agriculture despite being used for decades is the introduction of MPs into soils through the use of encapsulated plant protection products (PPPs). MP pollution in agriculture is increasingly recognized, with discussions on primary MP emissions to soils focusing on secondary MPs, such as from plastic mulches that degrade and primary MPs, such as seed coatings and fertilizers. In this context, the potential contribution from pesticide formulations using plastic-based microencapsulation is often overlooked. Recent reports by the Food and Agriculture Organization (FAO, 2021) of the United Nations, of the United Nations Environment Programme (UNEP, 2022) and the Center for International Environmental Law (CIEL) (Carlini and Drugmand, 2022) highlight the deliberate and direct introduction of MPs into agricultural soils, referring also to pesticide encapsulation as a potential contributor that may pose risks to food security. In the Annex XV Restriction Report on MPs (ECHA, 2019, Table 15), it is estimated that out of 10,000 tons of microplastics (MPs) in agricultural and horticultural products released into the environment, approximately 500 tons originate from capsule suspensions (CS) of plant protection products (PPPs).

From a scientific, but also from a regulatory perspective, pesticide risk assessments primarily address the active ingredient in isolation, with minimal or no consideration given to the environmental fate and potential risks of the full formulation, here including the polymeric shell materials (Cox and Surgan, 2006; Kookana, 2010). These considerations have only recently begun to receive attention. This lack of attention to the formulation as a whole, including polymer-based carriers, was also addressed in the viewpoint article of Nederstigt et al. (2024) and in the review of Brunning et al. (2022). In these, it is emphasized that improved environmental profile of advanced formulations often overlooks changes in exposure profiles and the persistence of encapsulations or carrier materials in pesticide formulations which often persist in the environment and may alter chemical exposure profiles. However, they remain largely unregulated and unstudied in both scientific and regulatory contexts. They emphasize that the environmental risk assessment of such formulations must consider not only the active substance but also the behavior and potential ecological impacts of the carrier materials themselves.

Microencapsulated pesticide formulations have already been on the market for several decades. In 1974, the Environmental Protection Agency (EPA) granted approval for commercial marketing of the first encapsulated pesticide product containing methyl parathion (American Chemical Society, 1974). Currently, numerous encapsulation techniques are documented in the scientific and patent literature. in

academic and patent literature, but only a few have been established as manufacturing methods. The most widely used technology, among the few established manufacturing techniques for encapsulation, is the use of interfacial polymerization. Interfacial polymerization is particularly suitable for non-polar (hydrophobic) active ingredients, which can either be used in their liquid form or dissolved in a water-immiscible solvent, thereby forming the oil phase (Pires-Oliveira et al., 2020). The encapsulation procedure generally involves two fundamental steps. First, the oil phase containing a non-polar monomer is emulsified into a continuous aqueous phase using an appropriate surfactant and/or nanoparticle. The aqueous phase contains a water-soluble monomer. In the second step, a rapid polymerization occurs at the interface of the dispersed droplets, resulting in the formation of the capsule wall. This interfacial polymerization can proceed at ambient temperature or under mild heating conditions, typically up to 50°C, which in the latter case is referred to as in situ polymerization (Pires-Oliveira et al., 2020). Microcapsules are commonly characterized by their size, shape, and microscopic morphology. Besides, the encapsulation efficiency is determined by the ratio between the amount of active ingredient retained in the final CS and the total quantity initially used during the encapsulation process. The encapsulation method offers advantages in terms of release control and formulation stability, making it relevant for industrial applications involving hydrophobic actives, also including the encapsulation of fragrances (Pires-Oliveira et al., 2020).

Therefore, microencapsulation has been recognized as a useful approach for agrochemical delivery, offering enhanced efficacy, safety, and environmental profile. The polymeric shell builds a barrier to early degradation processes such as hydrolysis and photolysis or to volatilization (Dailey, 2004; Fu et al., 2019; Wienhold and Gish, 1994), reducing application loads and prolonging application intervals. The interfacial polymerization technique enables precise control over the release rate of the active compound by adjusting the physical properties of the capsule wall. In addition to defining the capsule size, wall thickness and porosity can be influenced by the monomer concentration and the extent of crosslinking applied during synthesis. Thus, studies have demonstrated that encapsulation parameters, such as shell composition, particle size, and wall thickness, can significantly influence the release behavior and photostability of microencapsulated actives. Fu et al. (2019) encapsulated the light-sensitive pesticide avermectin using a 3,3′,4,4′-benzophenonetetracarboxylic dianhydride (BTDA)-modified polyurea (PUA) shell formed by interfacial polymerization, resulting in improved UV resistance and a prolonged release over approximately one week. Wang et al. (2018) reported similar improvements using polylactic acid (PLA) capsules of varying sizes, showing that smaller particle diameters enhanced release rates and reduced photodegradation. These observations align with results by Li et al. (2006), who demonstrated that shell thickness and particle size can be adjusted to fine-tune permeability and UV protection. However, it should be noted that increased cross-linking, while improving capsule stability, may reduce the biodegradability of the polymer shell, which requires consideration in light of the current regulatory developments on MPs. Moreover, covering the active

ingredient in polymer capsules can reduce their mobility in soils (Preisler et al., 2019) due to changes of sorption properties. Accordingly, the reduced mobility limits leaching into groundwater and decreases the risk of run-off reaching adjacent water bodies, thereby helping to prevent adverse effects on non-target organisms (Roy et al., 2014; Sopeña et al., 2009, 2007). Furthermore, the polymeric shell physically isolates the active ingredient, thereby reducing the risk of acute toxicity to users during handling and application by minimizing direct exposure through skin contact or inhalation (Pires-Oliveira et al., 2020). These attributed characteristics were reason to justify the extended eight-year transition period following the entry into force of the REACH restriction for PPPs, reflecting both the uncertainty regarding the availability of suitable biodegradable alternatives and the recognition of socio-economic benefits associated with such formulations, despite the objective of reducing MP emissions (Committee for Risk Assessment, ECHA; Committee for Socio-economic Analysis, ECHA, European Commission (2023)).

An example of a pesticide product containing a PUA microcapsule formulation is Prosper 300 CS (Prosper 300 CS https://www.cropscience.bayer.it/prodotti/fungicidi/prosper-300-cs, Bayer AG). It is a systemic fungicide containing the encapsulated active ingredient spiroxamine, specifically developed for the control of powdery mildew (*Uncinula necator*) on the leaves of grapevines (*Vitis vinifera*), which are cultivated for wine production. Powdery mildew is a widespread and economically critical fungal disease in viticulture, capable of highly impacting both yield and grape quality. Prosper 300 CS is formulated as a CS, allowing for controlled release and prolonged activity of the active compound. Application begins in early spring, at the budbreak stage, with an initial dose of recommended more than 0.7 L/ha. During the growing season, the recommended application rate is 1.00–1.30 ml/L water, which will be applied in rates of 1000 L/h, resulting in a total product dose of 1–1.3 L/ha. The product is applied every 10 to 14 days, with a maximum of three treatments per season to reduce the risk of resistance development. Alternation with fungicides of different modes of action is advised as part of integrated pest management strategies. With regard of the applied polymer content, comprising 1-5% w/w of PUA in the CS formulation, based on an approximate formulation density of 1 kg/m^3 and an application rate of one initial and three application within the growth season, the estimated MP release per season ranges from 37 to 230 g/ha per season, depending on the exact polymer content and applied amount of the product.

1.7 Background and Motivation of this Thesis

Synthetic polymer microcapsules used in PPP formulations are deliberately applied to agricultural soils and contribute to the diffuse and potentially persistent input of MPs into the environment. Understanding their biodegradability is essential, not only from a regulatory perspective, but also to evaluate their long-term environmental fate and potential impacts on soil ecosystems. This PhD project was therefore motivated by the urgent need to assess whether MPs, with special regard to PUA microcapsules, can be

biologically utilized by organisms and effectively biodegraded according to proposed test guidelines and under simulated environmentally relevant conditions. However, conducting meaningful investigations into the biodegradability of the polymeric material within the microcapsule suspension emerged to be technically challenging. For formulations containing more than one polymer or substantial non-polymeric organic content (>10% w/w), the regulation requires proof that each component contributes to the observed degradation. However, distinguishing the mineralization (e.g., CO_2-evolution) of the polymeric capsule shell, in this case typically representing only 1 to 5% of the overall formulation, from that originating from other organic constituents such as the encapsulated active ingredient and the oil-like solvent was practically impossible within the proposed biodegradation tests. Furthermore, testing the extracted polymeric shell is also challenging, as the extraction procedure itself can introduce bias. Karagianni et al. (2024) demonstrated that the method used to separate the capsule shell from other formulation components, especially from the encapsulated oil phase or additives, can significantly affect the outcome of biodegradation testing according to OECD TG 301F (OECD, 1992a). In addition, regulatory guidance requires that MPs be tested in a form that reflects their composition, size, shape, and surface characteristics as present in the final product. However, this requirement is challenged by the fact that extraction procedures can modify the shape and thickness of the polymeric material, which may affect its bioavailability and, consequently, its biodegradability. As previously mentioned (see subchapter 1.6), the polymeric shell is formed via interfacial polymerization of isocyanate and diamine, making it impossible to synthesize microcapsules without the inclusion of other carbonaceous components or to reproduce a polymer with identical structure and physicochemical properties. Thus, the approach of using a ^{14}C -radiolabeled polymer was selected to enable tracing and balancing the fate of the polymer and quantifying its mineralization through the measurement of released $^{14}CO_2$.

To broaden the environmental relevance of this work beyond intentionally added, formulation-derived MPs, linear low-density polyethylene (LLDPE) was also included as a representative secondary microplastic. LLDPE is widely used in agricultural applications, particularly in mulch films, which constitute one of the largest sources of microplastic emissions to agricultural soils as mentioned above (see subchapter 1.1). This approach enabled a broader assessment of microplastic degradation in soils and places the biodegradation behavior of PUA microcapsules in context with other plastic types typically present in agricultural environments.

In addition, the aim was to gain broader insights into the biodegradation of MPs or microcapsules and to investigate their fate with a focus on agricultural soils, where they are typically applied. Therefore, various analytical techniques such as pyrolysis-GC-MS, field-flow fractionation (FFF), and high-temperature GPC were initially considered to gather more detailed information on the structure and shape of the microcapsules within or after a biodegradation test. However, the polymer's cross-linked structure renders it insoluble, which precluded the use of GPC-based analytical methods. Furthermore,

the extraction of the small microcapsules (median size of 23 µm) or MPs from complex environmental matrices such as sludge or soil is particularly challenging due to their low concentration, small particle size, and rather adhesion to the surrounding material compared to larger MPs. These constraints complicate downstream analyses, such as Py-GC/MS or FFF, which require sufficiently purified and concentrated polymer fractions.

Moreover, abiotic factors such as sunlight (particularly UV radiation), temperature, oxygen availability, and moisture can influence the environmental degradation of polymeric materials. Photooxidation induced by sunlight exposure leads to chemical changes like chain scission, formation of oxygenated functional groups, and increased surface hydrophilicity, which may enhance microbial accessibility. Other abiotic factors play a more limited role but may still interact with biotic processes. Since current standardized tests omit these influences, incorporating abiotic stressors could improve the environmental relevance and robustness of biodegradability assessments for polymeric microcapsules.

1.8 Scope and Aims of this Thesis

Taken together, the explained scientific and regulatory challenges highlight the need for test systems that more accurately reflect the environmental degradation of MPs, including polymeric microcapsules. This requires improving existing guidelines by developing technically feasible methodological amendments and including complementary endpoints that extend beyond sole reliance on complete mineralization thresholds and account for relevant abiotic influences. These improvements are essential for better understanding their fate in agricultural soils and for more accurately estimating their environmental persistence.

Considering these challenges, the following specific research objectives guided this PhD project:

1. Development of analytical and extraction methods for qualitative characterization of MPs and their degradation products in environmental matrices according to relevant test guidelines, including OECD TG 301 and 307.
2. Optimization of biodegradation screening and simulation tests:
    a. Quantitative determination of polymer mineralization.
    b. Integration of qualitative analytical techniques to complement quantitative data.
3. Assessment of abiotic factors (e.g., simulated sunlight) on MP degradability.

The practical work was carried out over a three-year project period at Fraunhofer IME in Schmallenberg, in collaboration with RWTH Aachen University, INVITE GmbH in Leverkusen, and Bayer AG, Crop Science Division, in Monheim.

1.9 Structure of this Thesis

This thesis is divided into three parts, each addressing specific challenges related to the analysis and biodegradation assessment of MP particles, with a focus on PUA microcapsules.

The first part ("Part 1 – Broadening the Framework in Biodegradation Testing of Microplastics", see Figure 2 for the graphical abstract) focused on the applicability and robustness of the screening biodegradation test OECD TG 301B for assessing MPs. Radiolabeled ^{14}C-PUA microcapsule suspension was tested. To gain further insight into degradation pathways, a size distribution analysis was included. In addition, UHPLC-HRMS analysis was employed to investigate ^{14}C-molecules or ^{14}C-oligomers of the smallest fraction of the suspension (<0.2 µm), presumably initiating biodegradation.

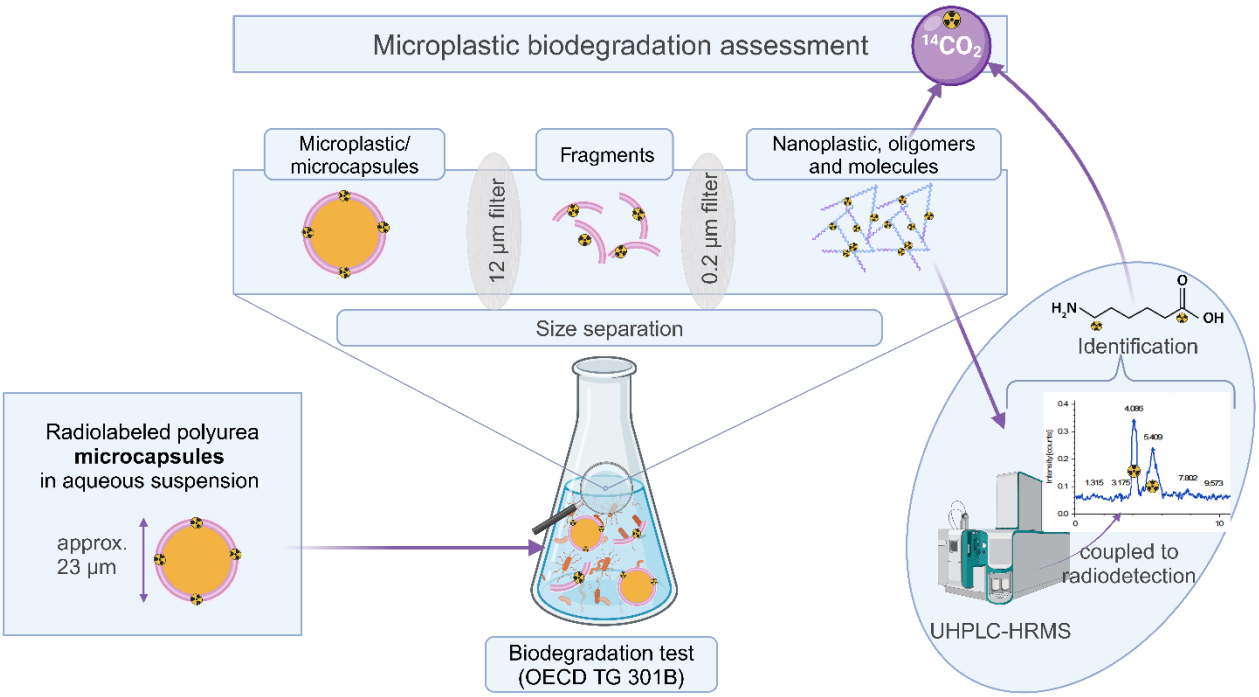

Figure 2. Graphical abstract of Teggers et al. (2025a) representing the employed methods, idea and key outcomes of the first part of the thesis.

The second part ("Part 2 – The Influence of Simulated Sunlight on the Biodegradation of Persistent Microplastics", see Figure 3 for the graphical abstract) focused on the influence of abiotic weathering, specifically simulated sunlight exposure, on the biodegradability of different MP types. Radiolabeled ^{14}C-PUA microcapsules and linear low-density polyethylene (LLDPE) MP particles were exposed to artificial sunlight to simulate environmental photooxidation. Subsequently, their biodegradability was assessed using standardized test protocols OECD TG 301B (aqueous systems) and OECD TG 307 (soil systems). In addition to biodegradation, changes in particle size and morphology were investigated.

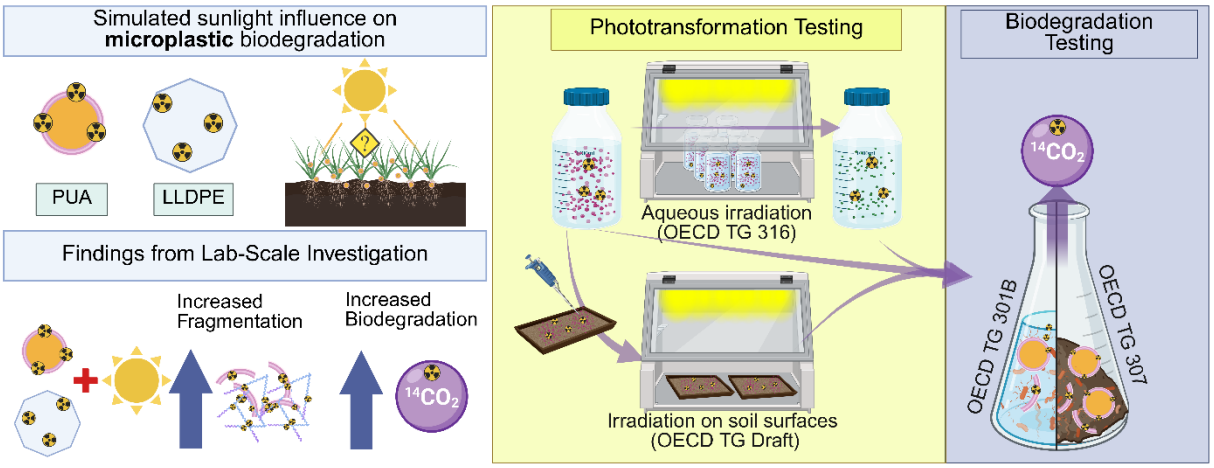

Figure 3. Graphical abstract of the second part of this thesis (Teggers et al., 2025c, under review), illustrating the performed methods and the general findings.

The third part ("Part 3 – Extraction of Pristine and Weathered Microplastics from Soil Using Modified Oil-Based Method", see Figure 4 for the graphical abstract) focused on developing an efficient and robust method for extracting MPs from soil matrices to enable further MP-specific analysis. Pristine and sunlight-irradiated PUA microcapsules and cryo-milled LLDPE were spiked into two reference agricultural soils. A conventional density separation method, as commonly applied in literature (Grause et al., 2022; Möller et al., 2020; Radford et al., 2021; Thomas et al., 2020), and a modified oil extraction method using n-octanol, adapted from the protocol of Crichton et al. (2017) were tested following an alkaline first extraction step.

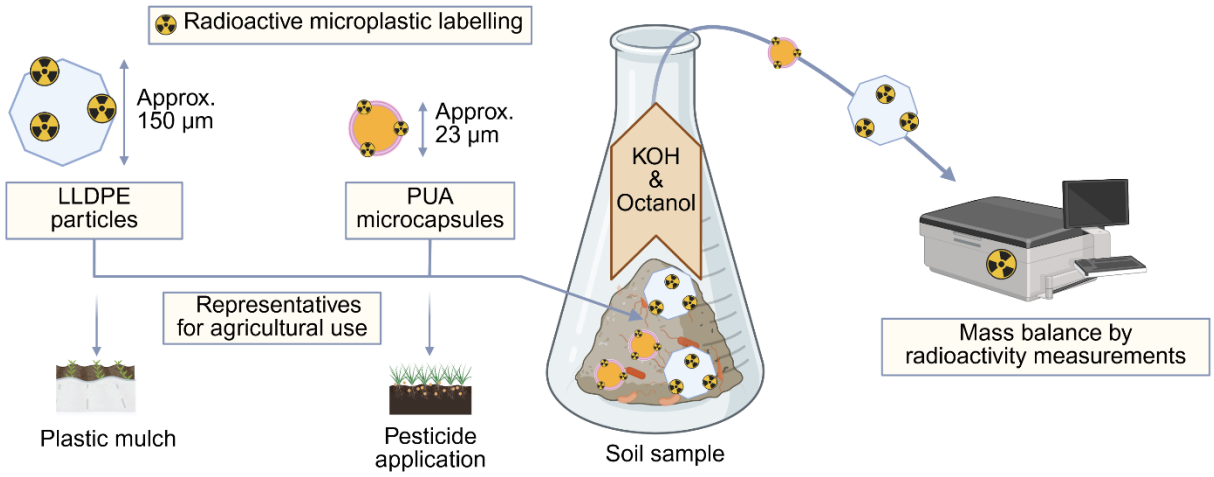

Figure 4. Graphical abstract of the third part of this thesis representing the materials and methods employed (reproduced from Teggers et al. (2025b).

2 Material and Methods

2.1 General Materials and Methods

2.1.1 Microcapsule Suspension

The synthesis of ^{14}C-labeled PUA microcapsules, with a specific radioactivity of approximately 3.49 MBq/mg (Bayer AG, Germany), followed a procedure adapted from the method disclosed in patent WO2021136758 (Krause and Egger, 2021). The capsules were produced through interfacial polymerization, where a diisocyanate and a polyamine reacted within an oil-in-water emulsion system. Radiolabeling was achieved using [1,6-^{14}C] hexamethylenediamine (HMDA, specific activity 1887 MBq/mmol, Tjaden Biosciences LLC, USA) comprising in conjunction with a modified polymeric diphenylmethane diisocyanate (pMDI). The pMDI component contained two or more reactive sites, enabling the formation of a crosslinked polymeric network.

The microcapsule suspension comprised an industrial aromatic solvent with oil-like properties with 8.59 wt% of the total undiluted microcapsule suspension (Solvesso 200 ND, ExxonMobil, USA), a surfactant at 0.23 wt% (Reax 88, Ingevity Holdings SPRL, USA), 0.08 wt% HMDA and pMDI with 0.24 wt% and water making up the remaining 90.9 wt%. A variation of this formulation, referred to as PUA_{mod}, was created using a pMDI derivative that featured ester linkages, with the goal of enhancing the biodegradability of the final microcapsule structure.

The PUA microcapsules are used for the encapsulation of pesticides and are present in certain pesticide formulations (e.g., in the fungicide Prosper 300 CS https://www.cropscience.bayer.it/prodotti/fungicidi/prosper-300-cs, Bayer AG) which are currently available on the European market. For the radiolabeled material of this study, both PUA and PUA_{mod} were synthesized on a smaller scale (approx. 200:1 to production scale and approx. 10:1 to normal lab scale), requiring lower concentrations and smaller high-shear equipment (ULTRA TURRAX Tube Disperser, IKA-Werke GmbH & CO. KG, Germany). The polymeric shell amounted to less than 1 weight% of the ^{14}C-suspension (w/w).

For the investigations of Part 2 and 3 of this thesis residual non-polymerized ^{14}C-labeled compounds were removed from both PUA and PUA_{mod} microcapsule suspensions by filtration through a cellulose nitrate membrane with a 12 µm pore size (Whatman AE 100, Cytiva, USA). After purification, the capsules were resuspended in ultra-high-purity water (PURELAB Ultra, ELGA LabWater, Germany) using an ultrasonic bath (Sonorex Super RK514H, Bandelin GmbH & Co. KG, Germany), following the methodology detailed in Part 1, based on Teggers et al. (2025a). The particle size distribution of both formulations was subsequently assessed via laser diffraction using a Mastersizer 2000 instrument (see Appendix - Table A2, Figure A1, Figure A2, Figure A3, Malvern Panalytical Ltd, UK).

2.1.2 LLDPE Particles

Linear low-density ^{14}C-polyethylene (LLDPE) was synthesized based on a modified method on the example 1 of Sinn et al. (1980) and Quijada et al. (1999) at the Fraunhofer IME (Schmallenberg, Germany). In this synthesis, the relative molar amount of Al- and Zr-compounds was increased by factor 10, compared to Sinn et al. Under inert conditions, 18 mL toluene and 2.6 mL ^{14}C-1-octadecene of a total radioactivity of 370 MBq (8.1 mmol of 2035 MBq/mmol, American Radiolabeled Chemicals Inc., USA) were transferred into a pressurized reactor provided with an ethene supply line. Then, 1625 mg 7%- methylaluminiumoxane solution (115 mg), 0.140 mg dichloro[rac-ethylenebis(indenyl)]zirconium(IV) and 1625 mg 7%-methylaluminiumoxane solution (115 mg) were added in sequence under inert gas atmosphere. The reaction mixture was heated up to 60°C in a water bath and ethene gas introduced into the reactor until a pressure of 4 bar was reached. Ethene was added again to the reactor in case of a decrease of the pressure down to 2 bar until a final pressure of 4 bar was reached again. The reaction was stopped after 1 hour by opening the reactor and a methanolic HCl solution (2 vol-%) was added. The LLDPE product precipitated as a white solid. The molar ratio of ethylene to octadecene in the product was 13.4: 1. In total, 370 MBq of ^{14}C-octadecene were used. The yield of the reaction was 96.4%. The final product was cryo-milled and sieved through a 200 µm sieve to imitate MP originating from agricultural mulch films. Particle size distribution was determined using the Analysette 22 NanoTec particle size analyzer (see Appendix - Table A2, Fritsch GmbH, Germany).

2.1.3 Utilized Soil Material

The reference soils RefeSol 01-A and 03-G (https://www.refesol.de/, Fraunhofer IME, Schmallenberg, Germany), both representatives of agricultural areas in Germany, were used in this project. These soils are widely applied in environmental research and accepted by the German Federal Environment Agency for use in regulatory guideline studies, such as those addressing the biodegradation of chemicals. The soils were collected from the top 25 cm of an extensively managed field with documented management practices. Soil analyses were performed according to the requirements of GLP (Good Laboratory Practice) and DACH (Deutsche Akkreditierungsstelle Chemie GmbH). The soil texture was determined following ISO 11277 (2020) for soil texture determination and organic carbon content was measured according to DIN EN 15936 (2022). Details of the soil analyses are provided in the Appendix-Table A4.

RefeSol 01-A is characterized as a sandy loam with light humic properties and an OC content of 1.03%, representing typical arable soil properties. In contrast, RefeSol 03-G is representative of grassland soils, with a silty loam texture and higher contents of silt, clay and OC (OC of 3.87%). Prior to testing, both soils were sieved to a particle size of 2 mm and adjusted to 50% of their maximum water holding capacity (WHC_max: 239 g/kg).

2.1.4 Quantification of Radioactivity in Different Compartments

In general, the degree of (bio)degradation was assessed by quantifying mineralization, determined through the measurement of evolved $^{14}CO_2$, which was trapped in NaOH in a flow through system. This CO_2 was captured in sodium hydroxide (NaOH) using a flow-through trapping system. For the soil biodegradation test in soil (OECD TG 307) and the phototransformation test on a soil surface (OECD Draft TG), additional traps were employed: sulfuric acid (H_2SO_4, 0.25M) to capture volatile alkaline ^{14}C-species and ethylene glycol to retain volatile organic ^{14}C-compounds. If ^{14}C-labeled polymers or substances were tested, the aeration of the flow-through system could be done using ambient air, otherwise, for the testing of non-labeled materials or substances, CO_2-free synthetic air was employed. At intervals ranging from 2 to 19 days throughout the incubation period, the NaOH traps were collected and replaced with fresh ones, depending on the current rate of $^{14}CO_2$ evolution. Accordingly, NaOH samples were initially collected after 2 or 3 days, with the timing of subsequent samplings adjusted based on the levels of radioactivity detected over the preceding two days. When only low levels of $^{14}CO_2$ were detected, the following sample was collected after an extended incubation period. In contrast, elevated radioactivity readings indicated rapid $^{14}CO_2$ formation, prompting more frequent sampling at shorter time intervals. Radioactivity in the absorption traps was measured using liquid scintillation counting (LSC). The selection of liquid scintillation cocktails was based on the chemical properties of the test media: alkaline, acidic, or organic. For alkaline conditions, either 0.5 or 1 mL of NaOH was mixed with 4 mL of Picofluor Plus (Perkin Elmer, Germany). In the case of organic solutions or samples, 0.5 mL of ethylene glycol was combined with 10 mL of Supersolve X (Zinsser Analytics, Germany). Acidic samples, consisting of 0.5 mL of H_2SO_4, were paired with 4 mL of Supersolve X. Radioactivity analysis was then performed using a HIDEX 600 SL liquid scintillation counter (HIDEX Oy, Finland). Additionally, for aqueous samples, such as those obtained at the end of the OECD TG 301B biodegradation test, 1 mL of sample was mixed with 4 mL of Supersolve X for quantification. After the irradiation on a soil surface (OECD Draft TG) or at the end of the biodegradation test in soil (OECD TG 307) the residual radioactivity in soil was determined by first drying (if required) and then combusting aliquots of approximately 300 mg using an oxidizer (HIDEX 600 OX, HIDEX Oy, Finland). The $^{14}CO_2$ generated during the combustion was trapped and transferred into the liquid scintillation cocktail Oxysolve C-400 (Zinsser Analytic GmbH, Germany) by the device and subsequently quantified through LSC.

2.1.5 Data Analysis

The recovered amounts of radioactivity were expressed as the average ± standard deviation (SD) of the percentage relative to the applied radioactivity ($\%_{AR}$). The $\%_{AR}$ was determined and allocated to each extraction fraction (e.g., NaOH, soil, KOH, octanol phase vs. $ZnCl_2$ phase, and water phase) to establish

a mass balance and regarding Part 3 of this thesis, to evaluate extraction efficiencies. In this context, the total recovery represents the sum of radioactivity detected across all phases and fractions.

The extraction efficiencies in Part 3 of this thesis are in contrast calculated by the total recovered $\%_{AR}$ excluding the portion retained in the soil fraction. Additionally, to enable direct comparison among the different extraction experiments, the radioactivity associated with each extraction fraction was normalized to the total recovery, expressed as the proportion of the total recovered radioactivity ($\%_{TRR}$). All calculations were performed using Microsoft Office Professional Plus Excel (2019). Graphical representations and statistical analysis were conducted with GraphPad Prism 6. To assess the significance of the difference in mineralization between irradiated and non-irradiated MPs at the end of the biodegradation test (MII-Procedure 4), an unpaired, non-parametric Mann-Whitney test was applied and selected due to the limited number of replicates (n = 3). Illustrations were created using BioRender.com.

2.2 Part 1 – Broadening the Framework in Biodegradation Testing of Microplastics

2.2.1 Overview of the Screening Biodegradation Test (OECD TG 301B)

In a first test (T1), the biodegradation of the aqueous bulk PUA_{mod} CS was tested in a modified OECD TG 301B (1992) "CO_2-Evolution Test". This modification included radiolabeling of the PUA_{mod} (see details in subchapter 2.1.1) and three methodological modifications: Firstly, the use of filtered supernatant from activated sewage sludge as inoculum (see subchapter 2.2.2), secondly, the extension of the test period beyond the standard duration (see subchapter "Biodegradation of the bulk capsule suspension"), and lastly, the implementation of sequential filtration for particle size fractionation of the samples (see subchapter "Biodegradation of the different size fractions of the CS").

Mineralization was determined by measuring the $^{14}CO_2$ evolved during the degradation process, which was captured in sodium hydroxide (NaOH) traps within a flow-through ventilation system, following the OECD TG 301B design. The trapped radioactivity was analyzed by LSC, as described in subchapter 2.1.4. Due to the incorporation of ^{14}C into the PUA_{mod} polymer structure, aeration with ambient air was sufficient, eliminating the need for CO_2-free synthetic air. NaOH trap sampling was conducted at intervals ranging from approximately 2 to 27 days, adjusted according to the $^{14}CO_2$ release observed at a sampling time.

To monitor the degradation performance of the inoculum, in all tests the degradability of the standard reference substance, ^{14}C-labeled sodium benzoate (benzoic acid [ring-^{14}C (U)] sodium salt, 130 mCi/mmol, American Radiolabeled Chemicals Inc., USA), was assessed in parallel.

2.2.2 Preparation of the Test Inoculum

To minimize the influence of matrix components such as sludge particles and to facilitate the combability with a broader range of analytical methods, filtered activated sewage sludge was used instead of a conventional standard inoculum (mineral medium with ca. 30 g/L (dry weight (dw) basis) of activated sludge suspended solids). To replace the standard inoculum, mineralization of the reference substance sodium benzoate (100 mg/L; 167 mg theoretical oxygen demand (ThOD/L) was tested in a preliminary biodegradation test according to OECD TG 301F (1992). In this context, ThOD refers to the calculated amount of oxygen required to completely oxidize the applied amount of sodium benzoate to CO_2. As required in the TG the standard inoculum consisted of 30 mg/L dry weight (dw) sewage sludge particles, and its degradation performance was compared to that of the filtered supernatant used in this study. Additional tests included 300 mg/L (dw) sewage sludge particles and non-filtered supernatant.

The filtered inoculum was prepared using activated sludge collected from the effluent stream of a municipal wastewater treatment plant (Ruhrverband Kläranlage, Sunthelle 6, 57392 Schmallenberg) two days before the start of the test. The sludge was allowed to settle for approximately 30 minutes at room temperature under diffuse light, promoting sedimentation of the majority of suspended solids. The supernatant was then decanted, centrifuged for 5 minutes at 10,000 g, and subsequently filtered through a cellulose filter (Macherey-Nagel, MN-672; pore retention range: 4–12 µm). Throughout both, the preparation and incubation phases, the inoculum was continuously aerated with ambient air.

2.2.3 Biodegradation of the Bulk PUA_{mod} CS (T1)

A macro-elemental analyzer (multi EA 4000, Analytik Jena) was used to measure the total carbon content in the CS prior to testing. Test preparations for both the CS and sodium benzoate were adjusted to reach a total carbon (TC) concentration near 20 mg/L, in accordance with OECD TG 301B requirements. At the beginning of the test, two sodium benzoate control samples were prepared, in addition to 16 samples for the PUA_{mod} CS treatment (see SI – Table S5). An overview of all samples and their associated incubation durations is provided in Figure 5.

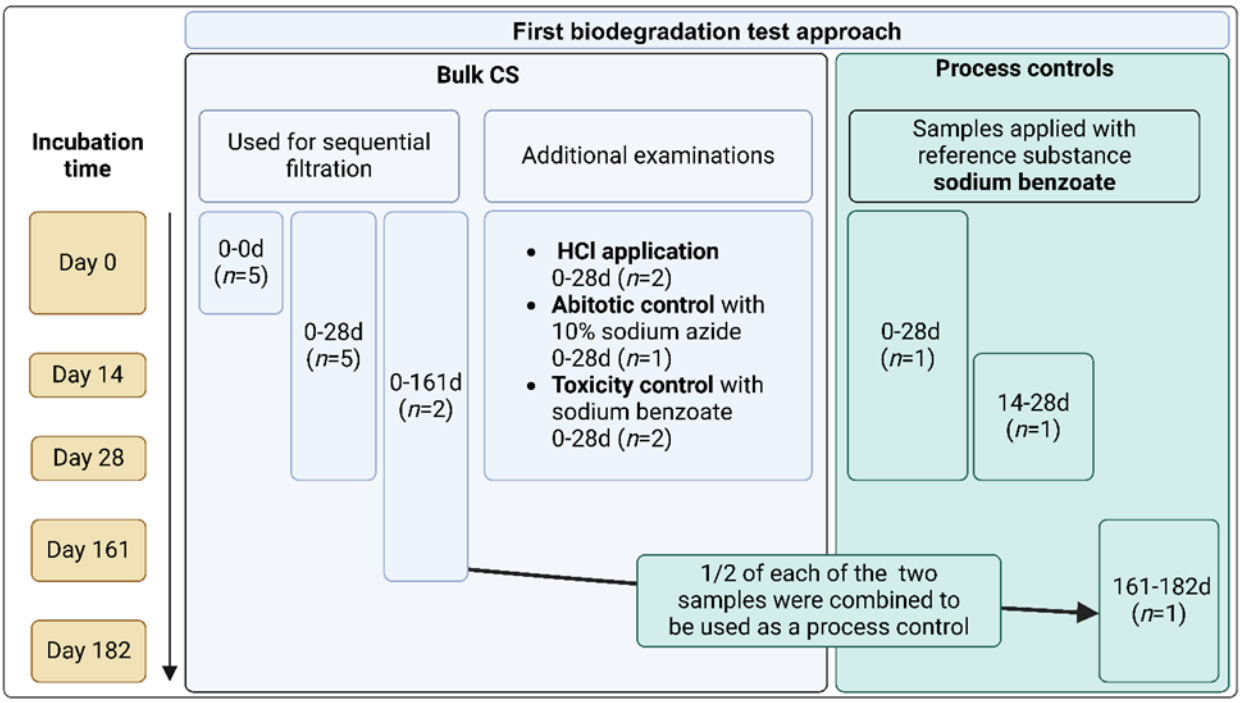

Figure 5. Incubation schedule of the bulk capsule suspension (CS) samples and process control samples supplied with sodium benzoate tested in the OECD TG 301B. Samples supplied with CS are displayed with light blue background and process controls, supplied with sodium benzoate are displayed with green background. At 161 d, one half of each CS sample duplicate was sampled and the other half was combined to a sample to which sodium benzoate was applied for using it as process control. Scheme reproduced from Teggers et al. (2025a).

To observe whether the degradation performance of the microbes was still functional throughout the incubation time, process controls were employed. For this, ^{14}C-sodium benzoate was applied to one inoculum sample at 0 d and to another at 14 d. The evolving $^{14}CO_2$ was monitored over time. To perform a sequential filtration (see subchapter 2.2.4) at different incubation time points, inoculum samples containing the CS were prepared.

To examine whether microbial activity remained stable over an extended period, a fraction of each of the duplicate sample containing the bulk CS, which were incubated for 161 d, were combined at the end of the test period (see Figure 6). To serve as another process control, the combined sample was applied with ^{14}C-sodium benzoate and its mineralization was monitored.

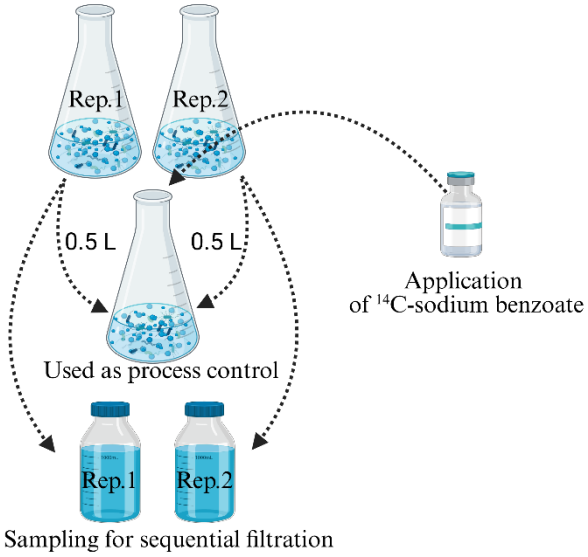

Figure 6. Preparation of the last process control at 161 d. Half of each duplicate sample incubated for 161 d with the bulk CS was combined. Subsequently, ^{14}C-sodium benzoate was applied to the combined sample.

Further investigations included (Figure 5):

(I) the determination of CO_2 bound as carbonic acid in the aqueous media by applying hydrochloric acid (HCl) at the end of the incubation time (28 d).

(II) and the evaluation of abiotic degradation (30 mL of a 10% sodium azide solution was introduced to a sample containing the CS).

(III) and the evaluation of potential inhibitory effects of the suspension on microbial activity. Therefore, a toxicity control was included in parallel with the main test. For this purpose, an easily biodegradable ^{14}C-labeled substance is added to the sample containing the CS. In this study, ^{14}C-sodium benzoate (20 mg C/L) was used to examine whether its mineralization was inhibited by the presence of the tested bulk CS. If the mineralization of ^{14}C-sodium benzoate is substantially decreased by the presence of the CS, it would suggest that the CS negatively impacts microbial activity.

After the application of either the unprocessed bulk CS (5 mL, 5.4 ± 0.1 kBq/mL) or the ^{14}C-sodium benzoate solution (5 mL, 65.8 ± 0.3 kBq/mL), the total radioactivity in each sample was verified to confirm the accuracy of AR at the beginning of the test. For this purpose, 1 mL aliquots were taken from each sample (n=3) and LSC analyzed as described in subchapter 2.1.4.

2.2.4 Sequential Filtration Integrated into the First Biodegradation Test (T1)

To assess changes in the size distribution of the MP, the first biodegradability test following the modified OECD TG 301B guideline, included a sequential filtration of test samples containing the bulk CS at different times during the incubation. For this purpose, 50 mL sample aliquots were sequentially passed through filters with differing pore sizes (Cytiva Whatman®, nitrocellulose filter, 12 µm pore size,

Z696919; Sartorius, cellulose acetate filter, 5 µm pore size, Type 12342; Sartorius, cellulose acetate filter, 0.45 µm pore size, Type 11106; Sartorius, cellulose acetate filter, 0.2 µm pore size, Type 11107) at day 0, day 28 and day 161 (see Figure 5). The radioactivity of the filters and the filtrate were quantified as described in subchapter 2.1.4.

2.2.5 Biodegradation of the Different Size Fractions of the PUA_{mod} Bulk CS (T2)

The second biodegradability test (OECD TG 301B) was performed with prior separated size fractions of the CS as illustrated in Figure 7. For this purpose, the CS was first filtered, and the size fractions of approximately >12 µm retained on the 12 µm pore-sized filter (Cytiva Whatman®, nitrocellulose filter, Z696919), as well as the fractions of approximately <12 µm that passed into the filtrate, were tested in separate test vessels. Thus, 500 mL of the aqueous stock suspension with a radioactivity of 1.6 ± 0.0 kBq/mL were produced, 50 mL CS aliquots were passed through the 12 µm pore-sized filter ($n = 3$) and each filtrate was sampled to be subsequently applied to the biodegradation test. The filters were washed with 100 mL of water prior to be applied to the inoculum of the biodegradation test. All samples were subsequently connected to the ventilation system to trap evolving $^{14}CO_2$. In addition, 50 mL aliquots of the unfiltered CS ($n = 3$) were tested as quality control, to confirm that the total mineralization evolved from both size fractions, (mineralization >12 µm retained on the filter plus the mineralization of the filtrate <12 µm) equals the mineralization of the bulk CS.

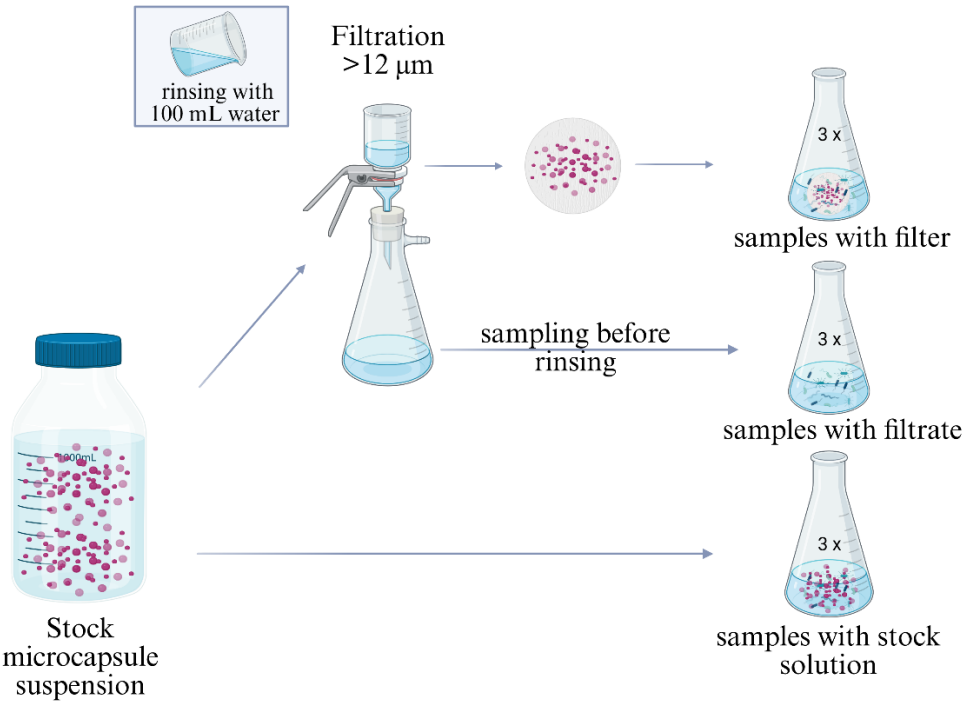

Figure 7. Preparation of the test samples for testing the separated size fractions of the bulk CS in an OECD TG 301B biodegradation test.

2.2.6 Ultra-High Performance Liquid Chromatography with High Resolution Mass Spectrometry (UHPLC-HRMS)

To investigate whether ^{14}C-labeled molecular compounds or unreacted monomers were present in the smallest size fraction (<0.2 µm) of the PUA_{mod} bulk suspension, a UHPLC HRMS analysis coupled with radio detection was employed. The set-up included a reversed-phase C18 column (RP18, ODS-AQ, YMC, USA) coupled to a Q-Exactive Plus Orbitrap mass spectrometer (HRMS, using the analysis software Qual Browser of Xcalibur Version 4.0, Thermo Fisher Scientific Inc., USA) and a radio detector (LB509 - YG 75 S6M, Berthold GmbH & Co. KG, Germany), as detailed in the Appendix - Table A5, Table A6 and Table A7. ^{14}C-labeled molecules identified by HRMS analysis were compared to known analytical standards of the respective compounds. To rule out potential adsorption of the analytes on the column matrix, the LC system was also verified by evaluating recovery of the eluted radioactivity. For this purpose, the eluate was collected over timed intervals (0–3.5 min, 3.5–7 min, 7–15 min, and every 7.5 min from 15–60 min), based on the radio signal from prior analyses. The radioactivity contained in these fractions was subsequently measured via LSC (see subchapter 2.1.4).

The last analysis focused on identifying molecules derived from the labeled [1,6-^{14}C]hexamethylenediamine used in polymer synthesis. To enable this, isotopic patterns of molecules present in both labeled and non-labeled forms were evaluated. The analysis focused on detecting specific mass shifts, which can be associated with substitutions of carbon isotopes, for example molecules containing different combinations of ^{12}C, ^{14}C or $^{14}C_2$ in addition to their characteristic intensity profiles.

Thus, molecules with matching mass shifts (with 5 ppm tolerance) and similar intensity patterns (20% deviation) were extracted from the mass spectra. Their signal intensities were then plotted against the retention time (RT).

2.3 Part 2 – The Influence of Simulated Sunlight on the Biodegradation of Persistent Microplastics

2.3.1 Simulated Sunlight Irradiation Settings

To simulate potentially, environmentally relevant photooxidative processes acting on the polymers and its influence on subsequent biodegradation, two irradiation approaches were performed (see Figure 8). The first approach (MI) was performed in an aqueous environment, following OECD TG 316 (2008) "Phototransformation of Chemicals in Water". The second (MII) irradiation method was performed on a soil surface based on the OECD Draft TG (2002) "Phototransformation of Chemicals on Soil Surfaces". After the execution of these methods the size distribution changes and the biodegradation were examined as illustrated in Figure 8 and Table 2 providing more details.

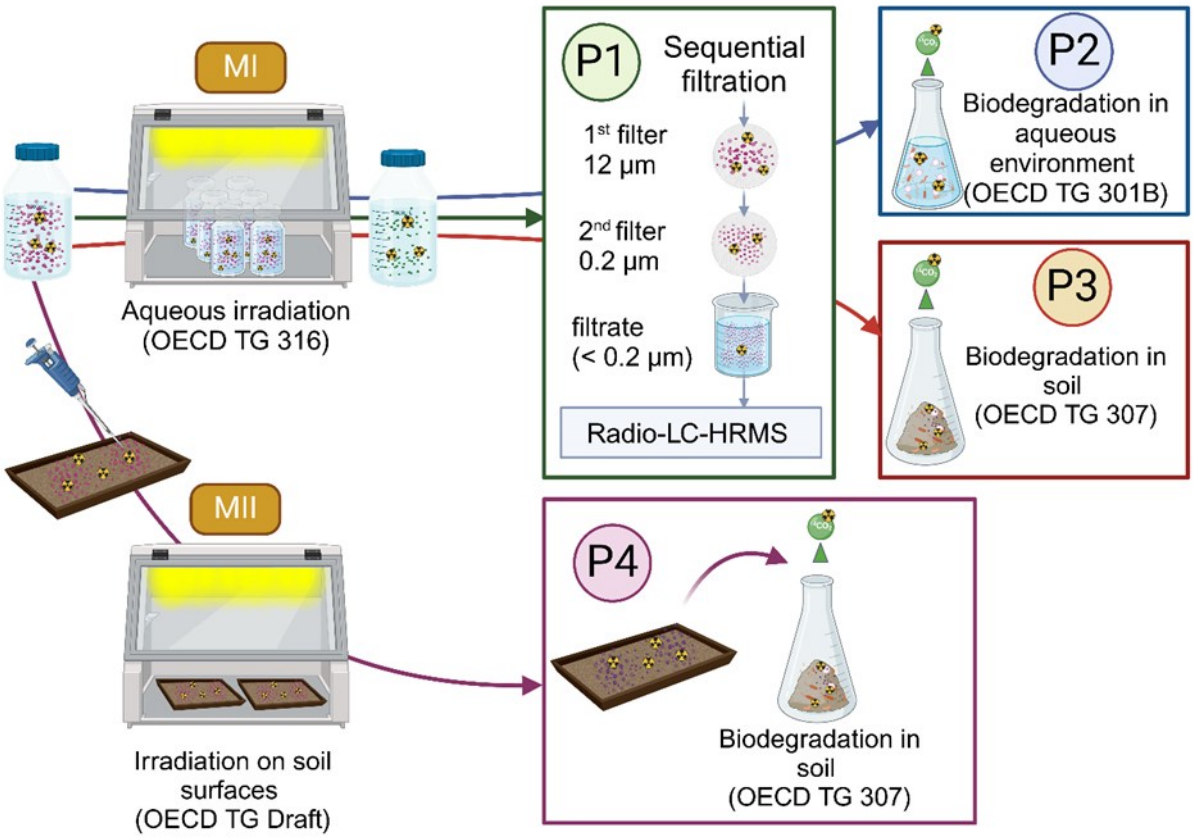

Figure 8. Procedures (P) to investigate the influence of simulated sunlight exposure of MPs by implementing two different irradiation methods (MI and MII) on the biodegradation and fragmentation of the MPs. Standardized testing guidelines were used in sucssession for irradiation and biodegradation tests. Details of the performed procedures are provided in Table 2.

The irradiation methods were carried out under continuous light exposure using the SUNTEST CPS+ chamber (Figure 9. A), Atlas Material Testing Technology GmbH, Germany), which emits radiation in the 295–800 nm range. The system is equipped with a Xenon lamp with an intensity of 75 W/m² in the 300–400 nm range, as specified by the manufacturer. The light intensity and wavelength range were verified with a BLACK-Comet UV-VIS Spectrometer (BLK-CR2, StellarNet, Inc., USA). Based on the following equation [1] of the OECD draft Test Guideline (2002), the irradiation energy was converted into the equivalent number of summer daylight exposure days (*d*) in the mid-latitude regions of the northern hemisphere (30–50°N). For this, the hours of irradiation (*h*) were multiplied by the ratio of irradiance (*r*) of the Xenon radiation (75 W/m^2) to that of summer light, which is specified as 67 W/m^2 for the northern hemisphere. The calculated irradiation energy was divided by the correction for the diurnal variation of natural sunlight (0.75), which was multiplied by the conversion factor of hours to days (12).

$$d = \frac{h \cdot r}{0.75 \cdot 12} \quad [1]$$

In Table 1 the irradiation duration and applied energy of the performed irradiation procedures are displayed.

Table 1. Irradiation duration and irradiation energy of the performed irradiation procedures

Irradiation Procedure	Days of Irradiation [d]	Equivalent to days of summers† [d]	Total irradiation energy per square meter* [kWh/m²]
Procedures 1 and 3			
PUA$_{mod}$	13.9	41.5	25.0
LLDPE	13.9	41.5	17.8
Procedure 2			
PUA$_{mod}$	13.9	41.5	25.0
Procedure 4			
PUA$_{mod}$	9.9	29.6	17.8
PUA			
LLDPE	10.1	30.1	18.1

*calculated using the manufacturer's specification of the SUNTEST CPS+ of 75 W/m² within a wavelength range of 300-400 nm; † calculated to the equivalent sunlight energy of natural summer days in the northern hemisphere (30-50°N) acc. to OECD draft TG

A cooling system using ethylene glycol was integrated alongside the built-in air conditioning of the SUNTEST CPS+ chamber at the base of the vials and the soil surface (Figure 9. E), F), G)), to maintain the temperature of the aqueous suspensions below 35°C and to ensure that soil surfaces remained at moderate temperatures. After the irradiation period, radioactivity levels were measured in both the soil and suspension phases to ensure mass balance calculations.

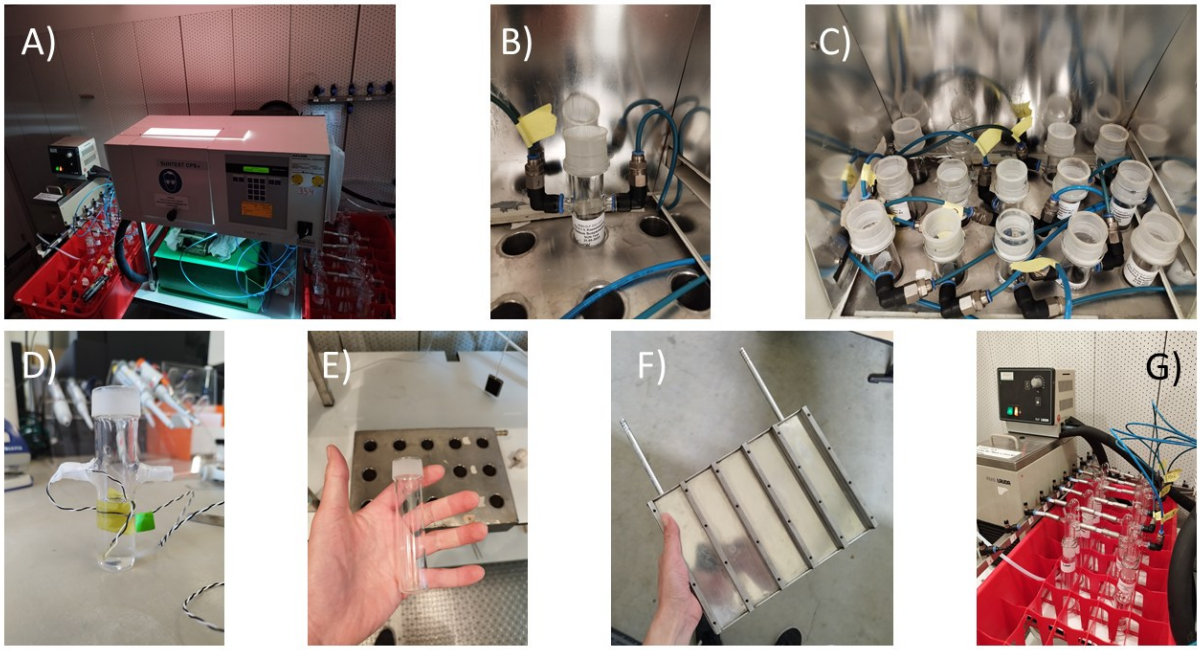

Figure 9. Images of the simulated sunlight irradiation set-up. A) SUNTEST CPS+ Equipped with a second cooling system (left) and ventilation system to trap evolving volatiles (red boxes with flasks). B) Vial with ventilation system adaptaters. C) Vials with and without ventilation sytem (set-up of procedure MI-Procedure 2). D) Installation of the temperature data logger for aqueous irradiation. E) Quartz glass vial equipped with basis used for ethylen gylcole circulation in the background. F) Basis used for ethylen gylcole circulation underneath the soil surfaces. G) Left side: Ethylen glycole cooling system and at the right side: connected flasks in red baskets connected with a flow through system for trapping volatiles.

The irradiation of the PUA_{mod} suspension in water (MI-P2, Figure 8 and Table 2) was performed using six replicates of 15 mL each, transferred into quartz glass vials (Ø 2.6 cm, 10.5 cm height, Figure 9 E)) and placed into the irradiation chamber. Three of the vials with PUA_{mod} suspension were sealed with gas-tight quartz glass lids and used for the downstream biodegradation test. The remaining three were sealed with glass lids and connected to a flow-through system to trap all evolving volatile ^{14}C-compounds (Figure 9. B), C)). The AR of MI-Procedure 2 was 5.23 ± 0.21 kBq/15 mL. In comparison, MI-P1 and MI-P3 were performed with higher AR values, with five replicates of 15 mL PUA_{mod} suspension with 3.5 ± 0.16 kBq/mL and 15 mL of the LLDPE suspension with 4.6 ± 1.95 kBq/mL

Table 2. Overview of the procedures used to assess the effect of simulated sunlight exposure on polymer biodegradation and fragmentation. The procedures are based on combined standardized OECD guidelines for irradiation and biodegradation testing and fragmentation was assessed through a sequential filtration. Figure 8 illustrates the test procedures

Procedure	Description	Tested Material	Irradiation/ biodegradation following
MI-P1	Aqueous irradiation and sequential filtration	PUA_{mod}; LLDPE	OECD TG 316
MI-P2	Aqueous irradiation followed by biodegradation in aqueous environment	PUA_{mod}	OECD TG 316, OECD TG 301B
MI-P3	Aqueous irradiation followed by biodegradation in soil	PUA_{mod}	OECD TG 316, OECD TG 307
MII-P4	Irradiation on soil surface followed by biodegradation in soil	PUA_{mod}; PUA; LLDPE	OECD TG 316, OECD TG 307

The irradiation of MII-P4 (Figure, Table 2) with the MP PUA, PUA_{mod} and LLDPE were performed on a soil surface. The experiment was performed following to the draft OECD TG "Phototransformation of Chemicals on Soil Surfaces" (2002). For this, 10 g of RefeSol 01-A soil (section 2.1.3) were suspended in water, poured into quartz glass dishes (18 x 3.5 x1 cm) and dried in a drying cabinet at 35°C to generate a dry soil layer with a thickness of approximately 2 mm. The application of the MPs and polymers were performed as follows: 1.5 mL of the PUA (AR of 31.7 ± 0.06 kBq/1.5 mL) and PUA_{mod} (AR of 26.0 ± 0.04 kBq/1.5 mL) were applied on four replicates of the dried soil each. Due to a high SD observed in previous tests regarding the application of LLDPE suspensions, exact amounts of 1.7, 1.9, 2.1 and 2.8 mg of LLDPE were weighted and mixed with 10 mL water and 10 g of RefeSol 01-A soil to be casted into the quartz glass dishes. By the determined specific radioactivity of 56.6 kBq/mg the AR were calculated to be 96.1, 107, 119 and 158 kBq, respectively. Generally, two out of the four applied soil layer replicates (R1 and R2) were irradiated. Following the draft OECD TG, the temperature of the irradiated soil layers must be kept at 20 ± 2°C. However, this proposed set-up unavoidably generates a temperature gradient, as the surface of the soil is directly exposed to air that is heated up upon irradiation by the xenon lamp, reaching measured temperatures of up to 80°C (Figure A5 and Figure A6). In contrast, the soil layer was cooled from underneath by the ethylene-glycol system, which is set to ≤ 5°C. Consequently, to meet the temperature specifications of the draft TG throughout the soil layer is not feasible and criticized ((European Food Safety Authority (EFSA) et al., 2022; Hassink et al., 2024).

Therefore, the two remaining replicates were prepared as dark and temperature controls by incubating them in a drying cabinet set to 80 °C, the highest soil surface temperature observed during irradiation, to simulate a worst-case scenario for potential temperature-induced degradation. This approach ensured a clear distinction between MP or polymer degradation induced by photolytic processes and that caused

solely by possible thermal degradation in the absence of light. During irradiation, the soil layers were connected to a flow-through system to trap volatile ^{14}C-compounds, including acidic species such as $^{14}CO_2$, as well as alkaline and organic volatiles released during exposure period (see subchapter 2.1.4 for quantification measures).

2.3.1 Biodegradation after Simulated Sunlight Exposure

Following MI-P2 (Figure 8, Table 3), after irradiation in water, the PUA_{mod} suspension was transferred to the biodegradation test, which was performed following OECD TG 301B "CO_2-Evolution Test". Deviating from the TG, the inoculum used consisted of filtered activated sludge supernatant rather than bulk sludge particles suspended in mineral medium as already used and examined in chapter 3.1. Furthermore, instead of total CO_2, only $^{14}CO_2$ was measured for sensitive attribution to the ^{14}C-PUA_{mod} degradation. The test also included biodegradation testing of a standard reference substance sodium benzoate form (benzoic acid [ring-^{14}C (U)] sodium salt, 130 mCi/mmol, American Radiolabeled Chemicals Inc., USA) to monitor the overall degradation performance as a process control (PC). The AR was 2.73 ± 0.04 kBq/8.5 mL for PUA_{mod} (n=3) and 58.3 ± 0.18 kBq/8.5 mL for ^{14}C-sodium benzoate (n=1).

The biodegradation tests in soil for procedure MI-P3 and MII-P4 were performed following OECD TG 307 (2002) "Aerobic and Anaerobic Transformation in Soil". The experiments were carried out at 20 ± 2 °C in the dark with sufficient aeration provided by the flow-through system. In Procedure MI-P3, 0.5 mL (1.75 kBq) of the irradiated PUA_{mod} suspension was applied to 25 g dry weight (dw) soil of reference soils (01-A and 03-G, respectively each in replicates of n=3). In procedure MII-P4, both replicated soil layers were placed at two different positions in the irradiation chamber inducing potential differences regarding the irradiation intensity. Therefore, irradiated and non-irradiated soil duplicate layers (n=2 each) on which PUA_{mod}, PUA and LLDPE were each combined and mixed thoroughly to generate a homogenous application soil material for the subsequent biodegradation test in soil. Prior to application the radioactivity of the combined soil layers was measured for accurate mass balancing in the subsequent biodegradation test (see chapter 2.1.4 for radioactivity analysis). For application, 5 g aliquots of the irradiated soil were each added to 50 g of biologically active and untreated reference soil (RefeSol 01-A and 03-G for MI-P3), which was preincubated in the sample flasks for 10 days at 20 ± 2 °C. The biodegradation test was performed in triplicates.

2.3.2 Sequential Filtration of the MPs Suspensions

The sequential filtration of procedure MI-P1 was performed similarly as described in subchapter 2.2.4 to evaluate the approximate size distribution. In this procedure, in water irradiated and non-irradiated suspensions of PUA_{mod} and LLDPE were investigated. For this, 0.5 mL of each irradiated (1.12 ± 0.01 kBq/0.5 mL AR of PUA_{mod} , 0.63 ± 0.15 kBq/0.5 mL LLDPE) and non-irradiated (1.75 ± 0.08 kBq/0.5

mL, 2.33 ± 0.98 kBq/0.5 mL LLDPE) stock solution was diluted in 49.5 mL water and sequentially passed through two filters in sequence: a 12 µm nitrocellulose membrane (Cytiva Whatman®, Z696919) followed by a 0.2 µm cellulose acetate membrane (Sartorius, Type 11107) (n = 3). After filtration, the filters were dried and the radioactivity retained on each filter was determined. In addition, the radioactivity of the filtrate (<0.2 µm) was analyzed for a complete mass balance. For details on quantification measures see subchapter 2.1.4.

To investigate potential release of the ^{14}C-labeled low molecular weight compounds from PUA_{mod} induced by photo-oxidation, the 0.2 µm filtrate was subjected to further analysis using UHPLC-HRMS (UHPLC-HRMS; m/z 100–6000, Xcalibur Qual Browser v4.0) analysis coupled to radiodetection (LB509 - YG 75 S6M, Berthold GmbH & Co. KG, Germany) using the same method as described in subchapter 2.2.6. Details of the analysis are given in Appendix - Table A5, Table A6, Table A7.

2.4 Part 3 – Extraction of Pristine and Weathered Microplastics from Soil Using a Modified Oil-Based Method

2.4.1 Overview of the Microplastic Extraction Procedures

Overall, three different extraction experiments were performed, which are displayed in Table 3. In the first experiment (I), a modified oil extraction method utilizing octanol was applied (Figure 10) and compared with the second experiment (II), which employed a density-based extraction using $ZnCl_2$. Both approaches incorporated a first extraction step with KOH (Figure 10). The third experiment (III) investigated whether repeating the KOH extraction step improves the efficiency of MP recovery by conducting two sequential alkaline treatments. Additionally, a separate experiment was conducted to assess the effect of varying pH levels during the first extraction step on the recovery of PUA_{mod}.

Table 3. Overview of the performed experiments. Not executed experiments are abbreviated by "N/A". LLDPE was only tested in experiment I). Reproduced from Teggers et al. (2025b).

	Extraction experiments	**Spiked MPs**		**Soils used for the experiments (Reference Soil RefeSol)**
		Pristine	**Light-exposed**	
I)	Modified oil extraction using octanol	PUA_{mod}, LLDPE	PUA_{mod}, LLDPE	03-G, 01-A
II)	Density extraction using $ZnCl_2$	PUA_{mod}	N/A	03-G, 01-A
III)	Repeated first extraction step using KOH	PUA_{mod}	N/A	03-G

2.4.2 Experiment I) - Modified Oil Extraction Using Octanol

Experiment I) ("Modified oil extraction using octanol") and Experiment II) ("Density extraction using $ZnCl_2$) both consist of two extraction steps of which the first extraction step is identical (Figure 10). This first extraction step was carried out using KOH to remove soil organic matter (SOM) to improve the MP extraction efficiency. In this step, 100 mL of a 10% KOH solution (prepared from potassium hydroxide pellets, Merck KGaA, Germany) were added to the soil samples spiked with PUA_{mod} or LLDPE MPs (n = 3 each). The samples were shaken on a horizontal shaker (Laboshake LS500, C. Gerhardt Analytical Systems GmbH & Co. KG, Germany) at 200 rpm for 22 h at room temperature followed by centrifugation (Multifuge 4KR, Heraeus GmbH, Germany) at 1700 g for 20 min. The supernatant was decanted and 100 mL of UHQ water were added to the soil samples to remove residual KOH. The samples were then shaken and centrifuged again to allow decantation of the aqueous supernatant. The volume of the extracts was measured to determine the contained radioactivity for assessing the extraction efficiency of the KOH. Given that the strongly alkaline conditions (pH 14) could potentially alter the MP particles, a parallel investigation was conducted in which morphological changes in the PUA_{mod} microcapsules were examined microscopically following incubation in KOH solution for up to five days.

A separate investigation was conducted to assess the influence of pH on the extraction efficiency of the first extraction step. For this purpose, 25 g of the RefeSol 03-G reference soil was treated with four solutions of varying pH in triplicates: hydrochloric acid (pH 3), UHQ water (pH 6), and two sodium hydroxide solutions (pH 11 and pH 14), prepared from a 2 M NaOH stock solution (Grüssing GmbH, Germany).

In the first experiment (I, Table 3), the second extraction step followed a modified oil extraction protocol by Crichton (2017), which originally used canola oil. Other studies that performed an oil extraction also used olive or castor oil. Following this method, water and oil are initially added to the soil sample and

the mixture is thoroughly shaken. The mixture is then left undisturbed until the phases separate clearly into two layers. Because of the polymers oleophilic properties MPs accumulate in the oil layer, which can then be decanted for subsequent analysis. To reduce variability caused due to the uncertain composition of natural, non-standardized oils, potentially affecting the extraction process, we substituted plant oil with the chemically defined compound n-octanol (Extra Pure, Merck KGaA, Germany) in our study.

Thus, after the performance of the first extraction step using KOH, 100 mL UHQ water and 10 mL octanol as a second extraction step were applied to the PUA_{mod} or LLDPE MPs spiked soil samples. As illustrated in Figure 10, the samples were shaken for 1 h at 200 rpm on the horizontal shaker, left to settle for around 18 h and then centrifuged for 20 min at 1700 g (Multifuge 4KR, Heraeus GmbH, Germany). This centrifugation step was essential to remove excess soil particles from the liquid phase, which would otherwise hinder effective filtration. Following centrifugation, the upper octanol phase was extracted using a Pasteur pipette and vacuum-filtered through a 12 µm cellulose nitrate filter (Whatman AE 100, Cytiva, USA). The filters subsequently rinsed with a 1:1 (v:v) ethanol-water solution to eliminate residual octanol. Finally, the aqueous phase was decanted. The volume of all extracts was measured and both, the soil and filters were air-dried prior combustion to determine their respective radioactivity and to calculate the overall mass balance.

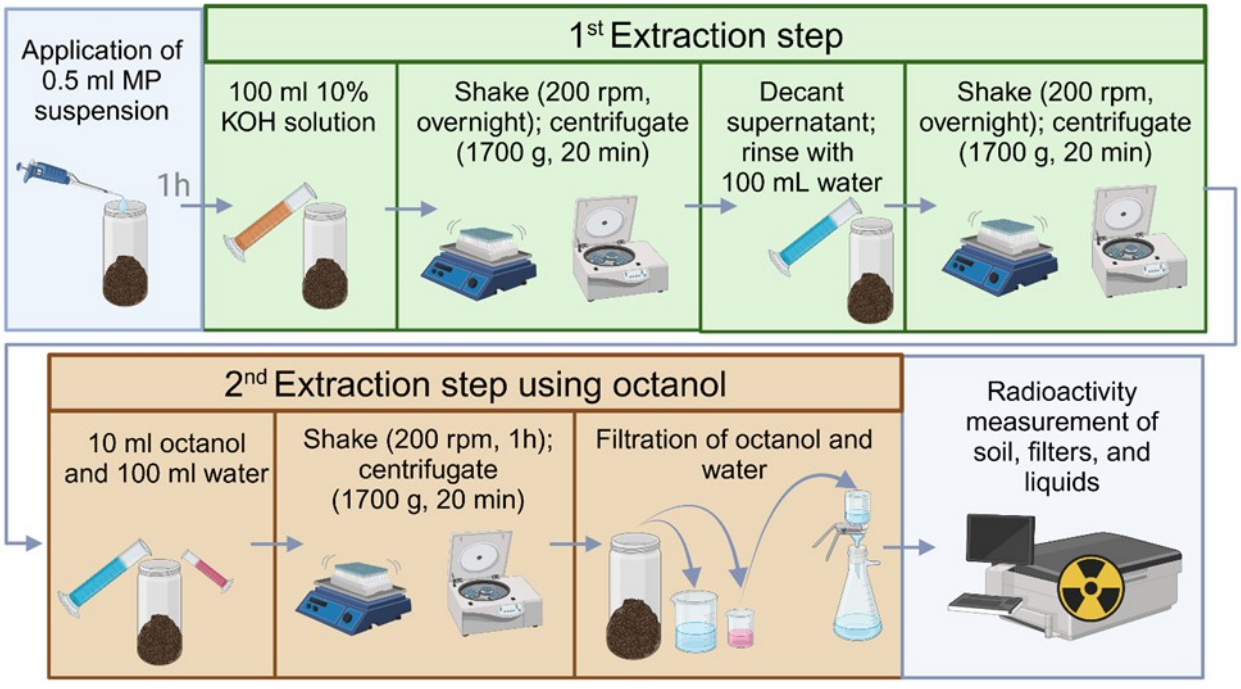

Figure 10. Protocol of the extraction experiment I). The modified oil extraction using octanol as an alternative to the density extraction (experiment II)). The first extraction step with KOH is shown in green (top row), followed by the second extraction step using octanol, shown in brown (bottom row). The density-based procedure employing zinc chloride as a second extraction step is not depicted. Reproduced from Teggers et al. (2025b).

2.4.3 Experiment II) - Density Extraction Using $ZnCl_2$

For the second extraction experiment (II, Table 3), a density-based extraction was conducted as an alternative second extraction step. An 8.8 M $ZnCl_2$ solution (made from anhydrous ZnCl2, 98+%, Thermo Fisher Scientific, USA) with a density of 1.57 g/cm^3 was used. A volume of 100 mL $ZnCl_2$ solution was added to the soil samples spiked with PUA_{mod} MPs following the first extraction step using KOH. In the next step the samples were shaken on a horizontal shaker at 200 rpm for 45 min and subsequently centrifuged at 1700 g for 20 min (Multifuge 4KR, Heraeus GmbH, Germany). The resulting supernatant was vacuum-filtered through a 12 µm cellulose nitrate filter (Whatman AE 100, Cytiva, USA). To remove most of the $ZnCl_2$ the filters were rinsed with UHQ water. The soil was then washed with 100 mL UHQ water, shaken, and centrifuged again. The second supernatant was decanted and vacuum-filtered. The volume of the extracts was measured, and the soil and filters were air-dried and combusted to ultimately determine the radioactivity of the respective fractions.

2.4.4 Experiment III) - Repeated KOH Extraction

For the third extraction experiment (III, Table 3), the first extraction step using KOH was performed twice to evaluate whether this repeated treatment might enhance the extraction efficiency.

2.4.5 pH Dependence of Microplastic Extraction Efficiency

In a separate experiment, a pH correlation test was performed to examine the dependence of pH on extraction efficiency by the first extraction step. For this, 25 g of reference soil (RefeSol 03-G) was treated with four solutions of varying pH: hydrochloric acid (pH = 3), UHQ water (pH = 6), and two sodium hydroxide solutions (pH = 11 and pH = 14), both prepared from a 2 M NaOH stock solution (Grüssing GmbH, Germany). The experiment was performed identically to the first extraction step (see subchapter 2.4.2), and the recovered radioactivity in the solutions was measured (see subchapter 2.1.4 for radioactivity quantification). All treatments were carried out in triplicate.

3 Results

3.1 Part 1 – Broadening the Framework in Biodegradation Testing of Microplastics

3.1.1 Biodegradation of the Bulk PUA_{mod} CS (T1)

To assess the biodegradation ability of the filtered supernatant compared to the standard inoculum used in the OECD TG 301 (1992), a preliminary biodegradation test acc. to OECD TG 301F was performed. In this test, both inoculums showed a comparable performance in the mineralization of sodium benzoate. Both reached over 60% mineralization after 2 days (<10-day window and within the first 14 days for test validity), with 67.9 ± 2.55%ThOD for the supernatant and 64.0 ± 0.42%ThOD for the standard inoculum (average ± SD of *n*=3; Figure 11). Compared to the standard inoculum, a lag phase on the first day after application was observed, with a delayed but rapid increase in mineralization at day two of the supernatant.

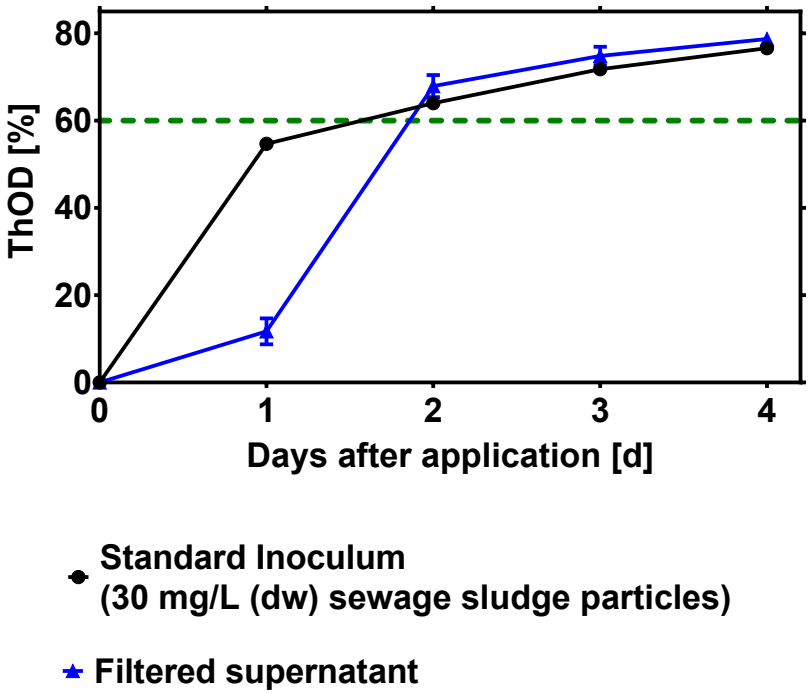

Figure 11. Biodegradation ability of the filtered supernatant opposed to the standard inoculum (30 mg/L dry weight (dw) sewage sludge particles) in the OECD TG 301F test. Compared was the cummulative mineralization of the reference substance sodium benzoate (100 mg/L; 167 mg theoretical oxygen demand (ThOD)/L). The green line represents the validity threshold of the OECD TG 301, wherein the reference needs to reach a degradation of 60% within a 10-day window. Means of *n*=3 ± SD. Reproduced from the Supplementary Information (SI) of Teggers et al., (2025a).

In both biodegradation tests based on OECD TG 301B (T1, testing the bulk PUA_{mod} suspension and T2, testing the separated size fractions of the PUA_{mod} suspension), the amount of evolved $^{14}CO_2$ from the

PCs applied on day 0 was below the validity criterion of 60%$_{AR}$ (see Figure 12). In T1, 58.6%$_{AR}$ was evolved as $^{14}CO_2$, corresponding to over 98% of the validity criterion, while in T2, only 26.6%$_{AR}$ was evolved as $^{14}CO_2$, meeting only 44% of the validity threshold. The PC to which sodium benzoate was applied on day 14 (T1) reached 48.2%$_{AR}$ (Figure 12). The process control, which was made of two samples with bulk suspension, started at 161 d and reached 67.1%$_{AR}$ within 21 d (Figure 12).

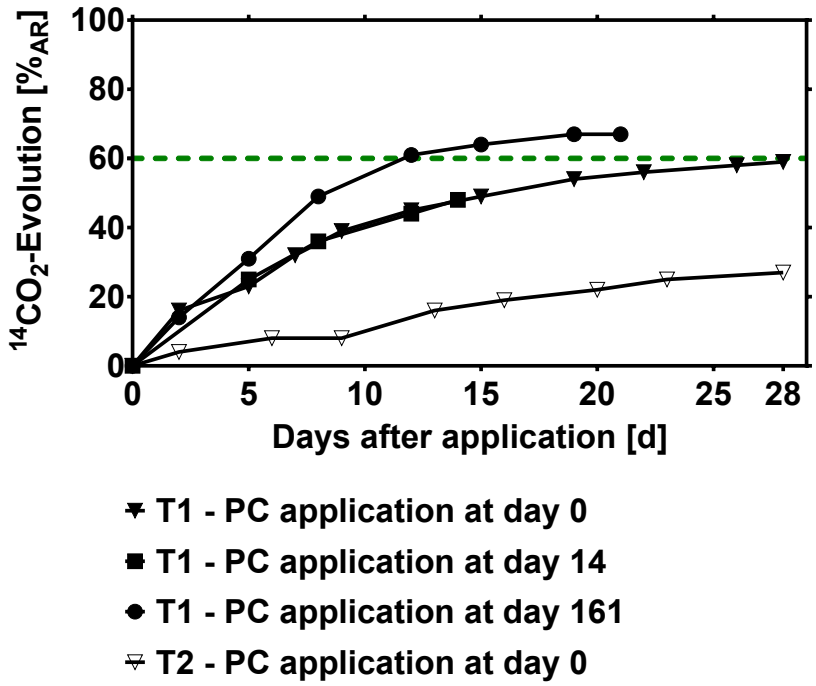

Figure 12. Biodegradation performance of the process controls (PC) within the two OECD TG 301B tests testing the bulk PUA$_{mod}$ suspension (T1) and the separated size fractions of the PUA$_{mod}$ suspension (T2). Displayed is the cummulative amount of evolved $^{14}CO_2$ in percentage of AR (%$_{AR}$) relative to the incubation time (days after application [d]), *n*=1). The green dotted line indicates the 60% threshold for ready biodegradation, which must be reached within a 10-day window to meet the validity criteria of the OECD 301B test. Reproduced from the SI of Teggers et al., (2025a).

In the first biodegradation test (T1, acc. to OECD TG 301B), the toxicity control, which reflects the combined mineralization of sodium benzoate and of the bulk CS and reached 83.6%$_{AR}$ (*n* = 1; Figure 13) at 28 d. Within the abiotic control, where the bacteriostatic substance sodium azide was applied to the CS sample, 13.3%$_{AR}$ (*n*=1) $^{14}CO_2$ evolved over the duration of 28 d with a lag phase of 17 d (Figure 13).

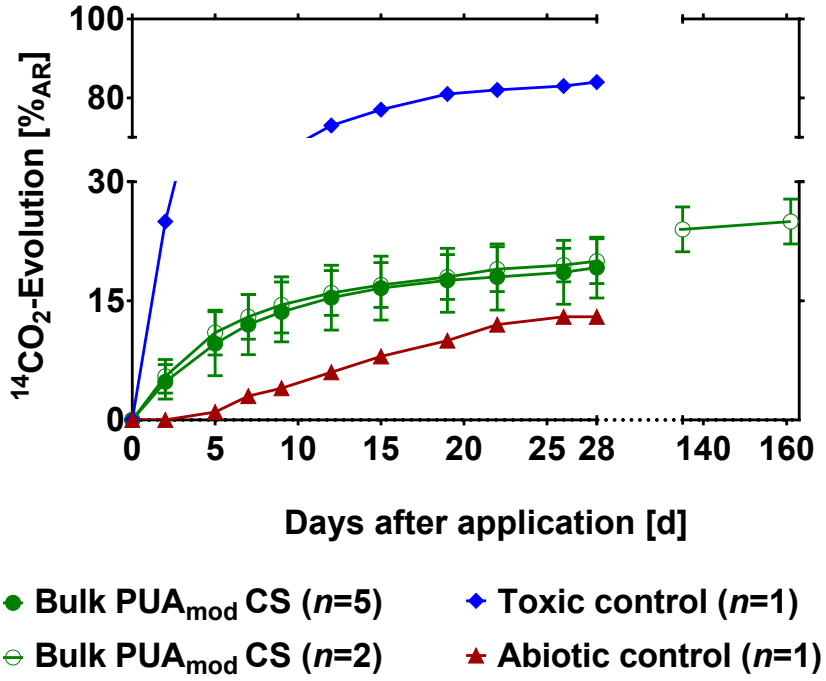

Figure 13. Biodegradation test results of the fist OECD TG 301B (T1) assessing the bulk PUA_{mod} capsule suspension (bulk PUA_{mod} CS). $^{14}CO_2$-Evolution of the bulk PUA_{mod} CS, the abiotic control (applied with sodium azide) and the toxicity control (sodium benzoate application supplemented to bulk PUA_{mod} CS). Plotted is the cumulative portion of applied radioactivity (AR) mineralized to $^{14}CO_2$ relative to the incubation time (average and SD). Reproduced from Teggers et al., (2025a).

After 28 d of incubation in the first biodegradation test (T1) examining the bulk PUA_{mod} CS 19.1 ± 3.96 %$_{AR}$ (average and stdev of *n*=5) evolved in form of $^{14}CO_2$ (Figure 13). The presence of dissolved $^{14}CO_2$ in form of carbonic acid ($H_2{}^{14}CO_3$) was neglectable, as no additional $^{14}CO_2$ was detected upon acidification with HCl in the two additional test samples (overall 23.0 ± 1.22 %$_{AR}$, *n*=2). The two samples with the bulk PUA_{mod} CS that were incubated for 161 d reached in total 25.0 ± 2.29 %$_{AR}$ (mean of *n*=2, stdev as range).

3.1.1 Sequential Filtration Integrated into the First Biodegradation Test (T1)

In the first biodegradation test (T1, based on OECD TG 301B) a sequential filtration experiment was integrated. At the start of the test (0 d), the majority of AR from the bulk PUA_{mod} CS was distributed predominantly between two size fractions (Figure 14). On the 12 µm filter 54.9 ± 3.64%$_{AR}$ were retained, while 49.7 ± 1.67%$_{AR}$ were detected in the filtrate (<0.2 µm). In contrast, a negligible amount of 2.93 ± 1.26%$_{AR}$ was found in the intermediate size fraction captured in sum on the 0.2 µm, 0.45 µm and 5 µm filters. This pattern is in line with the results of a laser diffraction analysis revealing a median size of the bulk suspension of 16.5 µm and 65.3%$_{particle\text{-}volume\text{-}based}$ being above 12 µm (measured size range 0.01 to 5.75 µm; Appendix - Table A2, Table A 3, Figure A1).

From 0 to 28 d, the AR in the smallest size fraction (filtrate, <0.2 µm) decreased by 18.4%$_{AR}$ resulting in a total remaining activity of 31.3 ± 2.64%$_{AR}$, while 19.1%$_{AR}$ $^{14}CO_2$ was formed as shown in subchapter 2.2.3 "Biodegradation of the Bulk PUAmod " (Figure 14). The AR in the intermediate fraction between 0.2 to 12 µm was reduced to a total of 1.58 ± 0.28 %$_{AR}$ (Figure 14). In addition, the AR of the largest fraction (>12 µm) of the samples decreased from day 0 to day 28 by 12.4 %$_{AR}$ (total of 42.5 ± 4.22 %$_{AR}$ at day 28, Figure 14).

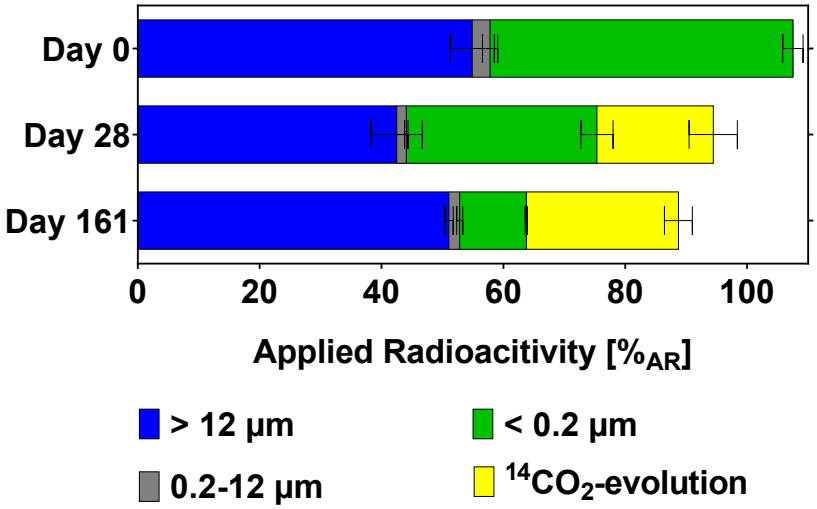

Figure 14. Results of the sequential filtration integrated in the first biodegradation test (T1), which was performed based on OECD TG 301B. Distribution of applied radioactivity (AR) across different filter pore sizes and in the filtrate following sequential filtration of test samples at day 0, day 28 (*n*=5), and day 161 (*n*=2). AR retained on the 12 µm filter is displayed as"> 12 µm" and "0.2 to 12 µm" represent the sum of the AR found on the three pore sized filters (0.2 µm, 0.45 µm and 5 µm). AR in the filtrate is displayed as "< 0.2 µm". Results are presented as average ± SD or range. Reproduced from Teggers et al., (2025a).

After 161 d of incubation, the smallest size fraction (filtrate <0.2 µm) was decreased by 38.8%$_{AR}$ compared to the test start (0 d) reaching a final amount of 10.9 ± 0.18 %$_{AR}$ as determined by the sequential filtration (Figure 14). The largest size fraction, retained by the 12 µm filter was increased by 8.57%$_{AR}$ from 28 d to 161 d, reaching a total of 51.1 ± 0.69%$_{AR}$, while the intermediate fraction (0.2-12 µm) remained at similar levels with 1.77 ± 0.49%$_{AR}$. The amount of evolved $^{14}CO_2$ reached in total 25.0 ± 2.29 %$_{AR.}$ (from day 0 to day 161, see subchapter 2.2.3 "Biodegradation of the Bulk PUAmod "). The recovery of the sequential filtration from 161 d (*n*=2) resulted in 88.7%$_{AR.}$

3.1.2 Biodegradation of the Different Size Fractions of the PUA$_{mod}$ Bulk CS (T2)

To investigate whether the only source of mineralization was from lower size fractions, the bulk PUA$_{mod}$ CS was submitted to a second biodegradation test (T2) performed similar to OECD TG 301B. For this, the bulk PUA$_{mod}$ CS was separated into two size fractions and tested separately (<12 µm and >12 µm) and compared to the mineralization amount of the bulk PUA$_{mod}$ CS. In this approach, the amount of

evolved $^{14}CO_2$ of the bulk PUA_{mod} CS was similar that from the smaller fraction (<12 µm filtrate). The deviation between the two was by a factor of 1.1, with $^{14}CO_2$-evolution of 7.77 ± 1.63 kBq for the bulk suspension *vs* 6.92 ± 1.28 kBq for the <12 µm filtrate (Figure 15). In contrast, no mineralization to $^{14}CO_2$ was observed for the size fraction of >12 µm (0.08 ± 0.02 kBq).

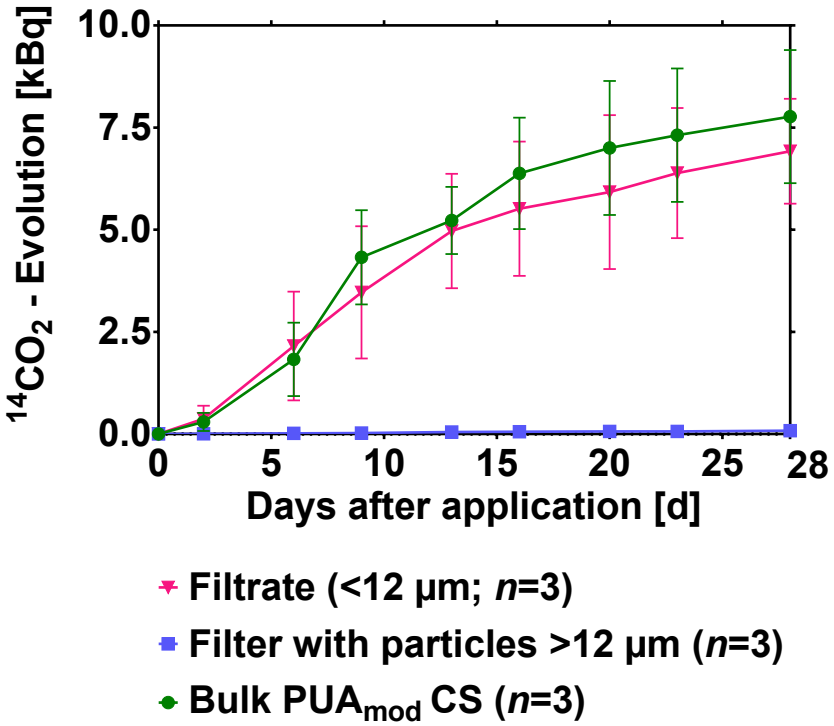

Figure 15. Biodegradation test results of the second OECD TG 301B (T2). $^{14}CO_2$-evolution of the Bulk CS and its separated size fractions: mineralization from filter with particles >12 µm and from the filtrate with compounds <12 µm. Plotted is the cumulative radioactivity (kBq) that was mineralized to $^{14}CO_2$ relative to the incubation time (average and stdev of *n*=3). Reproduced from Teggers et al., (2025a).

3.1.3 Ultra-High Performance Liquid Chromatography with High Resolution Mass Spectrometry (UHPLC-HRMS)

To identify ^{14}C components of the smallest particle size fraction (<0.2 µm) of the bulk CS a UHPLC-HRMS analysis (total mass range of 100-6000 m/z) coupled with a radio detector (Appendix Table A5, Table A6 and Table A7) was employed. Labeled and non-labeled aminocaproic acid (m/z range of 132.10125-132.1057; Figure 16) was detected by the HRMS analysis, based on the determined molecular formula using the Xcalibur Qual Browser (Version 4.0).

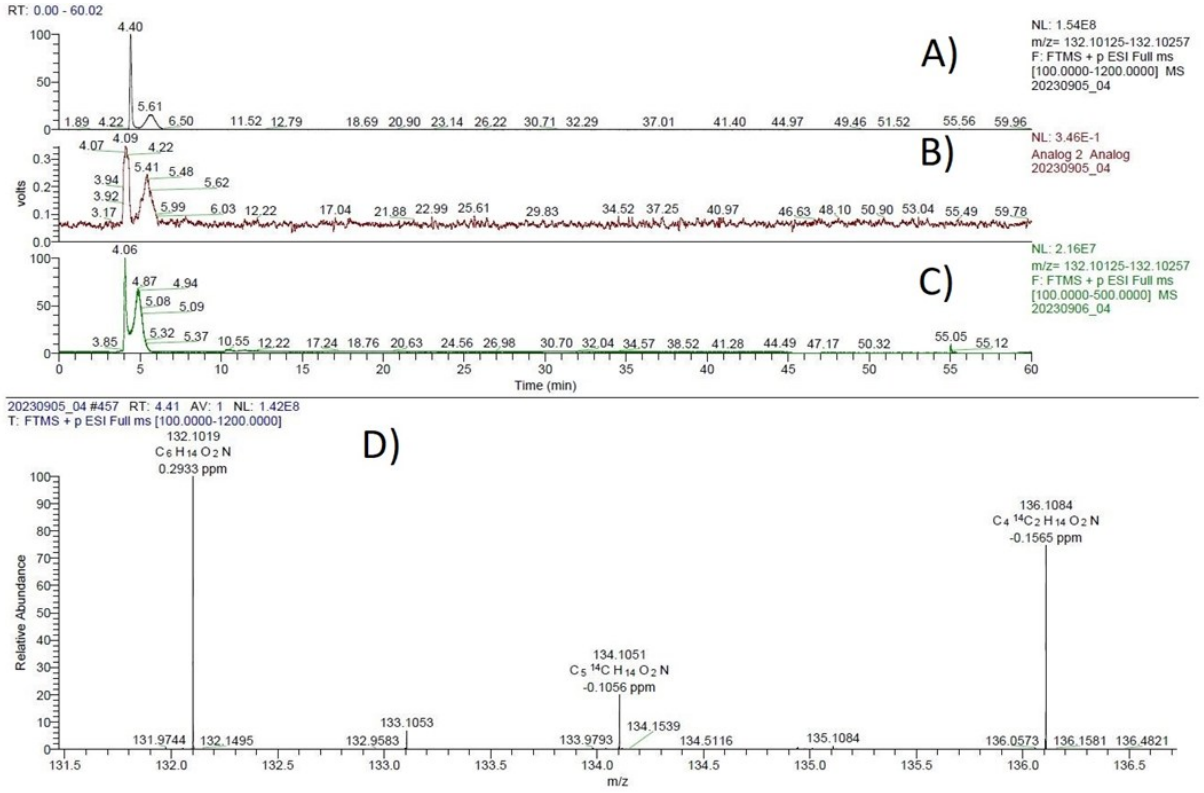

Figure 16. High-Resolution Mass Spectrometry (HRMS) analysis of the PUA_{mod} capsule suspension (CS) (<0.2 µm filtrate). A) Extracted mass chromatogram of aminocaproic acid (m/z 132.10125–132.1057) from the sample (100 µL); B) Corresponding radio detection signal; C) Extracted mass chromatogram of the aminocaproic acid reference standard (50 µL; Sigma-Aldrich, CAS No. 60-32-2); D) Isotopic pattern trace showing the relative abundance of non-labeled, ^{14}C-labeled and $^{14}C_2$-labeled aminocaproic acid in the PUA_{mod} CS filtrate. Reproduced from the SI of Teggers et al., (2025a).

To confirm the identification, a reference analysis was conducted using pure aminocaproic acid (≥99%, 10 ng/mL; Sigma-Aldrich Chemie GmbH, Germany), with results shown in Figure 16. Radiodetection of the eluate showed a primary peak of radioactivity aligning with the retention time of eluted aminocaproic acid (Figure 16). Additionally, column recovery analysis enabled quantification of the radioactivity eluting within the same retention time window as aminocaproic acid. The results showed that 83.3 ± 2.29% (average of n = 3; Figure 17) of the injected radioactivity was recovered between 3.5 and 7 minutes, matching the retention time of aminocaproic acid.

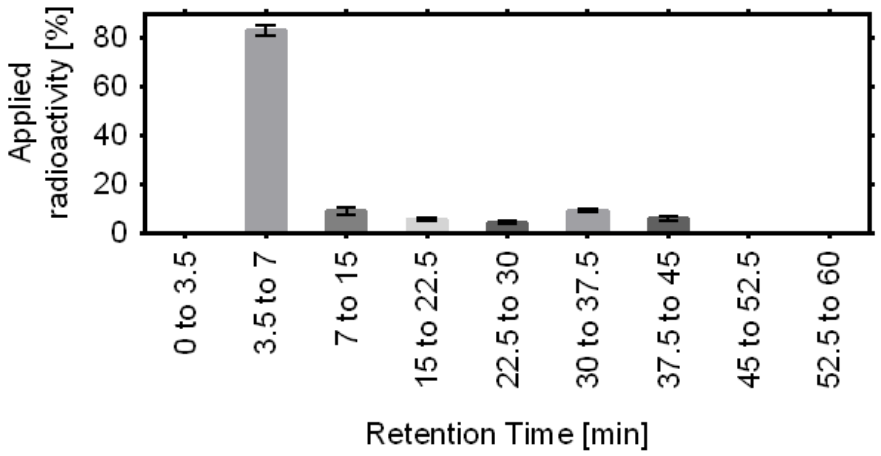

Figure 17. Ultra-high performance liquid chromatography (UHPLC) column recovery of the <0.2 µm filtrate from the bulk PUA_{mod} capsule suspension (CS).
Eluate fractions were collected across defined retention time intervals (0 to 3.5 min; 3.5 to 7 min; 7 to 15 min; from 15 to 60 minutes in 7.5 min intervals). The radioactivity in each fraction was measured via LSC. Data represent means of $n = 3$, with an average total recovery of 119 ± 2.8% of the injected radioactivity. Reproduced from the SI of Teggers et al., (2025a).

Isotopic pattern analysis was used to extract all molecules or oligomers sharing the same (^{12}C-, ^{14}C-, and $^{14}C_2$-)isotopic pattern as the identified aminocaproic acid into a chromatogram (Figure 18), where only two consecutive peaks corresponding to the RT of aminocaproic acid were observed.

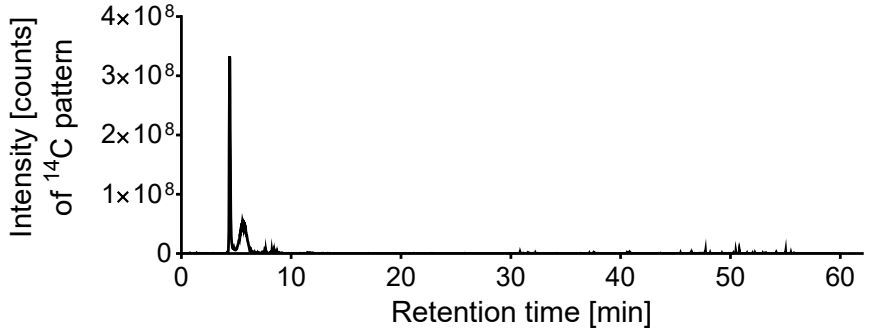

Figure 18. Isotopic pattern analysis of the PUA_{mod} capsule suspension (CS) filtrate (<0.2 µm) using UHPLC-HRMS analysis. The identified labeled aminocaproic acid was analyzed based on its specific isotopic mass shifts (^{12}C with 0.0000 m/z, ^{14}C with +2.00322 m/z and $^{14}C_2$ with +4.00652 m/z, not exceeding a deviation of 5 ppm) and its specific isotopic intensity pattern (^{12}C with 100%, ^{14}C with 18.90% and $^{14}C_2$ with 70.74% intensity, not exceeding 20% deviation) (Figure 16, D). Extracted chromatogram plotted as intensity counts against the retention time. Reproduced from the SI of Teggers et al., (2025a).

3.2 Part 2 – The Influence of Simulated Sunlight on the Biodegradation of Persistent Microplastics

3.2.1 Simulated Sunlight Irradiation

Table 4 summarizes the amount of evolved $^{14}CO_2$, the average irradiation temperature, the total recovery of the different irradiation methods (MI and M2) and the days of irradiation applying 75W/m^2 within the 300–400 nm wavelength range. Detailed temperature data, including average and maximum values as well as temperature profiles during irradiation, are provided in the Appendix (Figure A5, Figure A6, Figure A7, Figure A8, Figure A9).

While the temperature of the aqueous irradiation of PUA_{mod} within procedure MI-P1 and MI-P3 remained stable at 32.4 ± 1.60 °C, the aqueous irradiation of MI-P2 (PUA_{mod}) exhibited lower temperatures at 3.99 ± 0.77 °C and the evolution of $^{14}CO_2$ reached a maximum of 3.81 ± 1.53 $\%_{AR}$, with a total recovery of 92.2 ± 1.20 $\%_{AR}$. In comparison, the total recovered radioactivity of procedure MI-P1 and MI-P3 was lower with 73.4 ± 1.38$\%_{AR}$ but the evolution of $^{14}CO_2$ was not repeatedly determined. During the aqueous irradiation of LLDPE, a malfunction of the cooling system resulted in elevated temperatures with an average temperature of 53.0 °C ± 1.3 °C for 6.8 d out of 13.9 d of the exposure period and an overall average temperature of 43.8 ± 10.3 °C (max. temperature of 62.0 °C; Figure A9).

Table 4. Overview of the different irradiation procedures under 75 W/m² irradiation intensity within the 300–400 nm wavelength range. Shown are the average irradiation temperature, the irradiation time, the mineralization to $^{14}CO_2$ during irradiation and the total recovery for mass balancing both in the percentage of applied radioactivity [$\%_{AR}$] Details of the irradiation intensity and duration are shown in Table 1.

Irradiation Procedure	Average irradiation temperature [°C]		Mineralization to $^{14}CO_2$ [$\%_{AR}$]	Total recovery [$\%_{AR}$]	
	Dark	Irradiation	Irradiation	Dark	Irradiation
Procedures 1 and 3					
PUA_{mod}		32.4 ± 1.60			73.4 ± 1.38
LLDPE		43.8 ± 10.3			54.1 ± 12.5
Procedure 2					
PUA_{mod}	20.8 ± 1.66	3.99 ± 0.77	3.81 ± 1.53	85.1 ± 4.36	92.2 ± 1.20
Procedure 4					
PUA_{mod}	78.0 ± 1.13	70.5 ± 1.86	11.3 ± 4.63	107 ± 9.51	100
PUA			7.83 ± 8.88	104 ± 11.2	94.7
LLDPE	77.3 ± 0.77	69.3 ± 3.39	0.31 ± 0.22	52.4 ± 21.7	36.9

Unlike the aqueous irradiation of PU_{mod}, the exposure of the polymer microcapsules on the soil surfaces resulted in a higher detected mineralization to $^{14}CO_2$. More precisely, the mineralization of PUA_{mod} reached 14.6 $\%_{AR}$ and 8.02$\%_{AR}$ for replicate 1 and 2, respectively, while PUA reached 14.11 $\%_{AR}$ and 1.55$\%_{AR}$ for replicate 1 and 2, respectively. No additional ^{14}C-labeled alkaline or organic volatiles were detected in the H_2SO_4 or ethylene glycol traps. The total recovered radioactivity of both PUA and PUA_{mod} microcapsules applied to soil surfaces that were kept in the drying cabinet to serve as a temperature and dark control was high at 107 ± 9.51 $\%_{AR}$ PUA_{mod} and 104 ± 11.2 $\%_{AR}$ PUA. In contrast to the microcapsules, no $^{14}CO_2$ or other volatiles were detected during the irradiation of LLDPE on soil surfaces. The total recovery for irradiated LLDPE samples was low, amounting to 36.9 $\%_{AR}$, while in the dark controls 52.4 ± 21.7 $\%_{AR}$ was recovered. The temperature of the dark controls was generally maintained at approximately 6 to 7.5°C higher than for the irradiated samples (see Table 4).

3.2.2 Alterations of Size Distribution and Release of ^{14}C-Compounds

Irradiated and non-irradiated PUA_{mod} and LLDPE suspensions were sequentially filtrated through two different pore-sized filters (0.2 and 12 µm) for an approximate size distribution analysis, similarly as performed in the previous chapter (see subchapter 2.2.4). Figure 19 provides an overview of the results. Non-irradiated PUA_{mod} microcapsules predominantly remained on the 12 µm filter, accounting for

85.3 ± 5.84 $\%_{AR}$ and only minor fractions (0.75 ± 0.44 $\%_{AR}$) were found on the 0.2 µm filter or in the filtrate (<0.2 µm with 0.48 ± 0.25 $\%_{AR}$) yielding a total recovery of 86.5 ± 5.36 $\%_{AR}$. In contrast, upon exposure to simulated sunlight, most of the PUA_{mod} passed both filters (12 µm and 0.2 µm). Thus, while only 0.89 ± 0.69 $\%_{AR}$ and 0.59 ± 0.06 $\%_{AR}$ was retained on the 12 µm and the 0.2 µm filter, respectively, 102 ± 2.43 $\%_{AR}$ was recovered in the filtrate. The total recovery of the irradiated samples amounted to 106 ± 2.38 $\%_{AR}$.

Compared to sequential filtration results of the PUA_{mod} the overall recovered radioactivity of the irradiated and non-irradiated LLDPE samples was low (53.5 ± 8.36 $\%_{AR}$ and 57.6 ± 24.1 $\%_{AR}$, respectively, see Figure 19) and higher variations in the detected amounts of AR were observed. However, most of the recovered radioactivity of the non-irradiated LLDPE suspension was retained on the 12 µm filter amounting to 55.1 ± 24.07 $\%_{AR}$. Only minor fractions were detected on the 0.2 µm filter (1.52 ± 0.31 $\%_{AR}$) and in the filtrate (<0.2 µm) with 0.94 ± 0.97 $\%_{AR}$. After light exposure, the amount of radioactivity retained on the 12 µm filter decreased to 28.2 ± 7.13 $\%_{AR}$, while the retention on the 0.2 µm filter and the amount of AR in the filtrate increased to 4.79 ± 2.79 $\%_{AR}$ and 20.5 ± 1.97 $\%_{AR}$, respectively.

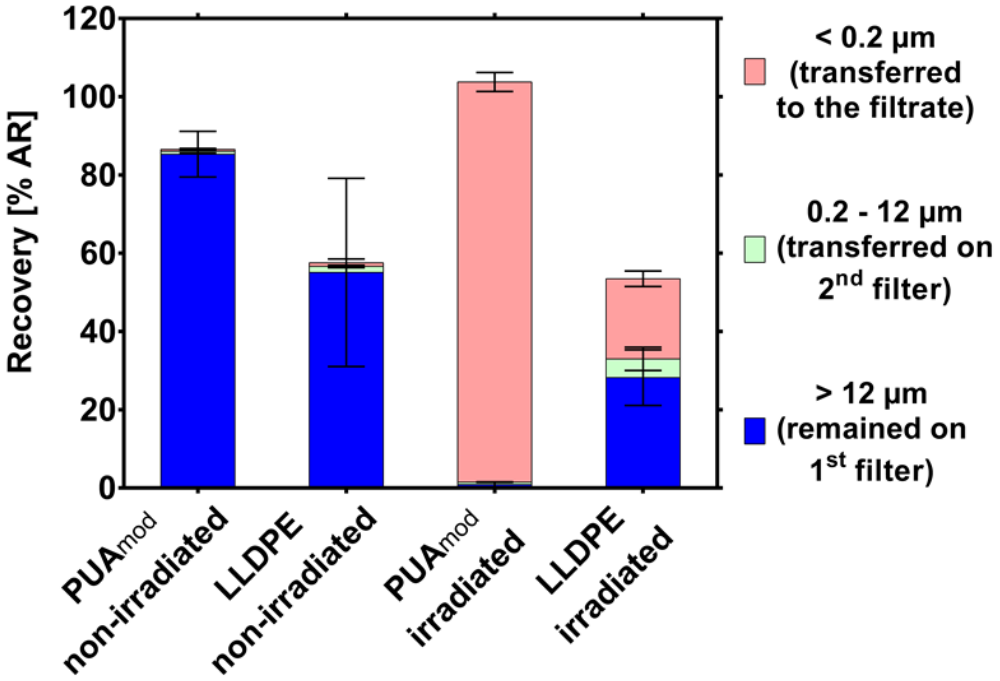

Figure 19. Proportion of applied radioactivity (AR) recovered in the different fractions obtained by sequential filtration. Displayed are the $\%_{AR}$ of the irradiated and non-irradiated PUA_{mod} and LLDPE suspensions, which was quantified on the first (12 µm pore size) and the second filter (0.2 µm) and in the filtrate (< 0.2 µm).

The irradiated filtrate (<0.2 µm) of PUA_{mod} was further analyzed by UHPLC-HRMS analysis coupled with radio detection, following the same methodology as described in chapter 2.2.6 and in the respective

publication by Teggers et al. (2025). In this analysis, radio detection showed one major broad peak, which eluted at a RT of 4.0-7.5 min (Figure 20).

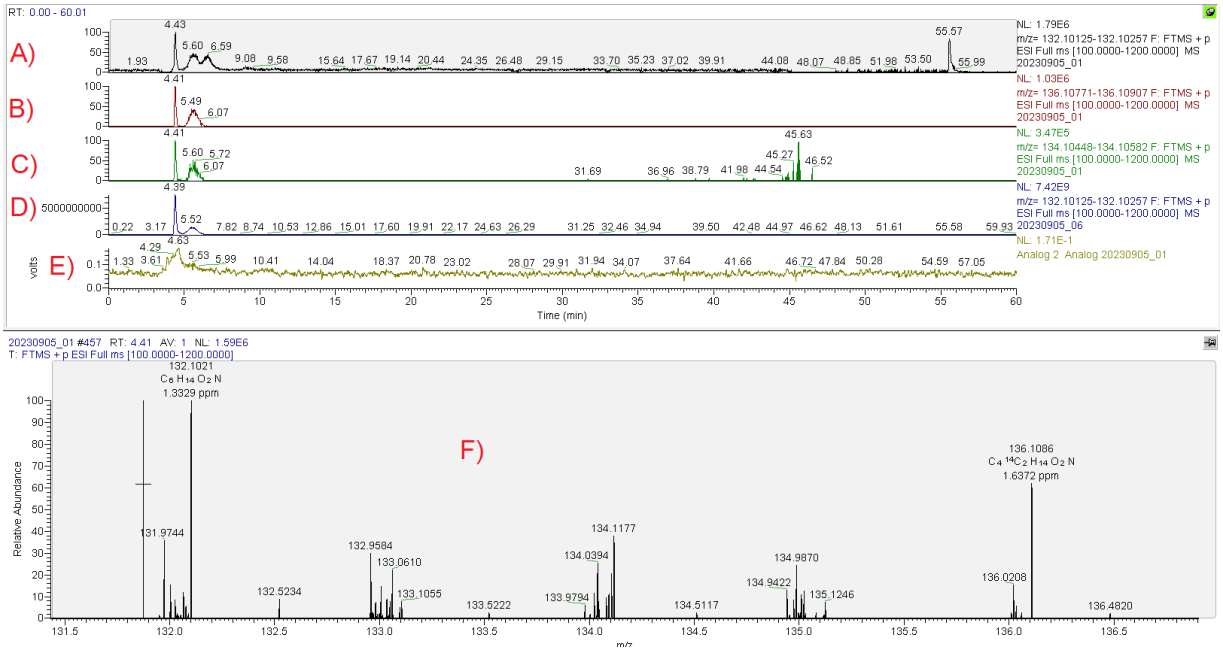

Figure 20. Ultra-High Performance Liquid Chromatography - High-Resolution Mass Spectrometry (HRMS) analysis for the investigation of the irradiated PUA_{mod} filtrate (<0.2µm). The extracted mass chromatogram of non-labeled (A) m/z range of 132.10125-132.1057), $^{14}C2$-labeled (B) m/z range of 136.10771-136.10907) and ^{14}C-labeled (C) m/z range of 134.10448-134.10582) aminocaproic acid of the irradiated PUA_{mod} microcapsule suspension (filtrate <0.2 µm; 100 µL), D) extracted mass chromatogram of aminocaproic acid (m/z range of 132.10125-132.1057, reference substance; 50 µL), E) the radio detection signal of the irradiated PUA_{mod} microcapsule suspension (filtrate <0.2 µm; 100 µL; A, B, C) is displayed. F) shows the relative abundance of non-labeled (^{14}C-labeled too low to be displayed) and $^{14}C2$-labeled aminocaproic acid of the irradiated PUA_{mod} microcapsule suspension (<0.2 µm) is represented (isotopic pattern trace of 12C with 100 %, ^{14}C with 18.90 % and $^{14}C2$ with 70.74 % relative intensity).

Within this peak (m/z range of 132.10125-132.1057) labeled and non-labeled aminocaproic acid were identified (Figure 20; A), B), C)) with a mass accuracy of 1.64 ppm for $^{14}C2$-labeled, 1.49 ppm for ^{14}C-labeled and 1.33 ppm for non-labeled aminocaproic acid. This outcome was additionally confirmed by analyzing and comparing pure (≥99 %, 10 ng/mL, Sigma-Aldrich Chemie GmbH, Germany) aminocaproic acid as reference compound with the obtained profiles (Figure 20, D)). However, in contrast to the radiodetection analysis, two consecutive peaks appeared in the extracted ion chromatogram (Figure 20). For robust validation of the identification, a mixture of the irradiated suspension filtrate and the aminocaproic acid reference was analyzed and resulted in identical retention times and matching MS spectra (Figure 21). Additionally, the isotopic pattern indicated a higher relative intensity of non-labeled aminocaproic acid (isotopic pattern trace of ^{12}C with 100 %, ^{14}C with 18.90 % and $^{14}C2$ with 70.74 % relative intensity, Figure 21, E)) compared to the ^{14}C- and $^{14}C2$-labeled forms (isotopic pattern trace with ^{12}C with 100 %, ^{14}C with 0.42 % and $^{14}C_2$ with 0.63 % relative intensity, Figure 20, F)).

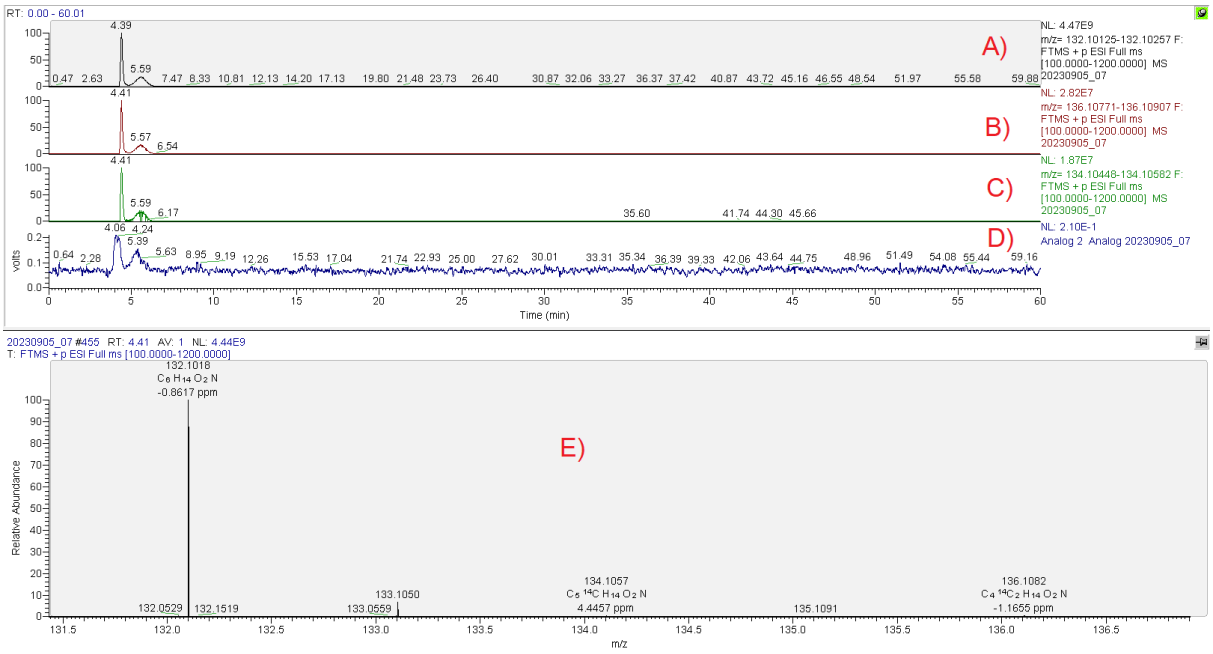

Figure 21. Ultra-High Performance Liquid Chromatography - High-Resolution Mass Spectrometry (HRMS) analysis for distinctive identification of aminocaproic acid in the filtrate (<0.2µm) of the irradiated PUA_{mod} with the addition of the reference compound aminocaproic acid.
The extracted mass chromatogram of non-labeled (A), $^{14}C_2$-labeled (B) and ^{14}C-labeled (C) aminocaproic acid of the mixture (filtrate <0.2 µm plus aminocaproic acid reference; 100 µL). D) displays the radio detection signal. E) shows the relative abundance of non-labeled (^{14}C-labeled and $^{14}C_2$-labeled too low to be displayed).

Within the isotopic pattern analysis, all molecules or oligomers comprising the isotopic pattern of the identified aminocaproic acid were extracted and visualized in a chromatogram. The corresponding molecules and oligomers eluted mostly within the respective RT window of aminocaproic acid but also at the end of the separation starting at a RT of 42 min (Figure 22).

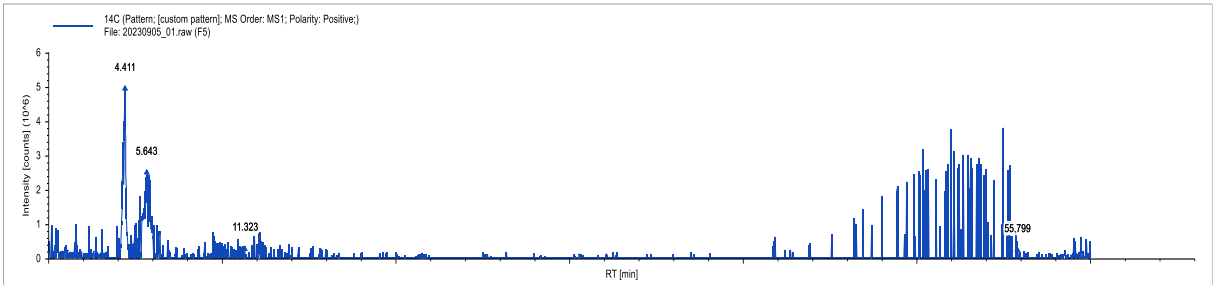

Figure 22. Isotopic pattern analysis of the irradiated PUA_{mod} microcapsule suspension (filtrate <0.2 µm; 100 µL) of the radio-UHPLC-HRMS analysis. Isotopic pattern (see Figure 20 – F)) of labeled aminocaproic acid with its specific mass shift of carbon isotopes (non-labeled 12C with 0.0000 m/z, 14C-labeled with 2.00322 m/z and $^{14}C2$-labeled aminocaproic acid with 4.00652 m/z, not exceeding a deviation of 5 ppm) and its specific intensity pattern (12C with 100 %, ^{14}C with 18.90 % and $^{14}C2$ with 70.74 % relative intensity, not exceeding 20 % deviation), quantified and plotted as intensity counts (y-axis: “Intensity [counts] (10^6)”) against the retention time (x-axis: “RT [min]). Bottom: radio detection signal of the analysis (y-axis: “Intensity [counts]”).

The results of the column recovery (see Figure 23) separating the irradiated PUA_{mod} suspension’s filtrate of <0.2 µm by UHPLC revealed that 48.5 ± 1.16 $\%_{AR}$ of the injected radioactivity eluted within the time frame of 4 to 7.5 min RT with a total recovery of 93.2 ± 1.93 $\%_{AR}$ of the analysis (n=3).

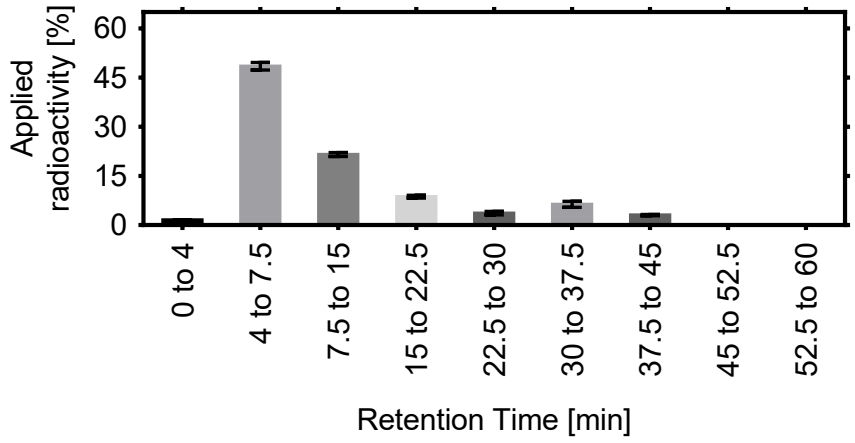

Figure 23.Results of the column recovery separating the irradiated capsule suspension's filtrate of <0.2 µm with the UHPLC. Eluates were collected for the following retention time intervals: 0 to 4 min; 4 to 7 min; 7.5 to 15 min and from 15 to 60 minutes in 7.5 min intervals. The radioactivity of the eluates was quantified by LSC. Means of *n*=3.

3.2.3 Biodegradation after Simulated Sunlight Exposure

Following MI-P2 (Figure 8; Table 2), the screening biodegradation test in aqueous medium (OECD TG 301B), performed after the irradiation of the PUA_{mod} suspension in water (similar to OECD TG 316), resulted in a biodegradation of 28.0 ± 4.05 $\%_{AR}$. In contrast, the preceding Part 1 of this thesis presented in chapter 3.1.2, based on Teggers et al. (2025), demonstrated that in the absence of simulated sunlight exposure, PUA_{mod} did not undergo biodegradation to $^{14}CO_2$ under the same experimental setup (OECD TG 301B, Figure 15).

In MI-P3 (Figure 8; Table 2), the PUA_{mod} suspension was first irradiated in an aqueous environment and then subjected to a biodegradation test in soil. This biodegradation test resulted in substantial $^{14}CO_2$ evolution, amounting to 63.2 ± 13.4 $\%_{AR}$ in RefeSol 01-A and 62.3 ± 9.65 $\%_{AR}$ in RefeSol 03-G within a short incubation time of 72 hours (Figure 24).

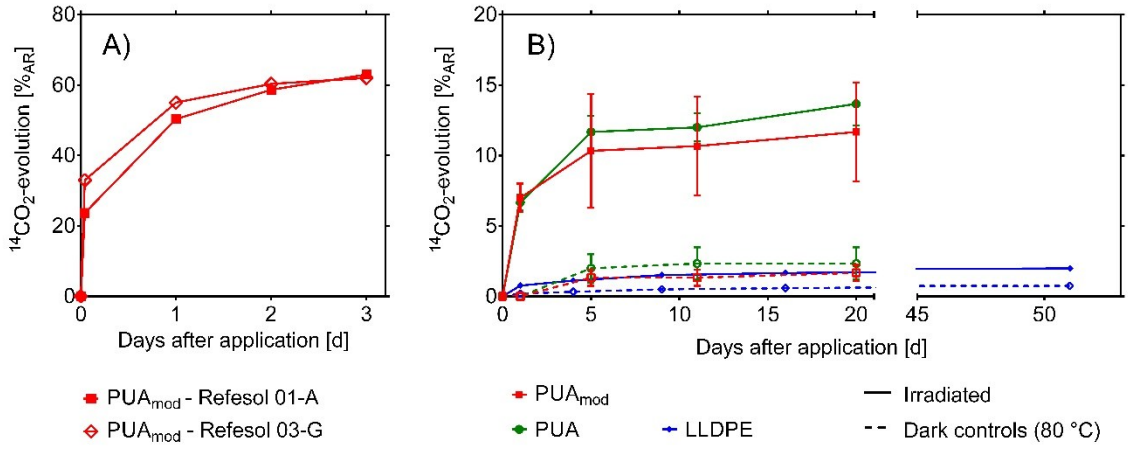

Figure 24. Biodegradation in soil following OECD TG 307. A) Biodegradation of irradiated PUA$_{mod}$ microcapsules in soil (Refesol 01-A and Refesol 03-G) after irradiation in the aqueous setting (MI-P3). B) Biodegradation of PUA microcapsules with/without ester-bond modification (PUA vs. PUA$_{mod}$) and LLDPE MPs in soil (Refesol 01-A) after simulated sunlight irradiation or in dark controls incubated at 80°C on soil surfaces (MII-Procedure 4). The biodegradation is plotted as the cumulative portion of applied radioactivity (AR) mineralized to $^{14}CO_2$ relative to the incubation time (average and SD of n=3).

In contrast, in procedure MII-P4 (Figure 8; Table 2) PUA and PUA$_{mod}$ microcapsules were irradiated directly on the soil surface (OECD draft TG) followed by a biodegradation test in soil according to OECD TG 307. Table 5 shows the amounts of mineralization regarding the biodegradation test of MII-P4. Performing this procedure, PUA and PUA$_{mod}$ showed similar degrees of mineralization (P=0.8 irradiated; P=0.6 non-irradiated, test of significance by an unpaired, non-parametric Mann-Whitney test; significant difference indicated by P<0.05). However, irradiation on the soil surface resulted in substantially lower $^{14}CO_2$ evolution within the biodegradation test, reaching 13.6 ± 1.44 %$_{AR}$ for PUA and 11.8 ± 3.64 %$_{AR}$ for PUA$_{mod}$ over a 20-day incubation period, compared to biodegradation of the aqueous irradiated samples. The dark controls, which were incubated at 80°C resulted in neglectable amounts of mineralization with 2.52 ± 0.96 %$_{AR}$ for PUA and 1.52 ± 0.29 %$_{AR}$ for PUA$_{mod}$. This result aligns with the results from the non-irradiated PUA$_{mod}$ samples in the OECD TG 301B aqueous biodegradation test, which also showed minimal mineralization.

Table 5. Mineralization and recovery of the biodegradation test in soil (OECD TG 307). Test of significance using an unpaired, non-parametric Mann-Whitney test to compare irradiated vs. non-irradiated materials.

MP Material	**Mineralization Dark controls**	**Mineralization Irradiated**	**Days of incubation**	**Significance of difference:** irradiated *vs*. non-irradiated	**Recovery Dark controls**	**Recovery Irradiated**
	[$\%_{AR}$]	[$\%_{AR}$]	[d]	P	[$\%_{AR}$]	[$\%_{AR}$]
PUA_{mod}	1.52 ± 0.29	11.8 ± 3.64	20	0.10	83.0 ± 8.12	82.0 ± 6.46
PUA	2.52 ± 0.96	13.6 ± 1.44	20	0.10	122 ± 20.8	109 ± 2.74
LLDPE	0.75 ± 0.14	1.99 ± 0.18	51	0.10	107 ± 37.5	84.0 ± 10.8

* Test of significance by an unpaired, non-parametric Mann-Whitney test; significant difference indicated by $P<0.05$.

With respect to the LLDPE MP particles, a slight increase in the biodegradation was observed compared to the non-irradiated dark control samples (1.99 ± 0.18 $\%_{AR}$ vs. 0.75 ± 0.14 $\%_{AR}$, respectively, Table 5). Recovery in the soil biodegradation tests exceeded 80%$_{AR}$ for all tested samples. However, greater variability was observed in some LLDPE dark control samples (see Table 3), with elevated standard deviations. Overall, the differences in mineralization between irradiated and non-irradiated samples following procedure MII-P4 were not statistically significant. Nevertheless, there was a trend ($P = 0.10$) toward increased mineralization following irradiation for PUA, PUA_{mod}, and LLDPE.

3.3 Part 3 – Extraction of Pristine and Weathered Microplastics from Soil Using a Modified Oil-Based Method

3.3.1 Extraction Efficiencies of the Different Extraction Experiments

The efficiency of the modified oil extraction method using octanol (Extraction Experiment I) was compared to the density-based extraction method (Extraction Experiment II), as summarized in Table 3. An overview of the results with the total recoveries including the extracted fractions and the total remaining radioactivity in the soil, as well as the extraction efficiencies across all experiments, is presented in Table 6.

The most efficient extraction of the pristine ^{14}C-PUA$_{mod}$ was achieved by applying extraction experiment I, which integrates a first extraction step using KOH followed by the oil extraction using octanol. This method led to efficiencies between 70.4 ± 5.1%$_{AR}$ from RefeSol 03-G and 74.6 ± 1.3%$_{AR}$ from RefeSol 01-A. The density extraction using $ZnCl_2$ (extraction experiment (II)), resulted in 10 to 15%$_{AR}$ lower extraction efficiencies than those of extraction experiment (I) (59.8 ± 2.6%$_{AR}$ RefeSol 01-A; 62.0 ± 4.9%$_{AR}$ RefeSol 03-G, Table 6). Regarding pristine ^{14}C-PUA, most of the AR was extracted in the KOH fraction, with extraction efficiencies of 50.3 ± 2.2%$_{AR}$ from RefeSol 01-A and 53.6 ± 3.7%$_{AR}$ from RefeSol 03-G in experiments (I) and (II), respectively (*n*=6).

Table 6. Overview of the total extraction recoveries (referring to the total applied radioactivity (AR)) and extraction efficiencies (excluding the AR recovered from the soil) of all performed extraction experiments (I-III), given in percentage of AR. Table reproduced from Teggers et al. (2025b).

Extraction Experiment	**Spiked MPs**		**Reference Soil**	**Total extraction recovery**		**Extraction efficiency**	
	Pristine	Light-exposed		AR Mean [%] (*n*=3)	AR SD [%] (*n*=3)	AR Mean [%] (*n*=3)	AR SD [%] (*n*=3)
Modified oil extraction using octanol (I)	PUA	no	01-A	84.6	4.92	74.6	1.33
	PUA	no	03-G	84.2	8.13	70.5	5.09
	LLDPE	no	01-A	50.6	9.61	50.3	9.49
	LLDPE	no	03-G	114	31.7	114	31.4
	PUA	yes	01-A	51.7*	9.23*	50.5*	9.09*
	PUA	yes	03-G	47.0	0.41	44.2	0.55
	LLDPE	yes	01-A	55.1	17.6	53.3	15.5
	LLDPE	yes	03-G	76.4	30.1	76.1	30.0
Density extraction using $ZnCl_2$ (II)	PUA	no	01-A	89.8	4.16	59.9	2.61
	PUA	no	03-G	88.1	6.17	62.0	4.89
Repeated first extraction step using KOH (III)	PUA	no	03-G	82.3	2.75	55.6	4.20

SD standard deviation; *(n=2, due to a high deviation of the first replicate)

When the KOH extraction was repeated, the total extraction efficiencies were 55.6 ± 4.2%$_{AR}$ (RefeSol 03-G, Table 6, Figure 26 (III)). Preliminary testing indicated that exposure to KOH solution (pH 14) for up to five days did not visibly alter the microcapsules, as assessed by light microscopy (Figure 25).

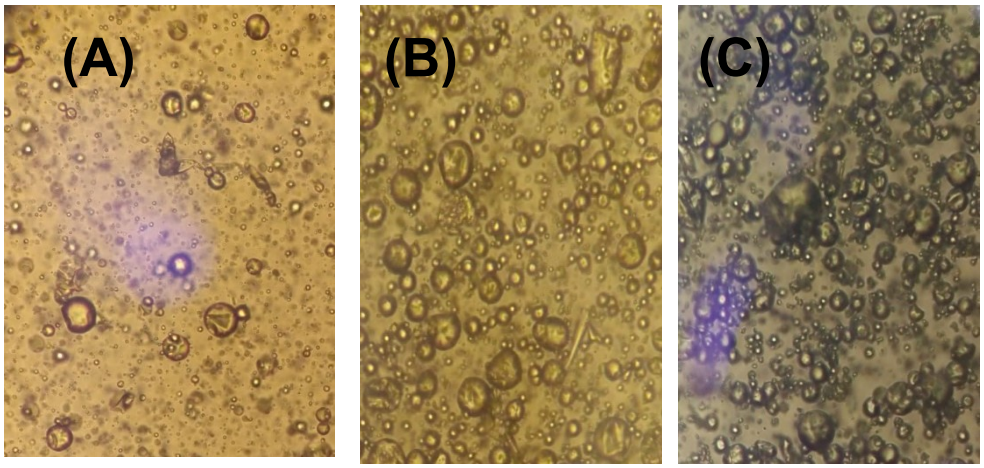

Figure 25. Microscopic image of the polyurea capsules (roundish shapes which look similar as bubbles. Some microcapsules were always found to be deformed) in (A) water and in KOH (pH 14) after (B) one hour and (C) after five days of incubation.

By introducing a second extraction step, using octanol (experiment I) or $ZnCl_2$ (experiment II), an additional fraction of the remaining ^{14}C-PUA$_{mod}$ was mobilized. This led to an improvement in total extraction efficiency by up to 14.9%$_{AR}$ when octanol was applied (comparison of I vs. III, RefeSol 03-G; Table 6), relative to experiment III which included a repeated first extraction step. Interestingly, even when the first extraction step was skipped, the octanol method alone recovered a comparable fraction of pristine PUA microcapsules, ranging from 19.0%$_{AR}$ (RefeSol 01-A) to 23%$_{AR}$ (RefeSol 03-G) (Appendix - Table A9, Octanol, "Modified oil extraction using octanol (I) w/o Step 1"). The density-based extraction in experiment II provided a maximum additional extraction efficiency of 6.4%$_{AR}$ recovered from soil compared to the repeated first extraction step (II vs. III, Table 6, RefeSol 03-G).

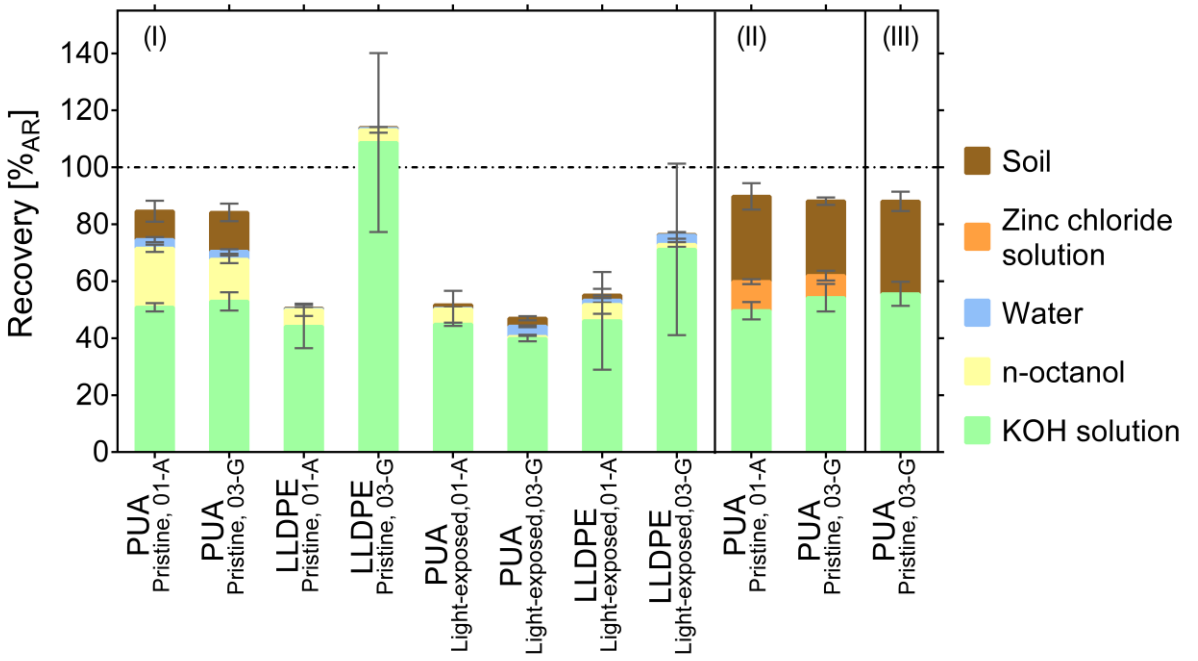

Figure 26. Recoveries of applied radioactivity (%AR) from various extraction experiments (I, II, III; see Table 3). Performance with spiked pristine or light-exposed ^{14}C-labeled PUA$_{mod}$ microcapsules and ^{14}C-labeled LLDPE microparticles (LLDPE) on two reference soils: RefeSol 01-A and 03-G. Means of n=3 with SD; except for the pristine PUA on RefeSol 01-A, means of n=2 with SD. Reproduced from Teggers et al. (2025b).

Substantial losses in balancing the recovered amount of AR were observed, particularly for light-exposed ^{14}C-PUA$_{mod}$ and both, pristine and light-exposed, ^{14}C-LLDPE MPs (see subchapter 3.3.3 "Impact of Sunlight Irradiation on the Extraction Efficiency" for results of light-exposed MP).

The applied amount of ^{14}C-LLDPE showed high variations (4.66 ± 1.96 kBq/mL) leading to substantial variations of AR across all replicates. For the total recoveries regarding ^{14}C-LLDPE were between 50.6 ± 9.6%$_{AR}$ (RefeSol 01-A) and 114 ± 31.6%$_{AR}$ (RefeSol 03-G) with overall higher deviations. Only 0.3 ± 0.2%$_{AR}$ (RefeSol 01-A, RefeSol 03 G) remained unextracted in soil (Figure 26 (I)) regarding the pristine ^{14}C-LLDPE.

Similar to the ^{14}C-PUA, the majority of ^{14}C-LLDPE were recovered with the first extraction step using KOH, with 44.1 ± 7.6%$_{AR}$ extracted from RefeSol 01-A and 109 ± 31.4%$_{AR}$ from RefeSol 03-G. In contrast, only a small additional fraction was recovered during the second extraction step with octanol.

3.3.2 Impact of Soil Types on the Extraction Efficiency

Across all performed extraction experiments, no distinct differences in the extraction efficiency were observed between the two soil types.

3.3.3 Impact of Sunlight Irradiation on the Extraction Efficiency

For the light-exposed ^{14}C-PUA microcapsules, total recoveries were generally relatively low, with 51.7 ± 9.2%$_{AR}$ for RefeSol 01-A and 47.0 ± 0.4%$_{AR}$ for RefeSol 03-G. By performing a biodegradation test in soil following the OECD TG 307 in Part 2 of this thesis (subchapter 3.2.3) we could show that 23.2 ± 7.3%$_{AR}$ (RefeSol 01-A) to 33.1 ± 2.1%$_{AR}$ (RefeSol 03 G) of the applied radioactivity were mineralized to $^{14}CO_2$ within the first hour. After the first extraction experiment, only 1.2 ± 0.0% to 2.8 ± 0.7% of the AR remained in the soil (RefeSol 01-A and RefeSol 03-G respectively).

As observed with the pristine material, the majority of the recovered radioactivity from light-exposed ^{14}C-PUA was extracted during the first extraction step using KOH, with recoveries of 44.9 ± 0.6%$_{AR}$ for RefeSol 01-A and 39.9 ± 1.0%$_{AR}$ for RefeSol 03-G (Figure 26 (I)). A small fraction was subsequently extracted by octanol from RefeSol 03-G, amounting to 0.7 ± 0.6%$_{AR}$ (n=3).

A notable variation in recovery was observed across the three replicates of RefeSol 01-A. In the first replicate, 37.5%$_{AR}$ of ^{14}C-PUA were recovered in the octanol phase, whereas replicates two and three showed substantially lower values (9.9%$_{AR}$ and 0.8%$_{AR}$, respectively). This discrepancy was also reflected in the total recoveries, with replicate one reaching 87.2%$_{AR}$, in contrast to 58.2%$_{AR}$ and 45.2%$_{AR}$ for the other two replicates. Due to this inconsistency, replicate one was excluded from the visualization in Figure 26 (I) as well as from the data presented in Table 6 and Appendix - Table A8 and - Table A9.

Compared to the pristine ^{14}C-PUA microcapsules, less radioactivity was found in the octanol phase (pristine ^{14}C-PUA in octanol: RefeSol 01-A: 20.7 ± 1.3%$_{AR}$; RefeSol 03-G: 14.8 ± 1.3%$_{AR}$; light-exposed ^{14}C-PUA in octanol: RefeSol 01-A: 5.3 ± 6.5%$_{AR}$; RefeSol 03-G: 0.7 ± 0.6%$_{AR}$); this also applied for the normalized TRR values (given in the percentage of the total recovered radioactivity, Appendix – Table A8, for better comparison regarding the highly deviating recoveries).

As with the pristine LLDPE, the light-exposed LLDPE was almost completely extracted from the soil, as shown by the low levels of residual radioactivity detected in soil (Figure 26 (I), Appendix – Table A8, - Table A9). The overall extraction efficiency was similar between the pristine and irradiated particles, ranging from 53.3 ± 15.5%$_{AR}$ in RefeSol 01-A to 76.1 ± 30.0%$_{AR}$ in RefeSol 03-G.

3.3.4 pH Dependence of Microplastic Extraction Efficiency

The separate investigation on the influence of the pH of the extraction solution regarding its extraction efficiency showed that by increasing the pH of the aqueous solution from 3 to 14, the extraction of ^{14}C-PUA was progressively increased, with maximum removal observed at pH 14 (Figure 27).

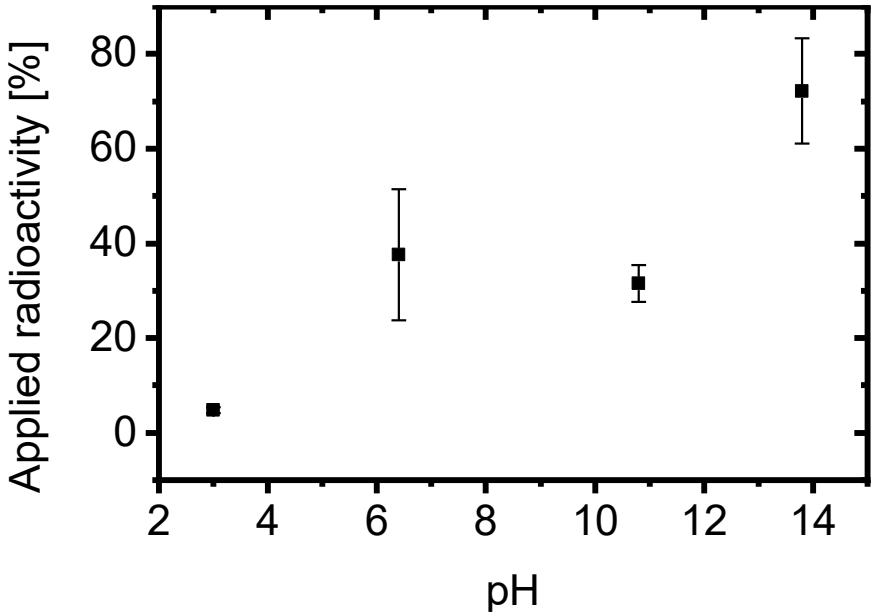

Figure 27. Proportion of the applied radioactivity (AR) recovered by four extraction solutions comprising different pHs. Results of the pH-correlation test extracting ^{14}C-PUA$_{mod}$ microcapsules with the following solutions: Hydrochloric acid (HCl) at pH = 3, UHQ water at pH = 6, and two NaOH solutions at pH = 11 and pH = 14. Means of n=3 with SD.

Additionally, the extract visibly darkened as the pH increased (Figure 28). In this pH correlation test using NaOH, extraction efficiencies were found to be comparable to those obtained with KOH, yielding 72.2 ± 11.2%$_{AR}$ (NaOH) and 63.0 ± 2.25%$_{AR}$ (KOH), respectively (RefeSol 03-G).

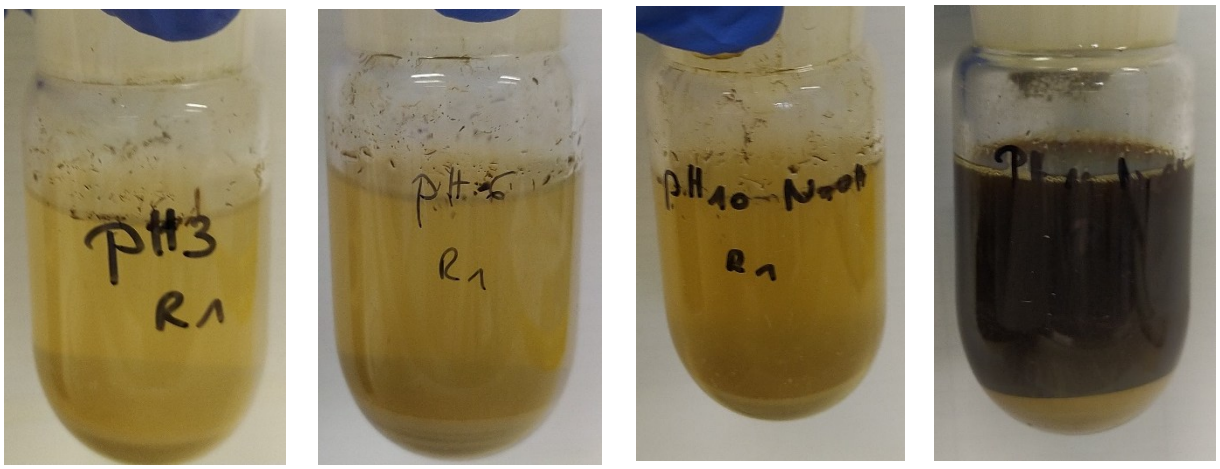

Figure 28. Turbidity of the different extraction solutions comprising different pHs. From left to right: Supernatant after the first extraction step using hydrochloric acid (HCl) at pH = 3, UHQ water at pH = 6, and two NaOH solutions at pH = 11 and pH = 14. Display of replicate one as a representative of n=3.

4 Discussion

4.1 Part 1 – Broadening the Framework in Biodegradation Testing of Microplastics

4.1.1 Biodegradation of Bulk PUA_{mod} CS (T1)

Objective of this work was first to assess mineralization to $^{14}CO_2$ as an endpoint for MP biodegradation, and second to implement additional MP-specific analyses into the OECD TG 301B screening biodegradation test. Analytical methods such as pyrolysis gas chromatography–mass spectrometry (Py-GC-MS), gel permeation chromatography (GPC), or field-flow fractionation (FFF) would have been conceivable at the start of this project. To be able to undertake such analyses, it is preferable to reduce environmental matrix effects. Therefore, as an initial approach, the standard inoculum of the screening biodegradation test OECD TG 301B containing activated sludge suspended solids was aimed to be replaced by a particle-free inoculum, the filtered activated sludge supernatant, to minimize the influence of matrix components and enhance compatibility with a wider range of analytical methods. For this replacement, the capability to mineralize sodium benzoate as reference compound for biodegradation was compared in an OECD TG 301F test. The result of this test proved that both filtered supernatant and the standard inoculum had a similar performance in the mineralization of sodium benzoate, with the filtered supernatant achieving a 3.9% higher ThOD after 2 days. Even though the filtered supernatant mineralized with a short lag phase, both inoculums reached the same level of mineralization, with over 60 % after 2 d (Figure 11). Thus, the filtered supernatant was classified as suitable for the OECD TG 301 tests and used in all following OECD TG 301 tests.

Regarding the mineralization performance of the PCs within biodegradation tests (T1 and T2), none would have been considered valid from a regulatory perspective, since they either failed to reach >60% mineralization in the time frame of 10 d or in case of the PCs to which sodium benzoate was applied on 161 d, the mineralization of >60% was not reached within 10 d window. However, even though the validity pass criterium of the OECD TG 301B was missed, the process controls, which serve to assess microbial activity using a reference substance, generally proved that the microbiome was sufficiently active during the whole incubation time to demonstrate biodegradation. It should be noted that the primary aim of these tests was not to confirm regulatory validity or absolute biodegradation rates, but rather to evaluate analytical methods, compare different incubation conditions (e.g. irradiated vs. non-irradiated), and test different types of MPs under standardized conditions.

The results of the toxicity control (used to assess possible toxicity of the CS to the microbial inoculum by combining it with a reference substance) showed the highest mineralization, both of the bulk PUA_{mod} CS and sodium benzoate, indicating that the CS itself exhibited neither toxic nor inhibitory effects.

In the abiotic control, the bacteriostatic substance sodium azide was added to the bulk PUA_{mod} CS. Sodium azide was selected due to its bacteriostatic properties, as it is known to effectively inhibit microbial respiration and enzymatic activity, presumably without altering the chemical structure of MP or interfering $^{14}CO_2$ measurements, since it primarily inhibits microorganism growth (Birch et al., 2022). Contrary to expectations, a mineralization of 13.3%$_{AR}$ was detected after 28 d of incubation. Since sodium azide is a bacteriostatic, rather than bactericidal agent (Blaschko, 1935), a partial recovery of the microbial activity, beginning around 5-7 d is conceivable. A similar delayed reactivation was also observed in a study by Süßmuth et al. (2024) on soil samples and is further supported by findings from Blaschko (1935), who demonstrated the reversible nature of sodium azide inhibition. Additionally, Hendrix et al. (2019) showed that sodium azide can interact with dissolved organic matter (DOM) in environmental samples, potentially reducing the inhibitor's effective concentration and thereby diminishing its inhibitory potential over time. Given that the filtered sewage sludge supernatant used in this test presumably contains a high level of DOM (Meng et al., 2009), such interactions may have occurred.

Considering the biodegradation results of the bulk PUA_{mod} CS, a relatively high degree of mineralization was reached, with approx. 40% of the pass criterion for biodegradability (>60% mineralization in the OECD TG 301B). Since PUA is a rigid and chemically stable material (see also section "Radioactive labeling and capsule suspension synthesis"), this result deviated from the initial assumption that only low levels of biodegradation would occur. Initially, it was hypothesized that the observed mineralization resulted from structural modifications to the polymer, specifically the incorporation of additional ester bonds to enhance biodegradability given that hydrolysis of ester bonds is a fundamental mechanism in polymer biodegradation (Singh and Sharma, 2008; Tokiwa et al., 2009). However, as it will be discussed in subchapter "4.1.4 Ultra-High Performance Liquid Chromatography with High Resolution Mass Spectrometry (UHPLC-HRMS)", this assumption was proved to be incorrect, and rather the ^{14}C-component aminocaproic acid was primary mineralized.

4.1.2 Sequential Filtration Integrated into the First Biodegradation Test (T1)

The sequential filtration procedure integrated into the first biodegradation test (T1), provided additional insights into the biodegradation of the bulk PUA_{mod} CS (Figure 14) by approximating its size distribution at the beginning (0 d) of the test and throughout the incubation period of the OECD TG 301 biodegradation test (28 d and 161 d).

As shown in subchapter 2.2.3 ("Biodegradation of the Bulk PUAmod "), 19.1 %$_{AR}$ of $^{14}CO_2$ evolved over 28 d from the bulk PUA_{mod} CS (Figure 13). The radioactivity released from the test sample through mineralization is inherently linked to the loss of radioactivity from one of the size fractions within the test sample. Thus, the 18.4%$_{AR}$ decrease in the smallest size fraction (<0.2 µm) is presumably associated with mineralization to $^{14}CO_2$, which also applies to the period up to 161 d of incubation. This deduction

is supported not only by the close match in the decreased amount of AR, but also by the fact that the bioavailability of plastics or MPs increases with decreasing particle or molecular size, which is discussed in the following subchapter 4.1.3.

In this context, the observed decrease in the largest size fraction from day 0 to day 28 raised the question of whether the largest particles, presumably microcapsules, were partially degraded into smaller fragments, molecules, or even fully mineralized. Alternatively, the reduction in the largest fraction could be attributed to imprecision in the filtration method. This question was addressed by the second biodegradation test (T2, see discussion subchapter 4.1.3 “3.1.2Biodegradation of the Different Size Fractions of the PUA_{mod} Bulk CS (T2)”).

The missing radioactivity in the smallest size fraction may be also attributed to a loss of $^{14}CO_2$ due to leakage from the used biodegradation setup. However, considering the extended biodegradation period and the complexity of the sequential filtration process, an overall recovery of 88.7%$_{AR}$ after 161 days is still considered high. Alternatively, it is possible that some of the radioactivity was adsorbed onto larger agglomerates, which is supported by the results of the largest size fraction, with an increase by 8.57 %$_{AR}$ from day 28 to day 161. Microorganisms in the test medium may have assimilated a portion of the ^{14}C-compounds, such as the identified ^{14}C-aminocaproic acid, from the smallest size fraction. These microorganisms, both living and dead, could have formed microbial aggregates or biofilms, potentially exceeding 12 µm in size. As a result, these aggregates may have adsorbed ^{14}C-activity and been retained by the 12 µm filter along with the microcapsules, potentially explaining the observed approx. 8%$_{AR}$ increase in the >12 µm size fraction after 161 days of incubation. Supporting this hypothesis, an increasing amount of flocculent material was visually observed in the sample vessels (Figure 28). Further investigations, such as analyzing the filter residue or microbial aggregates for ^{14}C-labeled lipids, proteins, or nucleic acids, which are clearly distinguishable from ^{14}C-labeled microcapsules >12 µm, could be valuable in future biodegradation studies. In this context, approaches similar to those reported by Weng et al. (2023) and Zumstein et al. (2018) may be useful for characterizing ^{14}C-assimilation by microbial cells, as also recommended by Zumstein et al. (2019) for plastic biodegradation assessments.

The proportion of AR in the size fraction between 0.2 and 12 µm remained relatively stable over the total incubation time, indicating that no relevant fragments emerged in that size range.

4.1.3 Biodegradation of the Different Size Fractions of the PUA_{mod} Bulk CS (T2)

The PUA_{mod} CS was subjected to a second OECD 301B biodegradation test (Figure 15). Due to the decrease in radioactivity in the >12 µm fraction from day 0 to 28 d of the sequential filtration (subchapter 3.1.1), the objective was to investigate whether particles larger than 12 µm were directly mineralized or whether the observed mineralization exclusively originated from smaller size fractions.

In this test, the bulk PUA_{mod} CS was mineralized to a similar degree as the <12 µm fraction of the filtrate, while no mineralization was observed for the >12 µm size fraction. This indicates that $^{14}CO_2$ evolution primarily originated from particles, monomers, and oligomers smaller than 0.2 µm, rather than from the larger PUA_{mod} microcapsules.

4.1.4 Ultra-High Performance Liquid Chromatography with High Resolution Mass Spectrometry (UHPLC-HRMS)

The sequential filtration results revealed that a larger fraction of AR was already present in the smallest size fraction at the start of the test. This finding led to the assumption that residual ^{14}C-molecules or ^{14}C-oligomers from synthesis present in the PUA_{mod} CS, causing the relatively high mineralization, as discussed in subchapters (4.1.2, 4.1.3).

To investigate the composition of the PUA_{mod} CS's filtrate (<0.2 µm) UHPLC-HRMS analysis coupled with a radiodetector was employed. This approach enabled the identification of both labeled and non-labeled aminocaproic acid, as confirmed by two characteristic peaks in the HRMS and radiodetector signal (RT 2.5–4 min; Figure 16). The presence of two peaks was attributed to aminocaproic acid existing in both ionized (more polar, eluting faster) and uncharged (less polar, adhering longer to the column) forms. Identification was further substantiated by UHPLC-HRMS analysis of a pure aminocaproic acid reference standard, as well as by column recovery analysis, which showed that the majority of injected radioactivity (83.3 ± 2.29%) co-eluted with the aminocaproic acid peaks. Notably, aminocaproic acid represents the oxidized derivative of the ^{14}C-labeled monomer ^{14}C-hexamethylenediamine used in the synthesis, distinguished by the presence of a carboxyl group.

In a subsequent step, isotopic pattern analysis was employed to identify other molecules or oligomers containing aminocaproic acid as a structural building block. Using this approach, all compounds with the same isotopic pattern as the previously identified aminocaproic acid were extracted in a chromatogram (Figure 18). This chromatogram displayed only the two previously observed consecutive peaks, which can be attributed to aminocaproic acid.

Taken together, the analyses strongly indicate that aminocaproic acid constituted a major proportion of the <0.2 µm filtrate from the PUA_{mod} suspension. This proportion of injected radioactivity (83.3 ± 2.3%) attributed to aminocaproic acid in the column recovery analysis was extrapolated to the total radioactivity of the bulk suspension. By multiplying this fraction with the relative share of radioactivity detected in the filtrate (<0.2 µm; 49.7 ± 1.67%$_{AR}$), it was estimated that approximately 41%$_{AR}$ of aminocaproic acid was present in the bulk PUA_{mod} CS. Consequently, we argue that the majority of the observed mineralization originated from the biodegradation of aminocaproic acid. Supporting this assumption, aminocaproic acid is classified as readily biodegradable, achieving 76% mineralization within 28 days according to its safety data sheet (OECD TG 301D). However, it is important to note

that the synthesized polymer shell consists not only of labeled HMDA but also includes co-polymerized isocyanates and other crosslinked, undefined structural components. Since only one monomer was radiolabeled, the resulting data and mineralization trends primarily reflect the fate of compounds containing this specific monomer. The degradation behavior and fate of non-labeled components within the polymer matrix were not addressed in the scope of this study.

Moreover, recent research has demonstrated that the biodegradation of MPs is influenced by particle size, with smaller MPs degrading more efficiently. This is primarily attributed to their larger surface area-to-volume ratio, which facilitates greater microbial colonization and enzymatic interaction (Chinaglia et al., 2018; ECETOC, 2020; García-Depraect et al., 2022; McDonough et al., 2017; Zhao et al., 2016). These insights highlight the importance of incorporating particle size analysis alongside mineralization measurements in biodegradability evaluations.

4.2 Part 2 – The Influence of Simulated Sunlight on the Biodegradation of Persistent Microplastics

4.2.1 Simulated Sunlight Irradiation

With respect to the temperatures within the aqueous irradiation procedures of PUA_{mod}, discrepancies in the detected average temperature were observed with MI-P2 exhibiting temperatures approximately 28°C higher than the temperatures in MI-P1 and -P3, where the temperature remained around 4°C. This variation is likely attributable to the differences in temperature sensor placement, which in MI-P1 and -P3 (Figure 8; Table 2) was positioned centrally and near the upper region of the vial, whereas in MI-P2, it may have been in contact with the vial wall or base. A photograph of the sensor setup is provided in Figure 9-D). Alternatively, if the discrepancy was not solely due to sensor positioning, the elevated temperatures in MI-P2 could have enabled increased $^{14}CO_2$ evolution. This assumption is supported by approximately $20\%_{AR}$ lower total recovered radioactivity of MI-P1 and -P3 compared to MI-P2 which may suggest increased mineralization to $^{14}CO_2$. However, as the flow-through system for trapping volatiles was not employed in MI-P1 and -P3, this interpretation remains speculative. The elevated temperature observed during the aqueous irradiation of LLDPE (MI-P3) was not considered substantial since LLDPE is considered thermally stable up to approx. 220°C in the presence of oxygen (Aniśko et al., 2023).

Regarding the irradiation of PUA_{mod} and PUA on soil surfaces, higher amounts of trapped$^{14}CO_2$ were detected. However, substantial deviations between replicates suggest that leakage in the flow-through system may have occurred. Since the soil layer was dried prior to simulated sunlight exposure, the formation of $^{14}CO_2$ is likely attributed to abiotic photooxidation rather than microbial catabolism. This assumption is supported by the complete total recovered radioactivity of the dark controls, indicating that no radiolabeled volatile compounds evolved without the influence of simulated sunlight. Bhargava

et al. (2015) have analyzed chemical changes of polyurethane-based coatings using attenuated total reflectance-Fourier transform infrared (ATR–FTIR) spectroscopy upon UV-light exposure at 0.7522 W/m^2/nm (with peak irradiance at 313 nm) over intervals of 200 h up to 1000 h. Similarly, Che et al. (2019) analyzed PUA coatings in marine atmosphere exposed to sunlight after 150 d of exposure using ATR-FTIR. Both studies detected notable reductions in absorbance peaks associated with urea (C–N), carbonyl (C=O), and ester (C–O–C) bonds, which can be associated with chain scission and cleavage of the mentioned bonds.

Considering our results, it is plausible that similar bond cleavages contributed to the release of $^{14}CO_2$. However, the introduction of additional ester bonds in the modified polyurethane (PUA_{mod}) compared to the unmodified PUA (see subchapter 2.1.1 “Microcapsule Suspension”) did not significantly affect the fraction mineralized to $^{14}CO_2$. Furthermore, results from the dark controls, which were incubated at elevated temperatures, exclude heat-induced degradation as a primary factor, as no loss of radioactivity due to volatilization was observed. The temperatures of the dark controls were maintained slightly higher than the highest observed temperature during irradiation.

4.2.2 Alterations of Size Distribution and Release of ^{14}C-Compounds

Sequential filtration analysis following MI-P1 (Figure 8; Table 2) demonstrated substantial changes in the size distribution of the PUA_{mod} suspension upon simulated sunlight exposure. Given that most of the AR was found in the filtrate, it can be derived that the microcapsules were almost completely disintegrated to sizes <0.2 µm. The potential photo-oxidation reactions discussed above (see subchapter 4.2.1), which may have contributed to release $^{14}CO_2$ from the PUA_{mod}, also likely caused chain scission and structural cleavage within the PUA_{mod} matrix leading to its disintegration. It should be considered that irradiating PUA_{mod} in an aqueous medium (MI, Figure 8) results in a larger exposed surface area compared to the irradiation on soil, where the microcapsules may aggregate or adhere to soil particles, thereby becoming partially shielded from light. Furthermore, the shell thickness of the PUA_{mod} microcapsules potentially influences the effect of light on the degradation. Du et al., (2022) reported shell thickness ranging from 0.4 to 2.5 µm for slightly larger microcapsules (approximately 79 µm) using Scanning Electron Microscopy (SEM). While the shell thickness generally correlates with capsule size, it also depends on the number of monomers and their ratios used during synthesis. In the context of this study, it can be assumed that a larger proportion of PUA_{mod} polymers was exposed and penetrated by simulated sunlight compared to the mono-constituent LLDPE polymeric particles. The results of the sequential filtration demonstrated that the irradiated LLDPE particles were partially disintegrated to smaller ^{14}C-particles or ^{14}C-compounds and a higher AR was detected in the filtrate compared to the non-irradiated suspension. Grause et al. (2020) investigated the transformation of polyolefins when subjected to UV irradiation in the presence of oxygen. Although polymers like polyethylene (PE) are known for their transparency and light-transmitting properties, they usually contain minor amounts of

chromophore groups, such as carbonyls or unsaturated bonds, that can form during manufacturing or thermal oxidation, e.g., during processing stages (Allen, 1986; Bracco et al., 2018; La Mantia, 1986; Rajakumar et al., 2009; Schnabel, 1981). These groups can initiate photodegradation reactions. In the case of LLDPE, the early formation of hydroperoxides is a key factor to induce degradation, potentially generating LMW compounds like carboxylic acids, alcohols, and, to a lesser extent esters (Gulmine et al., 2003; Tidjani, 2000). With regard to this study, the release of such ^{14}C-labeled LMW degradation products may explain the elevated radioactivity detected in the <0.2 µm filtrate of the irradiated suspension. According to Andrady et al. 2022, oxidative degradation in LLDPE is typically limited to a superficial layer of about 600 µm. In our study, the LLDPE particles had a median diameter of 147 µm (SI table S8), thus, the irradiation likely penetrated the particles fully, inducing fragmentation. This interpretation is supported by Pfohl et al. 2025, who observed increased fragmentation of LDPE under UV exposure in the presence of water. Additionally, since irradiation in an aqueous environment penetration from all directions is possible, the effective path lengths to the particle core may only be half the diameter.

The filtrate of the irradiated PUA_{mod} suspension was additionally examined using UHPLC-HRMS analysis coupled to radio detection to identify ^{14}C-labeled oligomers or ^{14}C-labeled molecules derived from the polymer as a result of simulated sunlight exposure. In this, the identification of both ^{14}C-labeled and non-labeled aminocaproic acid can be considered unequivocal, as it was supported by several lines of evidence: a distinct radio signal at 4.0–7.5 min RT, accurate mass detection in the HRMS within the expected m/z range for aminocaproic acid, isotopic pattern analysis consistent with the presence of labeled and non-labeled forms, and full alignment of retention time and spectral features with the reference compound, which was injected individually and in a co-injection experiment with the irradiated filtrate. Furthermore, the results of the column recovery analysis indicate that a substantial proportion of the ^{14}C-labeled molecules or oligomers introduced to this analysis can likely be attributed to the elution of ^{14}C-aminocaproic acid.

Presumably, the polyurea bonds within the PUA_{mod} shell underwent partial cleavage due to the action of reactive species formed during photo-oxidation, such as hydroxyl radicals (•OH) and superoxide anions (O_2•$^-$). The oxidative conditions appear to have contributed to the oxidation of HMDA into aminocaproic acid. Similar oxidative degradation mechanisms have been reported by Si et al. (2021), who demonstrated radical-induced deamination of primary amine groups (-NH_2).

4.2.1 Biodegradation after Simulated Sunlight Exposure

The observed partial biodegradation of approx. 28%$_{AR}$ of the irradiated PUA_{mod} suspension in the aqueous screening test (OECD TG 301B), performing procedure MI-P2 (Figure 8; Table 2), can to some extent be attributed to the mineralization of released readily biodegradable ^{14}C-labeled aminocaproic acid.

In contrast to the biodegradation observed in the aqueous screening test, the subsequent biodegradation test in soil (OECD TG 307) based on procedure MI-P3 (Figure 8; Table 2), demonstrated a substantially higher extent of mineralization within a short incubation time of 3 d on two types of reference soils (RefeSol 01-A and 03-G). This result is particularly remarkable, since biodegradation in soil, following OECD TG 307 as a simulation test, is typically slower than in the aqueous screening test (OECD TG 301B). The OECD TG 301B test is designed as a screening test with optimized conditions and a higher density of microorganisms to favor biodegradation. In contrast, the biodegradation test in soil represents a more realistic simulation of environmental conditions with the natural soil biome, rather slower mineralization and longer incubation times. The unexpectedly fast evolution of $^{14}CO_2$ already reaching 23-33% within the first hour raises the question, whether biotic or abiotic processes, such as chemical reactions were the key driver. In Part 2 of this thesis (based on Teggers et al., 2025b), performing the extraction procedure after the application to soil and a subsequent one-hour incubation, resulted in high losses of AR due to the evolution of $^{14}CO_2$.

The biodegradation in soil was substantially lower following irradiation of the PUA_{mod} microcapsules on a dry soil surface following procedure MII-P4 (Figure 8; Table 2), compared to irradiation in aqueous medium (MI-P3). In this case, irradiation on dry soil likely resulted in reduced phototransformation due to microcapsule aggregation and adsorption to the soil surface, which may have caused shading effects and limited light penetration compared to irradiation in water. Accordingly, the extent of biodegradation in soil was presumably lower.

Procedure MI-P 1–3 focused on testing PUA_{mod} microcapsules, while procedure MII-P4 also included the non-modified PUA. The modification of PUA did not significantly affect its biodegradability, as both modified and unmodified materials exhibited similar levels of mineralization.

The biodegradation in soil of the dark control LLDPE samples resulted in almost no biodegradation with less than $1\%_{AR}$. Similarly, the on soil surface irradiated LLDPE samples showed less than $2\%_{AR}$ biodegradation. Based on the results of procedure MI-P 1 (Figure 19), which demonstrated the release of ^{14}C-labeled compounds following irradiation in water, a higher degree of mineralization was expected. However, either the LLDPE particles released fragments or compounds that remained persistent in soil, or the irradiation on the soil surface led to less degradation compared to the aqueous environment. In the latter case, fragment formation and the release of ^{14}C-compounds were observed only after aqueous irradiation, as shown by applying the sequential filtration method (MI-P1). Since biodegradation of LLDPE particles after aqueous irradiation was not assessed in this study, this question remains unresolved.

Although the differences in biodegradation between irradiated and non-irradiated samples following procedure MII-P4 were not statistically significant for PUA, PUA_{mod}, and LLDPE, a clear trend toward increased biodegradation was observed.

4.3 Part 3 – Extraction of Pristine and Weathered Microplastics from Soil Using Modified Oil-Based Method

4.3.1 Extraction Efficiencies of the Different Extraction Experiments

The results of this study provide insights into the extraction of pristine and weathered MPs, specifically ^{14}C-PUA microcapsules and ^{14}C-LLDPE particles, from different types of soil.

The two types of MP particles analyzed in this study varied in several aspects, including size, morphology, polymer composition, and density. Especially, their internal composition differed substantially, as the PUA encapsulated a high proportion of an industrial aromatic solvent with oil-like properties (up to 94% by weight). Depending on the synthesis route, PUA can have hydrophilic properties through the incorporation of ionic or non-ionic hydrophilic segments within the polymer matrix, enabling the formation of hydrogen bonds with water. However, the PUA used in this study was synthesized with a crosslinked structure, promoting hydrogen bonding primarily within the polymer itself rather than with surrounding water molecules. This intramolecular bonding limited its interaction with water. Jiang et al. (2017) reported that such crosslinking and the presence of branched urea groups rendered PUA insoluble. Consequently, as insolubility increases, hydrophilicity typically decreases (Hill and Young, 2010). In contrast, LLDPE is a non-polar polymer and inherently hydrophobic (Yuan et al., 2008). Therefore, both particle types were largely hydrophobic and could be effectively isolated using a modified oil extraction protocol. Specifically, the most efficient recovery was achieved in experiment 1, which combined n-octanol extraction with a preliminary KOH extraction step, resulting in extraction efficiencies of up to approximately 75%$_{AR}$.

With respect to the ^{14}C-LLDPE, the considerable high deviations in the amount of AR were attributed to the heterogeneity of the MP suspension, which likely led to uneven distribution during application. As a result, the calculated total recoveries are considered unreliable, since accurate quantification of the initially AR was not possible. Unlike dissolved substances, suspended particles tend not to distribute uniformly within a given volume, introducing variability and inconsistency. Consequently, some calculated recoveries exceeded 100% of the estimated AR. Despite this issue, less than 1%$_{AR}$ of the particles remained in the soil after extraction, supporting the deduction that the modified oil extraction method (experiment 1) was effective and achieved an almost complete recovery of the ^{14}C-LLDPE MPs.

Overall, the modified oil extraction method (Experiment I) demonstrated greater efficiency compared to the classical density-based $ZnCl_2$ method (Experiment II), which was evaluated for the recovery of PUA microcapsules. This enhanced performance is likely due to the predominantly hydrophobic and oleophilic nature of both PUA, which facilitated their effective partitioning into the octanol phase.

Previous research has shown that both density-based (e.g., Prosenc et al., 2021; Radford et al., 2021; Vermeiren et al., 2020) and oil-based extraction techniques (Crichton, 2017; Mani et al., 2019; Prosenc

et al., 2021b; Radford et al., 2021; Scopetani et al., 2020b) generally yielded higher MP recovery rates than those achieved in this project. However, a key difference probably lies in the particle sizes investigated. In the study by Radford et al. (2021), for instance, a $ZnCl_2$-based density separation method was applied to MPs ranging from 0.5 to 5 mm in size (including PET, HDPE, PVC, LDPE, PP, and PS), and recovery efficiencies of around 80% were reported. Although a decrease in efficiency was observed with smaller particles, the smallest MPs in their study were still larger than those used in our experiments. The ^{14}C-labeled PUA microcapsules used here had a median diameter of approx. 23 µm, which is significantly smaller than the MPs used in most prior studies. This size difference, combined with their distinctive oil-filled polymer shell structure, likely contributed to the reduced recovery observed. Furthermore, it is possible that some microcapsules partially disintegrated, making fragmented shells more challenging to extract. The improved recovery of ^{14}C-LLDPE MPs, with lower residual radioactivity in the soil might be attributed to their larger size and differing physical-chemical characteristics.

Introducing KOH as the first step in the extraction process substantially enhanced overall recovery compared to procedures where this step was omitted (Appendix - Table A8 and - Table A9). Radford et al. (2021) similarly observed increased extraction efficiencies when SOM was removed prior to applying the oil-based extraction method, aligning with our findings. In the study by Nava and Leoni (2021), a comparable extraction efficiency of 60–67% was achieved for polyethylene terephthalate (PET) and nylon particles within the smallest tested size range (250–500 µm) using KOH as extraction solution. However, in many published studies, the specific contribution of soil organic matter (SOM) removal reagents to overall MP recovery is not reported separately. In some cases, SOM removal is conducted only after the primary extraction process (Rani et al., 2023). Repeating the initial extraction only led to marginal gains in efficiency in our study. Presumably, the additional amount of ^{14}C-PUA and ^{14}C-LLDPE extracted by the second extraction step using *n*-octanol or $ZnCl_2$, were not bound to SOM, but rather to other soil components, such as mineral components.

Since exposure to highly alkaline conditions (pH 14) was part of the extraction process, the potential impact on the microcapsules and LLDPE particles need to be considered, particularly in terms of suitability for subsequent potential analyses. Potential fragmentation or chemical alteration during this step cannot be excluded. Preliminary microscopic observations indicated that exposing the microcapsules to KOH solution (pH 14) for up to five days did not visibly alter their morphology (Figure 25). However, such optical assessments are limited to detecting obvious shape changes and do not provide information about potential physical or chemical modifications (e.g., on the surface) resulting from KOH exposure. Additionally, the mechanical stress introduced by centrifugation could potentially lead to MP disintegration. Nonetheless, a study by Pfohl et al. (2024) reported that particle size remained consistent with that of untreated MPs even under higher centrifugal forces than those applied in this work. However, the microcapsules used here may be more susceptible due to their thin-walled structure.

4.3.1 Impact of Soil Types on the Extraction Efficiency

To compare the MP extraction efficiencies of soils with different properties all extraction experiments were performed with two distinct reference soils. Both soils were representative of typical agricultural environments to which PUA microcapsules and LLDPE mulch films can end up. Due to the differences in soil composition (Appendix - Table A4), particularly in terms of organic matter content, variations in extraction performance were expected. It was therefore assumed that the higher organic matter content of RefeSol 03-G (6.7% SOM compared to 1.8% in RefeSol 01-A, measured according to DIN EN 15936; see Appendix - Table A4) would result in stronger retention of MPs within the soil matrix, thus negatively affecting the extraction efficiency. However, no notable differences in recovery rates between the two soils were observed, regardless of the extraction method applied (Appendix - Figure 26; Appendix -Table A8, and - Table A9). This result stands in contrast to findings from other studies such as Corradini et al. (2019), which reported decreased extraction efficiency in soils with higher SOM content. At the same time, our findings align with those of Radford et al. (2021) and Prosenc et al. (2021), who also did not observe a significant correlation between SOM content and MP recovery when using density-based extraction methods.

4.3.2 Impact of Sunlight Irradiation on the Extraction Efficiency

Mass balancing of the radioactivity applied to the soils proved valuable not only for assessing extraction efficiency but also for identifying potential losses of radioactivity associated with MP loss during the extraction process. Notably, lower total recoveries were observed for the light-exposed ^{14}C-PUA. It was suspected that simulated sunlight exposure had induced alterations to the polymer, which may have increased its susceptibility to degradation pathways, including biodegradation to $^{14}CO_2$ during the one-hour incubation period in soil prior to extraction. In Part 2 of this thesis (see subchapter 3.2.3), this assumption was confirmed, and a rapid transformation to $^{14}CO_2$ of the light-exposed ^{14}C-PUA was demonstrated through a biodegradation test in soil based on OECD TG 307.

The performance of extraction experiment 1 proved to be efficient since only less than 3%AR remained in soil. It is likely that light exposure increased the extractability of ^{14}C-PUA microcapsules during the initial KOH extraction step, resulting in reduced radioactivity detected in the octanol phase compared to the pristine ^{14}C-PUA microcapsules. This assumption is supported by previous studies demonstrating that light exposure can induce polymer alterations, including degradation processes that reduce molecular weight and overall mass, increase hydrophilicity, and enhance the susceptibility of plastics to microbial attack (Duan et al., 2022; Gu, 2003; Sivan, 2011; Sun et al., 2020; Yuan et al., 2020). On this background, it is reasonable that simulated sunlight exposure might have enhanced the hydrophilicity of the ^{14}C-PUA microcapsules, thereby promoting their accumulation into the aqueous KOH phase and increasing the extractability of this step. In addition, simulated sunlight irradiation likely caused physical

fragmentation of the microcapsules and the release of transformation products into the ^{14}C-PUA suspension, which was examined and proved in greater detail in Part 2 of this thesis. Some of these transformation products were presumably mineralized during the short incubation period between the application to the soil and the extraction experiment, which might have led to the notable reduction of the total recovery.

In contrast to our findings, in a study by Mani et al. (2019), oil-based extraction efficiencies were compared between sediments spiked with pristine MPs and environmental samples believed to contain naturally aged (weathered) MPs. The recovery from environmental samples was notably lower, at 74 ± 13% based on the number of particles visually recovered and counted by stereomicroscopy, compared to 99 ± 4% for samples with pristine MPs. The authors attributed this discrepancy, at least in part, to the weathered condition of the MPs. However, given that the weathered particles were sourced directly from the environment, it is also possible that differences in matrix composition or other environmental factors played a role in the reduced extraction performance compared to our investigation.

Similar to the pristine LLDPE, the light-exposed LLDPE was nearly entirely extracted from the soil, as shown by the low residual radioactivity detected in the soil. This outcome indicates that light-induced alterations had minor impact on the extractability of LLDPE MP particles.

Overall, it should be emphasized that the simulated sunlight exposure of this study followed standardized laboratory methods, which do not fully reflect the complexity of natural environmental sunlight exposure scenarios. In real-world settings, MPs are subjected to a combination of physico-chemical and biological processes that may alter their extraction behavior compared to particles exposed to light under controlled laboratory conditions. Additionally, in this study, the polymers were irradiated while suspended in water, allowing for hydrolytic processes and increasing the surface area exposed to light, in contrast to light exposure performed on a soil surface, as examined in the Part 2 of this thesis (see subchapter 2.3.1).

4.3.3 pH Dependence of Microplastic Extraction Efficiency

The separate investigation examining the influence of the pH of the solution used in the first extraction step provided more detailed insights into its correlation with extraction efficiency. The results of this investigation demonstrated that increasing the pH of the aqueous solution led to a progressive increase in the extraction efficiency of ^{14}C-PUA. In general, an increase in pH enhances the solubility of SOM, particularly humic substances due to the destruction of their molecular structure, for example through deprotonation of functional groups such as carboxylic and phenolic moieties (Powell and Fenton, 1996; You et al., 2006). Therefore, the high extraction efficiency of ^{14}C-PUA microcapsules observed in the alkaline solutions (KOH and NaOH) can likely be attributed to the mobilization of humic and fulvic acids from the soil, to which the ^{14}C-PUA presumably partly adhere. As a result, the KOH or NaOH treatment may have induced their subsequent release into the aqueous phase and facilitated their

extraction. In contrast, under more acidic conditions, humic acids tend to precipitate, which decreases their solubility. Consequently, it lowers the extraction efficiency of both organic matter and associated ^{14}C-PUA.

While pH is an important factor influencing the extraction outcome, different alkaline solutions, even at identical pH values, may produce varying results due to differences in ionic composition. The separate investigation employed NaOH instead of KOH, which was used in the extraction experiments. The specific properties of the sodium ion, including its relatively small ionic radius and binding behavior, may influence interactions with soil components. Notably, a previous study has shown that Na^+ and K^+ ions differ in their effects on soil aggregate stability (Li et al., 2023), suggesting that the choice of alkaline cation may also impact MP recovery. However, results obtained in our experiment using NaOH showed similar extraction efficiencies at comparable solution molarity (2 M vs. approx. 1.8 M, respectively), therefore only minor variations may have been introduced by the used type of solution.

4.4 General Discussion

Generally, it needs to be considered that both synthesized PUA shells investigated in this project were not solely composed of the radiolabeled HMDA monomer but also included co-polymerized isocyanates that did not contain the ^{14}C-label. Since the radiolabel was confined to only HMDA, the evaluation of degradation and polymer fate was limited to fragments containing the labeled component. Transformation products originating from the non-labeled polymer fractions were therefore not assessed in this project.

Nonetheless, radiolabeling proved to be a powerful tool for addressing several key challenges in MP biodegradation testing. It enabled precise tracking, quantification, and full mass balance of polymer-derived mineralization and was especially suitable for the small and structurally complex microcapsules investigated. At the same time, broader use of radiolabeling remains restricted due to high synthesis costs and regulatory requirements for authorized laboratories. Therefore, routine biodegradability testing will likely depend on validated alternative endpoints. Methods such as FTIR and Raman spectroscopy can provide insight into chemical transformation, while Scanning Electron Microscopy (SEM) can support visual characterization of morphological changes. However, the applicability of these alternatives depends on matrix complexity, particle size, detection sensitivity, and instrument accessibility for routine use.

The results of this thesis also highlight the importance of either thoroughly purifying or performing comprehensive characterization of the MP material prior to testing. The presence of soluble, low-molecular-weight residues in a microplastic suspension can substantially bias mineralization outcomes. This was in our study demonstrated through UHPLC-HRMS analysis, where apparent biodegradation of the bulk suspension was driven by soluble radiolabeled synthesis residues contained in the

suspension. In addition, Karagianni et al. (2024) demonstrated that the choice of extraction and purification method for the polymeric shell of microcapsules can significantly influence the outcome of biodegradation tests. Residual organic material or other non-polymeric constituents may lead to overestimated mineralization results if not adequately characterized and removed.

Furthermore, the investigations of this project, which are illustrated in Figure 29, demonstrated that simulated sunlight exposure in water caused fragmentation of PUA microcapsules and, to a lesser extent, LLDPE particle disintegration. For PUA, the release of a readily biodegradable molecule, aminocaproic acid, from the polymer was identified and likely contributed to increased mineralization in subsequent biodegradation tests. The enhanced biodegradability of PUA and PUA_{mod} following irradiation in water or on soil contrasts with that of LLDPE, whose biodegradability appeared largely unaffected by prior irradiation. This difference may be attributed to polymer-specific properties, in addition to the susceptibility of PUA's thin shell to full light penetration and photooxidation effects. While LLDPE irradiated in water released fragmentation products detectable by sequential filtration, no subsequent biodegradation tests were conducted under these conditions. In contrast, LLDPE particles irradiated on the soil surface did not exhibit increased biodegradation in the following soil test, suggesting that light exposure may have led to the formation of more persistent or less bioavailable degradation products.

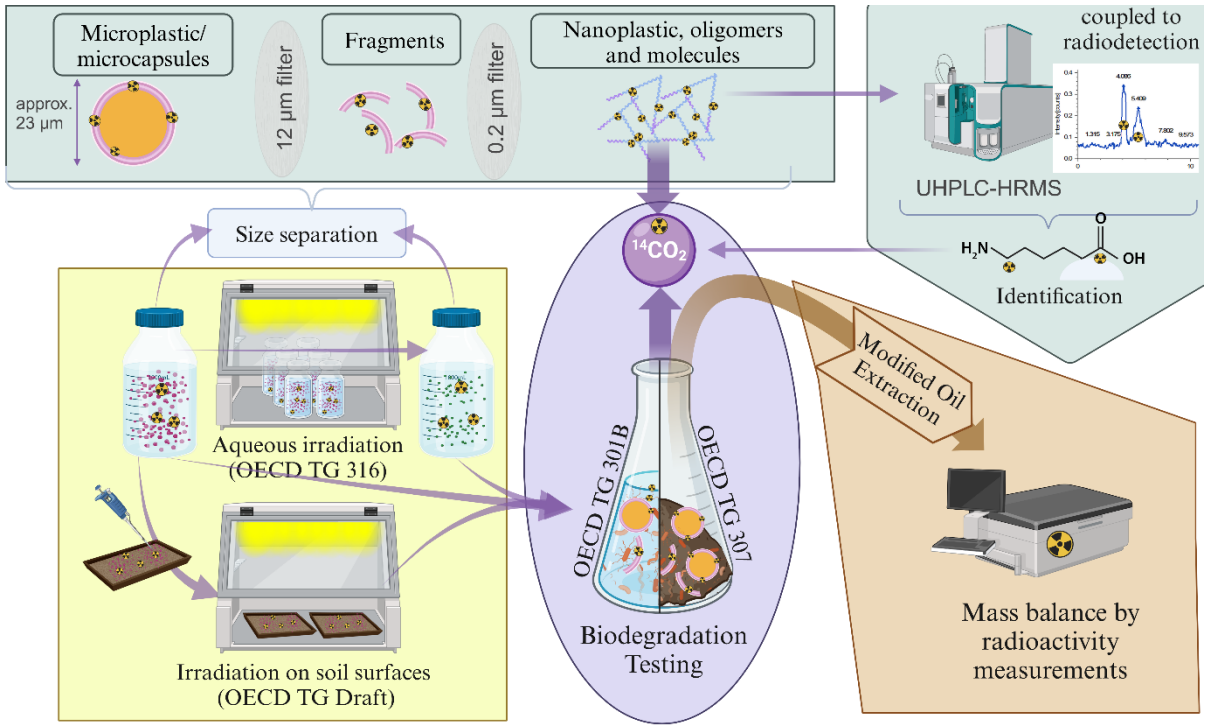

Figure 29. Overview of the main methods and ideas involved in this thesis.

It must be noted that the test results on photo-oxidation effects can only be partially extrapolated to real-world environmental conditions. In agricultural use scenarios, such as the foliar application of PUA-based pesticide formulations (e.g., Prosper 300 CS), microcapsules may be exposed to sunlight, potentially leading to their disintegration before reaching the soil. However, direct soil applications

would likely reduce sunlight exposure due to incorporation into deeper layers due to irrigation, plowing, or bioturbation. Light penetration into soil is known to be very limited in the sub-mm range (Tester and Morris, 1987; Ciani et al., 2005), which needs to be considered when interpreting the results.

In the final part of this thesis, the modified oil extraction method successfully recovered both pristine and irradiated ^{14}C-PUA and ^{14}C-LLDPE MPs from two soils with differing pedological characteristics. The method proved suitable for small particle sizes (<500 µm) and may be applicable to other hydrophobic polymers. However, potential polymer degradation during extraction must be considered, especially when using solvents like octanol or hexane, which are known to dissolve certain polymers (but not PUA and LLDPE). In addition to this, sunlight-induced polymer changes not only facilitated (bio)degradation but also altered extractability, effects that must be considered in future testing approaches.

5 Conclusion

This thesis investigated the biodegradability and environmental fate of microplastics (MPs), with a specific focus on polyurea (PUA) microcapsules intentionally added to plant protection products. The work addressed methodological and regulatory challenges by exploring key aspects of biodegradation testing in three experimental parts.

First, the findings of Part 1 demonstrated that purification was critical to avoid misleading biodegradation results. In particular, residual formulation components, such as soluble synthesis by-products, increased mineralization values and biased the interpretation of biodegradability. Filtration and resuspension effectively isolated the microcapsules, while size distribution analysis combined with UHPLC-HRMS of the smallest size fraction (<0.2 µm) provided a deeper understanding of the biodegradation process.

Second, the influence of abiotic factors was investigated in Part 2. Simulated sunlight exposure substantially affected the degradability of PUA microcapsules, as photooxidation promoted the formation of smaller, more bioavailable LMW molecules, oligomers or fragments. In contrast, LLDPE particles exhibited only limited disintegration and no clear increase in mineralization after irradiation. These findings underscore the importance of considering abiotic degradation processes under realistic exposure scenarios, as well as accounting for size fractionation when assessing MP degradation.

Third, Part 3 focused on the development of a robust extraction method for recovering MPs from soil. The modified oil-based approach was effective for isolating both pristine and weathered particles from different soil types, including small MPs. This method may enable further characterization and may support the extraction and identification of transformation products, contributing to a more comprehensive understanding of MP behavior in environmental matrices.

In summary, this thesis leads to three key conclusions and recommendations. First, thorough characterization and, where applicable, fractionation of MP test materials are essential for accurately interpreting biodegradation data. Second, the influence of abiotic factors such as irradiation with simulated sunlight should be considered in experimental testing designs when the respective MP is likely to be exposed to such conditions. Third, practical and efficient extraction methods, ideally standardized, are needed to enable meaningful analysis of MPs and their transformation products in complex matrices such as soil.

Due to uncertainty in real-world sunlight exposure, simulated photodegradation of PUA microcapsules requires validation. Lysimeter or field studies would be essential to verify if laboratory results apply under agricultural conditions and to confirm their environmental relevance.

6 Future Implications and Outlook

The findings of this thesis point to several key areas for further research and methodological refinement in the assessment of MP biodegradability under environmentally relevant conditions.

First, future studies should advance analytical strategies that go beyond simple mineralization endpoints. The combination of mineralization data with supporting physicochemical analyses, such as size distribution, chemical structure, and identification of soluble byproducts, proved essential in this work to correctly interpret degradation behavior. However, future challenges remain in developing standardized methodological amendments for integration into biodegradation testing and in introducing alternative approaches that do not rely on radiolabeling for broader applicability.

Second, a key point to be addressed in future studies is how transferable the results of laboratory studies are to more environmentally realistic scenarios, particularly with regard to simulated sunlight exposure and its influence on biodegradation of PUA microcapsules. Without knowledge of how much sunlight intensity microcapsules are actually exposed to under realistic application conditions, deductions regarding abiotic influences on biodegradation processes cannot be made, neither from a scientific nor from a regulatory perspective. In this study, the applied simulated sunlight exposure corresponded to 30 days of natural summer sunlight in the northern hemisphere. However, depending on the type and timing of application, as well as shading effects or the localization of the encapsulated PPPs, the actual effects of sunlight exposure likely vary. In the case of direct application of PUA-based pesticide formulations like Prosper 300 CS on plant leaves, the microcapsules may initially be exposed to sunlight before being washed off by rain and subsequently being incorporated into the soil. In contrast, when applied directly to the soil surface, exposure to sunlight is expected to decrease steeply. The microcapsules may quickly be incorporated into deeper soil layers by irrigation, bioturbation, or plowing. According to Tester and Morris (1987), physiologically and ecologically relevant amounts of light rarely penetrate more than 4–5 mm into soil. Ciani et al. (2005) measured light penetration depths in the range of 17–110 µm at 275 nm and 120–300 µm at 700 nm, depending on soil composition and structure. These studies indicate that direct light exposure under field conditions may also be limited or even negligible. To reduce speculation, controlled lysimeter studies or well-designed field trials are recommended to monitor microcapsule behavior and light exposure under agricultural conditions. These studies would bridge the gap between laboratory simulations and realistic environmental scenarios, improving both the scientific validity and regulatory relevance of test results.

Third, the development of practical and standardized extraction methods remains a cornerstone for future tests and environmental research. The modified oil-based extraction protocol evaluated in this thesis showed promising results for isolating both pristine and weathered MPs from soil. However, its broader applicability should be verified across more diverse polymer types, particle sizes, and environmental matrices. Integration of such extraction methods into standardized test guidelines would

allow for a more holistic assessment of MPs, enabling the quantification of residual material, detection of transformation products, and monitoring of changes in particle properties over time.

Taken together, future test strategies should combine thorough material characterization, environmentally relevant test designs, and adaptable protocols that incorporate complementary endpoints and analytical methods.

7 Contributions in Publications and Chapters

Parts of this dissertation are based on work published in the following peer-reviewed papers and related publications:

Abbreviations of names:

EMT	Eva-Maria Teggers	MS	Markus Simon
JH	Jonas Hardebusch	PD	Philipp Dalkmann
BM	Boris Meisterjahn	HE	Holger Egger
AJ	Annika Jahnke	RH	Roman Heumann
AS	Andreas Schäffer	SW	Svenja Winterhoff
DH	Dieter Hennecke	SH	Svetlana Heck

I. Part 1

Teggers, E.-M., Hardebusch, J., Meisterjahn, B., Simon, M., Hennecke, D., Heumann, R., Egger, H., Dalkmann, P., Schäffer, A., Jahnke, A., 2025a. Diversifying endpoints in biodegradation testing of microplastics. Environ Sci Eur 37, 65. https://doi.org/10.1186/s12302-025-01096-8

Contributions: EMT: conceptualization, data curation, formal analysis, investigation, visualization, methodology, writing the original draft and editing of reviewed manuscript; JH: UHPLC–HR-MS analysis investigation and evaluation; BM: methodology; AJ, AS, BM: writing—review and editing. AJ, AS, BM, DH, MS, PD, HE, RH: supervision. AS, BM, DH, MS, PD, HE: project administration, funding acquisition.

II. Part 2

Submitted manuscript: Teggers, E.-M., Winterhoff, S., Heck, Hardebusch, J., S., Meisterjahn, B., Simon, M., Hennecke, D., Heumann, R., Egger, H., Dalkmann, P., Jahnke, A., Schäffer, A., 2025c. Journal of Hazardous Materials. Under Review.

Contributions: EMT, SW, SH: Investigation, data curation, formal analysis, EMT: Conceptualization, visualization, methodology, writing of the original draft and editing of reviewed manuscript; JH: UHPLC-HRMS analysis investigation and evaluation; BM, AJ, AS: Supervision – review & editing; DH, MS, PD, HE, RH: Review & editing; AS, BM, DH, MS, PD, HE, RH: project administration, funding acquisition. All authors revised and edited the manuscript and approved the final version before submission.

III. Part 3

Teggers, E.-M., Heck, S., Meisterjahn, B., Simon, M., Hennecke, D., Heumann, R., Egger, H., Dalkmann, P., Jahnke, A., Schäffer, A., 2025b. Modified oil extraction of pristine and weathered synthetic polyurea microcapsules and polyethylene microplastics from soil. Microplastics and Nanoplastics. https://doi.org/10.1186/s43591-025-00121-0

Contributions: EMT: Conceptualization, visualization, methodology, data curation and formal analysis, writing—original draft preparation. SH: Investigation, methodology, data curation, writing—original draft. AJ, AS, BM, DH: writing—review & editing. AJ, AS, BM, DH, MS, RH, PD, HE: Supervision, project administration. AS, BM, DH, MS, RH, PD, HE: funding acquisition.

Chapter	Contribution	Includes parts of publication*
Zusammenfassung/ Summary	Conceptualization and writing: EMT	I, II, III
Introduction	Conceptualization and writing: EMT	I, II, III
Microplastic Pollution	Conceptualization and writing: EMT	I, II, III
REACH Restriction on the Use of Intentionally Added Microplastics in Products	Conceptualization and writing: EMT	I, II, III
Biodegradation of Polymers	Conceptualization and writing: EMT Visualization: EMT	I
Photodegradation of Polymers	Conceptualization and writing: EMT Visualization: EMT	II
Extraction of MPs from Soils	Conceptualization and writing: EMT Visualization: EMT	III
Synthetic Polymer Microcapsules used for Pesticide Applications	Conceptualization and writing: EMT	I, II, III
Background and Motivation of this	Conceptualization and writing: EMT	I, II, III
Scope and Aims of this Thesis	Conceptualization and writing: EMT	I, II, III

Structure of this thesis	Conceptualization and writing: EMT	I, II, III
Part 1 – Material and Methods	Conceptualization and writing: EMT Investigation: EMT (80%), UHPLC-HRMS analysis investigation: JH (90%), EMT (10%) Methodology: EMT Visualization: EMT	I
Part 2 – Material and Methods	Conceptualization and writing: EMT (100%) Investigation: SW (60%), EMT (20%), SH (10 %), UHPLC-HRMS analysis investigation: JH (8%), EMT (2%). Methodology: EMT (80%), SH (20%) Visualization: EMT (90%), SW (10%)	II
Part 3 – Material and Methods	Conceptualization and writing: EMT (100%) Investigation: SH (90%), EMT (10%) Methodology: EMT (70%), SH (30%) Visualization: EMT (90%), SW (10%)	III
Part 1 - Results	Conceptualization and writing: EMT Data curation and formal analysis: EMT Visualization: EMT	I
Part 2 - Results	Conceptualization and writing: EMT Data curation and formal analysis: EMT (50%), SH (50%) Visualization: EMT (70%), SH (30%)	II
Part 3 - Results	Conceptualization and writing: EMT Data curation and formal analysis: EMT (30%), SW (25%), SH (5%) Visualization: EMT (70%), SH (30%)	III
Part 1 - Discussion	Conceptualization and writing: EMT	I
Part 2 - Discussion	Conceptualization and writing: EMT	II
Part 3 - Discussion	Conceptualization and writing: EMT	III
General Discussion	Conceptualization and writing: EMT	I, II, III
Conclusion	Conceptualization and writing: EMT	I, II, III
Future Implications and Outlook	Conceptualization and writing: EMT	I, II, III

* Results from the publications of EMT et al. 2025 (I a, II b, III submitted), developed during the course of this doctoral research, are included in this dissertation with the consent of the journals and supervisors. The results are fully and accurately cited and are appropriately integrated into the context of the dissertation.

The following software assisted this work

1. ChatGPT3.5-4.o for literature research, rephrasing, shortening of self-written text
2. DeepL for translation

X. References

Albertsson, A., Karlsson, S., 1990. The influence of biotic and abiotic environments on the degradation of polyethylene. Progress in Polymer Science 15, 177–192. https://doi.org/10.1016/0079-6700(90)90027-X

Albright, V.C., Chai, Y., 2021. Knowledge Gaps in Polymer Biodegradation Research. Environ. Sci. Technol. 55, 11476–11488. https://doi.org/10.1021/acs.est.1c00994

Alimi, O.S., Claveau-Mallet, D., Kurusu, R.S., Lapointe, M., Bayen, S., Tufenkji, N., 2022. Weathering pathways and protocols for environmentally relevant microplastics and nanoplastics: What are we missing? Journal of Hazardous Materials 423, 126955. https://doi.org/10.1016/j.jhazmat.2021.126955

Allen, N.S., 1986. Recent advances in the photo-oxidation and stabilization of polymers. Chemical Society Reviews 15, 373–404.

Allen, S., Allen, D., Phoenix, V.R., Le Roux, G., Durántez Jiménez, P., Simonneau, A., Binet, S., Galop, D., 2019. Atmospheric transport and deposition of microplastics in a remote mountain catchment. Nat. Geosci. 12, 339–344. https://doi.org/10.1038/s41561-019-0335-5

American Chemical Society, 1974. Microencapsulated pesticide reaches market. Chem. Eng. News Archive, 52 15–16.

Anbumani, S., Kakkar, P., 2018. Ecotoxicological effects of microplastics on biota: a review. Environ Sci Pollut Res 25, 14373–14396. https://doi.org/10.1007/s11356-018-1999-x

Aniśko, J., Sałasińska, K., Barczewski, M., 2023. Thermal stability and degradation kinetics of bio-based low-density polyethylenes. p 68, 451–460. https://doi.org/10.14314/polimery.2023.9.1

Arnaud, R., Dabin, P., Lemaire, J., Al-Malaika, S., Chohan, S., Coker, M., Scott, G., Fauve, A., Maaroufi, A., 1994. Photooxidation and biodegradation of commercial photodegradable polyethylenes. Polymer Degradation and Stability 46, 211–224. https://doi.org/10.1016/0141-3910(94)90053-1

Bachmann, M., Zibunas, C., Hartmann, J., Tulus, V., Suh, S., Guillén-Gosálbez, G., Bardow, A., 2023. Towards circular plastics within planetary boundaries. Nat Sustain 6, 599–610. https://doi.org/10.1038/s41893-022-01054-9

Bai, Y., Zhou, Y., Che, X., Li, C., Cui, Z., Su, R., Qu, K., 2021. Indirect photodegradation of sulfadiazine in the presence of DOM: Effects of DOM components and main seawater constituents. Environmental Pollution 268, 115689. https://doi.org/10.1016/j.envpol.2020.115689

Bank, M.S., Mitrano, D.M., Rillig, M.C., Sze Ki Lin, C., Ok, Y.S., 2022. Embrace complexity to understand microplastic pollution. Nature Reviews Earth & Environment 3, 736–737.

Benedict, C.V., Cameron, J.A., Huang, S.J., 1983. Polycaprolactone degradation by mixed and pure cultures of bacteria and a yeast. J of Applied Polymer Sci 28, 335–342. https://doi.org/10.1002/app.1983.070280129

Bhargava, S., Kubota, M., Lewis, R.D., Advani, S.G., Prasad, A.K., Deitzel, J.M., 2015. Ultraviolet, water, and thermal aging studies of a waterborne polyurethane elastomer-based high reflectivity coating. Progress in Organic Coatings 79, 75–82. https://doi.org/10.1016/j.porgcoat.2014.11.005

Birch, H., Sjøholm, K.K., Dechesne, A., Sparham, C., Van Egmond, R., Mayer, P., 2022. Biodegradation Kinetics of Fragrances, Plasticizers, UV Filters, and PAHs in a Mixture─Changing Test Concentrations over 5 Orders of Magnitude. Environ. Sci. Technol. 56, 293–301. https://doi.org/10.1021/acs.est.1c05583

Blaschko, H., 1935. The mechanism of catalase inhibitions. Biochemical Journal 29, 2303–2312. https://doi.org/10.1042/bj0292303

Bläsing, M., Amelung, W., 2018. Plastics in soil: Analytical methods and possible sources. Science of The Total Environment 612, 422–435. https://doi.org/10.1016/j.scitotenv.2017.08.086

Borrelle, S.B., Ringma, J., Law, K.L., Monnahan, C.C., Lebreton, L., McGivern, A., Murphy, E., Jambeck, J., Leonard, G.H., Hilleary, M.A., Eriksen, M., Possingham, H.P., De Frond, H., Gerber, L.R., Polidoro, B., Tahir, A., Bernard, M., Mallos, N., Barnes, M., Rochman, C.M., 2020. Predicted growth in plastic waste exceeds efforts to mitigate plastic pollution. Science 369, 1515–1518. https://doi.org/10.1126/science.aba3656

Boucher, J., Friot, D., 2017. Primary microplastics in the oceans: A global evaluation of sources. IUCN International Union for Conservation of Nature. https://doi.org/10.2305/IUCN.CH.2017.01.en

Bracco, P., Costa, L., Luda, M.P., Billingham, N., 2018. A review of experimental studies of the role of free-radicals in polyethylene oxidation. Polymer Degradation and Stability 155, 67–83. https://doi.org/10.1016/j.polymdegradstab.2018.07.011

Bravo Rebolledo, E.L., Van Franeker, J.A., Jansen, O.E., Brasseur, S.M.J.M., 2013. Plastic ingestion by harbour seals (Phoca vitulina) in The Netherlands. Marine Pollution Bulletin 67, 200–202. https://doi.org/10.1016/j.marpolbul.2012.11.035

Brunning, H., Sallach, J.B., Zanchi, V., Price, O., Boxall, A., 2022. Toward a Framework for Environmental Fate and Exposure Assessment of Polymers. Environmental Toxicology and Chemistry 41, 515–540. https://doi.org/10.1002/etc.5272

Büks, F., Kaupenjohann, M., 2020. Global concentrations of microplastics in soils – a review. SOIL 6, 649–662. https://doi.org/10.5194/soil-6-649-2020

Carlini, G., Drugmand, D., 2022. Sowing a Plastic Planet: How Microplastics in Agrochemicals Are Affecting Our Soils, Our Food, and Our Future. Center for International Environmental Law.

Carmichael, N., 2014. European Centre for Ecotoxicology and Toxicology of Chemicals, in: Encyclopedia of Toxicology. Elsevier, pp. 547–548. https://doi.org/10.1016/B978-0-12-386454-3.00505-4

Chamas, A., Moon, H., Zheng, J., Qiu, Y., Tabassum, T., Jang, J.H., Abu-Omar, M., Scott, S.L., Suh, S., 2020. Degradation Rates of Plastics in the Environment. ACS Sustainable Chem. Eng. 8, 3494–3511. https://doi.org/10.1021/acssuschemeng.9b06635

Che, K., Lyu, P., Wan, F., Ma, M., 2019. Investigations on Aging Behavior and Mechanism of Polyurea Coating in Marine Atmosphere. Materials 12, 3636. https://doi.org/10.3390/ma12213636

Chen, C., Chen, L., Yao, Y., Artigas, F., Huang, Q., Zhang, W., 2019. Organotin Release from Polyvinyl Chloride Microplastics and Concurrent Photodegradation in Water: Impacts from Salinity, Dissolved Organic Matter, and Light Exposure. Environ. Sci. Technol. 53, 10741–10752. https://doi.org/10.1021/acs.est.9b03428

Chiellini, E., Corti, A., Swift, G., 2003. Biodegradation of thermally-oxidized, fragmented low-density polyethylenes. Polymer Degradation and Stability 81, 341–351. https://doi.org/10.1016/S0141-3910(03)00105-8

Chinaglia, S., Tosin, M., Degli-Innocenti, F., 2018. Biodegradation rate of biodegradable plastics at molecular level. Polymer Degradation and Stability 147, 237–244. https://doi.org/10.1016/j.polymdegradstab.2017.12.011

Cole, M., Webb, H., Lindeque, P.K., Fileman, E.S., Halsband, C., Galloway, T.S., 2014. Isolation of microplastics in biota-rich seawater samples and marine organisms. Sci Rep 4, 4528. https://doi.org/10.1038/srep04528

Corradini, F., Meza, P., Eguiluz, R., Casado, F., Huerta-Lwanga, E., Geissen, V., 2019. Evidence of microplastic accumulation in agricultural soils from sewage sludge disposal. Science of The Total Environment 671, 411–420. https://doi.org/10.1016/j.scitotenv.2019.03.368

Cox, C., Surgan, M., 2006. Unidentified Inert Ingredients in Pesticides: Implications for Human and Environmental Health. Environ Health Perspect 114, 1803–1806. https://doi.org/10.1289/ehp.9374

Crichton, E.M., 2017. A novel, density-independent and FTIR-compatible approach for the rapid extraction of microplastics from aquatic sediments. Analytical Methods.

Crichton, E.M., Noël, M., Gies, E.A., Ross, P.S., 2017. A novel, density-independent and FTIR-compatible approach for the rapid extraction of microplastics from aquatic sediments. Anal. Methods 9, 1419–1428. https://doi.org/10.1039/C6AY02733D

Cui, W., Gao, P., Zhang, M., Wang, L., Sun, H., Liu, C., 2022. Adverse effects of microplastics on earthworms: A critical review. Science of The Total Environment 850, 158041. https://doi.org/10.1016/j.scitotenv.2022.158041

da Costa, J.P., Duarte, A.C., 2022. Introduction to the Analytical Methodologies for the Analysis of Microplastics, in: Rocha-Santos, T., Costa, M.F., Mouneyrac, C. (Eds.), Handbook of Microplastics in the Environment. Springer International Publishing, Cham, pp. 3–32. https://doi.org/10.1007/978-3-030-39041-9_1

Dailey, O.D., 2004. Volatilization of alachlor from polymeric formulations. Journal of agricultural and food chemistry 52, 6742–6746.

Dehaut, A., Cassone, A.-L., Frère, L., Hermabessiere, L., Himber, C., Rinnert, E., Rivière, G., Lambert, C., Soudant, P., Huvet, A., Duflos, G., Paul-Pont, I., 2016. Microplastics in seafood: Benchmark protocol for their extraction and characterization. Environmental Pollution 215, 223–233. https://doi.org/10.1016/j.envpol.2016.05.018

DIN EN 15933, 2012. Schlamm, behandelter Bioabfall und Boden - Bestimmung des pH-Werts. https://doi.org/10.31030/1866552

DIN EN 15936, 2022. Boden, Abfall, behandelter Bioabfall und Schlamm - Bestimmung des gesamten organischen Kohlenstoffs (TOC) mittels trockener Verbrennung. https://doi.org/10.31030/3293536

DIN EN ISO 11260, 2018. Bodenbeschaffenheit - Bestimmung der effektiven Kationenaustauschkapazität und der Basensättigung unter Verwendung von Bariumchloridlösung. https://doi.org/10.31030/2809006

DIN EN ISO 14240-2, 2011. Bodenbeschaffenheit - Bestimmung der mikrobiellen Biomasse von Böden_- Teil_2: Fumigations-Extraktionsverfahren (ISO_14240-2:1997). https://doi.org/10.31030/1804006

DIN EN ISO 14852, 2021. Determination of the ultimate aerobic biodegradability of plastic materials in an aqueous medium – Method by analysis of evolved carbon dioxide.

Ding, L., Yu, X., Guo, X., Zhang, Y., Ouyang, Z., Liu, P., Zhang, C., Wang, T., Jia, H., Zhu, L., 2022. The photodegradation processes and mechanisms of polyvinyl chloride and polyethylene terephthalate microplastic in aquatic environments: Important role of clay minerals. Water Research 208, 117879. https://doi.org/10.1016/j.watres.2021.117879

Dissanayake, P.D., Kim, S., Sarkar, B., Oleszczuk, P., Sang, M.K., Haque, M.N., Ahn, J.H., Bank, M.S., Ok, Y.S., 2022. Effects of microplastics on the terrestrial environment: A critical review. Environmental Research 209, 112734. https://doi.org/10.1016/j.envres.2022.112734

Du, J., Ibaseta, N., Guichardon, P., 2022. Characterization of polyurea microcapsules synthesized with an isocyanate of low toxicity and eco-friendly esters via microfluidics: Shape, shell thickness, morphology and encapsulation efficiency. Chemical Engineering Research and Design 182, 256–272. https://doi.org/10.1016/j.cherd.2022.03.026

Duan, J., Li, Y., Gao, J., Cao, R., Shang, E., Zhang, W., 2022. ROS-mediated photoaging pathways of nano- and micro-plastic particles under UV irradiation. Water Research 216, 118320. https://doi.org/10.1016/j.watres.2022.118320

ECETOC, E.C. for E. and T. of C., 2020. Applicability of Analytical Tools, Test Methods and Models for Polymer Risk Assessment (No. 133–2). Elsevier, Brussels.

ECHA, E.C.A., 2021. Microplastics. hot- topics. URL https://echa.europa.eu/de/hot-topics/microplastics (accessed 3.7.24).

Eldsater, C., Erlandsson, B., Renstad, R., 2000. The biodegradation of amorphous and crystalline regions in film-blown poly(e-caprolactone).

European Chemicals Agency (ECHA), 2019. ANNEX XV Restriction Report, Proposal for a Restriction - Microplastics (No. 1.2). Helsinki.

European Commission, 2023. ANNEX to the Commission Regulation (EU) amending Annex XVII to Regulation (EC) No 1907/2006 of the European Parliament and of the Council concerning the Registration, Evaluation, Authorisation and Restriction of Chemicals (REACH) as regards synthetic polymer microparticles.

European Food Safety Authority (EFSA), Egsmose, M., Fait, G., Janzen, W., Jentzsch, F., Lava, R., Lythgo, C., Padovani, L., Pickl, C., Priegnitz, J., 2022. Scientific guidance on soil phototransformation products in groundwater – consideration, parameterisation and simulation in the exposure assessment of plant protection products. EFS2 20. https://doi.org/10.2903/j.efsa.2022.7119

Fan, W., Qiu, C., Qu, Q., Hu, X., Mu, L., Gao, Z., Tang, X., 2023. Sources and identification of microplastics in soils. Soil & Environmental Health 1, 100019. https://doi.org/10.1016/j.seh.2023.100019

FAO, F. and A.O. of the U.N., 2021. Assessment of agricultural plastics and their sustainability: A call for action. Rome, Italy.

Feldman, D., 2002. Polymer Weathering: Photo-Oxidation. Journal of Polymers and the Environment 10, 163–173. https://doi.org/10.1023/A:1021148205366

Fields, R.D., Rodriguez, F., Finn, R.K., 1974. Microbial degradation of polyesters: Polycaprolactone degraded by P. pullulans. J. Appl. Polym. Sci. 18, 3571–3579. https://doi.org/10.1002/app.1974.070181207

Fritscher, C., 1994. Degradable polymers. IJMPT 9, 482–495. https://doi.org/10.1504/IJMPT.1994.036434

Fu, Y., He, H., Liu, R., Zhu, L., Xia, Y., Qiu, J., 2019. Preparation and performance of a BTDA-modified polyurea microcapsule for encapsulating avermectin. Colloids and Surfaces B: Biointerfaces 183, 110400. https://doi.org/10.1016/j.colsurfb.2019.110400

Galafassi, S., Nizzetto, L., Volta, P., 2019. Plastic sources: A survey across scientific and grey literature for their inventory and relative contribution to microplastics pollution in natural environments, with an emphasis on surface water. Science of The Total Environment 693, 133499. https://doi.org/10.1016/j.scitotenv.2019.07.305

García-Depraect, O., Lebrero, R., Rodriguez-Vega, S., Bordel, S., Santos-Beneit, F., Martínez-Mendoza, L.J., Aragão Börner, R., Börner, T., Muñoz, R., 2022. Biodegradation of bioplastics under aerobic and anaerobic aqueous conditions: Kinetics, carbon fate and particle size effect. Bioresource Technology 344, 126265. https://doi.org/10.1016/j.biortech.2021.126265

GESAMP, G., 2016. Sources, fate and effects of microplastics in the marine environment: part two of a global assessment. IMO London 220.

Gewert, B., Plassmann, M.M., MacLeod, M., 2015. Pathways for degradation of plastic polymers floating in the marine environment. Environ. Sci.: Processes Impacts 17, 1513–1521. https://doi.org/10.1039/C5EM00207A

Gigault, J., Halle, A.T., Baudrimont, M., Pascal, P.-Y., Gauffre, F., Phi, T.-L., El Hadri, H., Grassl, B., Reynaud, S., 2018. Current opinion: What is a nanoplastic? Environmental Pollution 235, 1030–1034. https://doi.org/10.1016/j.envpol.2018.01.024

Grause, G., Chien, M.-F., Inoue, C., 2020. Changes during the weathering of polyolefins. Polymer Degradation and Stability 181, 109364. https://doi.org/10.1016/j.polymdegradstab.2020.109364

Grause, G., Kuniyasu, Y., Chien, M.-F., Inoue, C., 2022. Separation of microplastic from soil by centrifugation and its application to agricultural soil. Chemosphere 288, 132654. https://doi.org/10.1016/j.chemosphere.2021.132654

Gregory, M.R., 2009. Environmental implications of plastic debris in marine settings—entanglement, ingestion, smothering, hangers-on, hitch-hiking and alien invasions. Phil. Trans. R. Soc. B 364, 2013–2025. https://doi.org/10.1098/rstb.2008.0265

Gu, J.-D., 2003. Microbiological deterioration and degradation of synthetic polymeric materials: recent research advances. International Biodeterioration & Biodegradation 52, 69–91. https://doi.org/10.1016/S0964-8305(02)00177-4

Gulmine, J.V., Janissek, P.R., Heise, H.M., Akcelrud, L., 2003. Degradation profile of polyethylene after artificial accelerated weathering. Polymer Degradation and Stability 79, 385–397. https://doi.org/10.1016/S0141-3910(02)00338-5

Hahn, S., Hennecke, D., 2023. What can we learn from biodegradation of natural polymers for regulation? Environmental Sciences Europe 35, 50. https://doi.org/10.1186/s12302-023-00755-y

Haider, T.P., Völker, C., Kramm, J., Landfester, K., Wurm, F.R., 2019. Plastics of the Future? The Impact of Biodegradable Polymers on the Environment and on Society. Angew Chem Int Ed 58, 50–62. https://doi.org/10.1002/anie.201805766

Hamid, S., 2000. Handbook of Polymer Degradation. Marcel Dekker.

Hann, S., Sherrington, C., Jamieson, O., Hickman, M., Kershaw, P., Bapasola, A., Cole, G., 2018. Investigating options for reducing releases in the aquatic environment of microplastics emitted by (but not intentionally added in) products. Report for DG Environment of the European Commission 335.

Hartmann, N.B., Hüffer, T., Thompson, R.C., Hassellöv, M., Verschoor, A., Daugaard, A.E., Rist, S., Karlsson, T., Brennholt, N., Cole, M., Herrling, M.P., Hess, M.C., Ivleva, N.P., Lusher, A.L., Wagner, M., 2019. Are We Speaking the Same Language? Recommendations for a Definition and Categorization Framework for Plastic Debris. Environ. Sci. Technol. 53, 1039–1047. https://doi.org/10.1021/acs.est.8b05297

Hassink, J., Buda, J., Multsch, S., Nellen, S., Noe, S., Schmidt, T., 2024. Development of a new test design to investigate the degradation of pesticides in soil under sunlight conditions. Environ Sci Eur 36, 151. https://doi.org/10.1186/s12302-024-00974-x

He, D., Zhang, X., Hu, J., 2021. Methods for separating microplastics from complex solid matrices: Comparative analysis. Journal of Hazardous Materials 409, 124640. https://doi.org/10.1016/j.jhazmat.2020.124640

Hendrix, K., Bleyen, N., Mennecart, T., Bruggeman, C., Valcke, E., 2019. Sodium azide used as microbial inhibitor caused unwanted by-products in anaerobic geochemical studies. Applied Geochemistry 107, 120–130. https://doi.org/10.1016/j.apgeochem.2019.05.014

Hill, A.P., Young, R.J., 2010. Getting physical in drug discovery: a contemporary perspective on solubility and hydrophobicity. Drug Discovery Today 15, 648–655. https://doi.org/10.1016/j.drudis.2010.05.016

Hoang, V.-H., Nguyen, M.-K., Hoang, T.-D., Ha, M.C., Huyen, N.T.T., Bui, V.K.H., Pham, M.-T., Nguyen, C.-M., Chang, S.W., Nguyen, D.D., 2024. Sources, environmental fate, and impacts of microplastic contamination in agricultural soils: A comprehensive review. Science of The Total Environment 950, 175276. https://doi.org/10.1016/j.scitotenv.2024.175276

Horton, A.A., Dixon, S.J., 2018. Microplastics: An introduction to environmental transport processes. Wiley Interdisciplinary Reviews: Water 5, e1268.

Hurley, R.R., Lusher, A.L., Olsen, M., Nizzetto, L., 2018. Validation of a Method for Extracting Microplastics from Complex, Organic-Rich, Environmental Matrices. Environ. Sci. Technol. 52, 7409–7417. https://doi.org/10.1021/acs.est.8b01517

Imhof, H.K., Ivleva, N.P., Schmid, J., Niessner, R., Laforsch, C., 2013. Contamination of beach sediments of a subalpine lake with microplastic particles. Current Biology 23, R867–R868. https://doi.org/10.1016/j.cub.2013.09.001

International Organization for Standardization., 2023. Principles for the analysis of microplastics present in the environment.

ISO 11277, 2020. Soil quality — Determination of particle size distribution in mineral soil material — Method by sieving and sedimentation.

ISO 14851, 2019. Determination of the ultimate aerobic biodegradability of plastic materials in an aqueous medium — Method by measuring the oxygen demand in a closed respirometer.

ISO 17556, 2019. Plastics — Determination of the ultimate aerobic biodegradability of plastic materials in soil by measuring the oxygen demand in a respirometer or the amount of carbon dioxide evolved.

ISO 18830, 2016. Plastics — Determination of aerobic biodegradation of non-floating plastic materials in a seawater/sandy sediment interface — Method by measuring the oxygen demand in closed respirometer.

ISO 19679, 2020. Plastics — Determination of aerobic biodegradation of non-floating plastic materials in a seawater/sediment interface — Method by analysis of evolved carbon dioxide.

ISO 22404, 2019. Plastics — Determination of the aerobic biodegradation of non-floating materials exposed to marine sediment — Method by analysis of evolved carbon dioxide.

Jakubowicz, I., Yarahmadi, N., Arthurson, V., 2011. Kinetics of abiotic and biotic degradability of low-density polyethylene containing prodegradant additives and its effect on the growth of microbial communities. Polymer Degradation and Stability 96, 919–928. https://doi.org/10.1016/j.polymdegradstab.2011.01.031

Jiang, X., Zhu, X., Arnold, A.A., Kong, X.Z., Claverie, J.P., 2017. Polyurea Structure Characterization by HR-MAS NMR Spectroscopy. Ind. Eng. Chem. Res. 56, 2993–2998. https://doi.org/10.1021/acs.iecr.7b00192

Kale, G., Auras, R., Singh, S.P., Narayan, R., 2007. Biodegradability of polylactide bottles in real and simulated composting conditions. Polymer Testing 26, 1049–1061. https://doi.org/10.1016/j.polymertesting.2007.07.006

Karagianni, K., Kuntzmann-Dembele, F., Bocokic, V., Charbonnier, A., Harrison, I., Kreutzer, G., Mendoza, A., Jenner, K., 2024. Fragrance Encapsulates: Effect of Polymeric Shell Purification Method on the Accuracy of Biodegradability Testing. Enviro Toxic and Chemistry 43, 1242–1249. https://doi.org/10.1002/etc.5852

Kerschberger, M., Deller, B., Hege, U., Heyn, J., Kape, H.E., Krause, O., Pollehn, J., Rex, M.J., Severin, K., 2000. Bestimmung des Kalkbedarfs von Acker-und Grünlandböden. VDLUFA-Verlag: Darmstadt, Germany.

Koh, L.M., Khor, S.M., 2023. Biodegradation Process: Basics, Factors Affecting, and Industrial Applications, in: Ali, G.A.M., Makhlouf, A.S.H. (Eds.), Handbook of Biodegradable Materials. Springer International Publishing, Cham, pp. 19–56. https://doi.org/10.1007/978-3-031-09710-2_66

Kookana, R.S., 2010. The role of biochar in modifying the environmental fate, bioavailability, and efficacy of pesticides in soils: a review. Soil Res. 48, 627. https://doi.org/10.1071/SR10007

Krause, J., Egger, H., 2021. Aqueous Capsule Suspension Concentrates Based on Polyurea Shell Material Containing Polyfunctional Aminocarboxylic Esters. WO2021136758.

Kühn, S., Van Werven, B., Van Oyen, A., Meijboom, A., Bravo Rebolledo, E.L., Van Franeker, J.A., 2017. The use of potassium hydroxide (KOH) solution as a suitable approach to isolate plastics ingested by marine organisms. Marine Pollution Bulletin 115, 86–90. https://doi.org/10.1016/j.marpolbul.2016.11.034

La Mantia, F.P., 1986. Influence of processing conditions on the photo-oxidation of polypropylene films. Polymer degradation and stability 15, 283–290.

Lares, M., Ncibi, M.C., Sillanpää, Markus, Sillanpää, Mika, 2018. Occurrence, identification and removal of microplastic particles and fibers in conventional activated sludge process and advanced MBR technology. Water Research 133, 236–246. https://doi.org/10.1016/j.watres.2018.01.049

Lau, W.W.Y., Shiran, Y., Bailey, R.M., Cook, E., Stuchtey, M.R., Koskella, J., Velis, C.A., Godfrey, L., Boucher, J., Murphy, M.B., Thompson, R.C., Jankowska, E., Castillo Castillo, A., Pilditch, T.D., Dixon, B., Koerselman, L., Kosior, E., Favoino, E., Gutberlet, J., Baulch, S., Atreya, M.E., Fischer, D., He, K.K., Petit, M.M., Sumaila, U.R., Neil, E., Bernhofen, M.V., Lawrence, K., Palardy, J.E., 2020. Evaluating scenarios toward zero plastic pollution. Science 369, 1455–1461. https://doi.org/10.1126/science.aba9475

Lemaire, J., Arnaud, R., Lacoste, J., 1988. The prediction of the long-term photoageing of solid polymers. Acta Polymerica 39, 27–32. https://doi.org/10.1002/actp.1988.010390106

Li, S., Wang, B., Zhang, X., Wang, H., Yi, Y., Huang, X., Gao, X., Zhu, P., Han, W., 2023. Soil particle aggregation and aggregate stability associated with ion specificity and organic matter content. Geoderma 429, 116285. https://doi.org/10.1016/j.geoderma.2022.116285

Li, Z.-Z., Xu, S.-A., Wen, L.-X., Liu, F., Liu, A.-Q., Wang, Q., Sun, H.-Y., Yu, W., Chen, J.-F., 2006. Controlled release of avermectin from porous hollow silica nanoparticles: Influence of shell thickness on loading efficiency, UV-shielding property and release. Journal of Controlled Release 111, 81–88. https://doi.org/10.1016/j.jconrel.2005.10.020

Liu, P., Wu, X., Peng, J., Wang, H., Shi, Y., Huang, H., Gao, S., 2021. Critical effect of iron red pigment on photoaging behavior of polypropylene microplastics in artificial seawater. Journal of Hazardous Materials 404, 124209. https://doi.org/10.1016/j.jhazmat.2020.124209

Lucas, N., Bienaime, C., Belloy, C., Queneudec, M., Silvestre, F., Nava-Saucedo, J.-E., 2008. Polymer biodegradation: Mechanisms and estimation techniques – A review. Chemosphere 73, 429–442. https://doi.org/10.1016/j.chemosphere.2008.06.064

Lusher, A.L., McHugh, M., Thompson, R.C., 2013. Occurrence of microplastics in the gastrointestinal tract of pelagic and demersal fish from the English Channel. Marine Pollution Bulletin 67, 94–99. https://doi.org/10.1016/j.marpolbul.2012.11.028

MacLeod, M., Arp, H.P.H., Tekman, M.B., Jahnke, A., 2021. The global threat from plastic pollution. Science 373, 61–65. https://doi.org/10.1126/science.abg5433

Mani, T., Frehland, S., Kalberer, A., Burkhardt-Holm, P., 2019. Using castor oil to separate microplastics from four different environmental matrices. Anal. Methods 11, 1788–1794. https://doi.org/10.1039/C8AY02559B

Manshoven, S., Smeets, A., Malarciuc, C., Tenhunen-Lunkka, A., Mortensen, L.F., 2022. Microplastic pollution from textile consumption in Europe (No. ETC/CE 2022/1), Eionet Report. European Topic Centre Circular Economy and Resource Use.

Mao, R., Lang, M., Yu, X., Wu, R., Yang, X., Guo, X., 2020. Aging mechanism of microplastics with UV irradiation and its effects on the adsorption of heavy metals. Journal of Hazardous Materials 393, 122515. https://doi.org/10.1016/j.jhazmat.2020.122515

McDonough, K., Itrich, N., Casteel, K., Menzies, J., Williams, T., Krivos, K., Price, J., 2017. Assessing the biodegradability of microparticles disposed down the drain. Chemosphere 175, 452–458. https://doi.org/10.1016/j.chemosphere.2017.02.091

McNeill, K., Canonica, S., 2016. Triplet state dissolved organic matter in aquatic photochemistry: reaction mechanisms, substrate scope, and photophysical properties. Environ. Sci.: Processes Impacts 18, 1381–1399. https://doi.org/10.1039/C6EM00408C

Mekaru, H., 2020. Effect of Agitation Method on the Nanosized Degradation of Polystyrene Microplastics Dispersed in Water. ACS Omega 5, 3218–3227. https://doi.org/10.1021/acsomega.9b03278

Meng, F., Drews, A., Mehrez, R., Iversen, V., Ernst, M., Yang, F., Jekel, M., Kraume, M., 2009. Occurrence, Source, and Fate of Dissolved Organic Matter (DOM) in a Pilot-Scale Membrane Bioreactor. Environ. Sci. Technol. 43, 8821–8826. https://doi.org/10.1021/es9019996

Mie, G., 1908. Beiträge zur Optik trüber Medien, speziell kolloidaler Metallösungen. Annalen der physik 330, 377–445.

Mitrano, D.M., Wohlleben, W., 2020. Microplastic regulation should be more precise to incentivize both innovation and environmental safety. Nat Commun 11, 5324. https://doi.org/10.1038/s41467-020-19069-1

Möller, J.N., Löder, M.G.J., Laforsch, C., 2020. Finding Microplastics in Soils: A Review of Analytical Methods. Environ. Sci. Technol. 54, 2078–2090. https://doi.org/10.1021/acs.est.9b04618

Nava, V., Leoni, B., 2021a. Comparison of Different Procedures for Separating Microplastics from Sediments. Water 13, 2854. https://doi.org/10.3390/w13202854

Nava, V., Leoni, B., 2021b. Comparison of Different Procedures for Separating Microplastics from Sediments. Water 13, 2854. https://doi.org/10.3390/w13202854

Nederstigt, T.A.P., Brinkmann, B.W., Peijnenburg, W.J.G.M., Vijver, M.G., 2024. Sustainability Claims of Nanoenabled Pesticides Require a More Thorough Evaluation. Environ. Sci. Technol. 58, 2163–2165. https://doi.org/10.1021/acs.est.3c10207

Ng, E.-L., Huerta Lwanga, E., Eldridge, S.M., Johnston, P., Hu, H.-W., Geissen, V., Chen, D., 2018. An overview of microplastic and nanoplastic pollution in agroecosystems. Science of The Total Environment 627, 1377–1388. https://doi.org/10.1016/j.scitotenv.2018.01.341

Nishida, H., Tokiwa, Y., 1992. Effects of higher-order structure of poly(3-hydroxybutyrate) on its biodegradation. I. Effects of heat treatment on microbial degradation. J of Applied Polymer Sci 46, 1467–1476. https://doi.org/10.1002/app.1992.070460818

Nuelle, M.-T., Dekiff, J.H., Remy, D., Fries, E., 2014. A new analytical approach for monitoring microplastics in marine sediments. Environmental Pollution 184, 161–169. https://doi.org/10.1016/j.envpol.2013.07.027

OECD Draft TG (Ed.), 2002. Draft TG - Proposal for a new Guideline: Phototransformation of chemicals on soil surface. OECD Publishing, Paris.

OECD TG 301 (Ed.), 1992. Test No. 301: Ready Biodegradability, OECD Guidelines for the Testing of Chemicals, Section 3. OECD Publishing, Paris. https://doi.org/10.1787/9789264070349-en

OECD TG 302C (Ed.), 2009. Test No. 302C: Inherent Biodegradability: Modified MITI Test (II), OECD Guidelines for the Testing of Chemicals, Section 3. OECD Publishing, Paris. https://doi.org/10.1787/9789264070400-en

OECD TG 306 (Ed.), 1992. Test No. 306: Biodegradability in Seawater, OECD Guidelines for the Testing of Chemicals, Section 3. OECD Publishing, Paris. https://doi.org/10.1787/9789264070486-en

OECD TG 307 (Ed.), 2002. Test No. 307: Aerobic and Anaerobic Transformation in Soil, OECD Guidelines for the Testing of Chemicals, Section 3. OECD Publishing, Paris. https://doi.org/10.1787/9789264070509-en

OECD TG 308 (Ed.), 2002. Test No. 308: Aerobic and Anaerobic Transformation in Aquatic Sediment Systems, OECD Guidelines for the Testing of Chemicals, Section 3. OECD Publishing, Paris. https://doi.org/10.1787/9789264070523-en

OECD TG 309 (Ed.), 2004. Test No. 309: Aerobic Mineralisation in Surface Water Simulation Biodegradation Test, OECD Guidelines for the Testing of Chemicals, Section 3. OECD Publishing, Paris. https://doi.org/10.1787/9789264070547-en

OECD TG 310 (Ed.), 2006. Test No. 310: Ready biodegradability: CO2 in sealed vesels (Headspace test), OECD guidelines for the testing of chemicals. OECD Publishing, Paris.

OECD TG 316 (Ed.), 2008. Test No. 316: Phototransformation of Chemicals in Water Direct Photolysis, OECD Guidelines for the Testing of Chemicals, Section 3. OECD Publishing, Paris. https://doi.org/10.1787/9789264067585-en

Persson, L., Carney Almroth, B.M., Collins, C.D., Cornell, S., De Wit, C.A., Diamond, M.L., Fantke, P., Hassellöv, M., MacLeod, M., Ryberg, M.W., Søgaard Jørgensen, P., Villarrubia-Gómez, P., Wang, Z., Hauschild, M.Z., 2022. Outside the Safe Operating Space of the Planetary Boundary for Novel Entities. Environ. Sci. Technol. 56, 1510–1521. https://doi.org/10.1021/acs.est.1c04158

Pfohl, P., Roth, C., Wohlleben, W., 2024. The power of centrifugation: How to extract microplastics from soil with high recovery and matrix removal efficiency. MethodsX 12, 102598. https://doi.org/10.1016/j.mex.2024.102598

Piñon-Colin, T.D.J., Rodriguez-Jimenez, R., Rogel-Hernandez, E., Alvarez-Andrade, A., Wakida, F.T., 2020. Microplastics in stormwater runoff in a semiarid region, Tijuana, Mexico. Science of The Total Environment 704, 135411. https://doi.org/10.1016/j.scitotenv.2019.135411

Pires-Oliveira, R., Kfouri, M.S., Mendonça, B., Cardoso-Gustavson, P., 2020. Nanopesticides: From the bench to the market. Nanopesticides: From Research and Development to Mechanisms of Action and Sustainable Use in Agriculture 317–348.

Powell, H.K.J., Fenton, E., 1996. Size fractionation of humic substances: Effect on protonation and metal binding properties. Analytica Chimica Acta 334, 27–38. https://doi.org/10.1016/S0003-2670(96)00324-8

Preisler, A.C., Pereira, A.E., Campos, E.V., Dalazen, G., Fraceto, L.F., Oliveira, H.C., 2019. Atrazine nanoencapsulation improves pre-emergence herbicidal activity against Bidens pilosa without enhancing long-term residual effect on Glycine max. Pest Manag Sci.

Prosenc, F., Leban, P., Šunta, U., Bavcon Kralj, M., 2021a. Extraction and Identification of a Wide Range of Microplastic Polymers in Soil and Compost. Polymers 13, 4069. https://doi.org/10.3390/polym13234069

Prosenc, F., Leban, P., Šunta, U., Bavcon Kralj, M., 2021b. Extraction and Identification of a Wide Range of Microplastic Polymers in Soil and Compost. Polymers 13, 4069. https://doi.org/10.3390/polym13234069

Quijada, R., Narváez, A., Rojas, R., Rabagliati, F.M., Barrera Galland, G., Santos Mauler, R., Benavente, R., Pérez, E., Pereña, J.M., Bello, A., 1999. Synthesis and characterization of copolymers of ethylene and 1-octadecene using the rac-Et (Ind) 2ZrCl2/MAO catalyst system. Macromolecular Chemistry and Physics 200, 1306–1310.

Rabek, J.F., Rånby, B., 1974. Studies on the photooxidation mechanism of polymers. II. The role of quinones as sensitizers in the photooxidative degradation of polystyrene. J. Polym. Sci. Polym. Chem. Ed. 12, 295–306. https://doi.org/10.1002/pol.1974.170120204

Radford, F., Zapata-Restrepo, L.M., Horton, A.A., Hudson, M.D., Shaw, P.J., Williams, I.D., 2021. Developing a systematic method for extraction of microplastics in soils. Anal. Methods 13, 1695–1705. https://doi.org/10.1039/D0AY02086A

Rajakumar, K., Sarasvathy, V., Thamarai Chelvan, A., Chitra, R., Vijayakumar, C.T., 2009. Natural Weathering Studies of Polypropylene. J Polym Environ 17, 191–202. https://doi.org/10.1007/s10924-009-0138-7

Rani, M., Ducoli, S., Depero, L.E., Prica, M., Tubić, A., Ademovic, Z., Morrison, L., Federici, S., 2023. A Complete Guide to Extraction Methods of Microplastics from Complex Environmental Matrices. Molecules 28, 5710. https://doi.org/10.3390/molecules28155710

Richardson, K., Steffen, W., Lucht, W., Bendtsen, J., Cornell, S.E., Donges, J.F., Drüke, M., Fetzer, I., Bala, G., Von Bloh, W., Feulner, G., Fiedler, S., Gerten, D., Gleeson, T., Hofmann, M., Huiskamp, W., Kummu, M., Mohan, C., Nogués-Bravo, D., Petri, S., Porkka, M., Rahmstorf, S., Schaphoff, S., Thonicke, K., Tobian, A., Virkki, V., Wang-Erlandsson, L., Weber, L., Rockström, J., 2023. Earth beyond six of nine planetary boundaries. Sci. Adv. 9, eadh2458. https://doi.org/10.1126/sciadv.adh2458

Roy, A., Singh, S., Bajpai, J., Bajpai, A., 2014. Controlled pesticide release from biodegradable polymers. Open Chemistry 12, 453–469. https://doi.org/10.2478/s11532-013-0405-2

Rujnić-Sokele, M., Pilipović, A., 2017. Challenges and opportunities of biodegradable plastics: A mini review. Waste Manag Res 35, 132–140. https://doi.org/10.1177/0734242X16683272

Sa'adu, I., Farsang, A., 2023. Plastic contamination in agricultural soils: a review. Environ Sci Eur 35, 13. https://doi.org/10.1186/s12302-023-00720-9

Sadi, R.K., Fechine, G.J.M., Demarquette, N.R., 2013. Effect of prior photodegradation on the biodegradation of polypropylene/poly(3-hydroxybutyrate) blends. Polym Eng Sci 53, 2109–2122. https://doi.org/10.1002/pen.23471

Scheurer, M., Bigalke, M., 2018. Microplastics in Swiss Floodplain Soils. Environ. Sci. Technol. 52, 3591–3598. https://doi.org/10.1021/acs.est.7b06003

Schmidt, C., Kühnel, D., Materić, D., Stubenrauch, J., Schubert, K., Luo, A., Wendt-Potthoff, K., Jahnke, A., 2024. A multidisciplinary perspective on the role of plastic pollution in the triple planetary crisis. Environment International 193, 109059. https://doi.org/10.1016/j.envint.2024.109059

Schnabel, W., 1981. Polymer Degradation: Principles and Practice. Carl Hanser Verlag, Wien 2, 133.

Schwaferts, C., Niessner, R., Elsner, M., Ivleva, N.P., 2019. Methods for the analysis of submicrometer- and nanoplastic particles in the environment. TrAC Trends in Analytical Chemistry 112, 52–65. https://doi.org/10.1016/j.trac.2018.12.014

Scopetani, C., Chelazzi, D., Mikola, J., Leiniö, V., Heikkinen, R., Cincinelli, A., Pellinen, J., 2020a. Olive oil-based method for the extraction, quantification and identification of microplastics in

soil and compost samples. Science of The Total Environment 733, 139338. https://doi.org/10.1016/j.scitotenv.2020.139338

Scopetani, C., Chelazzi, D., Mikola, J., Leiniö, V., Heikkinen, R., Cincinelli, A., Pellinen, J., 2020b. Olive oil-based method for the extraction, quantification and identification of microplastics in soil and compost samples. Science of The Total Environment 733, 139338. https://doi.org/10.1016/j.scitotenv.2020.139338

Seo, Y., Zhou, Z., Lai, Y., Chen, G., Pembleton, K., Wang, S., He, J., Song, P., 2024. Micro- and nanoplastics in agricultural soils: Assessing impacts and navigating mitigation. Science of The Total Environment 931, 172951. https://doi.org/10.1016/j.scitotenv.2024.172951

Si, T., Kim, H.Y., Oh, K., 2021. One-Pot Direct Oxidation of Primary Amines to Carboxylic Acids through Tandem *ortho* -Naphthoquinone-Catalyzed and TBHP-Promoted Oxidation Sequence. Chemistry A European J 27, 18150–18155. https://doi.org/10.1002/chem.202103450

Silva, R.R.A., Marques, C.S., Arruda, T.R., Teixeira, S.C., De Oliveira, T.V., 2023. Biodegradation of Polymers: Stages, Measurement, Standards and Prospects. Macromol 3, 371–399. https://doi.org/10.3390/macromol3020023

Singh, B., Sharma, N., 2008. Mechanistic implications of plastic degradation. Polymer Degradation and Stability 93, 561–584. https://doi.org/10.1016/j.polymdegradstab.2007.11.008

Sinn, H., Kaminsky, W., Vollmer, H., Woldt, R., 1980. "Living Polymers" on Polymerization with Extremely Productive Ziegler Catalysts. Angew. Chem. Int. Ed. Engl. 19, 390–392. https://doi.org/10.1002/anie.198003901

Sivan, A., 2011. New perspectives in plastic biodegradation. Current Opinion in Biotechnology 22, 422–426. https://doi.org/10.1016/j.copbio.2011.01.013

Sopeña, F., Cabrera, A., Maqueda, C., Morillo, E., 2007. Ethylcellulose Formulations for Controlled Release of the Herbicide Alachlor in a Sandy Soil. Journal of Agricultural and Food Chemistry 55, 8200–8205. https://doi.org/10.1021/jf071459g

Sopeña, F., Maqueda, C., Morillo, E., 2009. Controlled release formulations of herbicides based on micro-encapsulation. CIENCIA E INVESTIGACIÓN AGRARIA 36.

Sridharan, S., Kumar, M., Saha, M., Kirkham, M.B., Singh, L., Bolan, N.S., 2022. The polymers and their additives in particulate plastics: What makes them hazardous to the fauna? Science of The Total Environment 824, 153828. https://doi.org/10.1016/j.scitotenv.2022.153828

Sun, Y., Yuan, J., Zhou, T., Zhao, Y., Yu, F., Ma, J., 2020. Laboratory simulation of microplastics weathering and its adsorption behaviors in an aqueous environment: A systematic review. Environmental Pollution 265, 114864. https://doi.org/10.1016/j.envpol.2020.114864

Surendran, U., Jayakumar, M., Raja, P., Gopinath, G., Chellam, P.V., 2023. Microplastics in terrestrial ecosystem: Sources and migration in soil environment. Chemosphere 318, 137946. https://doi.org/10.1016/j.chemosphere.2023.137946

Süßmuth, R., Shrestha, P., Andrea Diaz Navarrete, C., Wege, F.-F., Achten, C., Hennecke, D., 2024. Impact of different sterilisation techniques on sorption and NER formation of test chemicals in soil. Chemosphere 357, 141915. https://doi.org/10.1016/j.chemosphere.2024.141915

Teggers, E.-M., Hardebusch, J., Meisterjahn, B., Simon, M., Hennecke, D., Heumann, R., Egger, H., Dalkmann, P., Schäffer, A., Jahnke, A., 2025a. Diversifying endpoints in biodegradation testing of microplastics. Environ Sci Eur 37, 65. https://doi.org/10.1186/s12302-025-01096-8

Teggers, E.-M., Heck, S., Meisterjahn, B., Simon, M., Hennecke, D., Heumann, R., Egger, H., Dalkmann, P., Jahnke, A., Schäffer, A., 2025b. Modified oil extraction of pristine and weathered synthetic polyurea microcapsules and polyethylene microplastics from soil. Microplastics and Nanoplastics. https://doi.org/10.1186/s43591-025-00121-0

Teggers, E.-M., Winterhoff, S., Heck, S., Hardebusch, J., Meisterjahn, B., Simon, M., Hennecke, D., Heumann, R., Egger, H., Dalkmann, P., Schäffer, A., Jahnke, A., 2025c. Simulated Sunlight Exposure can be Prerequisite for the Biodegradation of Persistent Microplastics. Journal of Hazardous Materials.

Tester, M., Morris, C., 1987. The penetration of light through soil. Plant Cell & Environment 10, 281–286. https://doi.org/10.1111/j.1365-3040.1987.tb01607.x

Thomas, D., Schütze, B., Heinze, W.M., Steinmetz, Z., 2020. Sample Preparation Techniques for the Analysis of Microplastics in Soil—A Review. Sustainability 12, 9074. https://doi.org/10.3390/su12219074

Tidjani, A., 2000. Comparison of formation of oxidation products during photo-oxidation of linear low density polyethylene under different natural and accelerated weathering conditions. Polymer Degradation and Stability 68, 465–469. https://doi.org/10.1016/S0141-3910(00)00039-2

Tokiwa, Y., Calabia, B., Ugwu, C., Aiba, S., 2009. Biodegradability of Plastics. IJMS 10, 3722–3742. https://doi.org/10.3390/ijms10093722

UNEP, 2022. Resolution Adopted by the United Nations Environment Assembly on 2 March 2022. 5/5. Nature-based solutions for supporting sustainable development.

Vermeiren, P., Muñoz, C., Ikejima, K., 2020. Microplastic identification and quantification from organic rich sediments: A validated laboratory protocol. Environmental Pollution 262, 114298. https://doi.org/10.1016/j.envpol.2020.114298

Villarrubia-Gómez, P., Carney Almroth, B., Eriksen, M., Ryberg, M., Cornell., S.E., 2024. Plastics pollution exacerbates the impacts of all planetary boundaries. One Earth 7, 2119–2138. https://doi.org/10.1016/j.oneear.2024.10.017

Wang, A., Wang, Y., Sun, C., Wang, C., Cui, B., Zhao, X., Zeng, Z., Yao, J., Yang, D., Liu, G., Cui, H., 2018. Fabrication, Characterization, and Biological Activity of Avermectin Nano-delivery Systems with Different Particle Sizes. Nanoscale Res Lett 13, 2. https://doi.org/10.1186/s11671-017-2405-1

Wang, C., Wang, L., Ok, Y.S., Tsang, D.C.W., Hou, D., 2022. Soil plastisphere: Exploration methods, influencing factors, and ecological insights. Journal of Hazardous Materials 430, 128503. https://doi.org/10.1016/j.jhazmat.2022.128503

Wang, J., Chen, J., Qiao, X., Zhang, Y., Uddin, M., Guo, Z., 2019. Disparate effects of DOM extracted from coastal seawaters and freshwaters on photodegradation of 2,4-Dihydroxybenzophenone. Water Research 151, 280–287. https://doi.org/10.1016/j.watres.2018.12.045

Weng, J., Müller, K., Morgaienko, O., Elsner, M., Ivleva, N.P., 2023. Multi-element stable isotope Raman microspectroscopy of bacterial carotenoids unravels rare signal shift patterns and single-cell phenotypic heterogeneity. Analyst 148, 128–136. https://doi.org/10.1039/D2AN01603F

Wenzel, M., Fischer, B., Renner, G., Schoettl, J., Wolf, C., Schram, J., Schmidt, T.C., Tuerk, J., 2022. Efficient and sustainable microplastics analysis for environmental samples using flotation for sample pre-treatment. Green Analytical Chemistry 3, 100044. https://doi.org/10.1016/j.greeac.2022.100044

Wienhold, B.J., Gish, T.J., 1994. Chemical properties influencing rate of release of starch encapsulated herbicides: implications for modifying environmental fate. Chemosphere 28, 1035–1046.

Wohlleben, W., Bossa, N., Mitrano, D.M., Scott, K., 2024. Everything falls apart: How solids degrade and release nanomaterials, composite fragments, and microplastics. NanoImpact 34, 100510. https://doi.org/10.1016/j.impact.2024.100510

Wu, X., Liu, P., Gong, Z., Wang, H., Huang, H., Shi, Y., Zhao, X., Gao, S., 2021a. Humic Acid and Fulvic Acid Hinder Long-Term Weathering of Microplastics in Lake Water. Environ. Sci. Technol. 55, 15810–15820. https://doi.org/10.1021/acs.est.1c04501

Wu, X., Liu, P., Wang, H., Huang, H., Shi, Y., Yang, C., Gao, S., 2021b. Photo aging of polypropylene microplastics in estuary water and coastal seawater: Important role of chlorine ion. Water Research 202, 117396. https://doi.org/10.1016/j.watres.2021.117396

Xu, Y., Ou, Q., Van Der Hoek, J.P., Liu, G., Lompe, K.M., 2024. Photo-oxidation of Micro- and Nanoplastics: Physical, Chemical, and Biological Effects in Environments. Environ. Sci. Technol. 58, 991–1009. https://doi.org/10.1021/acs.est.3c07035

You, S.-J., Thakali, S., Allen, H.E., 2006. Characteristics of soil organic matter (SOM) extracted using base with subsequent pH lowering and sequential pH extraction. Environment International 32, 101–105. https://doi.org/10.1016/j.envint.2005.07.003

Yu, X., Xu, Y., Lang, M., Huang, D., Guo, X., Zhu, L., 2022. New insights on metal ions accelerating the aging behavior of polystyrene microplastics: Effects of different excess reactive oxygen species. Science of The Total Environment 821, 153457. https://doi.org/10.1016/j.scitotenv.2022.153457

Yuan, J., Ma, J., Sun, Y., Zhou, T., Zhao, Y., Yu, F., 2020. Microbial degradation and other environmental aspects of microplastics/plastics. Science of The Total Environment 715, 136968. https://doi.org/10.1016/j.scitotenv.2020.136968

Yuan, Z., Chen, H., Zhang, J., Zhao, D., Liu, Y., Zhou, X., Li, S., Shi, P., Tang, J., Chen, X., 2008. Preparation and characterization of self-cleaning stable superhydrophobic linear low-density polyethylene. Science and Technology of Advanced Materials 9, 045007. https://doi.org/10.1088/1468-6996/9/4/045007

Zhang, Y., Cheng, F., Zhang, T., Li, C., Qu, J., Chen, J., Peijnenburg, W.J.G.M., 2022. Dissolved Organic Matter Enhanced the Aggregation and Oxidation of Nanoplastics under Simulated Sunlight Irradiation in Water. Environ. Sci. Technol. 56, 3085–3095. https://doi.org/10.1021/acs.est.1c07129

Zhao, S., Li, K., Zhou, W., Qiu, S., Huang, S., He, P., 2016. Changes in soil microbial community, enzyme activities and organic matter fractions under long-term straw return in north-central China. Agriculture, Ecosystems & Environment 216, 82–88. https://doi.org/10.1016/j.agee.2015.09.028

Zhu, K., Sun, Y., Jiang, W., Zhang, C., Dai, Y., Liu, Z., Wang, T., Guo, X., Jia, H., 2022. Inorganic anions influenced the photoaging kinetics and mechanism of polystyrene microplastic under the simulated sunlight: Role of reactive radical species. Water Research 216, 118294. https://doi.org/10.1016/j.watres.2022.118294

Zumstein, M.T., Narayan, R., Kohler, H.-P.E., McNeill, K., Sander, M., 2019. Dos and Do Nots When Assessing the Biodegradation of Plastics. Environ. Sci. Technol. 53, 9967–9969. https://doi.org/10.1021/acs.est.9b04513

Zumstein, M.T., Schintlmeister, A., Nelson, T.F., Baumgartner, R., Woebken, D., Wagner, M., Kohler, H.-P.E., McNeill, K., Sander, M., 2018. Biodegradation of synthetic polymers in soils: Tracking carbon into CO_2 and microbial biomass. Sci. Adv. 4, eaas9024. https://doi.org/10.1126/sciadv.aas9024

XI. Appendix – General

Table A1. Overview of the five groups of test methods for demonstrating polymer degradability under the REACH MPs restriction (Appendix 15, Entry 78).
Groups 1-3 consist of OECD-based screening tests for ready and inherent biodegradability (OECD TG 301, 1992; OECD TG 302C, 2009; OECD TG 310, 2006). Group 4 includes ISO screening tests assessing degradation relative to reference materials (DIN EN ISO 14852, 2021; ISO 14851, 2019; ISO 17556, 2019; ISO 18830, 2016; ISO 19679, 2020; ISO 22404, 2019), while Group 5 comprises simulation tests under environmentally relevant conditions (OECD TG 306, 1992; OECD TG 307, 2002; OECD TG 308, 2002; OECD TG 309, 2004). Satisfying pass criteria in Groups 1-3 is sufficient for general compliance, whereas Groups 4–5 require demonstration of degradation in multiple environmental compartments, particularly for polymers used in agricultural and horticultural products.

Screening Test Methods				Simulation Test Methods
Group 1	**Group 2**	**Group 3**	**Group 4**	**Group 5**
"Ready Biodegradability"	"Ready Biodegradability"	"Inherent Biodegradability"	"degradation relative to a reference material"	"degradation under relevant environmental conditions"
Screening test methods and pass criteria	Modified and enhanced screening test methods and pass criteria	Screening test method and pass criteria	Screening test method and pass criteria	Simulation test methods and pass criteria
OECD TG 301B,C,D,F OECD TG 310	OECD TG 301 B,C,D,F OECD TG 310 OECD TG 306	OECD 302 C	EN ISO 14852:2021 EN ISO 14851:2019 EN ISO 19679:2020 EN ISO 18830:2016 EN ISO 17556:2019 ISO 22404:2019	OECD TG 307 OECD TG 308 OECD TG 309
Sufficient for demonstrating polymer degradability by..				
..meeting pass criteria in any of the test methods of group 1 to 3			..meeting pass criteria in three environmental compartments (group 4 or group 5)	
			For polymers in agricultural & horticultural products (other than fertilising products): ..meeting pass criteria in two environmental compartments (group 4 or group 5)	

Table A2. Particle size analysis of the polyurea microcapsule suspensions prior to washing off residues <12µm and LLDPE after cryo-milling. Measurements were performed using the Analysette 22 Nano TEC (Fritsch GmbH, Germany) for the measurements of LLDPE and the Mastersizer 2000 (Malvern, UK) for the polyurea microcapsules. Calculations were based on Mie diffraction theory (Mie, 1908).

Material	Form	Dispersant	Obscu r- ation	Particle refractive index (RI)	Percentile d(0.1) x in µm	Media n d(0.5) x in µm	Percentile d(0.9) x in µm
Linear low-density 14C-polyethylene (LLDPE)	Silage film, cryo-milled	Ethanol	8 %	1.52	48.8	147.0	342.7
Polyurea (PUA_{mod})	Initial microcapsule suspension	Water	5 %	1.52	2.1	16.5	37.1
Polyurea (PUA)	Initial microcapsule suspension	Water	4 %	1.52	4.8	15.4	32.7
Polyurea (PUA_{mod})	Microcapsule suspension after removal of residuals <12 µm	Calculative (based on measurement of the initial suspension)	-	-	14.2	22.9	45.7
Polyurea (PUA)	Microcapsule suspension after removal of residuals <12 µm	Calculative (based on measurement of the initial suspension)	-	-	13.0	20.2	36.8

Table A 3. Particle size distribution analysis size data of the unprocessed suspension (particle-volume-based). Given is the proportion of the total particle volume of a measured size class [µm] relative to the total volume of all particles. Measurements were performed in water by the Malvern Mastersizer 2000. Calculations were based on the Mie diffraction theory.

Size [µm]	Percentage of particle volume of the initial suspension [%particle-volume-based]	Size [µm]	Percentage of particle volume of the initial suspension [%particle-volume-based]	Size [µm]	Percentage of particle volume of the initial suspension [%particle-volume-based]
0.011	0	2.884	1	724.44	0
0.013	0	3.311	1.1	831.76	0
0.015	0	3.802	1.23	954.99	0
0.017	0	4.365	1.39	1096.5	0
0.02	0	5.012	1.6	1258.9	0
0.023	0	5.754	1.88	1445.4	0
0.026	0	6.607	2.2	1659.6	0
0.03	0	7.586	2.63	1905.5	0
0.035	0	8.71	3.16	2187.8	0
0.04	0	10	3.78	2511.9	0
0.046	0	11.482	4.49	2884	0
0.052	0	13.183	5.22	3311.3	0
0.06	0	15.136	5.94	3801.9	0
0.069	0	17.378	6.54	4365.2	0
0.079	0	19.953	6.98	5011.9	0
0.091	0	22.909	7.11	5754.4	0
0.105	0	26.303	6.96	6606.9	0
0.12	0	30.2	6.48	7585.8	0
0.138	0	34.674	5.71	8709.6	0
0.158	0	39.811	4.75	10000	0
0.182	0	45.709	3.68		
0.209	0	52.481	2.65		
0.24	0	60.256	1.73		
0.275	0.01	69.183	0.99		
0.316	0.09	79.433	0.51		
0.363	0.18	91.201	0.05		
0.417	0.27	104.71	0		
0.479	0.37	120.23	0		
0.55	0.48	138.04	0		
0.631	0.57	158.49	0		
0.724	0.66	181.97	0		
0.832	0.74	208.93	0		
0.955	0.8	239.88	0		
1.096	0.84	275.42	0		
1.259	0.88	316.23	0		
1.445	0.88	363.08	0		
1.66	0.87	416.87	0		
1.905	0.87	478.63	0		
2.188	0.89	549.54	0		
2.512	0.93	630.96	0		

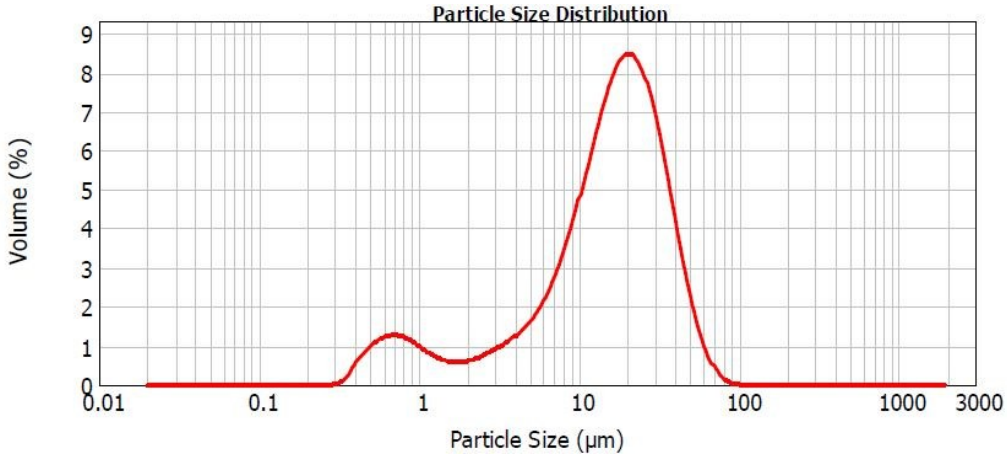

Figure A1. Particle size analysis of the unprocessed modified polyurea microcapsule suspension (PUA_{mod}). Measurements were performed in water by the Malvern Mastersizer 2000. Calculations were based on the Mie diffraction theory (Mie, 1908). Median and percentiles of the measurement are displayed in Table A2.

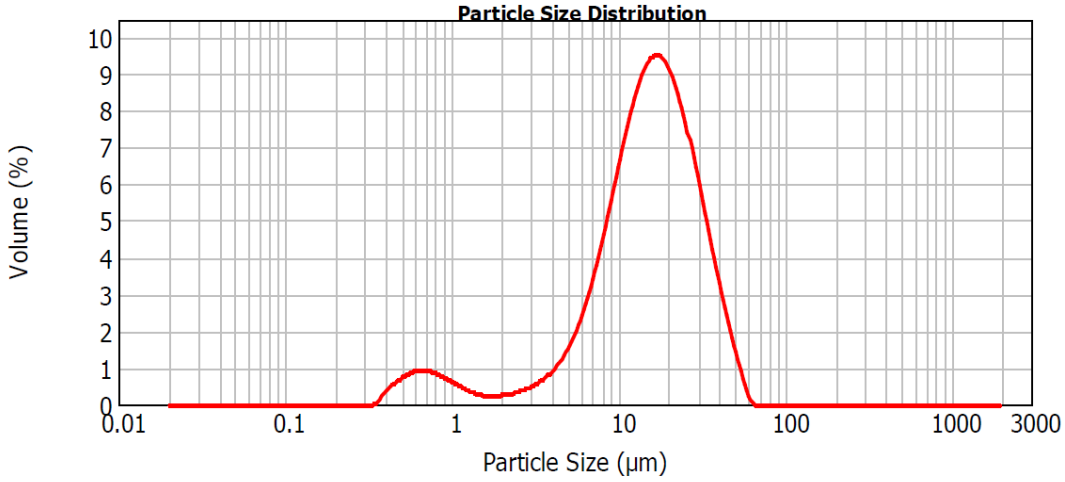

Figure A2. Particle size analysis of the unprocessed polyurea microcapsule suspension (PUA). Measurements were performed in water by the Malvern Mastersizer 2000. Calculations were based on the Mie diffraction theory (Mie, 1908). Median and percentiles of the measurement are displayed in Table A2.

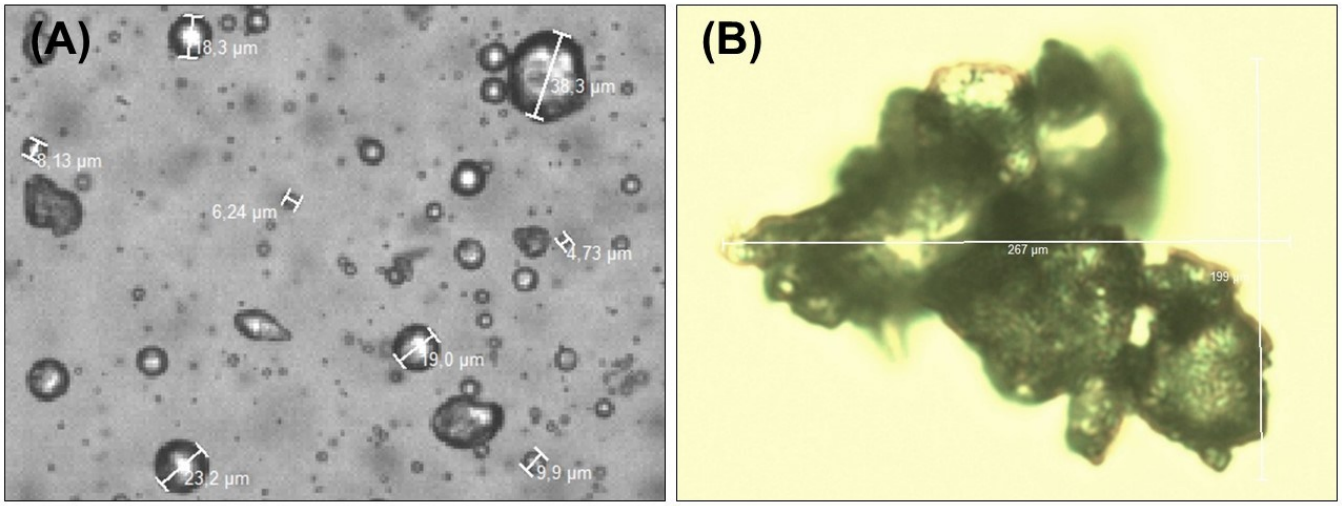

Figure A3. Microscopic image of the (A) polyurea capsules suspension (PUAmod) prior to washing off residues <12µm, (B) a LLDPE particle (approx. width of 267 µm and height of 199 µm).

XII. Appendix - Part 1

Table A4. Analyses Data of the Reference Soils (RefeSol 03-G and 01-A).

Date of sampling	Soil type and batch number	Sand	Silt	Clay	Soil texture		C_{org}	Total N	pH ($CaCl_2$)	pH (H_2O)	CEC_{eff}	Mg ($CaCl_2$)	WHC_{max}	Microbial biomass
		%	%	%			%	g/kg			mmol/kg	mg/kg	g/kg	mg/kg C_{mik}
07.08.2023	01-A-06	69.8	24.40	5.90	SI2	sandy loam	1.03	0.88	6.84	7.45	45.00	26.80	287.00	174.00
09.10.2023	01-A-07	74.10	17.10	8.80	Sl2	sandy loam	1.18	0.85	5.29	6.03	10.00		239.00	135.00
07.08.2023	03-G-05	13.10	62.70	24.20	Lu	silt loam	3.87	4.67	5.68	6.44	140.00	141.50	793.00	1711.00

Analytical Methods used:	
Soil texture:	acc. to ISO 11277 (2020)
Crganic carbon (C_{org})	DIN EN 15936 (DIN EN 15936, 2022)
Total N	Kjeldahlextraktion acc. to VDLUFA (Kerschberger et al., 2000)
pH	DIN EN 15933 (DIN EN 15933, 2012)
CEC_{eff}	DIN ISO 11260 (DIN EN ISO 11260, 2018)
Mg ($CaCl_2$)	Acc. to VDLUFA (Kerschberger et al., 2000)
WHC_{max}	Fraunhofer IME - SOP V3-370
Determination of the microbial biomass	DIN ISO 14240-2: 2011-09 (DIN EN ISO 14240-2, 2011)

Table A5. Summary of the specifications of the test column used for the UHPLC separation.

Column	Bonded phase	pH range	Physical dimension (mm)	Carbon load (%)	Particle size (µm)	Pore size (Å)	Modus
YMC-Pack ODS-AQ	C18 (RP18, ODS, Octadecyl)	2.0 - 7.5	2.1×250	14	3.0	120	Reversed phase (RP)

Table A6. The UHPLC instrumental analysis parameters for measurement of mass range of 100-1200 m/z (positive and negative ions) of the polyurea microcapsule suspension.

UHPLC conditions				
Column temperature (°C)	30			
Resolution	70,000			
Run time (min)	60			
Mobile phase	A: H_2O + 0.1 % formic acid B: ACN + 0.1 % formic acid			
Multi-Step Gradient profile	Time (min)	Flow rate (mL/min)	Percentage A (%)	Percentage B (%)
	0.0	0.20	100	0
	24.0	0.20	70	30
	40.0	0.20	70	30
	50.0	0.20	0	100
	60.0	0.20	100	0

Table A7. The UHPLC instrumental analysis parameters for measurement of mass range of 1000-6000 m/z (positive and negative ions) of the filtrate (<0.2 μm) of the polyurea microcapsule suspension.

UHPLC conditions				
Column temperature (°C)	30			
Resolution	70,000			
Run time (min)	60			
Mobile phase	A: H_2O + 0.1 % formic acid B: ACN + 0.1 % formic acid			
Multi-Step Gradient profile	Time (min)	Flow rate (mL/min)	Percentage A (%)	Percentage B (%)
	0.0	0.20	100	0
	24.0	0.20	95	5
	40.0	0.20	70	30
	50.0	0.20	0	100
	60.0	0.20	100	0

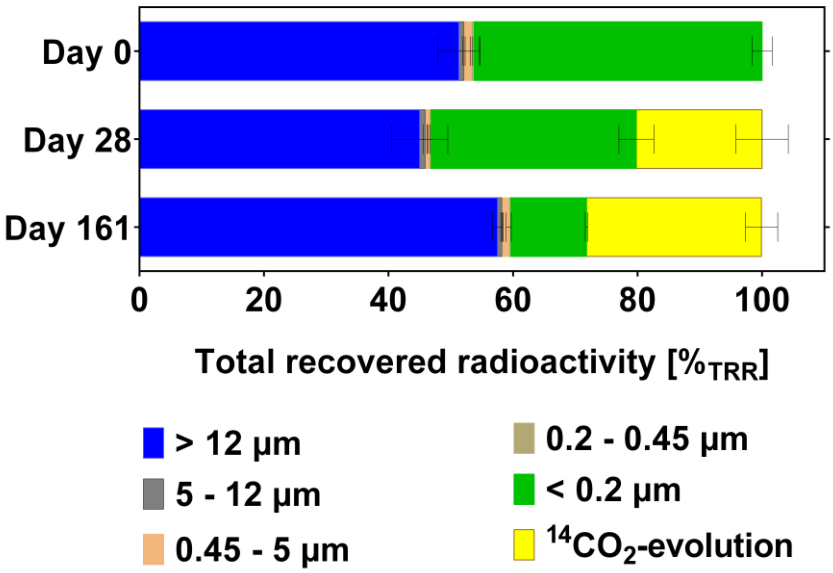

Figure A4. Results of the sequential filtration integrated in the first biodegradation test (T1), which was performed based on OECD TG 301B. Distribution of the total recovered radioactivity [$\%_{TRR}$] across different filter pore sizes and in the filtrate following sequential filtration of test samples at day 0, day 28 (n=5), and day 161 (n=2). $\%_{TRR}$ retained on the 12 µm filter is displayed as"> 12 µm"; $\%_{TRR}$ retained on the 5 µm filter is displayed as"5 - 12 µm"; $\%_{TRR}$ retained on the 0.45 µm filter is displayed as "0.45 – 5 µm" and $\%_{TRR}$ retained on the 0.2 µm filter is displayed as"0.2 µm – 0.45 µm". $\%_{TRR}$ in the filtrate is displayed as "< 0.2 µm". Results are presented as average ± SD or range.

XIII. Appendix – Part 2

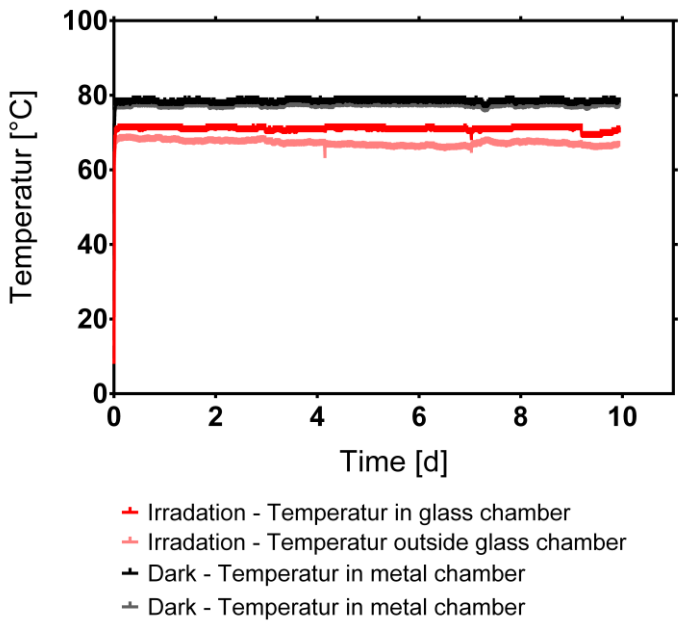

Figure A5. Temperature of the irradiation of Procedure 4 of soil surface samples applied with PUA and PUAmod irradiated similar as described in the OECD Draft TG (2002) in a SUNTEST CPS+ device. Simultanously, equally generated PUA and PUAmod samples were placed as dark controls in a drying cabinet which was set at 80°C. Highest measured temperatures: During irradiation in glass chamber: 71°C, outside the glass chamber: 68.3 °C, Dark incubation in drying cabinet: in metal

chamber: 78.5 °C, outside the metal chamber: 76.6 °C. Average temperature inside the glass chamber during irradiation: 70.5 ± 1.86 °C and average temperature during dark incubation in the metal chamber in the drying cabinet: 78.0 ± 1.13 °C.

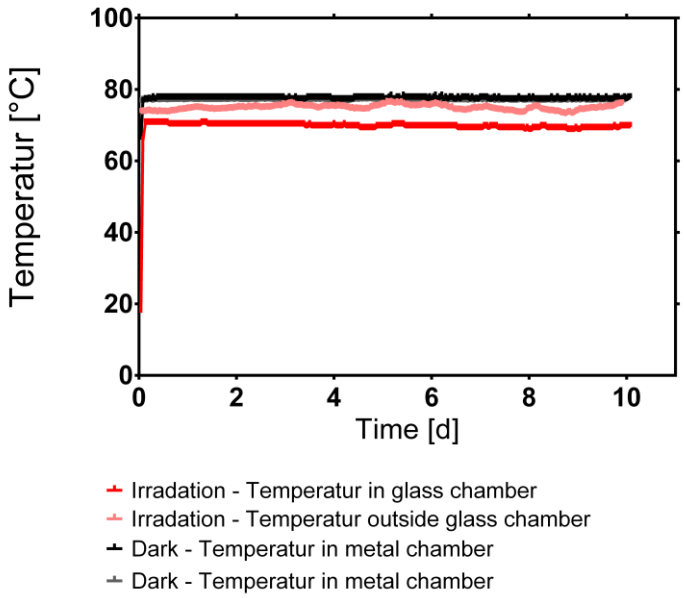

Figure A6. Temperature of the irradiation of Procedure 4 of soil surface samples consisting of LLDPE irradiated similar as described in the OECD Draft TG (2002) in a SUNTEST CPS+ device. Simultanously, equally generated LLDPE samples were placed as dark controls in a drying cabinet which was set at 80 °C. Highest measured temperatures: During irradiation in glass chamber: 70.5 °C, outside the glass chamber: 76.2 °C, Dark incubation in drying cabinet: in metal chamber: 78.0 °C, outside the metal chamber: 77.4 °C. Average temperature inside the glass chamber during irradiation: 69.3 ± 3.39 °C and average temperature during dark incubation in the metal chamber in the drying cabinet: 77.3 ± 0.77 °C.

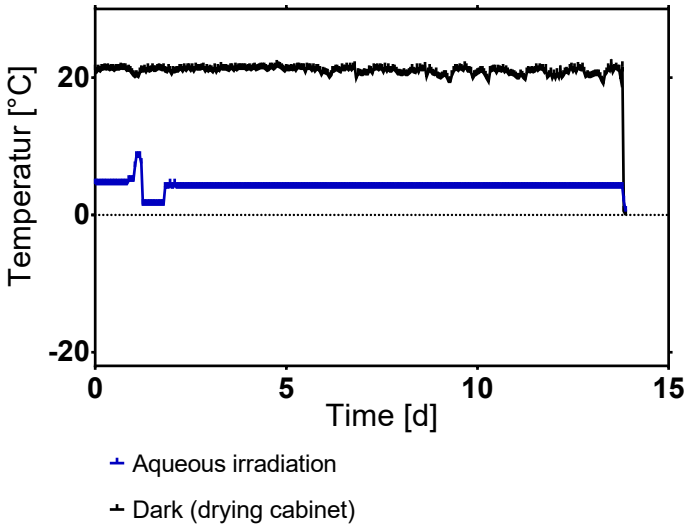

Figure A7. Temperature of the irradiation of Procedure 2 of the aquous PUA_{mod} microcapsule suspension irradiated similar as described in the OECD TG 316 of 2002 in a SUNTEST CPS+ device. Simultanously, equally generated PUAmod samples were placed as dark controls in a drying cabinet which was set at a similar temperture as observed in the SUNTEST CPS+. Mean ± SD temperature of the aqueous irradiation was 3.99 ± 0.77 °C, of the dry irradiation was 5.92 ± 4.66 °C and of the dark samples

in the drying cabinet was 20.9 ± 0.47 °C. Max. temperature of the aqueous irradiation: 8.5 °C, of the dry irradiation: 15.5 °C, and of the dark incubated samples in the drying cabinet: 21.9 °C.

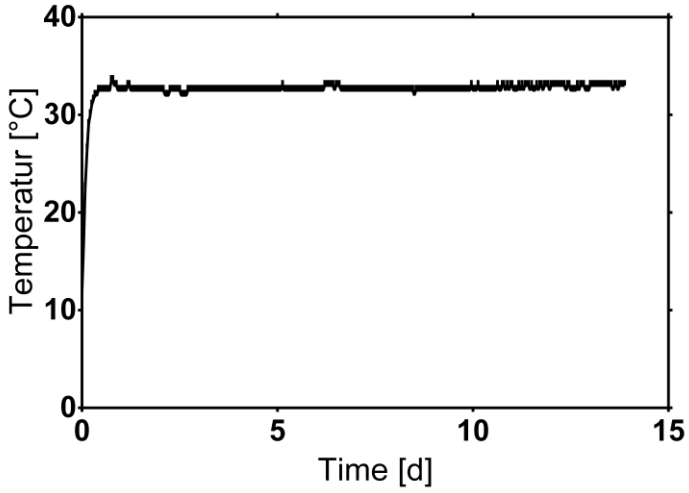

Figure A8. Temperature of the irradiation of Procedure 1&3 of the aquous PUAmod microcapsule suspension irradiated similar as described in the OECD TG 316 of 2002 in a SUNTEST CPS+ device. Simultanously, equally generated PUA_{mod} samples

were placed as dark controls in a drying cabinet which was set at a similar temperture as observed in the SUNTEST CPS+. Mean ± SD temperature of 32.4 ± 1.60 °C. Max. temperature 33.5 °C.

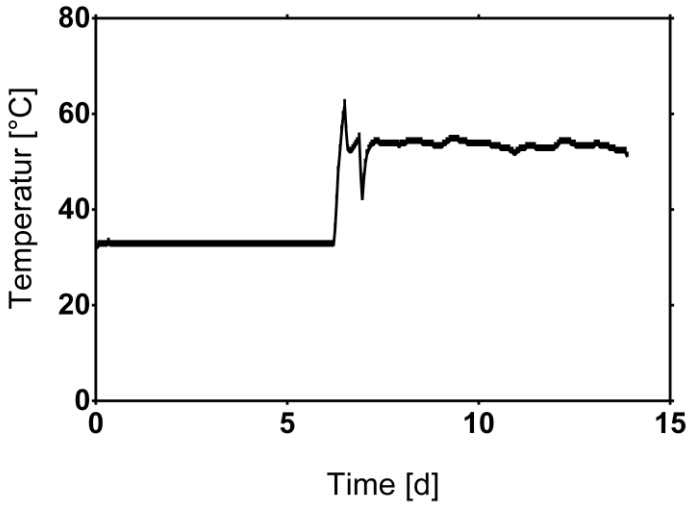

Figure A9. Temperature of the irradiation of Procedure 3 of the aquous LLDPE microplastic suspension irradiated similar as described in the OECD TG 316 of 2002 in a SUNTEST CPS+ device. Simultanously, equally generated LLDPE samples were

placed as dark controls in a drying cabinet which was set at a similar temperture as observed in the SUNTEST CPS+. Mean ± SD temperature of 43.8 ± 10.3 °C. Max. temperature 62.0 °C.

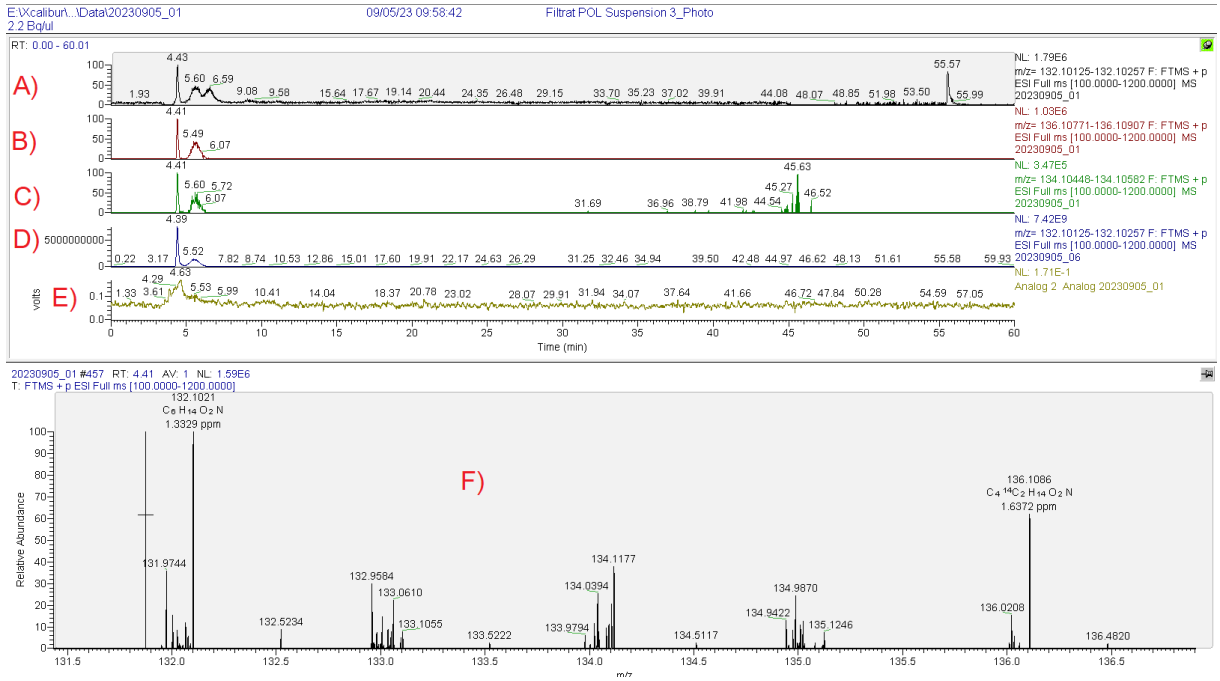

Figure A 10. High-Resolution Mass Spectrometry (HRMS) analysis. The extracted mass chromatogram of non-labeled (A) m/z range of 132.10125-132.1057), $^{14}C_2$-labeled (B) m/z range of 136.10771-136.10907) and ^{14}C-labeled (C) m/z range of 134.10448-134.10582) aminocaproic acid of the irradiated polyurea microcapsule suspension (filtrate <0.2 µm; 100 µL), D) extracted mass chromatogram of aminocaproic acid (m/z range of 132.10125-132.1057, reference substance; 50 µL; Sigma Aldrich, CAS-Nr.: 60-32-2), E) the radio detection signal of the irradiated polyurea microcapsule suspension (filtrate <0.2 µm; 100 µL; A, B, C) is displayed. F) shows the relative abundance of non-labeled (^{14}C-labeled too low to be displayed) and $^{14}C_2$-labeled aminocaproic acid of the irradiated polyurea microcapsule suspension (<0.2 µm) is represented (isotopic pattern trace of ^{12}C with 100 %, ^{14}C with 18.90 % and $^{14}C_2$ with 70.74 % relative intensity).

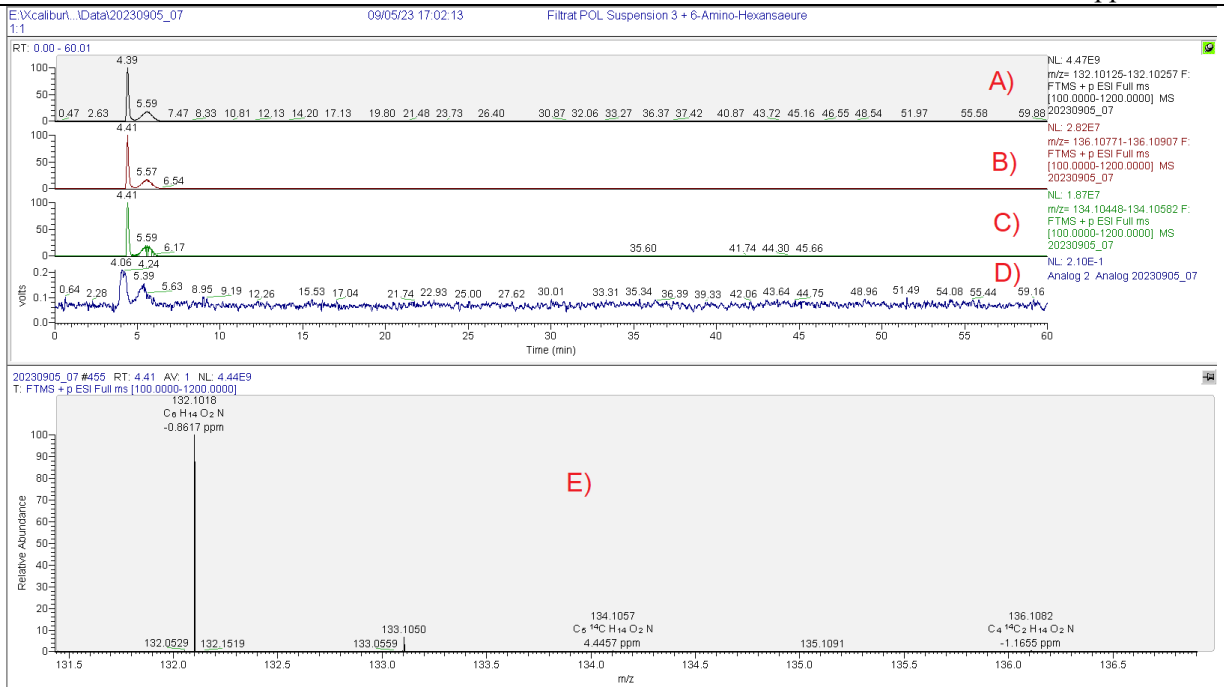

Figure A 11. High-Resolution Mass Spectrometry (HRMS) analysis. The extracted mass chromatogram of non-labeled (A) m/z range of 132.10125-132.1057), $^{14}C_2$-labeled (B) m/z range of 136.10771-136.10907) and ^{14}C-labeled (C) m/z range of 134.10448-134.10582) aminocaproic acid of the irradiated polyurea microcapsule suspension (filtrate <0.2 µm; 100 µL). D) with the Addition of the reference compound aminocaproic acid (reference substance; 50 µL; Sigma Aldrich, CAS-Nr.: 60-32-2) and E) the radio detection signal is displayed. F) shows the relative abundance of non-labeled (^{14}C-labeled and $^{14}C_2$-labeled too low to be displayed) (isotopic pattern trace of ^{12}C with 100 %, ^{14}C with 0.42 % and $^{14}C_2$ with 0.63 % relative intensity).

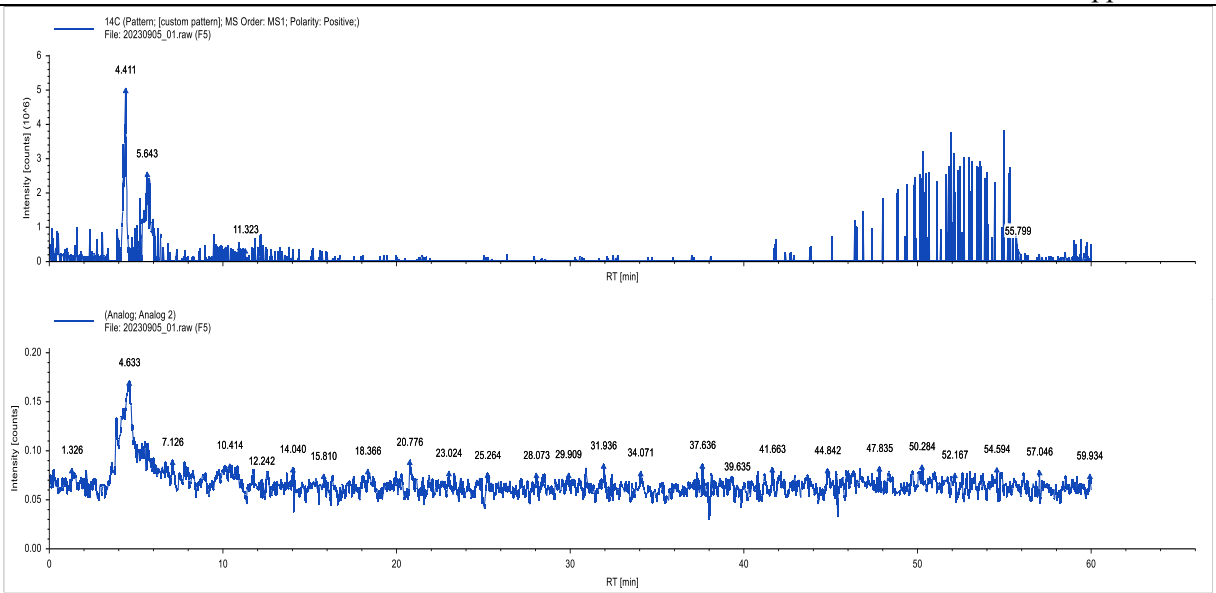

Figure A 12. Top: Isotopic pattern analysis of the irradiated polyurea microcapsule suspension (filtrate <0.2 µm; 100 µL) of the radio-UHPLC-HRMS analysis. Isotopic pattern (Figure S2, F)) of the identified labeled aminocaproic acid was analyzed with its specific mass shift of carbon isotopes (^{12}C with 0.0000 m/z, ^{14}C with 2.00322 m/z and $^{14}C_2$ with 4.00652 m/z,not exceeding a deviation of 5 ppm) and its specific intensity pattern (^{12}C with 100 %, ^{14}C with 18.90 % and $^{14}C_2$ with 70.74 % relative intensity, not exceeding 20 % deviation), quantified and plotted as intensity counts (y-axis: "Intensity [counts] (10^6)") against the retention time (x-axis: "RT [min]). Bottom: radio detection signal of the analysis (y-axis: "Intensity [counts]").

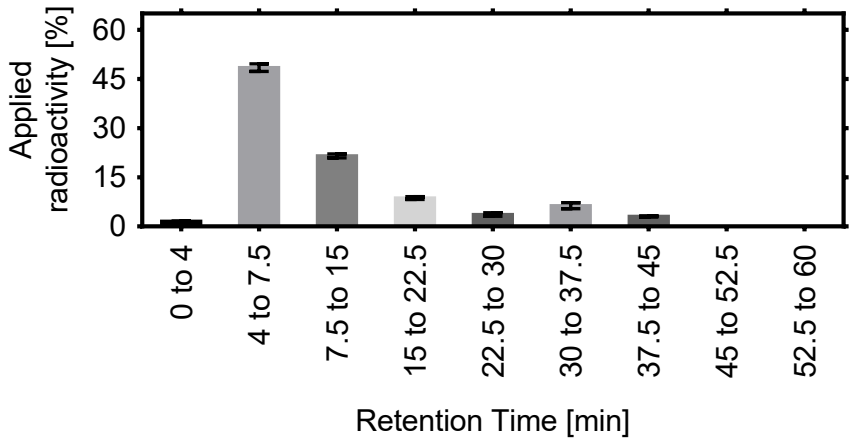

Figure A 13. Results of the column recovery separating the irradiated capsule suspension's filtrate of <0.2 µm with the UHPLC. Eluates were collected for certain retention time intervals (0 to 4 min; 4 to 7 min; 7.5 to 15 min; from 15 to 60 minutes in 7.5 min intervals), and the radioactivity of the eluates was quantified by LSC. Means of n=3 with an average total recovery of 93.2 ± 1.93 $\%_{AR}$ of the applied radioactivity.

XIV. Appendix – Part 3

Table A8. Overview of radioactivity recoveries from extraction solutions and residual soil radioactivity, relative to the **total recovered radioactivity (TRR)** of all extraction experiments and for experiments (I) and (II) without (w/o) the first extraction step.

Extraction experiment	**Spiked MPs**		**Ref. Soil**	**Zinc chloride solution**		**Octanol**		**Water**		**KOH solution**		**Soil**	
	Pristine	**Light-exposed**		TRR Mean [%] (n=3)	TRR SD [%] (n=3)	TRR Mean [%] (n=3)	TRR SD [%] (n=3)	TRR Mean [%] (n=3)	TRR SD [%] (n=3)	TRR Mean [%] (n=3)	TRR SD [%] (n=3)	TRR Mean [%] (n=3))	TRR SD [%] (n=3)
Modified oil extraction using octanol (I)	PUA	no	01-A			24.4	0.27	3.62	0.95	60.3	4.49	11.6	3.65
	PUA	no	03-G			17.6	0.86	3.26	0.59	63.0	2.25	16.2	2.02
	LLDPE	no	01-A			11.4	2.36	0.67	0.36	87.4	2.33	0.49	0.48
	LLDPE	no	03-G			4.23	1.78	0.41	0.08	95.2	1.52	0.21	0.18
	PUA	yes	01-A			9.35*	10.8*	0.44*	0.63*	87.8*	11.3*	2.39*	0.16*
	PUA	yes	03-G			1.47	1.19	7.65	0.57	84.9	2.45	5.99	1.50
	LLDPE	yes	01-A			11.8	9.47	3.05	2.33	82.5	10.7	2.58	3.11
	LLDPE	yes	03-G			2.33	1.18	4.77	2.98	92.2	3.36	0.75	0.97
Density extraction using $ZnCl_2$ (II)	PUA	no	01-A	11.4	1.48					55.4	2.88	33.2	3.43
	PUA	no	03-G	4.55	0.89					63.7	0.48	31.7	1.15
Repeated first extraction step using KOH (III)	PUA	no	03-G							67.5	3.40	32.5	3.40
Modified oil extraction using octanol (I) w/o Step 1	PUA	no	01-A			18.8	1.19	8.41	1.96			72.7	2.81
	PUA	no	03-G			24.8	2.19	3.70	1.09			71.5	1.48
Density extraction using $ZnCl_2$ (II) w/o Step 1	PUA	no	01-A	52.2	6.24							47.9	6.24
	PUA	no	03-G	56.4	1.86							43.6	1.86

SD standard deviation; Ref. Reference

*(n=2, due to a high deviation of the first replicate)

Table A9. Overview of radioactivity recoveries from extraction solutions and residual soil radioactivity, relative to the **applied radioactivity (AR)**, as used in Figure 2. The table also includes total extraction recoveries (referring to the total applied radioactivity) and efficiencies (referring to the total applied radioactivity except for the radioactivity in the soil) of all performed extraction experiments and for experiments (I) and (II) without (w/o) the first extraction step.

Extraction experiment	Spiked MPs		Ref. Soil	Zinc chloride solution		Octanol		Water		KOH solution		Soil		Total recovery		Efficiency	
	Pristine	Light-exposed		AR Mean [%] (n=3)	AR SD [%] (n=3)	AR Mean [%] (n=3)	AR SD [%] (n=3)	AR Mean [%] (n=3)	AR SD [%] (n=3)	AR Mean [%] (n=3)	AR SD [%] (n=3)	AR Mean [%] (n=3))	AR SD [%] (n=3)	AR Mean [%] (n=3)	AR SD [%] (n=3)	AR Mean [%] (n=3)	AR SD [%] (n=3))
Modified oil extraction using octanol (I)	PUA	no	01-A			20.7	1.27	3.08	0.89	50.9	1.46	9.96	3.70	84.6	4.92	74.6	1.33
	PUA	no	03-G			14.8	1.34	2.78	0.77	52.9	3.19	13.7	3.08	84.2	8.13	70.5	5.09
	LLDPE	no	01-A			5.87	2.16	0.33	0.16	44.1	7.60	0.26	0.24	50.6	9.61	50.3	9.49
	LLDPE	no	03-G			4.48	0.98	0.48	0.20	109	31.4	0.28	0.24	114	31.7	114	31.4
	PUA	yes	01-A			5.33	6.46	0.26	0.36	44.9	0.59	1.23	0.00	51.7*	9.23*	50.5*	9.09*
	PUA	yes	03-G			0.72	0.59	3.59	0.29	39.9	0.97	2.82	0.72	47.0	0.41	44.2	0.55
	LLDPE	yes	01-A			5.73	3.25	1.49	0.80	46.1	17.2	1.77	2.28	55.1	17.6	53.3	15.5
	LLDPE	yes	03-G			1.74	0.82	3.20	1.17	71.2	30.1	0.30	0.26	76.4	30.1	76.1	30.0
Density extraction using $ZnCl_2$ (II)	PUA	no	01-A	10.2	0.87					49.6	3.04	29.9	4.62	89.8	4.16	59.9	2.61
	PUA	no	03-G	7.76	1.73					54.2	4.83	26.1	1.29	88.1	6.17	62.0	4.89
Repeated first extraction step using KOH (III)	PUA	no	03-G							55.6	4.20	32.5	3.40	82.3	2.75	55.6	4.20
Modified oil extraction using octanol (I) w/o Step 1	PUA	no	01-A			19.0	0.54	9.05	0.99			73.4	5.36	102	3.97	28.0	1.41
	PUA	no	03-G			23.3	2.17	3.24	0.83			64.8	2.58	91.3	3.78	26.5	1.34
Density extraction using $ZnCl_2$ (II) w/o Step 1	PUA	no	01-A	47.1	4.92							43.3	6.23	90.3	1.31	47.0	4.92
	PUA	no	03-G	52.5	1.21							41.7	0.93	94.2	1.59	52.5	1.21

SD standard deviation; Ref. Reference

*(n=2, due to a high deviation of the first replicate)

XV. Appendix - Curriculum Vitae

Personal Data

Name	Eva-Maria Teggers
Nationality	German
Email	Eva.teggers@rwth-aachen.de
ORCiD	https://orcid.org/0009-0001-0164-9552

Academic Education

2021 - 2025 **Doctoral Candidate, Biology**

at the Institute for Environmental Research, Chair of Ecotoxicology and Environmental Risk Management, RWTH Aachen, Germany

in collaboration with

- Fraunhofer Institute for Molecular Biology and Applied Ecology, Department Ecological Chemistry, Schmallenberg, Germany
- INVITE GmbH, Sustainability and Innovation Group, Cologne, Germany
- Bayer AG, Crop Science Division, Monheim, Germany

Doctoral Thesis: "Environmental Fate of Microplastics, with a Focus on Polymer Microcapsule Formulations Used in Pesticide Applications"

2018 – 2021 **Master of Science, Ecotoxicology at the RWTH Aachen, Germany**

Master's Thesis: "The impact of organic amendments on the leaching of fertilizers and heavy metals, the water retention capacity, and the microbial activity of agricultural soils."

2016 **ERASMUS Semester, Biology at the La Rochelle University, France**

2014 - 2018 **Bachelor of Science, Biology at the Johannes Gutenberg University Mainz, Germany**

Bachelor's Thesis: "The effect of larvae and workers on behavior and physiology in Lasius niger queens."

Publications

2025 **Journal of Hazardous Materials (submitted manuscript, under review)**

ELSEVIER

Teggers, E.-M., Winterhoff, S., Heck, S., Hardebusch, J., Meisterjahn, B., Simon, M., Hennecke, D., Heumann, R., Egger, H., Dalkmann, P., Schäffer, A., Jahnke, A., 2025. Simulated Sunlight Exposure can be a Prerequisite for the Biodegradation of Persistent Microplastics. Journal of Hazardous Materials. Under Review.

2025 **Microplastics and Nanoplastics**

SpringerOpen

Teggers, E.-M., Heck, S., Meisterjahn, B., Simon, M., Hennecke, D., Heumann, R., Egger, H., Dalkmann, P., Jahnke, A., Schäffer, A., 2025. Modified oil extraction of pristine and weathered synthetic polyurea microcapsules and polyethylene microplastics from soil. Microplastics and Nanoplastics. https://doi.org/10.1186/s43591-025-00121-0.

2025 **Environmental Sciences Europe**

SpringerOpen

Teggers, E.-M., Hardebusch, J., Meisterjahn, B., Simon, M., Hennecke, D., Heumann, R., Egger, H., Dalkmann, P., Schäffer, A., Jahnke, A., 2025. Diversifying endpoints in biodegradation testing of microplastics. Environ Sci Eur 37, 65. https://doi.org/10.1186/s12302-025-01096-8.

2024 **Functional Ecology**

British Ecological Society

Majidifar, V.; Psalti, M. N.; Coulm, M.; Fetzer, E.; Teggers, E.; Rotering, F.; Grünewald, J.; Mannella, L.; Reuter, M.; Unte, D.; Libbrecht, R. Ontogeny of Superorganisms: Social Control of Queen Specialization in Ants. Functional Ecology 2024, 38 (5), 1044–1060. https://doi.org/10.1111/1365-2435.14536.

2023 **Soil Systems**

MDPI

Siedt, M.; Teggers, E.-M.; Linnemann, V.; Schäffer, A.; Van Dongen, J. T. Microbial Degradation of Plant Residues Rapidly Causes Long-Lasting Hypoxia in Soil upon Irrigation and Affects Leaching of Nitrogen and Metals. Soil Syst. 2023, 7 (2), 62. https://doi.org/10.3390/soilsystems7020062.

2022 **Scientific Reports**

Nature Portfolio

Teggers, E.-M.; Deegener, F.; Libbrecht, R. Fecundity Determines the Outcome of Founding Queen Associations in Ants. Sci Rep 2021, 11 (1), 2986. https://doi.org/10.1038/s41598-021-82559-9

Conferences and Workshops

2024 **MICRO - Plastic Pollution from Macro to Nano**

Presentation, Arrecife, Spain, 5th Edition

Titel: “Towards a Comprehensive Microplastic Fate Assessment: Integrating Size Analyses and Abiotic Degradation into Regulatory Testing”

2024 **Society of Environmental Toxicology and Chemistry (SETAC) Europe**

Two Presentations Sevilla, Spain, 34th Annual Meeting

Titel: “Towards an improved fate assessment of microplastics: Inclusion of specific analyses and abiotic degradation in regulatory tests”

Titel: “Photolysis on soil surface makes persistent microplastic biodegradable”

2024 **SETAC Young Environmental Scientists (YES) meeting**

Presentation, Landau, Germany, 12th Annual Meeting

Titel: “The inclusion of supplementary analysis within a standardized biodegradability testing framework has thepotential to provide enhanced comprehension of microplastic degradation”

2023 **Microplastics Workshop for Early Career Researchers**

Including a mandatory presentation, Ascona, Switzerland

Titel:“Improving the understanding of microplastic capsules degradation in a standard test setup”

2023 **Society of Environmental Toxicology and Chemistry (SETAC) Europe**

Presentation, Dublin, Irland, 33th Annual Meeting

Titel: “The integration of further analysis in a standardized biodegradability test system can lead to better insights into microplastic degradation.”

XVI. Appendix – Publications

1.1 Diversifying endpoints in biodegradation testing of microplastics

Environmental Sciences Europe

SpringerOpen

Teggers, E.-M., Hardebusch, J., Meisterjahn, B., Simon, M., Hennecke, D., Heumann, R., Egger, H., Dalkmann, P., Schäffer, A., Jahnke, A., 2025. Diversifying endpoints in biodegradation testing of microplastics. Environ Sci Eur 37, 65. https://doi.org/10.1186/s12302-025-01096-8.

1.2 Simulated Sunlight Exposure as a Prerequisite for the Biodegradation of Persistent Microplastics

Journal of Hazardous Materials (submitted manuscript, under review)

Elsevier

Teggers, E.-M., Winterhoff, S., Heck, S., Hardebusch, J., Meisterjahn, B., Simon, M., Hennecke, D., Heumann, R., Egger, H., Dalkmann, P., Schäffer, A., Jahnke, A., 2025. Simulated Sunlight Exposure can be a Prerequisite for the Biodegradation of Persistent Microplastics. Journal of Hazardous Materials. Under Review.

1.3 Modified oil extraction of pristine and weathered synthetic polyurea microcapsules and polyethylene microplastics from soil

Microplastics and Nanoplastics

SpringerOpen

Teggers, E.-M., Heck, S., Meisterjahn, B., Simon, M., Hennecke, D., Heumann, R., Egger, H., Dalkmann, P., Jahnke, A., Schäffer, A., 2025. Modified oil extraction of pristine and weathered synthetic polyurea microcapsules and polyethylene microplastics from soil. Microplastics and Nanoplastics. https://doi.org/10.1186/s43591-025-00121-0.

Environmental Sciences Europe

RESEARCH

Open Access

Diversifying endpoints in biodegradation testing of microplastics

Eva-Maria Teggers[1,2,3*], Jonas Hardebusch[1], Boris Meisterjahn[1*], Markus Simon[1], Dieter Hennecke[1], Roman Heumann[2], Holger Egger[4], Philipp Dalkmann[4], Andreas Schäffer[3†] and Annika Jahnke[3,5†]

Abstract

To counteract microplastic (MP) pollution the European Commission adopted a restriction of intentionally adding synthetic polymer microparticles to products, such as detergents, rinse-off cosmetics, controlled-release fertilizers or pesticides. Exempted are particles consisting of polymers that, e.g., meet the (bio)degradability pass criteria of the available test methods. The main criterion for proving biodegradability is the particle's mineralization rate, as set out, amongst others, in OECD testing guidelines 301B referenced by the REACH regulation of the European Union. Since present test methods are designed and validated to test low-molecular, soluble compounds adaptations regarding MP biodegradability testing are of high interest. In this study, the biodegradability of a polyurea (PUA) microcapsule suspension was tested using a standard degradation test method (OECD test guideline (TG) 301B). Since the polymeric component comprised less than 1% of the suspension, besides the aromatic solvent inside the microcapsule (8.6%) and water (90.9%), ^{14}C-labeling of the polymer was essential for specific detection throughout the experiments. Particle size determination of the tested PUA microcapsules indicated a bias in the test results due to the presence of a soluble ^{14}C-compound, a byproduct of synthesis, identified using ultra-high performance liquid chromatography–high resolution mass spectrometry (UHPLC–HRMS) coupled with radioactivity detection. This study highlights the need for proper characterization and purification of the tested particles prior to biodegradation testing and suggests how to diversify future regulatory testing for a comprehensive assessment of the biodegradation of MPs.

Keywords Biodegradation testing, Size fractionation, Radiolabeling, Transformation products, HRMS, Regulatory assessment, Polyurea, Microcapsules, Radioactivity detection, OECD TG 301B

†Andreas Schäffer and Annika Jahnke share the last authorship.

*Correspondence:
Eva-Maria Teggers
eva.teggers@rwth-aachen.de
Boris Meisterjahn
boris.meisterjahn@ime.fraunhofer.de
Full list of author information is available at the end of the article

Graphical abstract

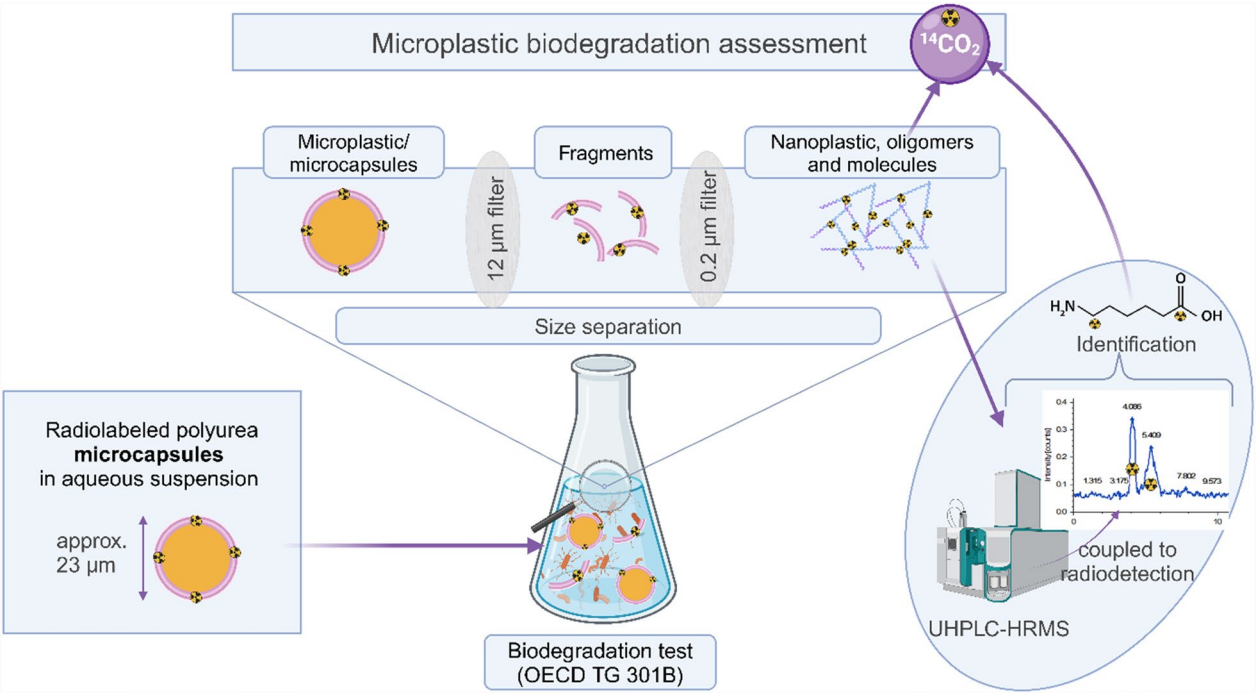

Background

The widespread presence of microplastic (MP) pollution, even on mountaintops and down to the deepest oceans, poses substantial challenges to efforts aimed at protecting environmental and human health from related hazards. Strategies to reduce plastic emissions to the environment include the adopted restriction of intentionally added MPs to products under REACH regulation by the European Commission [1]. In accordance with this restriction, MPs are to date defined as solid synthetic polymer particles in a size range of 100 nm to 5 mm. The restriction also includes polymers that are contained in particles constituting at least 1 wt% (percentage of the total weight of the product) or building a continuous surface coating on such particles. Exempted from the restriction are polymers that (i) have a solubility greater than 2 g/L in water, (ii) do not contain carbon atoms in their chemical structure, (iii) are natural and have not been chemically modified, or (iv) for which fulfilment of biodegradability criteria can be demonstrated. In this context, methods to prove biodegradability of MPs are of key relevance. There are overall 13 test methods accepted to prove synthetic polymer microparticle biodegradability, which are organized into 5 groups (screening and simulation test methods) (*Entry 78—Rules on proving degradability*, Appendix 15 of Annex XVII of (EC) No. 1907/2006 [1]) and are displayed in the supplementary information (SI—Table S1).

The present regulatory approach defines the main criterion for biodegradability of MP particles based on their mineralization, which refers to the biological breakdown of the polymer into carbon dioxide (CO_2) and water. Complete mineralization (also referred to as ultimate biodegradation) signifies that the polymer is fully degraded into CO_2 and biomass through microbial metabolism, leaving no residual transformation products. In regulatory testing, biodegradability is often assessed based on the extent of mineralization over a defined timeframe. For instance, reaching ≥ 60% mineralization within a specified test duration of 28–60 days (according to OECD TG 301 B, C, D, F, [2] and OECD TG 310 [3] for Group 1 and 2) is considered sufficient to demonstrate biodegradability.

Tests for MP biodegradability should be performed with particles of a comparable composition, shape, size and surface area as present in the product, if the product meets the "microplastic" definition. However, many products show a high degree of complexity, e.g., due to a wide range of components with different sizes and

particle shapes and/or chemical composition, which might be mineralized to different extents at varying rates. Consequently, the test results could be falsely interpreted.

From a scientific perspective, the biodegradation of polymers is divided into four steps: biodeterioration, depolymerization, bioassimilation and mineralization [4, 5]. During this process, Albright and Chai [6] defined the loss of one key property of the polymer, such as mass fragmentation or tensile strength, as primary degradation. However, a regulatory definition of primary degradation of polymers is still missing. Within the depolymerization the polymer is disintegrated into low-molecular weight compounds. The released organic compounds can be assimilated by microorganisms and, in the last step, either completely decomposed into simple, fully oxidized molecules like carbon dioxide (CO_2), methane, nitrate or ammonium to generate energy or transformed into biomass [5, 7, 8]. However, in addition to mineralization, other critical steps of polymer biodegradation, including biodeterioration, depolymerization, and bioassimilation, receive limited attention in the current regulatory framework for MPs. These intermediate degradation processes may influence the overall breakdown of polymers by altering their molecular structure, reducing particle size, and increasing bioavailability for microbial assimilation. Neglecting these factors in regulatory assessments may lead to incomplete evaluations of polymer degradability and potentially incorrect assumptions of the environmental persistence of MPs and the formation of persistent polymeric fragments.

The permitted test methods to prove biodegradability were designed and validated to test well-defined low molecular weight, mono-constituent and soluble or uniformly dispersed substances. For this type of substance, using the endpoint mineralization to CO_2 or related O_2 consumption is a reasonable and validated approach, however, transferring methods and endpoints to complex particulate polymers is criticized [6, 9–11]. The corresponding ring-trials of most of the standardized tests did not include polymeric particles, hence requiring further testing.

The inclusion of additional types of analysis, like size distribution and related changes of the tested material, can, besides describing or giving a hint for its degradation pathway, help to interpret test results of ultimate degradability (mineralization) and make them more robust and comprehensive. Since size can also play a major role regarding the bioavailability of MPs, characterizing their size distribution is meaningful in this context, too. However, integrating analytical approaches for studying biodegradation pathways is challenging and scarcely investigated.

Polymeric microcapsules used, e.g., for encapsulation of pesticides are also covered by the scope of the EU restriction. However, testing their biodegradation for regulatory purposes raises additional challenges. For example, it is practically impossible to distinguish the mineralization of the microcapsule shell, usually constituting approximately 1 to 5% of the product, from other organic components of the suspension, such as the oil and the pesticide inside the capsule, within the biodegradation test. To comprehensively monitor the biodegradation of synthetic MP capsules we used radioactive isotope-labeling of the polymer, i.e., ^{14}C-labeling, to quantify the $^{14}CO_2$-evolution exclusively as a result of the polymer mineralization, which can substantially enhance sensitivity and specificity.

In this study we investigated the biodegradation of a polyurea (PUA) capsule suspension (CS) used for pesticide applications using OECD TG 301B [2]. For specific tracking of the mineralization of the polymeric shell, the PUA was synthesized using a ^{14}C-labeled monomer ([1,6-^{14}C] hexamethylenediamine). To obtain information about the fragmentation of the capsules, we monitored changes in MP size distribution using sequential filtration. To analyze the presence of soluble compounds either released from the microcapsules or remaining from their synthesis we applied an ultra-high performance liquid chromatography—high resolution mass spectrometer (UHPLC–HR-MS) coupled to a radioactivity ("radio") detector. ^{14}C-labeling further served to examine the source of the detected $^{14}CO_2$ evolution during degradation of the PUA CS. This study aimed to (i) evaluate the biodegradability of PUA CS within the framework of a regulatory approved method and (ii) to assess the potential formation of polymeric fragments or transformation products.

Material and methods

Radioactive labeling and capsule suspension synthesis

The PUA CS was produced in a similar way as described by some of the authors in the WO2021136758 [12] applying the most widely used microcapsule synthesis [13], which is generated by the interfacial polymerization of diisocyanate and polyamine in an emulsion containing an organic-phase and water. For synthesis of radioactively labeled microcapsules, the synthesis procedure of the technical product was carried out on a small scale (factor of approx. 200:1 to production scale; approx. 10:1 to laboratory scale). Hence, a lower concentration and smaller high shear equipment (ULTRA TURRAX Tube Disperser, IKA-Werke GmbH & CO. KG, Germany) had to be used to be able to prepare the initial oil-in-water emulsion for the capsule synthesis. For the procedure, [1,6-^{14}C]hexamethylenediamine (0.08 Wt% of the

undiluted CS) and non-labeled modified polymeric diphenylmethane diisocyanate (pMDI), amounting to 0.24 Wt% of the undiluted CS, were used (3.49–3.57 MBq/mg, Bayer AG, Germany). Since the monomers consist of ≥ 2 binding sites the polymer rather crosslinked generating a polymer structure that is insoluble, more rigid and aging-resistant [14]. Given these properties, substantial biodegradation is not expected for the general polymer. However, for the tested polymer, the pMDI had been modified to include more ester bonds into the polymer structure with the goal of increasing biodegradability. Other components of the suspension included the organic phase, an oil (8.59 Wt% of the undiluted CS, Solvesso 200 ND, ExxonMobil, USA), a dispersant (0.23 Wt% of the undiluted CS, Reax 88, Ingevity Holdings SPRL, USA), and water (in total 90.9 Wt% of the undiluted CS).

The synthesized CS suspension was qualitatively examined by microscopic analysis (SI—Fig. S1) and a quantitative size distribution analysis was performed by laser diffraction using a particle size analyzer (Mastersizer 2000, Malvern, SI—Tables S2, S3 and S4, Fig. S2). In this analysis, the particle size distribution was expressed as a volume-based distribution, representing the percentage of the total sample volume occupied by particles within specific size classes ($\%_{\text{particle-volume-based}}$).

Biodegradability tests

The biodegradation of the aqueous PUA CS was tested in a modified OECD 301B "CO_2-Evolution Test" (OECD TG 301B [2]). In addition to the radiolabeling of the polymer (section "Radioactive labeling and capsule suspension synthesis"), the modifications included (I—section "Preparation of the test inoculum") the use of filtered activated sludge supernatant, (II—section "Biodegradation of the bulk capsule suspension") a prolongation of the test duration, and (III—section "Biodegradation of the different size fractions of the CS") a sequential filtration of the samples for size fractionation. Within the biodegradation tests, the proportion of mineralization was calculated based on the evolved $^{14}CO_2$, which was trapped in sodium hydroxide (NaOH) implementing a flow-through setup as proposed in the OECD TG 301B. The radioactivity within the traps was quantified using liquid scintillation counting (LSC) (section "Quantification and data analysis"). Since the PUA was ^{14}C-labeled, the aeration of the flow-through setup could be done using ambient air instead of CO_2-free synthetic air. The NaOH traps were sampled in intervals of approx. 2 to 27 d during the incubation time, depending on the current $^{14}CO_2$ evolution rate. In all tests the degradability of the standard reference substance, ^{14}C-labeled sodium benzoate (benzoic acid [ring-^{14}C (U)] sodium salt, 130 mCi/mmol, American Radiolabeled Chemicals Inc., USA), was assessed in parallel to monitor the overall degradation performance of the inoculum.

Preparation of the test inoculum

We used filtered activated sludge supernatant instead of the commonly used standard inoculum (mineral medium with activated sludge suspended solids), to reduce the impact of matrix (sludge particles) and to enable the application of as many analytical methods as possible. For this, in a preliminary biodegradation test (OECD TG 301 F [15]), the performance of the filtered activated sludge supernatant on mineralizing sodium benzoate was compared with the mineralization performance of the standard inoculum. For the preparation of the filtered inoculum, activated sewage sludge was collected from the outflow of a wastewater treatment plant (Ruhrverband Kläranlage, Sunthelle 6, 57392 Schmallenberg) 2 d before the start of the experiment and left standing at room temperature in diffuse light for approx. 30 min to let most of the particles settle. The formed supernatant was decanted, centrifuged (5 min at 10000*g*) and filtered (Macherey–Nagel, Mn- 672, Cellulose, average retention capacity 4–12 µm). During the preparation and incubation, overnight aeration of the aqueous inoculum with ambient air was provided.

Biodegradation of the bulk capsule suspension

The total carbon content of the CS was determined using a macro-elemental analyzer (multi EA 4000, Analytik Jena). Both the CS and sodium benzoate test samples were spiked to yield a total carbon (TC) content of approximately 20 mg/L, meeting the requirements of the OECD 301B guideline. At the test start a total of two samples were prepared for sodium benzoate application and 16 samples were prepared with inoculum for PUA CS application (SI—Table S5). All samples and corresponding incubation times are displayed in Fig. 1.

Process controls were implemented to observe whether the degradation performance of the microbes was still functional during the incubation time. For this purpose, ^{14}C-sodium benzoate was applied to an inoculum sample vessel at day 0 and to another inoculum sample vessel at day 14 and the $^{14}CO_2$ evolution over time was monitored. Inoculum samples containing the CS were used for (a) the sequential filtration (section "Biodegradation of the different size fractions of the CS"); (b) the determination the CO_2 bound as carbonic acid in the aqueous media by applying hydrochloric acid (HCl); (c) a toxic control tested in parallel to determine inhibitory effects of the suspension on microbial activity by adding a readily degradable reference compound, here ^{14}C sodium

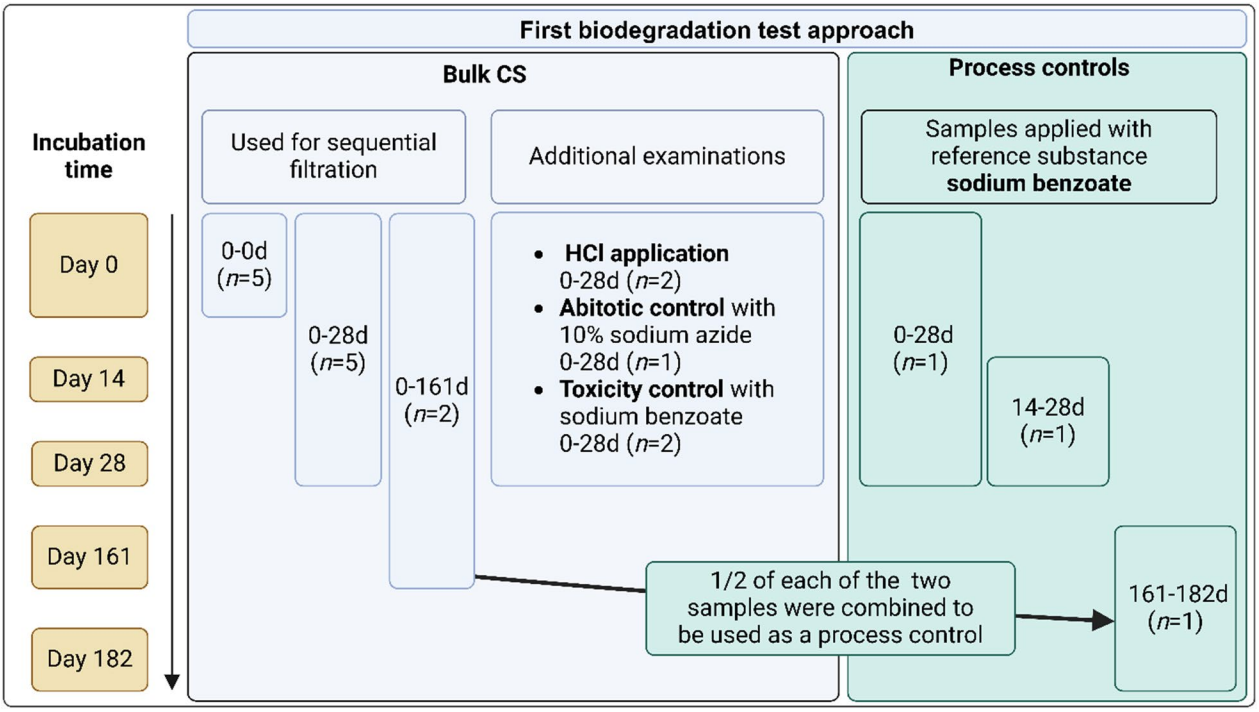

Fig. 1 Overview of samples and their incubation times, submitted to the OECD 301B biodegradability test of the bulk capsule suspension (CS). Samples supplied with CS are displayed with light blue background and process controls, supplied with sodium benzoate are displayed with green background. ½: half of each of the two replicates with bulk CS was sampled at 161 d and the other half combined to a sample to which the standard reference, sodium benzoate, was applied

benzoate (20 mg C/L, if microbial degradation of the reference compound was substantially reduced in the presence of suspension, it would indicate that the suspension has toxic or inhibitory effects on microbial activity); (d) abiotic degradation examined by adding 30 mL of a 10% sodium azide solution. Sodium azide was selected as a bacteriostatic agent because it effectively inhibits microbial respiration and enzymatic activity without altering the chemical structure of microplastic particles or interfering with CO_2 measurements, since it primarily inhibits microorganism growth [16]. Two samples containing CS were incubated for a prolonged test duration (161 d instead of the standard duration of 28 d), to verify that the mineralization potential of the microorganisms had not decreased over this prolonged incubation time. For this, a fraction of the volume of each duplicate was sampled and the remaining fraction of both duplicates was combined to one sample to which the standard reference sodium benzoate was applied, as a last process control starting at 161 d.

The applied radioactivity of each sample was determined after the respective application of the unprocessed stock CS (5 mL with 5.4 ± 0.1 kBq/mL) or of the sodium benzoate stock solution (5 mL with 65.8 ± 0.3 kBq/mL). The radioactivity of the samples was verified at the test start using 1 mL aliquots of each sample ($n = 3$), which were submitted to combustion and LSC determination (section "Quantification and data analysis").

Biodegradation of the different size fractions of the CS

In the first biodegradability test (OECD TG 301B) a sequential filtration was performed to assess changes in the size distribution of the ^{14}C-labeled synthetic polymer microparticles over the incubation time. For this purpose, sample aliquots of 50 mL were sequentially passed through several filters connected in series (12 µm pore size (Cytiva Whatman®, nitrocellulose filter, Z696919), 5 µm pore size (Sartorius, cellulose acetate filter, Type 12,342), 0.45 µm pore size (Sartorius, cellulose acetate filter, Type 11,106) and 0.2 µm pore size (Sartorius, cellulose acetate filter, Type 11,107)) at day 0, day 28 and day 161 (see Fig. 1), and the radioactivity of the filters and the filtrate was quantified.

In a second biodegradability test (OECD TG 301B) the size fractions of the CS were tested separately, by first filtering the CS and testing the size fractions of approx. > 12 µm (filter, Cytiva Whatman®, nitrocellulose filter, 12 µm pore size, Z696919) and approx. < 12 µm (filtrate) separately. For this purpose, 500 mL of the aqueous

stock suspension with a radioactivity of 1.6 ± 0.0 kBq/mL were produced. After thorough shaking, 50 mL CS aliquots were filtered through a 12 µm pore-sized filter ($n = 3$). Each filtrate was sampled for the application to the biodegradation test. The filter was then washed with 100 mL water. Each filtered material and each filtrate were subsequently applied to the inoculum of the biodegradation test and connected to the ventilation system. The same was done with 50-mL aliquots of the unfiltered stock CS ($n = 3$) as a quality control, to verify whether the sum of the mineralization of the fractions on the filter and in the filtrate corresponded to the mineralization of the original 50 mL CS.

Ultra-high performance liquid chromatography with high-resolution mass spectrometry (UHPLC–HR-MS)

The UHPLC–HR-MS analysis coupled with radio detection was used to analyze the smallest filtration fraction (filtrate < 0.2 µm) of the PUA CS and thus, to verify if ^{14}C-labeled molecular compounds remaining from capsule synthesis were present in this fraction. Therefore, UHPLC equipped with a C18 (RP18, ODS, Octadecyl) reversed phase (ODS-AQ, YMC, USA) column, coupled to a Q-Exactive Plus Orbitrap mass spectrometer (HR-MS, using the analysis software Qual Browser of Xcalibur Version 4.0, Thermo Fisher Scientific Inc., USA) and additionally to a radio detector (LB509—YG 75 S6M, Berthold GmbH & Co. KG, Germany) (SI—Tables S6, S7, S8) was employed for qualitative assessment. The LC system was also evaluated in terms of possible adsorption of the analytes to the column matrix. Thus, a recovery test of the radioactivity eluted from the column was performed, by sampling the eluate in time intervals (0–3.5 min; 3.5–7 min; 7–15 min; from 15–60 min in 7.5 min intervals) based on the signal of the radio detector during the whole analytical run. The eluted radioactivity was then determined by LSC (HIDEX 600 SL Counter, HIDEX, Germany). Furthermore, identified molecules within HR-MS analysis were compared to analytical standards of the respective substance. In a next step, we screened for molecules that originated from the labeled [1,6-^{14}C]hexamethylenediamine used for polymer synthesis by performing an isotopic pattern analysis. For this purpose, the isotopic patterns of molecules, present in labeled and non-labeled form, were assessed. In this approach, specific mass shifts of carbon isotopes (e.g., molecules consisting of different compositions of ^{12}C, ^{14}C or $^{14}C_2$, and the specific intensity of ^{12}C-, ^{14}C- or $^{14}C_2$-molecules) were determined. All molecules that eluted with the same mass shift (within 5 ppm) and intensity characteristics (within 20% deviation) were then extracted from the mass spectra. The intensity counts of those molecules were plotted against their retention time (RT). Details of the analysis are given in the supplementary data (SI—Fig. S3).

Quantification and data analysis

In general, the radioactivity of the CS was determined by applying an aliquot of 1 mL in a cellulose cone, leaving it for air-drying overnight followed by combustion in an oxidizer (HIDEX, 600 OX) and quantification of the trapped $^{14}CO_2$ by LSC (HIDEX 600SL). Regarding the quantification of radioactivity remaining on each filter within the sequential filtration, filters were air-dried and combusted. Similarly, the radioactivity of the filtrate was determined by drying 5 × 1 mL aliquots on a cellulose cone followed by combustion. For all remaining radioactive liquid samples or stock solutions, aliquots were directly applied into 4 mL LSC cocktail (Supersolve X, Zinsser Analytics) prior to the LSC determination.

The results are presented as percentage of the recovered radioactivity relative to the applied radioactivity ($\%_{AR}$). For all calculations Microsoft Office Professional Plus Excel (2019) was used. Graphpad Prism 6 was employed for the graphical representation. The graphical abstract and Fig. 1 were created with BioRender.com.

Results and discussion

Biodegradation of the bulk CS

In a pretest, we compared the filtered supernatant and the standard inoculated mineral medium by the biodegradation of the standard reference compound sodium benzoate in an OECD TG 301 F [15] by means of the oxygen demand. In this test, no substantial differences regarding mineralization performance for the reference substance and the related test validity, namely mineralization of > 60% of the reference substance within a 10-d window, were observed (SI—Fig. S4).

Regarding the biodegradation performance of the modified OECD 301B biodegradation test run examining the bulk suspension, 58.6%$_{AR}$ was mineralized by the process control applied on 0 d, approaching the validity threshold (i.e., 60%) set by the TG. Overall, the process controls proved that the microbiome of the filtered supernatant was sufficiently active during the whole incubation time (SI—Fig. S5). The toxicity control showed the combined mineralization of sodium benzoate and the CS (83.6%$_{AR}$; $n = 1$; Fig. 2), revealing that the CS itself did not show toxic or inhibitory effects. In the abiotic control (with sodium azide added), 13.3%$_{AR}$ ($n = 1$) $^{14}CO_2$ was formed over the duration of 28 d with a lag phase of 5 d (Fig. 2) after the microbiome recovered from the sodium azide application from day 7 onwards. Since sodium azide has a bacteriostatic rather than a bactericidal effect [17], a recovered viability of the test inoculum during the incubation time is possible which might delay

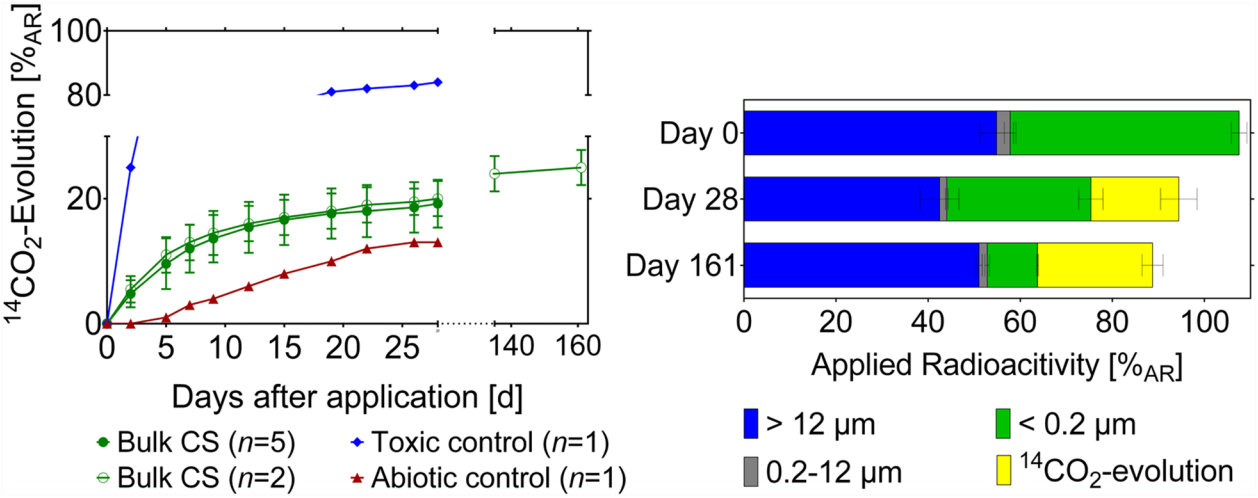

Fig. 2 Biodegradation test results of the fist OECD TG 301B. Left: $^{14}CO_2$-evolution of the bulk polyurea capsule suspension (Bulk CS), the abiotic control (sodium azide-treated) and the toxicity control (sodium benzoate added to the bulk CS). Plotted is the cumulative portion of applied radioactivity (AR) mineralized to $^{14}CO_2$ relative to the incubation time (mean and SD). Right: applied radioactivity (AR) on the different pore-sized filters and in the filtrate at day 0, at day 28 ($n = 5$) and at day 161 ($n = 2$) of test samples after the sequential filtration (mean and SD). Residues remaining on the 12-µm pore-sized filter are displayed as " > 12 µm" and "0.2 to 12 µm" represent the sum of the AR found on the three pore sized filters (0.2, 0.45 and 5 µm). The radioactivity in the filtrate is displayed as the fraction " < 0.2 µm"

the mineralization, which was also observed in a study of Süßmuth et al. [18] for soil samples. Investigations of Blaschko et al. [17] showed that the inhibition by sodium azide can be reversible. Furthermore, a study of Hendrix et al. [19] showed that the addition of sodium azide to environmental samples can lead to reactions with dissolved organic matter causing a lowered concentration of the inhibitor in the solution.

The biodegradation test of the bulk CS resulted in 19.1 ± 3.96%$_{AR}$ (average and stdev of $n = 5$) $^{14}CO_2$-evolution after the standard incubation time of 28 d (Fig. 2). A negligible amount of $^{14}CO_2$ (carbonic acid ($H_2{}^{14}CO_3$)) was dissolved in the sample, as from the two bulk CS samples no $^{14}CO_2$ evolved after acidification with HCl (23.0 ± 1.22%$_{AR}$, $n = 2$). The two bulk CS samples that were incubated for 161 d reached 25.0 ± 2.29%$_{AR}$ (mean of $n = 2$, range). Considering that PUA is a rigid and stable material (see also section "Radioactive labeling and capsule suspension synthesis"), this relatively high degree of mineralization (approx. 40% of the pass criterion for biodegradability using this test method (OECD TG 301B, group 1 and 2)), was unexpected. Initially, it was hypothesized that the observed mineralization may have resulted from the structural modification of the polymer, specifically the inclusion of additional ester bonds intended to enhance biodegradability. Since a crucial biodegradation mechanism is the hydrolysis of ester bonds to liberate monomers [20, 21], the moderate (bio) degradation may have been a result of this modification. However, as demonstrated in subchapter "Biodegradation of the different size fractions of the CS", this assumption was incorrect, and the main component that was mineralized—aminocaproic acid—was identified.

Biodegradation of the different size fractions of the CS

The sequential filtration experiments provided further insights into the (bio)degradation of the bulk CS (Fig. 2) by approximating the size distribution of the bulk CS, not only at the start of the experiment, but also during the incubation time within the OECD 301 biodegradation test.

Generally, the radioactivity was found to fall almost completely in two fractions of the applied sequential filtration approach for the bulk CS at the test start (0 d): 54.9 ± 3.64%$_{AR}$ was found on the 12-µm filter and 49.7 ± 1.67%$_{AR}$ was found in the filtrate < 0.2 µm (0 d, Fig. 2), while the summed up AR of the size range in-between 0.2 and 12 µm, remaining on the 0.2, 0.45 and 5 µm filters, was low (2.93 ± 1.26%$_{AR}$). Thus, slightly more than half was larger than 12 µm as expected, in line with the results of a laser diffraction analysis (SI—Table S3) revealing a median size of the bulk suspension of 16.5 µm (measured size range 0.01–5.75 µm; SI—Table S2, Table S4 and Fig. S2), whereas almost half was present in the filtrate.

As mentioned above, 19.1%$_{AR}$ evolved to $^{14}CO_2$ at 28 d for the bulk suspension (Fig. 2). The radioactivity that had been released from the test medium by mineralization (0 d to 28 d) was presumably reflected in the reduction of radioactivity in the smallest size fraction with a decrease of 18.4%$_{AR}$ resulting in a total remaining activity of 31.3

± 2.64%$_{AR}$ recovered 28 d after application (Fig. 2). In this context, the radioactivity in the fraction between 0.2 to 12 µm was only reduced by approximately 1%$_{AR}$ down to a total of 1.58 ± 0.28%$_{AR}$ (Fig. 2). Notably, the largest fraction (> 12 µm) of the sample—attributed to ^{14}C-labeled microcapsules—also decreased in the amount of radioactivity from d 0 to d 28 by 12.4%$_{AR}$ (total of 42.5 ± 4.22%$_{AR}$ at d 28, Fig. 2). This decrease raised the question whether also the largest particles (presumably microcapsules) were partly degraded to smaller fragments, molecules or even mineralized.

Finally, the sequential filtration results of 161 d incubation showed that the smallest size fraction (filtrate < 0.2 µm) decreased by a total of 38.8%$_{AR}$ compared to d 0, ending at 10.9 ± 0.18%$_{AR}$ (Fig. 2). However, this reduction in radioactivity exceeded the amount mineralized to $^{14}CO_2$ (25.0 ± 2.29%$_{AR}$ from d 0 to d 161). This missing radioactivity in the smallest fraction may be attributed either to a loss of $^{14}CO_2$ through leakage or to the adsorption of radioactivity onto larger agglomerates. Given the lengthy biodegradation period and the complex sequential filtration process, an overall recovery of 88.7%$_{AR}$ at 161 d remains high. The minor observed losses might be attributed to the smallest fraction. Yet, the missing AR in the smallest size fraction might also result from sorption or assimilation into the largest size fraction, retained by the 12-µm filter, which increased by 8.57%$_{AR}$ from d 28 to d 161, reaching a total of 51.1 ± 0.69%$_{AR}$ (n = 2, Fig. 2). Microorganisms of the test medium may have assimilated a portion of ^{14}C-compounds from the smallest size fraction. The living and dead microorganisms might stick together as a microbial aggregate or biofilm which might have reached sizes above 12 µm. Thus, theoretically these microbial aggregates containing assimilated ^{14}C were retained by the 12 µm filter along with the microcapsules to cause an 8%$_{AR}$ -increase in the size fraction > 12 µm after an incubation of 161 d. Supporting this, an increasing amount of flocculant was observed in the sample vessels (SI—Fig. S6). Further investigations, e.g., by analyzing the filter residue or the biofilm aggregates for ^{14}C-lipids, ^{14}C-proteins or ^{14}C-nucleic acid, which can be clearly differentiated from ^{14}C-microcapsules > 12 µm, could be useful to be implemented in future biodegradation testing. For instance, approaches similar as reported by Weng et al. [22] and Zumstein et al. [23] might be useful for characterization of the ^{14}C-uptake of microbial cells, which is also proposed by Zumstein et al. [24] to be considered for biodegradation assessment of plastics. In addition, the proportion of AR in the size fraction between 0.2 and 12 µm remained stable compared to 28 d with 1.77 ± 0.49%$_{AR}$ at 161 d (Fig. 2), indicating that no relevant fragments emerged in that size range.

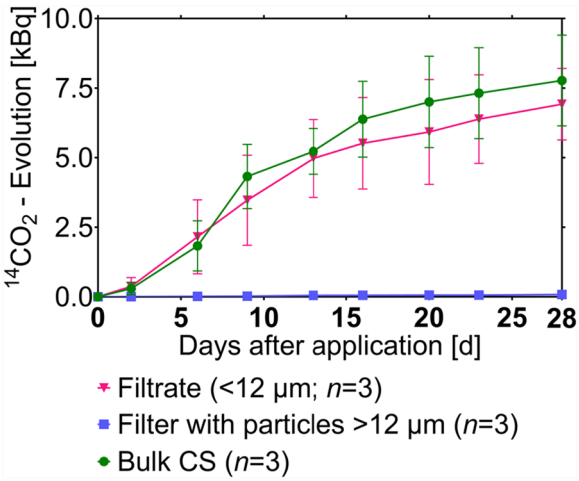

Fig. 3 Biodegradation test results of the second OECD TG 301B. $^{14}CO_2$-evolution of the Bulk CS and its separated size fractions: filter with particles > 12 µm and filtrate with compounds < 12 µm in the second OECD TG 301B. Plotted is the cumulative radioactivity (kBq) that was mineralized to $^{14}CO_2$ relative to the incubation time (mean and SD of n = 3)

The CS was submitted to a second OECD 301B biodegradation test (Fig. 3). Since the radioactivity found in the fraction > 12 µm decreased from d 0 to d 28 within the sequential filtration, the aim was to investigate whether particles (> 12 µm) were mineralized or whether the only source of mineralization was from lower size fractions and the decrease found in the largest size fraction originated from fragmentation or the imprecision of the method. Therefore, in this test, the CS was separated into two size fractions prior to biodegradation testing (< 12 µm and > 12 µm). The compounds and particles < 12 µm were in this approach mineralized to a similar degree as the bulk suspension (deviation by a factor of 1.1, $^{14}CO_2$-evolution of 6.92 ± 1.28 kBq for filtrate < 0.2 µm *vs* 7.77 ± 1.63 kBq for the bulk suspension; Fig. 3). However, for the size fraction of > 12 µm no mineralization to $^{14}CO_2$ was observed (0.08 ± 0.02 kBq). Hence, this experiment clearly showed that biodegradation with respect to $^{14}CO_2$ evolution largely originated from particles, mono- and oligomers with sizes below 0.2 µm instead of the PUA microcapsules.

Ultra-high performance liquid chromatography with high resolution mass spectrometry (UHPLC–HR-MS)

It was assumed that a higher fraction of radioactivity of the bulk suspension might be present in ^{14}C-molecules or ^{14}C-oligomers remaining from synthesis rather than ^{14}C-particles that were mineralized. The UHPLC–HR-MS analysis (total range of 100–6000 m/*z*) coupled with a radio detector (SI—Tables S6, S7, S8) was thus

employed to investigate of the filtrate (< 0.2 µm) of the pristine bulk suspension, which was used as the application solution. It was aimed to identify which components of the smallest particle size fraction (< 0.2 µm) of the bulk suspension might have been biodegraded to $^{14}CO_2$.

In this analysis, labeled and non-labeled aminocaproic acid (*m/z* range of 132.10125–132.1057; SI—Fig. S7) was detected based on the determined molecular formula using the Xcalibur Qual Browser (Version 4.0) in the HR-MS analysis. This molecule is the oxidized derivative of the ^{14}C-labeled monomer ^{14}C-hexamethylenediamine used for synthesis, containing a carboxyl group. For verification, HR-MS analysis of pure (≥ 99%) aminocaproic acid as a reference compound (10 ng/mL, Sigma-Aldrich Chemie GmbH, Germany, SI—Fig. S7) was performed. Focusing on the eluted radioactivity, within the radiodetection analysis of the eluate, the main radioactivity peak was detected in the same RT range (SI—Fig. S7) as the eluted aminocaproic acid. Furthermore, by means of the column recovery, the amount of radioactivity that eluted during the same RT as the aminocaproic acid peak was quantified. In this analysis, it could be demonstrated that 83.3 ± 2.29% (average of $n = 3$; SI—Fig. S8) of the injected radioactivity, more precisely of all ^{14}C-labeled molecules or oligomers introduced to this analysis, eluted at the same RT as aminocaproic acid (RT including both peaks from 3.5 to 7 min—Fig. S7).

Using the isotopic pattern analysis, all molecules or oligomers that consist of the same isotopic pattern of the discovered aminocaproic acid were extracted to a chromatogram. In this chromatogram (SI—Fig. S3) no other molecules or oligomers containing aminocaproic acid as building block eluted, since only the two consecutive peaks were present. This gives further evidence that aminocaproic acid constituted a high fraction of all ^{14}C-labeled molecules that were present in the filtrate of the CS (< 0.2 µm). Besides, the emerging two peaks of aminocaproic acid were presumably due to a part of the molecules being present in an ionized form and therefore more polar causing a faster elution. The other part was uncharged and therefore adhered more strongly to the non-polar column, prolonging RT.

Taken together, our analyses strongly implied that aminocaproic acid was present in high fractions above 80% in the suspension's filtrate (< 0.2 µm) attributable to the oxidized form of the hexamethylenediamine used for the synthesis of the PUA shell of the capsules. The proportion of radioactivity quantified within the column recovery (< 0.2 µm; 83.3 ± 2.3% of the injected radioactivity), that was attributable to aminocaproic acid, was then extrapolated to the radioactivity of the bulk suspension by multiplying this proportion with the relative amount of the bulk suspension's radioactivity in the filtrate (49.7 ± 1.67%$_{AR}$), resulting in approx. 41%$_{AR}$ of aminocaproic acid being dissolved in the bulk suspension. Therefore, presumably most of the observed mineralization originated from the degradation of aminocaproic acid. Supporting this deduction, aminocaproic acid is classified as readily biodegradable according to its safety data sheet with 76% mineralization in 28 d (OECD TG 301D [25]). However, the synthesized polymeric shell did not only consist of the labeled HMDA, but also of components of the co-polymer isocyanate and general crosslinked undefined, random structures. By labeling one monomer, the mineralization and tracking was focused on compounds and building blocks consisting of this monomer. The fate of compounds or molecules consisting of building blocks from (non-labeled) other parts of the polymer was not addressed in this study.

Methodological considerations for microplastic biodegradability testing: a comparative perspective

Our findings emphasize the necessity of characterizing and purifying polymer particles before biodegradation testing, as soluble low-molecular-weight residues can bias the derived mineralization rates. This outcome aligns with Karagianni et al. [26], who demonstrated that depending on the extraction of the polymeric shell and their purification method from the oil and soluble and insoluble ingredients of a microcapsule used for fragrances, the biodegradation test results (OECD 301 F [25]) largely differed, underscoring the necessity of eliminating non-polymeric components prior to testing.

Given the complexity of MP biodegradation assessments, radiolabeling provides distinct advantages for method validation, precise quantification and mass-balancing of polymer-derived mineralization. The advantages of isotope labeling in tracking the biodegradation and mineralization of polymers or polymer fractions of a product were highlighted by a study on radiolabeling approaches for polymer degradation [27]. Such labeling is particularly useful for tracking difficult-to-detect polymer particles, such as microcapsules with low polymer content. However, the high synthesis costs and the need for specialized laboratories with respective license and specific analytical instrumentation limits its application to applied research and method validation rather than routine testing. Once alternative endpoints are identified and methods are established, testing should ideally be possible without radiolabeling. Alternative analytical techniques might support here. Fourier transform infrared (FTIR) and Raman spectroscopy could be used to analyze polymer particles at different stages of biodegradation, providing

chemical characterization throughout the process. Scanning electron microscopy (SEM) can offer valuable insights into morphological changes and fragmentation. However, the feasibility of replacing radiolabeling with these methods depends on potential matrix interferences, MP particle size and their detection sensitivities as well as the availability of those analytical methods for routine testing.

Furthermore, recent studies have indicated size-dependent biodegradation of synthetic polymer particles showing that smaller MPs degrade more efficiently due to their higher surface area-to-volume ratio, enhancing microbial colonization and impact of enzymatic activity [28–34]. These findings support the need to integrate size monitoring alongside mineralization endpoints in biodegradability assessments.

Conclusion

This study supports two major recommendations for future biodegradation testing: Firstly, the tested material needs purification to exclude potential bias from the biodegradation of impurities or alternatively, a comprehensive characterization of the bulk product needs to be conducted. Secondly, monitoring the size distribution of the tested microparticles is useful, to obtain a more comprehensive picture including primary biodegradation. Integrating additional parameters such as particle size and the release or presence of bioavailable compounds gives more insights into how MPs degrade. The parameters substantiate the biodegradation test results within regulatory assessments to support accurate and valid classifications regarding MP degradability.

The UHPLC–HR-MS analysis of this study revealed that the apparent CS biodegradation was biased due to radiolabeled, low-molecular weight, soluble residues from polymer synthesis that caused the $^{14}CO_2$ evolution reaching 29%$_{AR}$ (day 161). We demonstrated that microcapsules from an aqueous suspension can be isolated (purified) by filtration with a rinsing step and subsequent resuspension in water. This procedure could also be applicable for non-labeled biodegradation testing.

The results demonstrate that ^{14}C-labeling is a powerful tool for distinguishing the polymer biodegradation from the mineralization of other constituents, in particular if the tested particles are more complex and contain more than the polymeric material. In addition, ^{14}C-labeling facilitates identification and quantification of compounds of interest, if further specific analyses coupled to radiodetection, such as UHPLC–HR-MS analysis, are implemented.

Abbreviations

PUA	Polyurea
CS	Capsule suspension
AR	Applied radioactivity
HCl	Hydrochloric acid
LSC	Liquid scintillation counting
MP	Microplastic
NaOH	Sodium hydroxide
RT	Retention time
TC	Total carbon
TG	Testing guideline
UHPLC–HR-MS	Ultra-high performance liquid chromatography with high-resolution mass spectrometry

Supplementary Information

The online version contains supplementary material available at https://doi.org/10.1186/s12302-025-01096-8.

Additional file1

Acknowledgements
We sincerely thank the laboratory technicians Christoph Eggenstein-Deimel, Thomas Hennecke, and Joana Bräutigam of the Fraunhofer IME Schmallenberg for their exceptional technical expertise and unwavering support throughout this project. Their contributions have been truly indispensable.

Author contributions
EMT: conceptualization, data curation, formal analysis, investigation, visualization, methodology, writing the original draft and editing of reviewed manuscript; JH: UHPLC–HR-MS analysis investigation and evaluation; BM: methodology; AJ, AS, BM: writing—review and editing. AJ, AS, BM, DH, MS, PD, HE, RH: supervision. AS, BM, DH, MS, PD, HE: project administration, funding acquisition. All authors revised and edited the manuscript and approved the final version before submission.

Funding
Open Access funding enabled and organized by Projekt DEAL. This project was funded by Bayer AG, Crop Science Division.

Availability of data and material
The data used and analyzed during the current study are available from the corresponding author on reasonable request.

Declarations

Conflict of interest
Philipp Dalkmann and Holger Egger are employees of the Bayer AG Division Crop Science, a leading manufacturer of agricultural chemicals. Roman Heumann is and Eva-Maria Teggers was employed at INVITE GmbH, Germany, a cross-industry company with 50% business shares belonging to Bayer AG and 50% business shares belonging to universities (Technical University of Dortmund, Germany, and Heinrich Heine University Düsseldorf, Germany).

Ethical approval and consent to participate
Not applicable.

Consent for publication
All authors consent for the publication of this work. They have reviewed the final manuscript for accuracy.

Author details
[1]Fraunhofer-Institute for Molecular Biology and Applied Ecology IME, Auf dem Aberg 1, 57392 Schmallenberg, Germany. [2]INVITE GmbH, Otto-Bayer-Straße 32, 51061 Cologne, Germany. [3]Institute for Environmental Research, RWTH Aachen University, Worringerweg 1, 52074 Aachen, Germany. [4]Bayer AG, Research & Development, Alfred-Nobel-Straße 50, 40789 Monheim, Germany. [5]Department of Exposure Science, Helmholtz Centre for Environmental Research - UFZ, Permoserstraße 15, 04318 Leipzig, Germany.

Received: 18 December 2024 Accepted: 3 April 2025
Published online: 26 April 2025

References

1. European Commission (2023) ANNEX to the Commission Regulation (EU) amending Annex XVII to Regulation (EC) No 1907/2006 of the European Parliament and of the Council concerning the Registration, Evaluation, Authorisation and Restriction of Chemicals (REACH) as regards synthetic polymer microparticles
2. OECD (1992) OECD guideline for testing chemicals—ready biodegradability; 301B CO2 Evolution Test
3. OECD (2006) OECD Guideline for testing chemicals - ready biodegradability; 310 CO2 in sealed vessels (Headspace Test)
4. Haider G, Steffens D, Moser G, Müller C, Kammann CI (2017) Biochar reduced nitrate leaching and improved soil moisture content without yield improvements in a four-year field study. Agr Ecosyst Environ 237:80–94. https://doi.org/10.1016/j.agee.2016.12.019
5. Lucas N, Bienaime C, Belloy C, Queneudec M, Silvestre F, Nava-Saucedo J-E (2008) Polymer biodegradation: mechanisms and estimation techniques—a review. Chemosphere 73:429–442. https://doi.org/10.1016/j.chemosphere.2008.06.064
6. Albright VC, Chai Y (2021) Knowledge gaps in polymer biodegradation research. Environ Sci Technol 55:11476–11488. https://doi.org/10.1021/acs.est.1c00994
7. Haider TP, Völker C, Kramm J, Landfester K, Wurm FR (2019) Plastics of the future? The impact of biodegradable polymers on the environment and on society. Angew Chem Int Ed 58:50–62. https://doi.org/10.1002/anie.201805766
8. Silva RRA, Marques CS, Arruda TR, Teixeira SC, De Oliveira TV (2023) Biodegradation of polymers: stages, measurement, standards and prospects. Macromol 3:371–399. https://doi.org/10.3390/macromol3020023
9. Carmichael N (2014) European centre for ecotoxicology and toxicology of chemicals. In: Encyclopedia of toxicology. Elsevier, pp 547–548
10. Hahn S, Hennecke D (2023) What can we learn from biodegradation of natural polymers for regulation? Environ Sci Eur 35:50. https://doi.org/10.1186/s12302-023-00755-y
11. Mitrano DM, Wohlleben W (2020) Microplastic regulation should be more precise to incentivize both innovation and environmental safety. Nat Commun 11:5324. https://doi.org/10.1038/s41467-020-19069-1
12. Krause J, Egger H (2021) Aqueous capsule suspension concentrates based on polyurea shell material containing polyfunctional aminocarboxylic esters (WO2021136758). World Intellectual Property Organization (WIPO).
13. Pires-Oliveira R, Kfouri MS, Mendonça B, Cardoso-Gustavson P (2020) Nanopesticides: from the bench to the market. In: Fraceto, L.F., S.S. de Castro, V.L., Grillo, R., Ávila, D., Caixeta Oliveira, H., Lima, R. (Eds.), Nanopesticides: From Research and Development to Mechanisms of Action and Sustainable Use in Agriculture. Springer International Publishing, Cham.
14. Zhang R, Huang W, Lyu P, Yan S, Wang X, Ju J (2022) Polyurea for blast and impact protection: a review. Polymers 14:2670. https://doi.org/10.3390/polym14132670
15. OECD (1992) OECD guideline for testing chemicals—ready biodegradability; 301F Manometric Respiratory Test
16. Birch H, Sjøholm KK, Dechesne A, Sparham C, Van Egmond R, Mayer P (2022) Biodegradation kinetics of fragrances, plasticizers, UV filters, and PAHs in a mixture—changing test concentrations over 5 orders of magnitude. Environ Sci Technol 56:293–301. https://doi.org/10.1021/acs.est.1c05583
17. Blaschko H (1935) The mechanism of catalase inhibitions. Biochemical Journal 29:2303–2312. https://doi.org/10.1042/bj0292303
18. Süßmuth R, Shrestha P, Andrea Diaz Navarrete C, Wege F-F, Achten C, Hennecke D (2024) Impact of different sterilisation techniques on sorption and NER formation of test chemicals in soil. Chemosphere 357:141915. https://doi.org/10.1016/j.chemosphere.2024.141915
19. Hendrix K, Bleyen N, Mennecart T, Bruggeman C, Valcke E (2019) Sodium azide used as microbial inhibitor caused unwanted by-products in anaerobic geochemical studies. Appl Geochem 107:120–130. https://doi.org/10.1016/j.apgeochem.2019.05.014
20. Singh B, Sharma N (2008) Mechanistic implications of plastic degradation. Polym Degrad Stab 93:561–584. https://doi.org/10.1016/j.polymdegradstab.2007.11.008
21. Tokiwa Y, Calabia B, Ugwu C, Aiba S (2009) Biodegradability of plastics. IJMS 10:3722–3742. https://doi.org/10.3390/ijms10093722
22. Weng J, Müller K, Morgaienko O, Elsner M, Ivleva NP (2023) Multi-element stable isotope Raman microspectroscopy of bacterial carotenoids unravels rare signal shift patterns and single-cell phenotypic heterogeneity. Analyst 148:128–136. https://doi.org/10.1039/D2AN01603F
23. Zumstein MT, Schintlmeister A, Nelson TF, Baumgartner R, Woebken D, Wagner M, Kohler H-PE, McNeill K, Sander M (2018) Biodegradation of synthetic polymers in soils: Tracking carbon into CO_2 and microbial biomass. Sci Adv 4:eaas9024. https://doi.org/10.1126/sciadv.aas9024
24. Zumstein MT, Narayan R, Kohler H-PE, McNeill K, Sander M (2019) Dos and do nots when assessing the biodegradation of plastics. Environ Sci Technol 53:9967–9969. https://doi.org/10.1021/acs.est.9b04513
25. OECD (1992) OECD guideline for testing chemicals—ready biodegradability; 301D Closed Bottle Test
26. Karagianni K, Kuntzmann-Dembele F, Bocokic V, Charbonnier A, Harrison I, Kreutzer G, Mendoza A, Jenner K (2024) Fragrance encapsulates: effect of polymeric shell purification method on the accuracy of biodegradability testing. Environ Toxic Chemy 43:1242–1249. https://doi.org/10.1002/etc.5852
27. Adeleh S, Bol R, Becker T, Herres-Pawlis S, Vereecken H, Pütz T (2024) Radiolabeling for polymers degradation studies: opportunities and challenges ahead. Polym Degrad Stab 230:111053. https://doi.org/10.1016/j.polymdegradstab.2024.111053
28. McDonough K, Itrich N, Casteel K, Menzies J, Williams T, Krivos K, Price J (2017) Assessing the biodegradability of microparticles disposed down the drain. Chemosphere 175:452–458. https://doi.org/10.1016/j.chemosphere.2017.02.091
29. García-Depraect O, Lebrero R, Rodriguez-Vega S, Bordel S, Santos-Beneit F, Martínez-Mendoza LJ, Aragão Börner R, Börner T, Muñoz R (2022) Biodegradation of bioplastics under aerobic and anaerobic aqueous conditions: kinetics, carbon fate and particle size effect. Biores Technol 344:126265. https://doi.org/10.1016/j.biortech.2021.126265
30. Chinaglia S, Tosin M, Degli-Innocenti F (2018) Biodegradation rate of biodegradable plastics at molecular level. Polym Degrad Stab 147:237–244. https://doi.org/10.1016/j.polymdegradstab.2017.12.011
31. ECETOC EC for E and T of C (2020) Applicability of analytical tools, test methods and models for polymer risk assessment. Elsevier, Brussels
32. Zhao J, Wang X, Zeng J, Yang G, Shi F, Yan Q (2005) Biodegradation of poly(butylene succinate) in compost. J Appl Polym Sci 97:2273–2278. https://doi.org/10.1002/app.22009
33. Rogers KL, Carreres-Calabuig JA, Gorokhova E, Posth NR (2020) Micro-by-micro interactions: How microorganisms influence the fate of marine microplastics. Limnol Oceanogr Letters 5:18–36. https://doi.org/10.1002/lol2.10136
34. Hino S, Kawasaki N, Yamano N, Nakamura T, Nakayama A (2023) Effects of particle size on marine biodegradation of poly(l-lactic acid) and poly(ε-caprolactone). Mater Chem Phys 303:127813. https://doi.org/10.1016/j.matchemphys.2023.127813

Publisher's Note

Journal of Hazardous Materials 500 (2025) 140424

Contents lists available at ScienceDirect

Journal of Hazardous Materials

journal homepage: www.elsevier.com/locate/jhazmat

Simulated sunlight exposure as a prerequisite for the biodegradation of persistent microplastics

Eva-Maria Teggers [a,b,c,*], Svenja Winterhoff [a], Svetlana Heck [a], Jonas Hardebusch [a], Boris Meisterjahn [a,**], Markus Simon [a], Dieter Hennecke [a], Roman Heumann [b], Holger Egger [d], Philipp Dalkmann [d], Andreas Schäffer [c,1], Annika Jahnke [c,e,1]

[a] Fraunhofer Institute for Molecular Biology and Applied Ecology IME, Auf dem Aberg 1, Schmallenberg 57392, Germany
[b] INVITE GmbH, Otto-Bayer-Straße 32, Cologne 51061, Germany
[c] Institute for Environmental Research, RWTH Aachen University, Worringerweg 1, Aachen 52074, Germany
[d] Bayer AG, Research & Development, Alfred-Nobel-Straße 50, Monheim 40789, Germany
[e] Helmholtz Centre for Environmental Research - UFZ, Department of Exposure Science, Permoserstraße 15, Leipzig 04318, Germany

HIGHLIGHTS

- Photooxidation led to fragmentation and release of ^{14}C-labeled compounds.
- Aminocaproic acid was identified as a photooxidation product of polyurea.
- Simulated sunlight increased polyurea biodegradation in laboratory tests.
- Coupled OECD test methods can reflect potential environmental degradation pathways.
- Radiolabeling allowed precise tracking of polymer mineralization to $^{14}CO_2$.

GRAPHICAL ABSTRACT

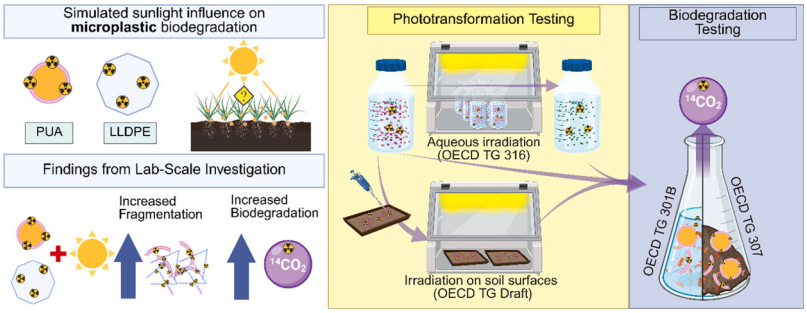

ARTICLE INFO

Keywords:
Microplastics
Photooxidation
Biodegradation
Polyurea microcapsules
Radiolabeling

ABSTRACT

The environmental fate and biodegradability of microplastics (MPs) are key concerns in regulatory and scientific contexts. Standard biodegradation testing effectively evaluate microbial decomposition, but overlook crucial abiotic processes, particularly photooxidation, which may significantly alter polymer structures and their susceptibility to microbial breakdown. Therefore, we investigated how simulated sunlight exposure influences the subsequent (bio)degradability of radiolabeled ^{14}C-polyurea (PUA) microcapsules and ^{14}C-linear low-density polyethylene (LLDPE) particles. Using standardized OECD test guidelines, we conducted coupled photo- and biodegradation experiments in both aqueous and soil environments. Our results demonstrate that simulated sunlight exposure led to fragmentation of PUA microcapsules and the release of low-molecular-weight ^{14}C-labeled compounds, such as aminocaproic acid. Irradiated PUA microcapsules showed significantly enhanced biodegradation in aqueous (up to $28 \pm 4.05\ \%_{AR}$, OECD TG 301B) and soil-based tests (up to $63.2 \pm 13.4\ \%_{AR}$, OECD TG 307), compared to negligible biodegradation in non-irradiated controls. In contrast, LLDPE MPs

* Corresponding author at: Fraunhofer Institute for Molecular Biology and Applied Ecology IME, Auf dem Aberg 1, Schmallenberg 57392, Germany.
** Corresponding author.
E-mail addresses: eva.teggers@rwth-aachen.de (E.-M. Teggers), boris.meisterjahn@ime.fraunhofer.de (B. Meisterjahn).
[1] Andreas Schäffer and Annika Jahnke share the last authorship.

https://doi.org/10.1016/j.jhazmat.2025.140424
Received 4 June 2025; Received in revised form 31 October 2025; Accepted 7 November 2025
Available online 8 November 2025

demonstrated only minor changes. These findings establish that abiotic weathering processes substantially influence MP biodegradability for certain polymer types, and demonstrate the necessity of incorporating realistic environmental exposure conditions into standardized testing protocols. This study improves the understanding of MP degradation pathways and supports more comprehensive regulatory evaluation strategies.

1. Introduction

The extensive production of plastics, including microplastics (MPs), and their uncontrolled emissions into the environment raise major concerns for human and environmental health. While most MP research has focused on aquatic systems, MP pollution in agricultural soils has been less investigated but its relevance is increasingly recognized. A major source of MPs in soil is the fragmentation of plastic mulch films by weathering, including abiotic processes such as sunlight exposure. Primary MPs, intentionally manufactured, also receive attention, with examples including polymer seed coatings and controlled-release fertilizers.

Encapsulated plant protection products (PPPs), represent a lesser-known source of primary MPs. In such products, the active ingredient is enclosed within a polymer microcapsule to enable controlled release and prolonged efficacy. Reports by the Food and Agriculture Organization [26], the United Nations Environment Programme [68], and the Center for International Environmental Law (CIEL, [11]) identify encapsulated pesticides as a potential contributor to MP pollution in soils and related food security risks. In the past, regulatory risk assessments for PPP have considered only the active ingredient, neglecting the fate and potential persistence of the polymeric shell [18,38]. Only recently attention has been given to the full formulation, including polymer-based carriers, as highlighted by Brunning et al. [10] and Nederstigt et al. [48]. The EU Annex XV Restriction Report [22] estimated that capsule suspensions of PPPs account for ~ 500 t of MPs released annually to agricultural soils in Europe.

One example is Prosper 300 CS (Bayer AG), a systemic fungicide contained in polyurea (PUA) microcapsules. Based on product application rates, the estimated worst-case scenario for microplastic (MP) emissions is 150 g/ha per season, assuming a polymer content of 1–5 % and up to three applications. These capsule suspensions are directly applied to agricultural soils, hence their environmental fate, in particular the assessment of their persistence, demands further investigation.

The European Union has recently restricted intentionally added MPs, targeting primary MPs 0.1–5 mm in size added to products such as cosmetics, fertilizers, detergents, and paints. Excluded are soluble, naturally polymerized, non-carbonaceous, and biodegradable primary MPs. For the latter, biodegradability must be demonstrated according to Appendix 15 of Annex XVII to Regulation (EC) No 1907/2006 (REACH, [23]). Current standard methods (OECD, ISO, SI – Table S1) focus on ultimate biodegradability, usually measured as CO_2 evolution, without accounting for abiotic weathering processes such as photooxidation, mechanical stress, hydrolysis, or thermal degradation, even though these can strongly influence MP environmental fate [13,28,46,73].

Recent literature has noted limitations of existing test methods for MPs' biodegradability [12,31,32,47,61,64]. Biodegradability tests were designed for soluble or low-molecular-weight (LMW) chemicals, where defining biodegradation solely by mineralization is reasonable for degradation screening. For polymers and plastics, which may consist of a complex mixture of molecules with varying molecular weights, likely including additives or other plastic-associated compounds, mineralization as only endpoint can misrepresent persistence. Polymeric microcapsules pose additional challenges. Due to their low polymer content and multi-component composition they complicate biodegradation testing, not to mention MP extraction procedures that can bias test results [37]. From a scientific perspective biodegradation of polymers is usually divided into four steps: biodeterioration, depolymerization, bioassimilation, and mineralization [32,43]. Therefore, alterations such as MP fragmentation and the release of plastic-associated compounds and transformation products might be relevant endpoints for degradation testing.

Photooxidation is a primary driver of polymer aging [27,33,41,44], altering surface chemistry and increasing susceptibility to microbial attack. Impurities or sorbed pollutants can accelerate photooxidation or promote indirect photolysis through reactive oxygen species (ROS) formation [21,73]. Dissolved substances such as cations, anions, dissolved organic matter (DOM), and minerals may further modulate these processes [15,19,74,77]. While DOM can act as a photosensitizer [6,45,55,69,75], other constituents may quench ROS, resulting in slower degradation [42,71,72].

Environmental fate comprises multiple processes, yet most studies address them separately (e.g., photochemical or biodegradation). Recent reviews and studies highlight that photooxidation can substantially alter polymer chemistry, size distributions, sorption behavior, and corresponding bio-interactions but understanding its influence on subsequent biodegradation remains largely absent from current testing strategies. This represents not only a scientific knowledge gap but also a regulatory gap in assessing the environmental persistence of MPs under realistic conditions, particularly for microcapsule MPs. The European Food Safety Authority (EFSA) has explicitly cautioned that excluding surface processes such as photolysis from persistence assessments can lead to overestimated degradation half-lives ($DegT_{50}$) and false-positive classifications of substances as persistent [24].

Our study addresses these gaps by investigating whether simulated sunlight exposure impacts the subsequent biodegradability of MPs. Using PUA microcapsules as a representative primary MP and linear low-density polyethylene (LLDPE) as a source for persistent secondary MP, we assessed biodegradation in both aqueous and soil systems subsequent to phototransformation. The study is particularly relevant as it demonstrates a sequential testing strategy combining established regulatory guidelines [52] and an OECD Draft TG [49] for simulated sunlight exposure, OECD TG 301 [50] for screening biodegradation, and OECD TG 307 [51] for biodegradation in soil, linking abiotic weathering to biodegradation outcomes. We used radiolabeled polymers to enable a precise mass balance analysis, mineralization tracking, and identification of transformation products.

2. Material and methods

2.1. Polymers

^{14}C-labeled PUA microcapsules (approx. 3.49 MBq/mg, Bayer AG, Germany) were synthesized in a similar way as described in the patent publication WO2021136758 [39]. The synthesis was performed by the interfacial polymerization of diisocyanate and polyamine in an oil-in-water emulsion. For the radioactive labeling, [1,6-^{14}C] hexamethylenediamine (HMDA, 1887 MBq/mmol, Tjaden Biosciences LLC, USA), together with modified polymeric diphenylmethane diisocyanate (pMDI) were used. The pMDI comprised ≥ 2 binding sites, creating a crosslinked polymer structure. Additional components in the suspension included an organic phase, an oil (8.59 wt% of the undiluted CS, Solvesso 200 ND, ExxonMobil, USA), a dispersant (0.23 wt%, Reax 88, Ingevity Holdings SPRL, USA), and water (90.9 wt%). In a second approach, PUA was synthesized with a modified pMDI additionally containing ester functions in the structure with the intention to increase biodegradability of the final polymer structure (PUA_{mod}). The PUA microcapsules are used for the encapsulation of pesticides and are present

in certain pesticide formulations (e.g., in the fungicide Prosper 300 CS https://www.cropscience.bayer.it/prodotti/fungicidi/prosper-300-cs, Bayer AG) which are currently available on the European market. For the radiolabeled material of this study, both PUA and PUA_{mod} were synthesized on a smaller scale (approx. 200:1 to production scale and approx. 10:1 to normal lab scale), requiring lower concentrations and smaller high-shear equipment (ULTRA TURRAX Tube Disperser, IKA-Werke GmbH & CO. KG, Germany). The polymeric shell amounted to less than 1 wt% of the ^{14}C-suspension (w/w).

The PUA and PUA_{mod} were purified by filtration through a 12 µm pore-sized cellulose nitrate filter (Whatman AE 100, Cytiva, USA) to remove residual non-polymerized ^{14}C-compounds and subsequently resuspended in ultra-high-quality (UHQ) water (PURELAB Ultra, ELGA LabWater, Germany) by ultrasonic bath treatment (Sonorex Super RK514H, Bandelin GmbH & Co. KG, Germany) as described by Teggers et al. [64]. The size distribution of the PUA and PUA_{mod} suspensions was determined using laser diffraction particle size analysis (PSA, Mastersizer 2000, Malvern Panalytical Ltd, UK).

^{14}C-labeled LLDPE MPs (70.46 MBq/g) were synthesized based on methods described by Sinn et al. [62] and Quijada et al. [54], using ^{14}C-1-octadecene (2035 MBq/mmol, American Radiolabeled Chemicals Inc., USA) and cryo-milled in order to imitate MPs originating from agricultural mulch films, and their particle size distribution was analyzed using PSA by Analysette 22 NanoTec, Fritsch GmbH, Germany. For our experiments, the ^{14}C-cellulose was dissolved in 1 N sodium hydroxide (NaOH) and for application, 700 µL NaOH was dissolved in 7.5 mL UHQ water for application with a radioactivity of 10.1 ± 0.07 kBq (average of $n = 4$ and standard deviation (SD)).

2.2. Test soils

Reference soils RefeSol 01-A and 03-G (https://www.refesol.de/, Fraunhofer IME, Schmallenberg, Germany; Supplementary information (SI - Table S2) were utilized for the photodegradation and biodegradation tests. RefeSol 01-A soil consists of a sandy loam with light humic properties and an organic carbon (OC) content of 1.03 %, representative of typical arable soil properties. RefeSol 03-G represents a grassland soil, with a silty loam texture, comprising higher contents of silt, clay and organic carbon (OC: 3.87 %). Both are representative of agricultural areas in Germany and are accepted by the German Federal Environment Agency for use in regulatory guideline studies, e.g., addressing the biodegradation of chemicals. Prior to testing, the soil was sieved to achieve a particle size of ≤ 2 mm, and its water content was adjusted to 50 % of its maximum water holding capacity of 239 g/kg (WHC_{max}, SI – Table S2).

2.3. Quantification of radioactivity in different compartments

Generally, the extent of mineralization as an endpoint of (bio) degradation was calculated based on the evolved $^{14}CO_2$, which was trapped in NaOH in a flow-through system. For the biodegradation test in soil (OECD TG 307) and for the irradiation on soil surfaces (OECD Draft TG), additional absorption traps containing sulfuric acid (H_2SO_4) and ethylene glycol were used to trap volatile alkaline and organic ^{14}C-compounds, respectively. Since we tested ^{14}C-labeled polymers, the aeration of the flow-through setup could be done using ambient air instead of CO_2-free synthetic air. The NaOH traps were sampled every 2–19 days during the incubation period, depending on the current rate of $^{14}CO_2$ development. The first NaOH samples were taken after 2 or 3 d, and subsequent sampling intervals were adjusted based on the radioactivity measured in the previous 2 d. If only a small amount of $^{14}CO_2$ had developed, the next sample was taken after a longer incubation period. Conversely, high levels of detected radioactivity suggested a rapid formation of $^{14}CO_2$. Therefore, sampling was performed in shorter sampling intervals. The radioactivity within the traps was quantified using liquid scintillation counting (LSC). For this purpose and depending on the test medium (alkaline, acidic, organic), 0.5 mL or 1 mL NaOH were combined with 4 mL of the LSC cocktail Picofluor Plus (Perkin Elmer, Germany), 0.5 mL ethylene glycol was combined with 10 mL of the LSC cocktail Supersolve X (Zinsser Analytics, Germany), and 0.5 mL H_2SO_4 was combined with 4 mL of the LSC cocktail Supersolve X and measured with a liquid scintillation counter (HIDEX 600 SL LSC, HIDEX Oy, Finland). The activity in aqueous phases was quantified, e.g., after the end of the OECD TG 301B biodegradation test by combining 1 mL of the sample with 4 mL Supersolve X. The remaining radioactivity in soil, either after irradiation (OECD Draft TG) or upon terminating the biodegradation test (OECD TG 307), was quantified by first drying the soil, where necessary, and then combusting subsamples of approx. 300 mg in an oxidizer (HIDEX 600 OX, HIDEX Oy, Finland). The resulting $^{14}CO_2$ from the combustion was collected in specific LSC-cocktail Oxysolve C-400 (Zinsser Analytic GmbH, Germany) and quantified by LSC-analysis.

2.4. Simulated sunlight irradiation

2.4.1. General irradiation settings

Two different irradiation methods (MI and MII, Fig. 1) were applied to simulate potential, relevant environmental photooxidation to which the pristine polymers might be exposed in order to assess the size distribution after simulated sunlight exposure and the biodegradation. The irradiation was either performed in an aqueous setting following the OECD TG 316 [52] "Phototransformation of Chemicals in Water" (MI) or on soil surfaces (MII) as described in OECD Draft TG [49] "Phototransformation of Chemicals on Soil Surfaces".

All procedures were performed under continuous irradiation in the chamber of a SUNTEST CPS+ device (295–800 nm, Atlas Material Testing Technology GmbH, Germany), equipped with a Xenon lamp of a light intensity of 75 W/m^2 at 300–400 nm according to the manufacturer's specification. The intensity was verified using the BLACK-Comet UV–VIS Spectrometer (BLK-CR2, StellarNet, Inc., USA). The irradiation energy was translated to equivalent days of natural sunlight of summer days in the Northern hemisphere (30–50°N) according to the calculation as described in the OECD Draft TG [49]. Table 1 provides an overview of the exposure durations applied in the respective testing procedures for each irradiation method.

In addition to the air conditioning system of the SUNTEST CPS+, a cryostat using ethylene glycol for cooling the base of the soil surface and the base of the vials was installed (see SI - Fig. S1- E), F)) to maintain a temperature of less than 35 °C in the aqueous suspensions and to cool down the soil surface temperature. The temperature during all irradiation experiments was monitored using thermo data loggers (EL-USB-TP and EL-USB-TP-LCD; accuracy ±0.55 °C), with measurements recorded at hourly intervals. The sensor positions are shown in the SI - Fig. S1, D) and H). For the OECD Draft TG one sensor was placed in the soil surface chamber and one outside the chamber. For the aqueous irradiation the sensor was placed at the bottom of the irradiated Quartz glass vial. After light exposure, the radioactivity of the suspension and of the soil was determined for mass balance analysis.

2.4.2. Aqueous irradiation (MI)

For the aqueous irradiation of the PUA_{mod} (**MI-Procedure 2**, Fig. 1 and Table 2), six replicates of 15 mL PUA_{mod} consisting of an applied radioactivity (AR) of 5.23 ± 0.21 kBq/15 mL were prepared in quartz glass vials (Ø 2.6 cm, 10.5 cm height, SI - Fig. S2) and placed in the irradiation chamber. Three vials were sealed with gas-tight quartz glass lids and used for the downstream biodegradation test (OECD TG 301B) and the remaining three were closed with quartz glass lids, which were equipped with an input and an output that were connected to a flow-through system to trap potentially evolving $^{14}CO_2$ in NaOH (see Section 2.3 for details on the quantification of radioactivity). **MI-Procedure 1** and **MI-Procedure 3** (Fig. 1, Table 2) were performed with a higher AR than 5.23 ± 0.21 kBq/15 mL. Five replicates each containing 15 mL

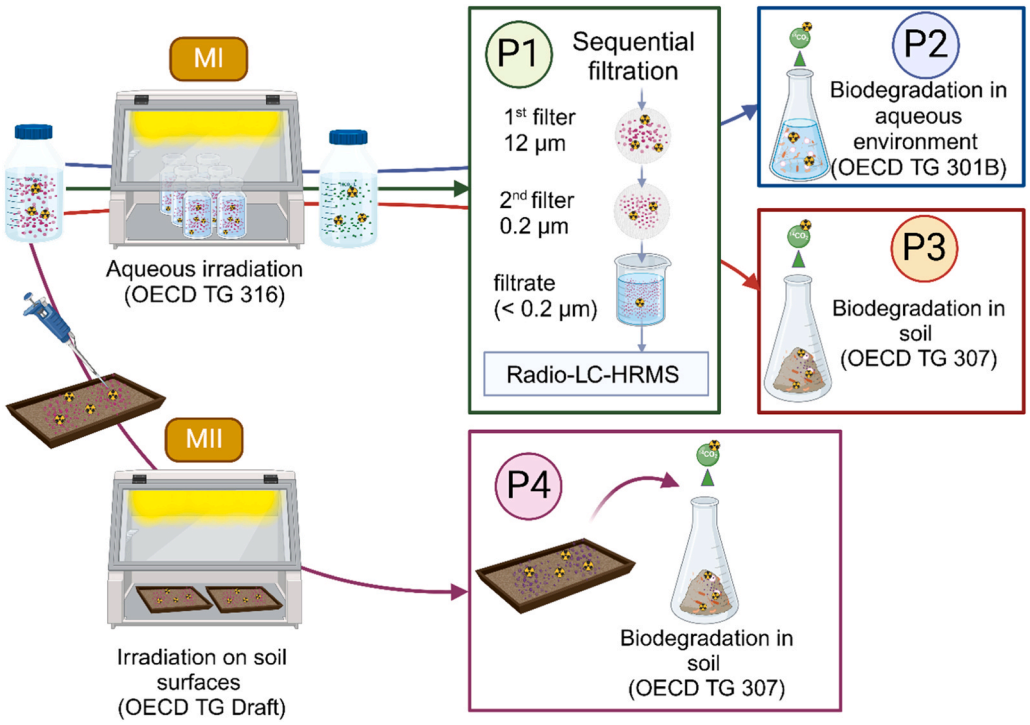

Fig. 1. Procedures (P) to investigate the influence of simulated sunlight exposure of MPs by implementing two different irradiation methods (MI and MII) on the biodegradation and fragmentation of the MPs using coupled standardized guidelines for irradiation and biodegradation tests. Details of the performed procedures are provided in Table 2.

Table 1
Overview of irradiation exposure durations and test materials used in the respective testing procedures.

Procedure	Irradiation Method	Material	Days of Irradiation [d]/eq. summer days[a]
Procedure 1 and 3	MI - Aqueous Irradiation	PUAmod	13.9/41.5
		LLDPE	13.9/41.5
Procedure 2		PUAmod	13.9/41.5
Procedure 4	MII – Irradiation on soil surface	PUAmod	9.9/29.6
		PUA	
		LLDPE	10.1/30.1

[a] Calculated to the equivalent sunlight energy of natural summer days in the Northern hemisphere (30–50°N) acc. to OECD draft TG.

Table 2
Procedures to investigate the influence of light exposure of MP on their biodegradation and fragmentation using coupled standardized OECD guidelines for irradiation and biodegradation tests. (See Fig. 1 for the illustration of the test methods.).

	Procedure description	Irradiation/ biodegradation following	Tested Material
Procedure 1 (P1)	Aqueous irradiation and sequential filtration	OECD TG 316	PUA_{mod}; LLDPE
Procedure 2 (P2)	Aqueous irradiation followed by biodegradation in aqueous environment	OECD TG 316, OECD TG 301B	PUA_{mod}
Procedure 3 (P3)	Aqueous irradiation followed by biodegradation in soil	OECD TG 316, OECD TG 307	PUA_{mod}
Procedure 4(P4)	Irradiation on soil surface followed by biodegradation in soil	OECD TG 316, OECD TG 307	PUA_{mod}; PUA; LLDPE

of the PUA_{mod} suspension (3.5 ± 0.16 kBq/mL) and five replicates of 15 mL of the LLDPE suspension (4.6 ± 1.95 kBq/mL) were placed in the irradiation chamber.

2.4.3. *Irradiation on soil surfaces (MII)*

For **MII-Procedure 4** (Fig. 1, Table 2), the irradiation of the polymers (PUA_{mod}, PUA, Cellulose and PE) on the soil surface, the setup was according to the draft OECD TG "Phototransformation of Chemicals on Soil Surfaces" [51]. In a first step, 10 g_{dw} (dry weight) soil (RefeSol 01-A, see Section 2.2) were suspended in water in order to be cast in quartz glass dishes (18 × 3.5 × 1 cm, SI - Fig. S2). Thereafter, the dishes were placed in a drying cabinet at 35 °C to generate a dry soil layer with a thickness of approx. 2 mm.

For the application 1.5 mL of PUA or PUA_{mod} (31.7 ± 0.06 kBq/1.5 mL PUA; 26.0 ± 0.04 kBq/1.5 mL PUA_{mod}) were applied ($n = 4$ of the dried soil each). Since in previous tests the SD observed for the aqueous application of the LLDPE suspension was high, in this test exact amounts of 1.7, 1.9, 2.1, and 2.8 mg of LLDPE with a determined specific radioactivity of 56.6 kBq/mg were weighted and mixed into the 10 mL water aliquots (equals to a total applied radioactivity (AR) of 96.1, 107, 119, 158 kBq respectively). These aliquots were then used for preparation of the soil suspension used for generating the soil layer. Overall, two replicates (R1 and R2) were irradiated. According to the draft OECD TG, the temperature of the irradiated soil layer shall be kept at 20 ± 2 °C. However, the proposed set-up of the draft OECD TG inevitably generates a temperature gradient, as the lower part of the soil layer is in close proximity to the cooling system, which is set to ≥ 5 °C and the surface of the soil is directly exposed and heated up upon irradiation from the xenon lamp, reaching up to approx. 80 °C (SI – Fig. S3 and S4).

This means that the soil layer is exposed to extreme temperature conditions and the temperature requirement of the guideline cannot fully be maintained [25,35]. Hence, the two remaining replicates were prepared as dark controls in a drying cabinet in which the temperature was set at the highest observed soil temperature (80°C) during irradiation as worst case for possible temperature-induced degradation. This

approach aimed to reliably distinguish between degradation induced by thermal effects from that induced by temperature combined with the photolytic degradation. The light-exposed soil layers were connected to the flow-through system to trap evolving volatile acidic compounds such as $^{14}CO2$, alkaline and organic compounds during irradiation.

2.5. Biodegradation tests

We applied a two-step testing approach in which simulated sunlight exposure, performed according to OECD TG 316 (aqueous medium) or the OECD Draft TG (soil-surface photolysis), was followed by biodegradation testing using OECD TG 301B or TG 307. This sequence reflects a potential realistic environmental pathway for surface-exposed MPs, where sunlight-driven phototransformation can accelerate microbial degradation. The approach aims to align with current regulatory photolysis guidance, including EFSA recommendations for assessing soil phototransformation products [24].

2.5.1. Biodegradation of light-exposed PUAmod microcapsules in the aqueous medium

The biodegradation of aqueous irradiated PUA_{mod} was investigated following OECD TG 301B "CO_2-Evolution Test" (**MI-Procedure 2,** Fig. 1**,** Table 2). As inoculum we applied filtered supernatant of activated sludge instead of bulk sludge, and the test was modified by measuring $^{14}CO_2$ instead of CO_2 for sensitive assignment to the ^{14}C-PUA_{mod} degradation [64]. To monitor the overall degradation performance of the inoculum, the biodegradation of a standard reference substance for ready biodegradability, labeled sodium benzoate form (benzoic acid [ring-^{14}C (U)] sodium salt, 130 mCi/mmol, American Radiolabeled Chemicals Inc., USA), was included in the same test run. The amount of AR was 2.73 ± 0.04 kBq/8.5 mL for PUA_{mod} ($n = 3$) and 58.3 ± 0.18 kBq/8.5 mL for ^{14}C-sodium benzoate ($n = 1$). Table 3 provides an overview of the incubation times of all applied biodegradation tests.

2.5.2. Biodegradation of light-exposed MPs in soil

For **MI-Procedure 3** (Fig. 1, Table 2) and **MII-Procedure 4** (Fig. 1, Table 2) biodegradation tests following the OECD TG 307 "Aerobic and Anaerobic Transformation in Soil" were performed in the dark with sufficient air supply via the flow-through ventilation system at a temperature of 20 ± 2 °C. For **MI-Procedure 3** 0.5 mL (1.75 KBq) of the irradiated PUA_{mod} suspension was applied to 25 g_{dw} of reference soil (01-A and 03-G). For **MII-Procedure 4**, the irradiated ($n = 2$) and non-irradiated ($n = 2$) soil replicate layers applied with PUA_{mod}, PUA, LLDPE was each combined separately for each material, due to their different positions in the irradiation chamber and related possible differences regarding the irradiation intensity or shading effects. Therefore, both replicates were mixed thoroughly to allow homogenous application and the radioactivity of the soil was determined for balancing the mass in the downstream biodegradation test. For application to the biodegradation test (OECD TG 307) after the soil irradiation experiments, 5 g aliquots of the irradiated soil (SI – Table S4) were applied to 50 g untreated biologically active soil (RefeSol 01-A, 10 days preincubated at 22 ± 3 °C) in triplicates each.

Table 3
Overview of the incubation times of the different biodegradation tests.

Procedure	Irradiation method	Biodegradation test	Material	Days of incubation [d]
Procedure 2	MI – Aqueous irradiation	Screening biodegradation (OECD TG 301B)	PUAmod	28
Procedure 3	MI – Aqueous irradiation	Biodegradation in soil (OECD TG 306)	PUAmod	3
Procedure 4	MII – Irradiation on soil surface	Biodegradation in soil (OECD TG 306)	PUAmod PUA LLDPE	20 20 51

2.6. Sequential filtration of the light-exposed MPs suspensions

For **MI-Procedure 1** (Fig. 1, Table 2) the aqueous irradiated and non-irradiated PUA_{mod} and LLDPE were subjected to sequential filtration. For this size distribution analysis, 0.5 mL of the irradiated (1.12 ± 0.01 kBq/0.5 mL PUA_{mod}, 0.63 ± 0.15 kBq/0.5 mL LLDPE) or non-irradiated (1.75 ± 0.08 kBq/0.5 mL, 2.33 ± 0.98 kBq/0.5 mL LLDPE) PUA_{mod} or LLDPE stock solution was diluted in 49.5 mL water and sequentially filtrated by a 12 µm (Cytiva Whatman®, nitrocellulose filter, Z696919) and a 0.2 µm pore-sized filter (Sartorius, cellulose acetate filter, Type 11107) ($n = 3$). The filters were then dried and the remaining radioactivity sorbed and retained to the filter was determined. Furthermore, the radioactivity of the filtrate (< 0.2 µm) was measured (see Section 2.3).

The filtrate of PUA_{mod} (< 0.2 µm) was further analyzed using ultra-high performance liquid chromatography with high resolution mass spectrometry (UHPLC-HRMS, total range of 100–6000 *m/z;* using the Xcalibur Qual Browser (Version 4.0).) coupled to radiodetection (LB509 - YG 75 S6M, Berthold GmbH & Co. KG, Germany) similar to Teggers et al. [64] to examine whether ^{14}C-labeled LMW compounds had been released from the PUA_{mod} shells due to photodegradation. Details of this analysis are given in the SI – Table S5–S7.

2.7. Data analysis

The recovered amounts of radioactivity were calculated as average values with their respective (±) SD of percentage relative to the applied radioactivity ($\%_{AR}$). For all calculations Microsoft Office Professional Plus Excel (2019) was used. Graphpad Prism 6 was employed for the graphical representation and for testing the significance of the difference between the amount of mineralization of irradiated vs. non-irradiated MPs at the end of the biodegradation test (**MII-Procedure 4**) using an unpaired, non-parametric (due to the small number of replicates of $n = 3$) Mann-Whitney test. However, statistical test results should be regarded with caution due to the small number of replicates per treatment and a restricted number of sampling dates within the OECD 301B and 307 tests. This constrained design reduces the statistical power to detect small or moderate differences and can lead to results that appear non-significant even when biological differences exist. The illustration of Fig. 1 and the graphical abstract was created with BioRender.com.

3. Results and discussion

3.1. Analysis of MPs

The PSA of the PUA_{mod} and PUA resulted in a median particle size of 16.5 µm (10th percentile of 2.1 µm and 90th percentile of 37.1 µm; SI – Table S8) and 15.4 µm (10th percentile of 4.8 µm and 90th percentile of 32.7 µm; SI - Table S8) prior purification. The size distribution of the suspension purified by sequential filtration was reevaluated by including a 12 µm cut-off, resulting in a median particle size of 22.9 µm (PUA_{mod},10th percentile of 14.2 µm and 90th percentile of 45.7 µm) and 20.2 µm (PUA,10th percentile of 13.0 µm and 90th percentile of 36.8 µm) (SI - Table S8, SI – Figs. S5 and S6). The LLDPE MPs had a median size of 147 µm (10th percentile of 48.8 µm to 90th percentile of 343 µm, SI - Table S8) after cryo-milling. Microscopic analysis (SI - Fig. S7) provided qualitative data on the PUA microcapsules and LLDPE MPs.

3.2. Simulated sunlight irradiation (MI and MII)

The average temperatures and the irradiation duration, the degree of

mineralization to $^{14}CO_2$ and the total recovery of the different irradiation procedures (**MI** and **MII**) are presented in Table 5. Details, such as the maximum temperatures and the temperature curves during irradiation are shown in the SI – Figs. S3, S4, S8–S10. $^{14}CO_2$ evolving during irradiation of the aqueous PUA_{mod} suspension of **MI-Procedure 2** did not exceed 3.81 ± 1.53 $\%_{AR}$, in which the recovery was 92.2 ± 1.20 $\%_{AR}$ and the average temperature of the aqueous irradiated samples was 3.99 ± 0.77 °C.

The temperatures of the aqueous irradiations in these procedures remained stable at 32.4 ± 1.60 °C, which was notably higher than the temperatures observed in **MI-Procedure 2**. This discrepancy is likely attributable to the positioning of the temperature sensor, which in **MI-Procedures 1** and **3** was positioned centrally and near the upper region of the vial, rather than in contact with the vial wall or base as it might have been the case in **MI-Procedure 2**. A photograph of the sensor setup is provided in SI – Fig. S1-D). Alternatively, if the temperature difference was not solely due to sensor placement, the elevated temperature in **MI-Procedures 1** and **3** relative to **2** could have contributed to increased $^{14}CO_2$ evolution. The total recovery of radioactivity of **MI-Procedures 1** and **3** was 73.4 ± 1.38 $\%_{AR}$, compared to 92.2 ± 1.20 $\%_{AR}$ in **MI-Procedure 2**. This reduction may indicate a greater loss of radioactivity through mineralization. However, as $^{14}CO_2$ was not quantitatively determined in **MI-Procedures 1** and **3**, this interpretation remains speculative.

Due to a failure of the cooling system during irradiation, the aqueous LLDPE suspension (**MI-Procedure 3)** was exposed to higher temperatures reaching an average temperature of 53.0 °C ± 1.3 °C for 6.8 days out of 13.9 days of the exposure period with an overall average temperature of 43.8 ± 10.3 °C (max. temperature of 62.0 °C; SI – Fig. S10). However, LLDPE is considered thermally stable up to approx. 220 °C in the presence of oxygen [3] and therefore the deviation in temperature was not regarded as relevant.

In contrast to the aqueous irradiation of PUA_{mod}, during the exposure on soil surfaces (**MII-Procedure 4**) to simulated sunlight a higher photomineralization to $^{14}CO_2$ was observed, which amounted to 14.6 $\%_{AR}$ (R1) and 8.02 $\%_{AR}$ (R2) for PUA_{mod} and for PUA to 14.11 $\%_{AR}$ (R1) and 1.55 $\%_{AR}$ (R2), respectively (Table 2). The high deviations between both replicates is most likely caused by a leakage of the flow-through system. No other alkaline or organic ^{14}C-volatiles were found in the H_2SO_4 and ethylene glycol traps, respectively. Since the soil layer was dried before light exposure, the formation of $^{14}CO_2$ most likely resulted from abiotic photooxidation reactions rather than biological processes converting the polymer into $^{14}CO_2$. Supporting this finding, 107 ± 9.51 $\%_{AR}$ PUA_{mod} and 104 ± 11.2 $\%_{AR}$ PUA of total AR were recovered from the samples that were kept in darkness, indicating that no radiolabeled volatile compounds evolved without light exposure. Thus, the observed $^{14}CO_2$ formation is attributable to abiotic oxidation and cleavage of the polymer backbone, indicating the occurrence of photo-initiated mineralization. Such abiotic mineralization, though limited in extent, also reflects the degree of chemical functionalization and chain scission that likely influenced the polymers' subsequent particle size changes and biodegradability (see Sections 3.4 and 3.5). Studies of Bhargava et al. [8] and Che et al. [14] investigated the chemical changes of PUA and polyurethane coating by attenuated total reflectance-Fourier transform infrared (ATR–FTIR) spectroscopy after UV-light exposure (0.7522 $W/m^2/nm$) with irradiance at the peak radiation wavelength of 313 nm, tested every 200 h up to 1000 h) and after 150 days exposure in the marine atmosphere, respectively. They found that the absorbance peaks that can be attributed to urea bonds (C-N), carbonyl groups (C═O) and ester bonds (C–O–C) had been decreased after the exposure, which indicated chain scission and cleavage of these bonds. Regarding our findings, it is conceivable that similar cleavages led to the release of $^{14}CO_2$. However, the implementation of more ester bonds as a modification within the PUA (PUA vs. PUA_{mod}, see Section 2.1) had no substantial influence on the fraction that was mineralized to $^{14}CO_2$. Additionally, by implementing the dark controls, which were incubated at higher temperatures, heat-related degradation as the main affecting factor could be excluded, since no radioactivity was lost due to volatilization. The temperature of the dark controls was maintained at 78.0 ± 1.13 °C (SI - Fig. S3), i.e., higher than for the irradiated samples 70.5 ± 1.86 °C (SI – Fig. S3, Table 4).

Regarding the irradiation of LLDPE on soil surfaces, no $^{14}CO_2$ or other ^{14}C-volatiles were detected (Table 4). The recovery was generally low in the dark controls and the irradiated samples of LLDPE with 52.4 ± 21.7 $\%_{AR}$ and 36.9 $\%_{AR}$, respectively, which could not be explained.

3.3. Alterations of size distribution and release of ^{14}C-compounds (MI – Procedure 1)

The results of the sequential filtration (**MI-Procedure 1**, Fig. 2) revealed that the size distribution of the PUA_{mod} suspension was highly altered by the simulated sunlight exposure (Fig. 2) which indicated disintegration of the PUA_{mod} microcapsules. The PUA_{mod} microcapsules that were kept in darkness still showed a retention of 85.3 ± 5.84 $\%_{AR}$ on the 12 μm filter, as expected (Fig. 2). Minor fractions of the dark controls reached the 0.2 μm filter (0.75 ± 0.44 $\%_{AR}$) or the filtrate (< 0.2 μm) (0.48 ± 0.25 $\%_{AR}$, total recovery of 86.5 ± 5.36 $\%_{AR}$). After light exposure, the majority of the applied radioactivity passed the 12 μm and 0.2 μm filters and was hence found in the filtrate (< 0.2 μm) (102 ± 2.43 $\%_{AR}$) with an overall recovery of 106 ± 2.38 $\%_{AR}$ (Fig. 2). Only negligible amounts of labeled particles were retained by the 12 μm (0.89 ± 0.69 $\%_{AR}$) and 0.2 μm (0.59 ± 0.06 $\%_{AR}$) filters, respectively, after irradiation (total recovery of 102 ± 2.46 $\%_{AR}$). The above-mentioned photooxidation reactions (see Section 3.2) that might lead to chain scission and cleavages within the PUA structure had likely led to the disintegration of the microcapsules to sizes smaller than 0.2 μm. Here, the small size (a median particle size of 22.9 μm), the comparably thin PUA_{mod} microcapsules and the exposure in an aqueous medium need to be considered. Du et al. [20] determined the shell thickness of slightly larger PUA microcapsules (approx. 79 μm) to be between 0.4 and 2.5 μm using Scanning Electron Microscopy (SEM). However, shell thickness is not only related to capsule size, but also influenced by the number of monomers used during microcapsule synthesis. Nonetheless, transferring these findings to our experiments, a much higher proportion of the PUA microcapsules was likely to be exposed to the simulated sunlight than for the bulk polymer LLDPE, and PUA was thus likely more affected than the thicker and mono-constituent LLDPE polymeric particles.

Accordingly, reduced effect was observed for the LLDPE particles that were exposed to simulated sunlight (Fig. 2). Prior to irradiation, the vast majority of the recovered LLDPE particles (total recovery of 57.6 ± 24.1 $\%_{AR}$) were retained by the 12 μm filter 55.1 ± 24.07 $\%_{AR}$ opposed to the second filter (0.2 μm, 1.52 ± 0.31 $\%_{AR}$) or the filtrate (< 0.2 μm, 0.94 ± 0.97 $\%_{AR}$). After light exposure, only 28.2 ± 7.13 $\%_{AR}$ remained on the first filter (12 μm) and 4.79 ± 2.79 $\%_{AR}$ was recovered from the second filter (0.2 μm). When interpreting these results, it has to be kept in mind that the overall recovered radioactivity of this analysis was low and some of the detected amounts differed considerably. Nevertheless, the sequential filtration indicated that LLDPE had partially disintegrated to smaller ^{14}C-compounds or ^{14}C-particles that were released upon simulated sunlight exposure, as a higher amount was recovered in the filtrate (< 0.2 μm, 20.5 ± 1.97 $\%_{AR}$, total recovery 53.5 ± 8.36 $\%_{AR}$) (Fig. 2) upon simulated sunlight irradiation.

A review of Grause et al. [29] summarized the changes of polyolefins due to weathering, especially regarding the exposure to UV irradiation in the presence of oxygen. Even though some polymers such as PE are light-transmitting (transparent), they inevitably include certain fractions of chromophore compounds (e.g., carbonyl functionalities or chain unsaturation), which are formed during production and thermooxidation (e.g., during processing, [1,9,40,56,59]) that can induce photodegradation. Focusing on LLDPE, the initial production of hydroperoxides plays a major role, inducing reactions that may liberate

Table 4
Overview of the different irradiation procedures. Shown are the average irradiation temperature, the mineralization to $^{14}CO_2$ during irradiation and the total recovery for mass balancing both in the percentage of applied radioactivity [$\%_{AR}$].

Irradiation Procedure	Average irradiation temperature [°C]		Minerali-zation to $^{14}CO_2$ [$\%_{AR}$]	Total recovery [$\%_{AR}$]	
	Dark	Irradiation	Irradiation	Dark	Irradiation
Procedures 1 and 3					
PUA_{mod}	-	32.4 ± 1.60	-	-	73.4 ± 1.38
LLDPE	-	43.8 ± 10.3	-	-	54.1 ± 12.5
Procedure 2					
PUA_{mod}	20.8 ± 1.66	3.99 ± 0.77	3.81 ± 1.53	85.1 ± 4.36	92.2 ± 1.20
Procedure 4					
PUA_{mod}	78.0 ± 1.13	70.5 ± 1.86	11.3 ± 4.63	107 ± 9.51	100
PUA			7.83 ± 8.88	104 ± 11.2	94.7
LLDPE	77.3 ± 0.77	69.3 ± 3.39	0.31 ± 0.22	52.4 ± 21.7	36.9

*The irradiation was performed with 75 W/m^2 within of a wavelength range of 300–400 nm (see details in SI – Table S3).

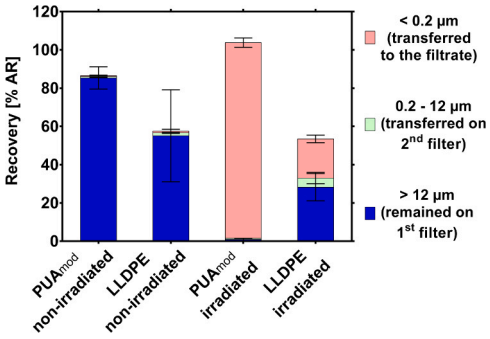

Fig. 2. Proportion of applied radioactivity (AR) recovered in the different fractions obtained by sequential filtration. Displayed are the $\%_{AR}$ of the irradiated and non-irradiated PUA_{mod} and LLDPE suspensions, which was quantified on the first (12 µm pore size) and the second filter (0.2 µm) and in the filtrate (< 0.2 µm).

LMW compounds including carboxylic acid, alcohols and to a lower extent esters [30,67]. Possibly, the liberation of such LMW ^{14}C-compounds resulted in the increased radioactivity in the filtrate (< 0.2 µm) after light exposure.

Andrady et al. [2] found that oxidation reactions were limited to a thin surface layer of the LLDPE of approx. 600 µm. Since the LLDPE in this study had a median size of 147 µm (SI – Table S8) it is likely that the LLDPE particles were completely penetrated by the irradiation and partly fragmented. Supporting this, findings from Pfohl et al. [53] showed that photooxidation in the presence of water increased the fragmentation of LDPE particles under UV aging. In addition, considering that irradiation in an aqueous medium can penetrate from all directions, the distance required to reach the center may be only half the total diameter for spherical particles.

The UHPLC-HRMS analysis of the filtrate (< 0.2 µm) of PUA_{mod} revealed the release of ^{14}C LMW compounds as a result of the light-induced disintegration, which is detailed in SI – Text S2. The radio chromatogram showed one peak (SI – Fig. S11-E)), corresponding to labeled and non-labeled aminocaproic acid (SI – Fig. S11-A), B), C)). By analyzing pure (≥ 99 %) aminocaproic acid as a reference compound (10 ng/mL, Sigma-Aldrich Chemie GmbH, Germany) and a mixture of the reference compound together with the PUA_{mod} filtrate (SI – Fig. S11-D), SI – Fig. S12-D)), the presence of aminocaproic acid was proven. Furthermore, the isotopic pattern analysis (SI – Fig. S13, SI - Text S2) substantiated these findings. ^{14}C-aminocaproic acid is similar to the ^{14}C-labeled monomer ^{14}C-hexamethylenediamine (^{14}C-HMDA) used for synthesis, except that it contains a carboxyl instead of an amine group.

Most likely, the PUA bonds were partially broken by formed radicals and photooxidation processes. Due to formed hydroxyl radicals (•OH) and superoxide anions ($O_2^{\bullet-}$) apparently HDMA was oxidized to produce aminocaproic acid. Oxidative processes were also shown by Si et al. [60], where deamination of primary amines (-NH_2) was induced by radicals. By means of a column recovery test, the eluted radioactivity within the retention time of ($^{14}C_{(2)}$-) aminocaproic acid was quantified and represented 48.5 ± 1.16 $\%_{AR}$ (SI – Fig. S14, recovery of 93.2 ± 1.93 %) of the injected radioactivity. This observation indicates that a large portion of ^{14}C-labeled molecules or oligomers introduced to this analysis can likely be attributed to the elution of ^{14}C-aminocaproic acid.

According to ECHA data (https://echa.europa.eu/es/registration-dossier/-/registered-dossier/22890/5/3/2), aminocaproic acid is readily biodegradable, non-toxic to aquatic organisms and not bioaccumulative suggesting a low environmental concern. Overall, the identification of specific degradation products remains analytically challenging, particularly when dealing with complex polymeric matrices and trace-level compounds. From an environmental perspective, it is important to investigate whether transformation products may form due to environmental exposure conditions that could alter the risk profile of the material. In this case, release of a non-persistent and biodegradable compound was identified. However, other types of polymers and their associated additives may generate different transformation products upon exposure to sunlight, which is a growing concern highlighted in a recent assessment supported by the UNEP but remains largely underexplored [36]. For example, the degradation of side-chain fluorinated polymers has been shown to release perfluorinated substances, including perfluorooctanoic acid (PFOA), over decades under environmental conditions such as those found in soil and water [70]. This observation highlights the importance of investigating whether polymeric materials might release environmentally persistent or toxic transformation products following abiotic processes like light exposure.

In this context, it is important to note that the polymeric shell included not only the radiolabeled HMDA monomer but also co-polymerized isocyanates. As the radiolabel was incorporated into one specific monomer, the assessment of mineralization and degradation pathways was limited to fragments containing that labeled unit. Consequently, the behavior and fate of degradation products derived from non-labeled portions of the polymer were beyond the scope of this study. For a comprehensive understanding of the degradation processes, experiments with isotope labels at other positions of the molecules would be required.

3.4. Biodegradation of light-exposed PUA_{mod} microcapsules in the aqueous medium (MI – Procedure 2)

The results of **MI-Procedure 2**, the aqueous irradiation (Fig. 1) of PUA_{mod} with the downstream biodegradation test resulted in a biodegradation of 28.0 ± 4.05 $\%_{AR}$ in the irradiated suspension. The test outcome is significantly higher than the $^{14}CO_2$ evolution observed in a previous OECD TG 301B study with non-irradiated PUA_{mod} reaching

0.81 $\%_{AR}$ ([64], p = .0303; irradiated vs. non-irradiated PUA_{mod}, test of significance by an unpaired, non-parametric Mann-Whitney test; significant difference indicated by $p < 0.05$) demonstrates that simulated sunlight exposure significantly increased biodegradation. It is likely that the partial biodegradation of the irradiated PUA_{mod} suspension observed in this experiment originated from the mineralization of the released ^{14}C-aminocaproic acid. This interpretation is supported by its safety data sheet's information stating that aminocaproic acid is classified as readily degradable, determined in an OECD TG 301D test with 76 % biodegradation within 28 days of incubation.

3.5. Biodegradation of light-exposed MPs in soil (MI – Procedure 3 and MII – Procedure 4)

With regard to **MI-Procedure 3**, the PUA_{mod} suspension was irradiated in an aqueous environment (see 2.4.2) and subsequently applied to the biodegradation test in soil. Biodegradation of the irradiated PUA_{mod} applying this procedure $^{14}CO_2$ formation amounted to 63.2 ± 13.4 $\%_{AR}$ (RefeSol 01-A) and 62.3 ± 9.65 $\%_{AR}$ (RefeSol 03-G) in the reference soil RefeSol 01-A within 72 h (Fig. 3, right panel). In a parallel study, significant losses were observed for the extraction recoveries of irradiated PUA_{mod} applied to soil [65]. This observation might be attributable to the fast biodegradation of the PUA_{mod}. Therefore, the results of this study may also be relevant for studies investigating extraction methods of aged polymers or plastics. Compared to the biodegradation test results of the irradiated PUA_{mod} in the aqueous setting the CO_2-evolution of the microcapsules irradiated on soil surfaces (**MII-Procedure 4**) reached only 13.6 ± 1.44 $\%_{AR}$ (PUA) and 11.8 ± 3.64 $\%_{AR}$ (PUA_{mod}) (Fig. 3) during 20 days of incubation in soil. The microcapsules of the dark controls showed a negligible biodegradation of 2.52 ± 0.96 $\%_{AR}$ (PUA) and 1.52 ± 0.29 $\%_{AR}$ (PUA_{mod}) (Fig. 3). In this case, irradiation on dry soil likely led to reduced phototransformation due to microcapsule aggregation and adsorption onto the soil surface, which may have caused shading effects and limited light penetration compared with irradiation in water. Consequently, the extent of biodegradation in soil was presumably lower.

The testing in **MI-Procedures 1–3** focused on PUA_{mod} microcapsules, whereas in **MII-Procedure 4** we additionally tested regular, non-modified PUA and LLDPE. PUA modification did not alter biodegradability since both materials were mineralized to similar degrees (p= 0.8 irradiated; p = 0.6 non-irradiated, test of significance by an unpaired, non-parametric Mann-Whitney test; significant difference indicated by $p < 0.05$). Table 5 shows the amounts of mineralization.

The biodegradation of LLDPE MPs was slightly enhanced after their irradiation on the soil surface compared to the non-irradiated dark controls (1.99 ± 0.18 $\%_{AR}$ vs. 0.75 ± 0.14 $\%_{AR}$, respectively, Table 5). The recovery of the biodegradation test in soil for all tested samples was above 80 %, but with a higher variability (elevated standard deviation) for some LLDPE dark controls (see Table 5). Overall, the differences observed between irradiated and non-irradiated PUA and PUA_{mod} samples in the degree of mineralization in the soil biodegradation test indicate a statistical trend ($p < 0.10$, Table 5) toward increased mineralization following simulated light exposure on a soil surface. For LLDPE particles, however, the increase in biodegradation after irradiation, although statistically significant, was minimal and practically not measurable, indicating negligible biological relevance.

3.6. Overall discussion

Our results demonstrate that phototransformation can be a decisive unlocking step in the biodegradation of certain MPs. With regard to PUA microcapsules, simulated sunlight caused near-complete disintegration (~ 98 % of recovered radioactivity in < 0.2 µm size fraction) and the release of a readily biodegradable LMW compound, ^{14}C-aminocaproic acid. These abiotic processes were closely associated with a 28 % mineralization in aqueous OECD 301B tests and > 60 % mineralization in soil OECD 307 tests following aqueous irradiation. Compared with irradiation in water, irradiation on a dry soil surface likely reduced phototransformation due to particle aggregation and surface adsorption, causing shading effects and limiting light penetration, which in turn constrained biodegradation. In contrast, LLDPE particles fragmented to ~ 20.5 $\%_{AR}$ in submicron fractions (< 0.2 µm) after simulated sunlight exposure in an aqueous medium. The increase after soil surface irradiation in mineralization from approximately ~ 1 $\%_{AR}$ to ~ 2 $\%_{AR}$ biodegradation in soil after soil surface irradiation was statistically significant. However, this change represents a rather negligible increase that is not practically measurable, consistent with the chemical resistance of LLDPE to oxidative functionalization [13,28]. These quantified differences confirm that fragmentation alone does not ensure biodegradability; the production of bioavailable transformation products is essential. The results are consistent with the conceptual framework of stepwise polymer degradation (biodeterioration/fragmentation →depolymerization→assimilation→mineralization) and provide regulatory-relevant quantification of each step for two contrasting polymer types.

By applying sequential testing (OECD TG 316 or OECD draft soil-surface photolysis → OECD TG 301B/307), we translated the conceptual link between abiotic and biotic processes into an easily applicable

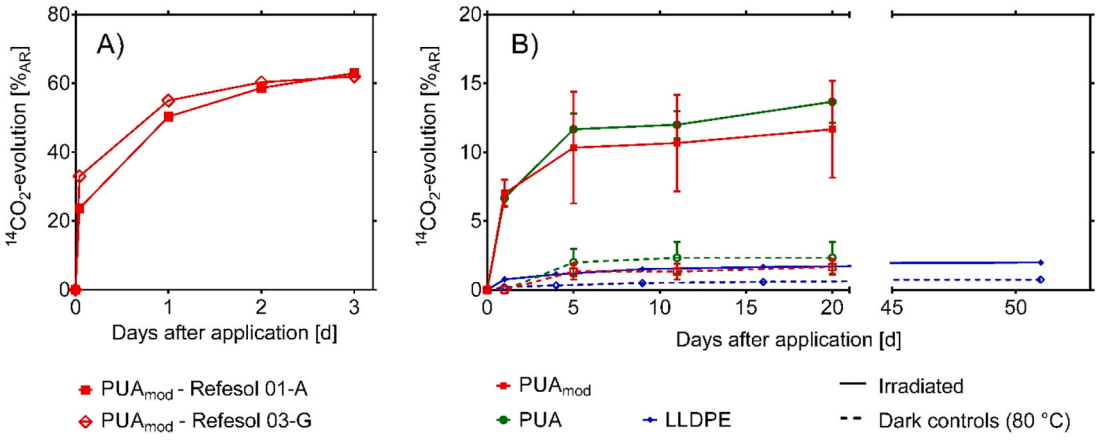

Fig. 3. A) Biodegradation of irradiated PUA_{mod} microcapsules in soil (Refesol 01-A and Refesol 03-G) after irradiation in the aqueous setting (**MI-Procedure 3**). B) Biodegradation of PUA microcapsules with/without ester-bond modification (PUA vs. PUA_{mod}) and LLDPE MPs in soil (Refesol 01-A) after simulated sunlight irradiation or in dark controls incubated at 80 °C on soil surfaces (**MII-Procedure 4**). The biodegradation is plotted as the cumulative portion of applied radioactivity (AR) mineralized to $^{14}CO_2$ relative to the incubation time (average and SD of $n = 3$).

Table 5
Mineralization and recovery of the biodegradation test in soil (OECD TG 307). Test of significance using an unpaired, non-parametric Mann-Whitney test to compare irradiated vs. non-irradiated materials.

MP Material	Mineralization Dark controls [$\%_{AR}$]	Mineralization Irradiated [$\%_{AR}$]	Days of incubation [d]	Significance of difference: irradiated vs. non-irradiated p	Recovery Dark controls [$\%_{AR}$]	Recovery Irradiated [$\%_{AR}$]
PUA_{mod}	1.52 ± 0.29	11.8 ± 3.64	20	0.0873	83.0 ± 8.12	82.0 ± 6.46
PUA	2.52 ± 0.96	13.6 ± 1.44	20	0.0873	122 ± 20.8	109 ± 2.74
LLDPE	0.75 ± 0.14	1.99 ± 0.18	51	* 0.0204	107 ± 37.5	84.0 ± 10.8

* Test of significance by an unpaired, non-parametric Mann-Whitney test; significant difference indicated by $p < 0.05$.

standardized testing approach. While earlier studies have documented photo-oxidative effects on polymers, they rarely quantify both structural changes and mineralization within a regulatory testing framework. Our results show that the influence of phototransformation on subsequent biodegradation is both polymer- and medium-dependent, which becomes apparent only when these processes are examined in sequence. This sequential approach, grounded in established guidelines, reveals mechanistic and regulatorily relevant information that single tests cannot capture.

Previous research has repeatedly suggested that abiotic weathering, particularly photooxidation, can facilitate microbial degradation of plastics, yet direct linkage between observed structural changes and measured ultimate biodegradation (mineralization) within a regulatory testing framework remains rare. For example, Gewert et al. [28] reviewed degradation pathways for marine plastics and highlighted UV- or photooxidation as a prerequisite for microbial colonization. Several studies have confirmed this facilitation effect and have shown that UV- or light-weathering pre-treatments can accelerate fragmentation and promote microbial colonization and breakdown of plastics [7,58,76]. CO_2 evolution measurements in various studies have demonstrated that prior phototransformation can enhance the biodegradability of certain polymers: Rose et al. [57], used the American Society for Testing and Materials (ASTM) D5208 standard "Practice for Fluorescent Ultraviolet (UV) Exposure of Photodegradable Plastics" [5] to UV-aged LDPE and oxo-LDPE prior to aqueous CO_2-respirometry tests. Tantawi et al. [63] applied simulated sunlight in combination with marine biodegradation assays following ASTM D6691-17 [4] "Standard Test Method for Determining Aerobic Biodegradation of Plastic Materials in the Marine Environment by a Defined Microbial Consortium or Natural Sea Water Inoculum" and ISO 23977-1 "*Plastics - Determination of the Aerobic Biodegradation of Plastics Exposed to Seawater - Part 1: Method by Analysis of Released Carbon Dioxide*.". Chen et al. [16] photoaged MPs before degradation was studied in soil microcosms. However, CO_2-based biodegradation studies that support the principle that abiotic processes can facilitate biotic degradation have been rarely conducted. Our work extends this concept by applying a regulatorily relevant sequential testing strategy aligned with OECD guidelines, directly addressing contexts such as the EU MPs restriction and ongoing initiatives to extend REACH provisions to cover polymers. This sequential design bridges observed photooxidative changes to quantifiable biodegradation endpoints in a format suitable for regulatory assessment, enabling interpretation within emerging regulatory frameworks. In contrast to earlier research, we focused on MPs, including PUA microcapsules used for application of PPPs, a formulation type whose environmental fate remains largely unexplored.

PUA microcapsules, such as those in Prosper 300 CS, are applied at relatively low amounts, with a maximum of 150 g/ha permitted per season. In our tests, aqueous irradiation produced high biodegradation (OECD TG 301B with 28 $\%_{AR}$ and ~ 62–63 $\%_{AR}$ in OECD TG 307 in soil), whereas soil-surface irradiation yielded much lower mineralization (12–13.5 $\%_{AR,}$ in OECD TG 307), underscoring the influence of the investigated medium and corresponding light penetration. LLDPE mulch films, applied at ~ 180 kg/ha per season [26], are partially recovered post-use (75–95 %, Hann et al. [34]) but can release persistent residues. In our experiments, even after fragmentation, LLDPE mineralization remained negligible. Such polymer-specific responses indicate that persistence assessments based solely on inherent chemical structure may misrepresent the actual environmental fate.

However, extrapolation of these laboratory results to real environmental conditions must be made with caution. In agricultural contexts, such as the application on plant leaves of PUA-based pesticide formulations like Prosper 300 CS, microcapsules may indeed be exposed to sunlight initially, before potentially being incorporated in the soil. If applied directly to the soil, their exposure to sunlight will probably be minor, compared to the lab experiment, since the MPs might be incorporated to deeper soil layers through irrigation, bioturbation or plowing. According to Tester and Morris [66], physiologically and ecologically relevant amounts of light rarely penetrate more than 4–5 mm into the soil, and Ciani et al. [17] measured that the light penetration depths for soils are in the range of 17–110 μm at 275 nm and 120–300 μm at 700 nm, respectively. Nonetheless, our controlled results illustrate the mechanistic potential for sunlight to alter environmental persistence and highlight conditions under which this process is relevant.

3.7. Regulatory gaps and recommendations

Biodegradability tests according to OECD (e.g. TG 301, TG 307) or ISO guidelines determine whether a chemical is subject to microbial metabolism. These tests were designed for soluble substances for which mineralization is a meaningful endpoint. However, the approach cannot be directly transferred to insoluble polymers, and thus to microplastic particles. For these materials, bioavailability can be constrained by particle size, morphology, and surface chemistry, meaning that mineralization endpoints may underestimate the degradation potential, especially if relevant abiotic transformation processes are not considered. The linkage between abiotic weathering processes, such as photooxidation, and subsequent biodegradation is largely disregarded in current testing strategies, representing a critical scientific and regulatory gap. This combined degradation is particularly relevant for agricultural polymer-based microcapsules or carrier materials, which may undergo structural changes under environmental conditions that may alter their fate. Relying solely on mineralization as an endpoint risks overlooking partial degradation steps or transformations that could be captured by polymer-specific analyses, such as particle size distribution, molecular weight changes, surface analysis and chemical functional group analysis.

Our findings show that for the tested crosslinked PUA MPs, which are classified as persistent, simulated sunlight can be a prerequisite for measurable biodegradation in standard tests. Where there is evidence of environmentally relevant light exposure for a given MP application (to be established by future studies under field conditions), the influence of simulated sunlight (e.g., TG 316 or draft soil-surface photolysis at a defined equivalent sunlight dose) on subsequent biodegradation testing (TG 301/307) should be considered. Ideally, such assessments should report both primary degradation metrics (fragmentation, low-molecular-weight product release) and ultimate mineralization, supported by a mass balance where feasible. This integrated approach

would align regulatory testing with realistic environmental exposure scenarios and reduce the risk of false persistence classifications.

4. Conclusions

The results of this study are not only relevant scientifically, but also from a regulatory perspective. They underscore the need for more comprehensive and realistic assessments of the fate of MPs, particularly by the inclusion of sunlight irradiation as a key abiotic degradation mechanism. By coupling existing standardized guidelines for abiotic and biological degradation, we demonstrated that photooxidation substantially influenced the environmental fate and biodegradability of MPs. Furthermore, our findings highlight that changes in particle size distribution and the formation of phototransformation products, in our case aminocaproic acid, can critically affect the outcome of biodegradation tests. We therefore recommend including such physicochemical characterization in future assessments of the fate of MPs. The use of radiolabeling in the applied tests was crucial for distinguishing $^{14}CO_2$ derived from polymer (bio)degradation from the CO_2 originating from other components in the tested sample. Moreover, the ability to perform precise mass balances based on total recovered radioactivity served as a reliable tool for validating the experimental outcomes. Overall, this study extends the understanding of the environmental fate of MPs, but should be expanded to include related studies under real field conditions.

Environmental Implication

This study demonstrates that abiotic processes, particularly simulated sunlight exposure, can be a prerequisite for the biodegradation of persistent microplastics, such as polyurea (PUA) microcapsules. The results show that phototransformation substantially alters polymer structure, and can lead to increased microbial mineralization in standard laboratory tests. These findings indicate that photodegradation can critically influence polymer fate. Including realistic environmental exposure processes may support more comprehensive assessments of microplastic biodegradation.

CRediT authorship contribution statement

Holger Egger: Writing – review & editing, Supervision, Project administration, Funding acquisition. **Roman Heumann:** Writing – review & editing, Supervision, Project administration, Funding acquisition. **Dieter Hennecke:** Writing – review & editing, Supervision, Project administration, Funding acquisition. **Markus Simon:** Writing – review & editing, Supervision, Project administration, Funding acquisition. **Boris Meisterjahn:** Writing – review & editing, Supervision, Project administration, Funding acquisition. **Jonas Hardebusch:** Methodology, Investigation. **Svetlana Heck:** Investigation, Formal analysis, Data curation. **Svenja Winterhoff:** Investigation, Formal analysis, Data curation. **Eva-Maria Teggers:** Writing – original draft, Visualization, Software, Methodology, Investigation, Formal analysis, Data curation, Conceptualization. **Annika Jahnke:** Writing – review & editing, Supervision. **Andreas Schäffer:** Writing – review & editing, Supervision, Project administration, Funding acquisition. **Philipp Dalkmann:** Writing – review & editing, Supervision, Project administration, Funding acquisition.

Declaration of Generative AI and AI-assisted technologies in the writing process

During the preparation of this work the authors used ChatGPT 4o and 5 Pro and Perplexity Pro (Version August, 2025) for rephrasing and shortening of self-written text. After using this tool/service, the authors reviewed and edited the content as needed and take full responsibility for the content of the publication.

Funding sources

This project was funded by Bayer AG, Crop Science Division. Open Access funding enabled and organized by Projekt DEAL.

Declaration of Competing Interest

The authors declare the following financial interests/personal relationships which may be considered as potential competing interests: Eva-Maria Teggers, Jonas Hardebusch, Boris Meisterjahn, Dieter Hennecke, Markus Simon, Philipp Dalkmann, Holger Egger, Roman Heumann reports financial support was provided by Bayer AG. Philipp Dalkmann, Holger Egger, Roman Heumann, Eva-Maria Teggers reports a relationship with Bayer AG and INVITE GmbH that includes: employment. Holger Egger has patent #WO2021136758 Aqueous Capsule Suspension Concentrates Based on Polyurea Shell Material Containing Polyfunctional Aminocarboxylic Esters licensed to Bayer AG. Philipp Dalkmann and Holger Egger are employees of the Bayer AG Division Crop Science, a leading manufacturer of agricultural chemicals. Roman Heumann and Eva-Maria Teggers are or were employed at INVITE GmbH, Germany, during the investigation time. INVITE GmbH is a cross-industry company with with 50 % business shares belonging to Bayer AG and 50 % business shares belonging to universities (Technical University of Dortmund, Germany and Heinrich Heine University Düsseldorf, Germany). If there are other authors, they declare that they have no known competing financial interests or personal relationships that could have appeared to influence the work reported in this paper.

Acknowledgements

The authors gratefully acknowledge the technical support provided by the team at Fraunhofer IME. In particular, we thank Thomas Hennecke, Christoph Eggenstein-Deimel, and Joana Bräutigam for their valuable advice regarding the experimental work.

Appendix A. Supporting information

Supplementary data associated with this article can be found in the online version at doi:10.1016/j.jhazmat.2025.140424.

Data availability

Data will be made available on request.

References

[1] Allen, N.S., 1986. Recent advances in the photo-oxidation and stabilization of polymers. Chem Soc Rev 15, 373–404.
[2] Andrady, A.L., Lavender Law, K., Donohue, J., Koongolla, B., 2022. Accelerated degradation of low-density polyethylene in air and in sea water. Sci Total Environ 811, 151368. https://doi.org/10.1016/j.scitotenv.2021.151368.
[3] Aniśko, J., Sałasińska, K., Barczewski, M., 2023. Study on thermal stability and degradation kinetics of bio-based low-density polyethylene. Aniśko Polimery 68, 451–460. https://doi.org/10.14314/polimery.2023.9.1.
[4] ASTM. D6691-17 – test method for determining aerobic biodegradation of plastic materials in the marine environment by a defined microbial consortium or natural sea water inoculum; n.d. ⟨https://doi.org/10.1520/D6691-17⟩.
[5] ASTM. D5208 – practice for fluorescent ultraviolet (UV) exposure of photodegradable plastics; 2022. ⟨https://doi.org/10.1520/D5208-14R22⟩.
[6] Bai, Y., Zhou, Y., Che, X., Li, C., Cui, Z., Su, R., et al., 2021. Indirect photodegradation of sulfadiazine in the presence of DOM: effects of DOM components and main seawater constituents. Environ Pollut 268, 115689. https://doi.org/10.1016/j.envpol.2020.115689.
[7] Bao, R., Cheng, Z., Hou, Y., Xie, C., Pu, J., Peng, L., et al., 2022. Secondary microplastics formation and colonized microorganisms on the surface of conventional and degradable plastic granules during long-term UV aging in various environmental media. J Hazard Mater 439, 129686. https://doi.org/10.1016/j.jhazmat.2022.129686.
[8] Bhargava, S., Kubota, M., Lewis, R.D., Advani, S.G., Prasad, A.K., Deitzel, J.M., 2015. Ultraviolet, water, and thermal aging studies of a waterborne polyurethane elastomer-based high reflectivity coating. Prog Org Coat 79, 75–82. https://doi.org/10.1016/j.porgcoat.2014.11.005.

[9] Bracco, P., Costa, L., Luda, M.P., Billingham, N., 2018. A review of experimental studies of the role of free-radicals in polyethylene oxidation. Polym Degrad Stab 155, 67–83. https://doi.org/10.1016/j.polymdegradstab.2018.07.011.
[10] Brunning, H., Sallach, J.B., Zanchi, V., Price, O., Boxall, A., 2022. Toward a framework for environmental fate and exposure assessment of polymers. Environ Toxicol Chem 41, 515–540. https://doi.org/10.1002/etc.5272.
[11] Carlini, G., Drugmand, D., 2022. Sowing a plastic planet: how microplastics in agrochemicals are affecting our soils, our food, and our future. Center for International Environmental Law.
[12] Carmichael, N., 2014. European centre for ecotoxicology and toxicology of chemicals. In: Encyclopedia of toxicology. Elsevier, pp. 547–548. https://doi.org/10.1016/B978-0-12-386454-3.00505-4.
[13] Chamas, A., Moon, H., Zheng, J., Qiu, Y., Tabassum, T., Jang, J.H., et al., 2020. Degradation rates of plastics in the environment. ACS Sustain Chem Eng 8, 3494–3511. https://doi.org/10.1021/acssuschemeng.9b06635.
[14] Che, K., Lyu, P., Wan, F., Ma, M., 2019. Investigations on aging behavior and mechanism of polyurea coating in marine atmosphere. Materials 12, 3636. https://doi.org/10.3390/ma12213636.
[15] Chen, C., Chen, L., Yao, Y., Artigas, F., Huang, Q., Zhang, W., 2019. Organotin release from polyvinyl chloride microplastics and concurrent photodegradation in water: impacts from salinity, dissolved organic matter, and light exposure. Environ Sci Technol 53, 10741–10752. https://doi.org/10.1021/acs.est.9b03428.
[16] Chen, Y., Gao, B., Yang, Y., Pan, Z., Liu, J., Sun, K., et al., 2022. Tracking microplastics biodegradation through CO2 emission: Role of photoaging and mineral addition. J Hazard Mater 439, 129615. https://doi.org/10.1016/j.jhazmat.2022.129615.
[17] Ciani, A., Goss, K. -U., Schwarzenbach, R.P., 2005. Light penetration in soil and particulate minerals. Eur J Soil Sci 56, 561–574. https://doi.org/10.1111/j.1365-2389.2005.00688.x.
[18] Cox, C., Surgan, M., 2006. Unidentified inert ingredients in pesticides: implications for human and environmental health. Environ Health Perspect 114, 1803–1806. https://doi.org/10.1289/ehp.9374.
[19] Ding, L., Yu, X., Guo, X., Zhang, Y., Ouyang, Z., Liu, P., et al., 2022. The photodegradation processes and mechanisms of polyvinyl chloride and polyethylene terephthalate microplastic in aquatic environments: important role of clay minerals. Water Res 208, 117879. https://doi.org/10.1016/j.watres.2021.117879.
[20] Du, J., Ibaseta, N., Guichardon, P., 2022. Characterization of polyurea microcapsules synthesized with an isocyanate of low toxicity and eco-friendly esters via microfluidics: shape, shell thickness, morphology and encapsulation efficiency. Chem Eng Res Des 182, 256–272. https://doi.org/10.1016/j.cherd.2022.03.026.
[21] Duan, J., Li, Y., Gao, J., Cao, R., Shang, E., Zhang, W., 2022. ROS-mediated photoaging pathways of nano- and micro-plastic particles under UV irradiation. Water Res 216, 118320. https://doi.org/10.1016/j.watres.2022.118320.
[22] ECHA, E.C.A., 2019. Annex XV restriction report – microplastics, proposal for restriction of intentionally added microplastics.
[23] European Commission. ANNEX to the Commission Regulation (EU) amending Annex XVII to Regulation (EC) No 1907/2006 of the European Parliament and of the Council concerning the Registration, Evaluation, Authorisation and Restriction of Chemicals (REACH) as regards synthetic polymer microparticles; 2023.
[24] European Food Safety Authority, 2014. EFSA guidance document for evaluating laboratory and field dissipation studies to obtain DegT50 values of active substances of plant protection products and transformation products of these active substances in soil. In: EFS2, 12. https://doi.org/10.2903/j.efsa.2014.3662.
[25] European Food Safety Authority (EFSA), Egsmose, M., Fait, G., Janzen, W., Jentzsch, F., Lava, R., et al., 2022. Scientific guidance on soil phototransformation products in groundwater – consideration, parameterisation and simulation in the exposure assessment of plant protection products. EFS2 20. https://doi.org/10.2903/j.efsa.2022.7119.
[26] FAO, F and AO of the UN. Assessment of agricultural plastics and their sustainability: a call for action. Rome, Italy; 2021.
[27] Feldman, D., 2002. Polymer weathering: photo-oxidation. J Polym Environ 10, 163–173. https://doi.org/10.1023/A:1021148205366.
[28] Gewert, B., Plassmann, M.M., MacLeod, M., 2015. Pathways for degradation of plastic polymers floating in the marine environment. Environ Sci Process Impacts 17, 1513–1521. https://doi.org/10.1039/C5EM00207A.
[29] Grause, G., Chien, M.-F., Inoue, C., 2020. Changes during the weathering of polyolefins. Polym Degrad Stab 181, 109364. https://doi.org/10.1016/j.polymdegradstab.2020.109364.
[30] Gulmine, J.V., Janissek, P.R., Heise, H.M., Akcelrud, L., 2003. Degradation profile of polyethylene after artificial accelerated weathering. Polym Degrad Stab 79, 385–397. https://doi.org/10.1016/S0141-3910(02)00338-5.
[31] Hahn, S., Hennecke, D., 2023. What can we learn from biodegradation of natural polymers for regulation? Environ Sci Eur 35, 50. https://doi.org/10.1186/s12302-023-00755-y.
[32] Haider, T.P., Völker, C., Kramm, J., Landfester, K., Wurm, F.R., 2019. Plastics of the future? The impact of biodegradable polymers on the environment and on society. Angew Chem Int Ed 58, 50–62. https://doi.org/10.1002/anie.201805766.
[33] Hamid, S., 2000. Handbook of polymer degradation. Marcel Dekker.
[34] Hann, S., Fletcher, E., Sherrington, C., Molteno, S., Elliott, L., 2021. Conventional and biodegradable plastics in agriculture. Report for DG environment of the European Commission.
[35] Hassink, J., Buda, J., Multsch, S., Nellen, S., Noe, S., Schmidt, T., 2024. Development of a new test design to investigate the degradation of pesticides in soil under sunlight conditions. Environ Sci Eur 36, 151. https://doi.org/10.1186/s12302-024-00974-x.
[36] Jansen, M.A.K., Andrady, A.L., Bornman, J.F., Aucamp, P.J., Bais, A.F., Banaszak, A.T., et al., 2024. Plastics in the environment in the context of UV radiation, climate change and the Montreal protocol: UNEP environmental effects assessment panel, update 2023. Photochem Photobiol Sci 23, 629–650. https://doi.org/10.1007/s43630-024-00552-3.
[37] Karagianni, K., Kuntzmann-Dembele, F., Bocokic, V., Charbonnier, A., Harrison, I., Kreutzer, G., et al., 2024. Fragrance encapsulates: effect of polymeric shell purification method on the accuracy of biodegradability testing. Environ Toxic Chem 43, 1242–1249. https://doi.org/10.1002/etc.5852.
[38] Kookana, R.S., Boxall, A.B.A., Reeves, P.T., Ashauer, R., Beulke, S., Chaudhry, Q., et al., 2014. Nanopesticides: guiding principles for regulatory evaluation of environmental risks. J Agric Food Chem 62, 4227–4240. https://doi.org/10.1021/jf500232f.
[39] Krause, J., Egger, H., 2021. Aqueous capsule suspension concentrates based on polyurea shell material containing polyfunctional aminocarboxylic esters [WO2021136758].
[40] La Mantia, F.P., 1986. Influence of processing conditions on the photo-oxidation of polypropylene films. Polym Degrad Stab 15, 283–290.
[41] Lemaire, J., Arnaud, R., Lacoste, J., 1988. The prediction of the long-term photoageing of solid polymers. Acta Polym 39, 27–32. https://doi.org/10.1002/actp.1988.010390106.
[42] Liu, P., Wu, X., Peng, J., Wang, H., Shi, Y., Huang, H., et al., 2021. Critical effect of iron red pigment on photoaging behavior of polypropylene microplastics in artificial seawater. J Hazard Mater 404, 124209. https://doi.org/10.1016/j.jhazmat.2020.124209.
[43] Lucas, N., Bienaime, C., Belloy, C., Queneudec, M., Silvestre, F., Nava-Saucedo, J.-E., 2008. Polymer biodegradation: mechanisms and estimation techniques – a review. Chemosphere 73, 429–442. https://doi.org/10.1016/j.chemosphere.2008.06.064.
[44] Mao, R., Lang, M., Yu, X., Wu, R., Yang, X., Guo, X., 2020. Aging mechanism of microplastics with UV irradiation and its effects on the adsorption of heavy metals. J Hazard Mater 393, 122515. https://doi.org/10.1016/j.jhazmat.2020.122515.
[45] McNeill, K., Canonica, S., 2016. Triplet state dissolved organic matter in aquatic photochemistry: reaction mechanisms, substrate scope, and photophysical properties. Environ Sci Process Impacts 18, 1381–1399. https://doi.org/10.1039/C6EM00408C.
[46] Mekaru, H., 2020. Effect of agitation method on the nanosized degradation of polystyrene microplastics dispersed in water. ACS Omega 5, 3218–3227. https://doi.org/10.1021/acsomega.9b03278.
[47] Mitrano, D.M., Wohlleben, W., 2020. Microplastic regulation should be more precise to incentivize both innovation and environmental safety. Nat Commun 11, 5324. https://doi.org/10.1038/s41467-020-19069-1.
[48] Nederstigt, T.A.P., Brinkmann, B.W., Peijnenburg, W.J.G.M., Vijver, M.G., 2024. Sustainability claims of nanoenabled pesticides require a more thorough evaluation. Environ Sci Technol 58, 2163–2165. https://doi.org/10.1021/acs.est.3c10207.
[49] OECD Draft TG (Ed.), 2002. Draft TG – proposal for a new guideline: phototransformation of chemicals on soil surface. OECD Publishing, Paris.
[50] OECD TG 301 (Ed.), 1992. Test No. 301: ready biodegradability, OECD guidelines for the testing of chemicals, section 3. OECD Publishing, Paris. https://doi.org/10.1787/9789264070349-en.
[51] OECD TG 307 (Ed.), 2002. Test no. 307: aerobic and anaerobic transformation in soil, OECD guidelines for the testing of chemicals, section 3. OECD Publishing, Paris. https://doi.org/10.1787/9789264070509-en.
[52] OECD TG 316 (Ed.), 2008. Test no. 316: phototransformation of chemicals in water direct photolysis, OECD guidelines for the testing of chemicals, section 3. OECD Publishing, Paris. https://doi.org/10.1787/9789264067585-en.
[53] Pfohl, P., Santizo, K., Sipe, J., Wiesner, M., Harrison, S., Svendsen, C., et al., 2025. Environmental degradation and fragmentation of microplastics: dependence on polymer type, humidity, UV dose and temperature. Microplast Nanoplast 5, 7. https://doi.org/10.1186/s43591-025-00118-9.
[54] Quijada, R., Narváez, A., Rojas, R., Rabagliati, F.M., Barrera Galland, G., Santos Mauler, R., Benavente, R., Pérez, E., Pereña, J.M., Bello, A., 1999. Synthesis and characterization of copolymers of ethylene and 1-octadecene using the rac-Et (Ind)2ZrCl2/MAO catalyst system. Macromol Chem Phys 200, 1306–1310.
[55] Rabek, J.F., Rånby, B., 1974. Studies on the photooxidation mechanism of polymers. II. The role of quinones as sensitizers in the photooxidative degradation of polystyrene. J Polym Sci Polym Chem Ed 12, 295–306. https://doi.org/10.1002/pol.1974.170120204.
[56] Rajakumar, K., Sarasvathy, V., Thamarai Chelvan, A., Chitra, R., Vijayakumar, C. T., 2009. Natural weathering studies of polypropylene. J Polym Environ 17, 191–202. https://doi.org/10.1007/s10924-009-0138-7.
[57] Rose, R.-S., Richardson, K.H., Latvanen, E.J., Hanson, C.A., Resmini, M., Sanders, I. A., 2020. Microbial degradation of plastic in aqueous solutions demonstrated by CO2 evolution and quantification. IJMS 21, 1176. https://doi.org/10.3390/ijms21041176.
[58] Sander, M., Weber, M., Lott, C., Zumstein, M., Künkel, A., Battagliarin, G., 2023. Polymer biodegradability 2.0: a holistic view on polymer biodegradation in natural and engineered environments. In: Künkel, A., Battagliarin, G., Winnacker, M., Rieger, B., Coates, G. (Eds.), Synthetic biodegradable and biobased polymers, advances in polymer science. Springer International Publishing, Cham, pp. 65–110. https://doi.org/10.1007/12_2023_163.
[59] Schnabel, W., 1981. Polymer degradation: principles and practice, 2. Carl Hanser Verlag, Wien, p. 133.

[60] Si, T., Kim, H.Y., Oh, K., 2021. One-pot direct oxidation of primary amines to carboxylic acids through tandem *ortho* -naphthoquinone-catalyzed and TBHP-promoted oxidation sequence. Chem A Eur J 27, 18150–18155. https://doi.org/10.1002/chem.202103450.

[61] Silva, A.B., Bastos, A.S., Justino, C.I.L., Da Costa, J.P., Duarte, A.C., Rocha-Santos, T.A.P., 2018. Microplastics in the environment: challenges in analytical chemistry – a review. Anal Chim Acta 1017, 1–19. https://doi.org/10.1016/j.aca.2018.02.043.

[62] Sinn, H., Kaminsky, W., Vollmer, H., Woldt, R., 1980. Living Polymers" on Polymerization with Extremely Productive Ziegler Catalysts. Angew Chem Int Engl 19, 390–392. https://doi.org/10.1002/anie.198003901.

[63] Tantawi, O., Joo, W., Martin, E.E., Av-Ron, S.H.M., Bannister, K.R., Prather, K.L.J., et al., 2025. Designing for degradation: the importance of considering biotic and abiotic polymer degradation. Environ Sci Process Impacts 27, 1303–1316. https://doi.org/10.1039/D5EM00079C.

[64] Teggers, E.-M., Hardebusch, J., Meisterjahn, B., Simon, M., Hennecke, D., Heumann, R., et al., 2025. Diversifying endpoints in biodegradation testing of microplastics. Environ Sci Eur 37, 65. https://doi.org/10.1186/s12302-025-01096-8.

[65] Teggers, E.-M., Heck, S., Meisterjahn, B., Simon, M., Hennecke, D., Heumann, R., et al., 2025. Modified oil extraction of pristine and weathered synthetic polyurea microcapsules and polyethylene microplastics from soil. Microplast Nanoplast. https://doi.org/10.1186/s43591-025-00121-0.

[66] Tester, M., Morris, C., 1987. The penetration of light through soil. Plant Cell Environ 10, 281–286. https://doi.org/10.1111/j.1365-3040.1987.tb01607.x.

[67] Tidjani, A., Arnaud, R., 1993. Photo-oxidation of linear low density polyethylene: a comparison of photoproducts formation under natural and accelerated exposure. Polym Degrad Stab 39, 285–292. https://doi.org/10.1016/0141-3910(93)90003-2.

[68] UNEP. Resolution adopted by the United Nations Environment Assembly on 2 March 2022. 5/5. Nature-based solutions for supporting sustainable development; 2022.

[69] Wang, J., Chen, J., Qiao, X., Zhang, Y., Uddin, M., Guo, Z., 2019. Disparate effects of DOM extracted from coastal seawaters and freshwaters on photodegradation of 2,4-dihydroxybenzophenone. Water Res 151, 280–287. https://doi.org/10.1016/j.watres.2018.12.045.

[70] Washington, J.W., Jenkins, T.M., Rankin, K., Naile, J.E., 2015. Decades-scale degradation of commercial, side-chain, fluorotelomer-based polymers in soils and water. Environ Sci Technol 49, 915–923. https://doi.org/10.1021/es504347u.

[71] Wu, X., Liu, P., Gong, Z., Wang, H., Huang, H., Shi, Y., et al., 2021. Humic acid and fulvic acid hinder long-term weathering of microplastics in lake water. Environ Sci Technol 55, 15810–15820. https://doi.org/10.1021/acs.est.1c04501.

[72] Wu, X., Liu, P., Wang, H., Huang, H., Shi, Y., Yang, C., et al., 2021. Photo aging of polypropylene microplastics in estuary water and coastal seawater: Important role of chlorine ion. Water Res 202, 117396. https://doi.org/10.1016/j.watres.2021.117396.

[73] Xu, Y., Ou, Q., Van Der Hoek, J.P., Liu, G., Lompe, K.M., 2024. Photo-oxidation of micro- and nanoplastics: physical, chemical, and biological effects in environments. Environ Sci Technol 58, 991–1009. https://doi.org/10.1021/acs.est.3c07035.

[74] Yu, X., Xu, Y., Lang, M., Huang, D., Guo, X., Zhu, L., 2022. New insights on metal ions accelerating the aging behavior of polystyrene microplastics: effects of different excess reactive oxygen species. Sci Total Environ 821, 153457. https://doi.org/10.1016/j.scitotenv.2022.153457.

[75] Zhang, Y., Cheng, F., Zhang, T., Li, C., Qu, J., Chen, J., et al., 2022. Dissolved organic matter enhanced the aggregation and oxidation of nanoplastics under simulated sunlight irradiation in water. Environ Sci Technol 56, 3085–3095. https://doi.org/10.1021/acs.est.1c07129.

[76] Zhang, S., Li, Y., Jiang, L., Cao, M., Xing, Z., Dong, D., et al., 2025. Insights on the characteristics of plastic surface degradation and biofilm microorganisms: exploring the impacts of three aerobic composting (AC) as well as UV irradiation and cycles of freeze-thaw (CFTs). J Hazard Mater 495, 138960. https://doi.org/10.1016/j.jhazmat.2025.138960.

[77] Zhu, K., Sun, Y., Jiang, W., Zhang, C., Dai, Y., Liu, Z., et al., 2022. Inorganic anions influenced the photoaging kinetics and mechanism of polystyrene microplastic under the simulated sunlight: role of reactive radical species. Water Res 216, 118294. https://doi.org/10.1016/j.watres.2022.118294.

Microplastics and Nanoplastics

RESEARCH

Open Access

Modified oil extraction of pristine and weathered synthetic polyurea microcapsules and polyethylene microplastics from soil

Eva-Maria Teggers[1,2,5*], Svetlana Heck[2,5], Boris Meisterjahn[2], Markus Simon[2], Dieter Hennecke[2], Roman Heumann[1], Holger Egger[4], Philipp Dalkmann[4], Annika Jahnke[3,5*†] and Andreas Schäffer[5,6,7†]

Abstract

Microplastics (MPs) in soil are an emerging environmental concern due to their widespread distribution, persistence, potential toxicity to soil organisms, possible transfer into crops and groundwater as well as their potential ability to alter soil functions. MP polymers, such as linear low-density polyethylene (LLDPE) and polyurea (PUA) are commonly applied to soils for mulching and pesticide application and their fate needs to be better understood. For qualitative and quantitative analysis, MPs need to be efficiently isolated from soils using suitable extraction methods. Therefore, we developed a modified oil extraction method using *n*-octanol and compared it with the widely used density extraction method, both preceded by a potassium hydroxide (KOH) extraction step. Pristine and artificially weathered (light-irradiated) small-sized LLDPE mulch film particles (cryo-milled to a median size of 147 µm) and PUA microcapsules used for pesticide applications (median diameter of 2 µm) were spiked into 25 g samples of two standard agricultural soils. Both MP types differed in size, shape, density and especially their composition, as the PUA microcapsules predominantly consisted of oil. After MP isolation, precise MP quantification was facilitated by ^{14}C-radiolabelling of the polymers, which enabled accurate mass balancing while eliminating potential interferences from background polymers. The modified oil extraction method, achieved extraction efficiencies of up to 75% of the applied radioactivity (AR), compared to a maximum efficiency of 62%$_{AR}$ using the conventional density extraction method combined with KOH.

Keywords Microplastics, Polyethylene, Polyurea, Microcapsules, Light-weathered, Extraction methods, Agricultural soil, Isotopic labelling

†Annika Jahnke and Andreas Schäffer share the last authorship.

*Correspondence:
Eva-Maria Teggers
eva.teggers@rwth-aachen.de
Annika Jahnke
annika.jahnke@ufz.de
Full list of author information is available at the end of the article

Graphical Abstract

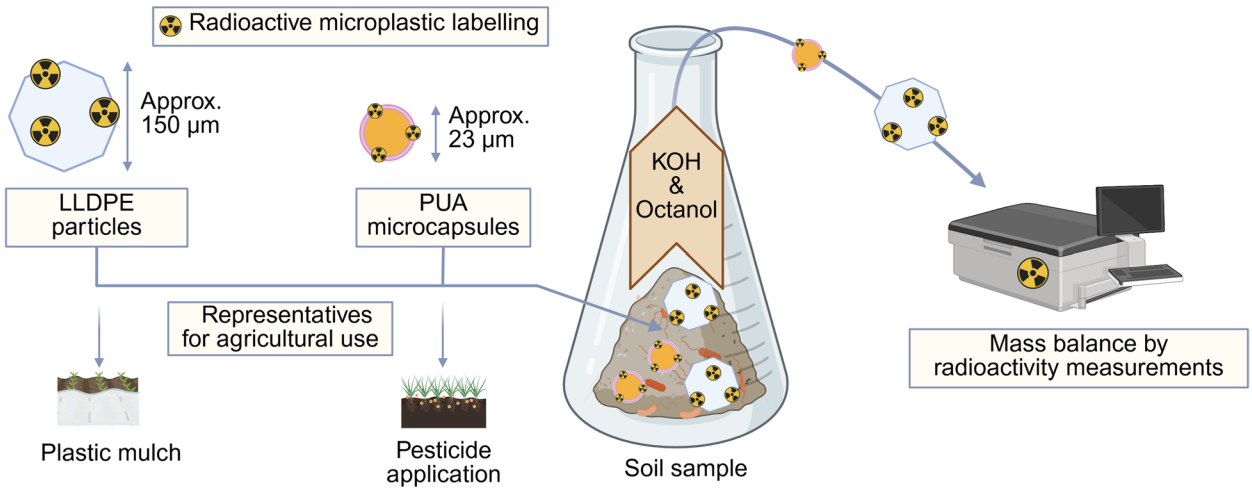

Introduction

Environmental pollution by synthetic polymer microparticles, commonly referred to as microplastics (MPs), has become a major concern in recent decades. The extensive dispersion, the persistence leading to slow fragmentation and degradation of MPs and the possible adverse effects on organisms are key aspects of concern [2, 5, 10, 13, 21, 30, 37]. The size range for MPs varies across studies and organizations [17, 19, 31, 33]. Hartmann et al. [25] discussed this inconsistency, highlighting the importance of establishing a standardized definition. They proposed a standardized size range of 1 µm to 1 mm. MPs are either directly released into the environment ("primary MPs") or generated by the fragmentation of larger plastic debris ("secondary MPs") [7, 39]. Calculating MP release is challenging due to the lack of standardized analytical methods, variations in sampling and analysis techniques, limited data on specific sources and the complex behaviour of MPs in different environmental compartments as reviewed by Galafassi et al. [18]. Based on Hann et al. [24], the European Chemicals Agency [16] estimated that 176,300 tonnes of secondary MPs are released into surface waters of the European environment per year. Regarding primary MPs Boucher and Friot [4] estimated that 1.5 million tons per year are globally released into the ocean but the values should be taken with caution according to the authors. In this study the prevailing sources of primary MPs pollution to the ocean are synthetic textiles (35%), followed by car tyres (28%), city dust (24%), road markings (7%), marine coatings (3.7%), personal care products (2%) and plastic pellet losses (0.3%). Secondary MPs typically comprise mismanaged plastic waste, e.g., from littered plastic packaging or discarded fishing gear [39]. Emissions of MPs to terrestrial ecosystems, analytical methods, and MP impacts on soil organisms and human health have been reviewed [3, 28, 58, 62]. According to the authors, estimating MPs and their sources to soils is difficult due to, among other issues, analytical limitations. Major MP emissions to agricultural soils comprise the use of plastic mulch (39%) of which 100,000 tonnes are used but only 32% are collected at the end of the farming period. Other sources are sewage sludge (16%), compost (15%), whereas coated fertilizers (3%) represent minor sources [54]. Encapsulated plant protection products are likely another minor source, but not systematically considered in studies to date.

In order to counteract the continued emissions of primary MPs in the environment, the European Commission recently adopted a restriction on intentionally adding synthetic polymer microparticles to products [17]. Exempted are natural, water-soluble polymers and MPs for which biodegradability can be proven by standardised tests according to OECD and ISO test guidelines (TG) [17]. For polymer-encapsulated pesticides, biodegradability must be proven in two environmental compartments: (i) in either fresh, estuarine or marine water and (ii) in soil. For regulatory test purposes, only the mineralisation to CO_2 is a valid criterion to show biodegradability, whereas the assessment of possible fragmentation or transformation products is to date not considered. However, for a more comprehensive description of biodegradation pathways and general environmental fate

assessment, efficient and robust extraction methods for MPs from soils are needed.

Most of the published extraction methods are based on density separation [23, 40, 49, 51] or oil extraction [9, 38, 49, 51, 57]. Other, less common extraction methods comprise electrostatic extraction, magnetic extraction or froth flotation [26, 42, 67]. Generally, the extraction efficiency to remove MPs from soils can be improved by soil organic matter (SOM) removal [26, 29, 51]. Common reagents used for this purpose include acids, bases like potassium hydroxide (KOH), hydrogen peroxide, or Fenton's reagent [42, 56]. However, the role of these reagent solutions and the physical and chemical processes in extracting MPs remain largely unexplored [44, 49]. A study by Nava and Leoni [43] found that nylon and polyethylene terephthalate (PET) MPs of three size categories (250–500 µm, 500–2000 µm, 2–5 mm) were efficiently extracted using 10% KOH at 60 °C for 30 min with constant stirring, followed by sieving through a 250 µm mesh, with reliable recovery results (60–100% for nylon and 67–100% for PET MPs > 250 µm). The study also demonstrated that smaller-sized MPs were less efficiently extracted, which poses an additional challenge. Möller et al. [42] and da Costa and Duarte [11] reviewed the challenges associated with the identification and quantification of MPs following extraction, particularly for particles with smaller sizes, with error rates ranging up to 70% (visual identification), issues due to matrix effects (e.g., Fourier-Transform Infrared spectroscopy (FTIR)) or other drawbacks.

Further challenges for the extraction process arise due to MP alterations caused by extraction solvents [12, 29, 35, 55] but also from natural weathering processes, such as photooxidation in the environment, that can change MP characteristics [1]. When MPs are exposed to sunlight, high energy UV-radiation can induce chain cleavage of the polymer, the creation of free radicals and the addition of oxygen-containing functional groups on the MP surface. These transformations enhance the hydrophilicity of the MP surface and render its structure more brittle, thereby increasing their susceptibility for fragmentation [1, 15]. In addition, changes in the physical and chemical properties of MPs can modify their interactions with soil particles and influence their aggregation behaviour. This, in turn, may compromise the overall efficiency of MP extraction [15].

The aim of this study was to develop an efficient and robust method for the extraction of MPs from soil matrices. Pristine and sunlight-irradiated (weathered) polyurea (PUA) microcapsules used for pesticide encapsulation and cryo-milled linear low-density polyethylene (LLDPE), which is commonly used as mulch film material, were spiked to reference soils. Two MP extraction methods were compared: The widely used density separation [20, 42, 51, 64], and a modified oil extraction method, inspired by the protocol of Crichton et al. [9]. The methods were tested on two diverse reference soils to evaluate potential differences in the sorption behaviour of the polymers. The MP mass quantification was performed based on ^{14}C-radiolabelling the polymer which enabled the sensitive and specific tracking of the tested MPs. The calculation of the percentage of applied radioactivity (AR) allowed for a comprehensive evaluation of extraction performance while excluding potential bias due to contamination of other polymers that might be present in the soil.

Materials and methods

MP materials

^{14}C-labelled PUA microcapsules (approx. 3.49 MBq/mg, Bayer AG, Germany) were synthesised as described in the patent paper of Krause and Egger [34] using [1,6-^{14}C]hexamethylenediamine (1887 MBq/mmol, Tjaden Biosciences LLC, USA). The utilised ^{14}C-labelled LLDPE microparticles (70.46 MBq/g) were generated by cryo-milling after synthesis based on the procedure of Sinn et al. [59] and Quijada et al. [50] using labelled ^{14}C-1-octadecene (2035 MBq/mmol, American Radiolabeled Chemicals Inc., USA) at the Fraunhofer IME (Schmallenberg, Germany). More details of the PE synthesis and particle generation can be found in the SI—Text S1. Both types of MPs were prepared in an aqueous suspension and used either in their pristine or light-exposed form (see below). The polymeric content of the PUA suspension was represented by the microcapsules' shell that only amounted to < 1% on a w/w basis of the suspension.

The initial suspension of the PUA microcapsules was characterised by laser diffraction particle size analysis (PSA, Mastersizer 2000, Malvern Panalytical Ltd, Great Britain) and shown to comprise a median size of 16.5 µm (10% percentile of 2.1 µm and a 90% percentile of 37.1 µm) (SI—Table S2, Figure S1). Following a method of Teggers et al. [63], residual non-polymerised material (e.g., identified labelled molecules) was removed by filtering the PUA suspension with a 12 µm pore-sized cellulose nitrate filter (Whatman AE 100, Cytiva, USA) and by rinsing the filter with 100 mL ultra-high quality (UHQ) water (PURELAB Ultra, ELGA LabWater, Germany). Then, the microcapsules remaining on the filter were resuspended in 10 mL of UHQ water in an ultrasonic bath for ten minutes (Sonorex Super RK514H, Bandelin GmbH & Co. KG, Germany). The filter was removed, and the new suspension with a determined radioactivity of 3.5 kBq/mL was used for application of soil samples in the extraction tests. The median of the microcapsules' size of the new suspension (fraction > 12 µm) was calculated to be

Table 1 Overview of the performed experiments. Not executed experiments are abbreviated by "N/A". LLDPE was only tested in the first experiment (I)

	Extraction experiments	Spiked MPs		Soils used for the experiments (RefeSol)
		Pristine	Light-exposed	
I)	Modified oil extraction using octanol	PUA, LLDPE	PUA, LLDPE	03-G, 01-A
II)	Density extraction using $ZnCl_2$	PUA	N/A	03-G, 01-A
III)	Repeated first extraction step using KOH	PUA	N/A	03-G

22.9 µm (10% percentile of 14.2 µm and a 90% percentile of 45.7 µm; SI—Table S2). The PUA microcapsules are estimated to have a density ranging from 1.10 to 1.23 g/cm^3 [14, 41].

The ^{14}C-labelled LLDPE microparticles with a general density [66] of 0.91 g/cm^3, varied in size (10% percentile of 48.8 µm to a 90% percentile of 342.7 µm; SI—Table S2) with a median of 147.0 µm within the PSA (Analysette 22 NanoTec, Fritsch GmbH, Germany, SI—Table S2). The application suspension was prepared by transferring 6 mg of LLDPE into 50 mL of UHQ water. Microscopic images of representative MPs of PUA microcapsules (prior to washing off compounds < 12 µm) and one LLDPE particle are shown in the SI—Figure S2.

To evaluate the extraction performance with more environmentally relevant, artificially weathered particles, both PUA and LLDPE MPs were exposed to artificial sunlight (295–800 nm, SUNTEST CPS+, Atlas Material Testing Technology GmbH, Germany). This process simulated potential phototransformation that the pristine polymers might undergo under field conditions. The irradiation setup was inspired by the OECD draft TG [45] "Phototransformation of Chemicals on Soil Surfaces" and the OECD TG 316 [46] "Phototransformation of Chemicals in Water". Five replicates each containing 15 mL of the PUA suspension (3.5 ± 0.16 kBq/mL) and five replicates of 15 mL of the LLDPE suspension (4.6 ± 1.95 kBq/mL) were transferred into 20 mL quartz glass vials with gas-tight quartz glass lids and placed in the irradiation chamber. A Xenon lamp with a light intensity of 54.5 W/m^2 (300–400 nm) was operated for 13.8 days (approx. 18.1 kWh/m^2), corresponding to an irradiation similar to 30 summer days in the Northern hemisphere (30–50°N) according to the OECD draft TG [45]. Two cooling systems were employed at the base and the surface of the vials to maintain the temperature of the polymer suspension at approximately 32 °C. Due to a failure in the SUNTEST CPS+ device, the LLDPE suspension was exposed to higher temperatures reaching approximately 50 °C for the last 6.8 days of the exposure period. Following the light exposure, the radioactivity of the suspension was determined.

Test soils and MP application

The different extraction methods were tested on two reference soils: RefeSol 01-A and RefeSol 03-G (https://www.refesol.de/, Fraunhofer IME, Schmallenberg, Germany, Supplementary Information (SI)—Table S1). Both soils are representative of agricultural areas in Germany and are accepted by the German Environment Agency for use in regulatory guideline studies, e.g., addressing the biodegradation of chemicals. RefeSol 01-A represents the soil characteristics of an arable land, with a sandy loam texture as well as light humic and organic carbon content (OC: 1.03%). RefeSol 03-G represents grassland soils, with a silty loam texture, comprising higher contents of silt, clay and organic carbon (OC: 3.87%).

The soils were sieved to a particle size smaller than 2 mm, and their water content was adjusted to 50% of their maximum water-holding capacity (WHC_{max}, SI – Table S1). The extraction experiments were performed with 25 g soil ($n = 3$) on a dry weight basis (dw) to which 0.5 mL MP suspension (PUA microcapsules: 1.75 ± 0.08 KBq; LLDPE particles: 2.33 ± 0.97 KBq) was applied. To ensure thorough incorporation of the spiked MPs, the soil samples were carefully mixed with a spatula. They were then left uncovered at room temperature for one hour before MP extraction, allowing the suspension moisture to evaporate and to ensure better interaction between the soil matrix and the MPs.

MP extraction procedures

Three extraction experiments were conducted, as summarized in Table 1. The first experiment (I) involved a modified oil extraction method using octanol (Fig. 1), which was compared to the second experiment (II), a density extraction using $ZnCl_2$. Both methods included a first extraction step with KOH (Fig. 1). In the third experiment (III), the first extraction step using KOH extraction was performed twice in sequence to determine whether repeated alkaline treatment enhances MP extraction efficiency. In a separate experiment, the first extraction step was performed using sodium hydroxide (NaOH) solutions with different pH values in order to investigate their influence on the ability to extract PUA MPs.

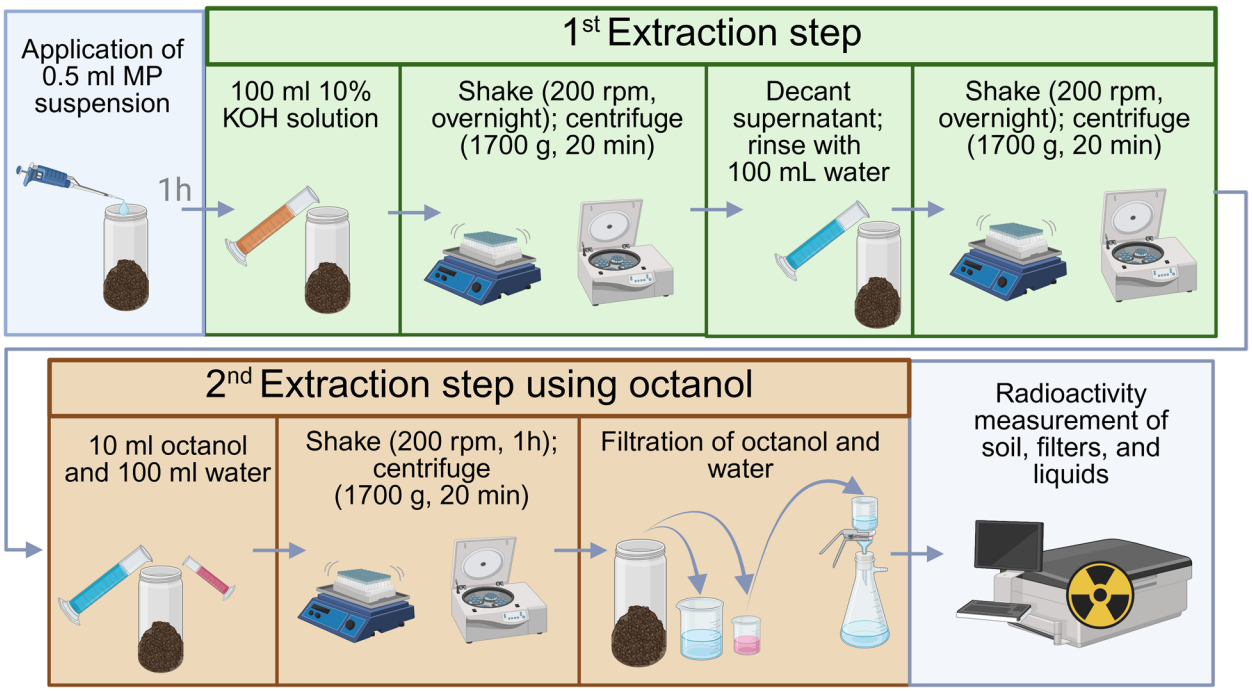

Fig. 1 Scheme of the first extraction experiment (I)—the modified oil extraction using octanol, as an alternative to the density extraction procedure. The first extraction step with KOH is shown with a green background (upper row) and the second extraction step using octanol is displayed with brown background below. The density extraction procedure using a $ZnCl_2$ solution as the second extraction step is not displayed

In all three expermiments, the first extraction step with KOH was performed to remove the SOM and hence to improve the efficiency of the MP extraction. For this purpose, 100 mL of a 10% KOH solution (prepared from KOH pellets, Merck KGaA, Germany) were added to the soil samples spiked with PUA or LLDPE MPs ($n=3$ each). The samples were shaken for 22 h at room temperature on a horizontal shaker (Laboshake LS500, C. Gerhardt Analytical Systems GmbH & Co. KG, Germany) at 200 rpm and centrifuged for 20 min at 1700 g (Multifuge 4KR, Heraeus GmbH, Germany). The resulting supernatant was decanted, and the radioactivity of the KOH solution was determined. To remove residual KOH, 100 mL of UHQ water were added. The samples were shaken and centrifuged to allow the supernatant to be decanted. The volume of the extracts was measured and the contained radioactivity determined to assess the extraction efficiency of the KOH (Fig. 1). Since the strongly alkaline conditions of the extraction may alter the MP particles, a microscopic examination of morphological changes of the PUA microcapsules was performed after incubating the suspension in KOH (pH 14) for up to 5 d.

In the first experiment (I, Table 1), the second extraction step followed a modified version of the oil extraction protocol by Crichton et al. [9], which originally used olive, canola, or castor oil. According to this method, water and oil are first added to the soil sample, followed by thorough shaking. The mixture is then left to settle until the phases are clearly separated. Due to the oleophilic properties of the polymers, MPs accumulate in the upper oil layer, which can be decanted for further analysis. To minimize variations caused by the composition of natural, non-standardized oils, which could affect the extraction process, we replaced plant oil with the well-defined chemical *n*-octanol (Extra Pure, Merck KGaA, Germany) in our study.

After the first extraction step using KOH, 100 mL UHQ water and 10 mL octanol as a second extraction step were applied to each soil sample spiked with PUA or LLDPE MPs. As demonstrated in Fig. 1, the samples were shaken for 1 h on the horizontal shaker (200 rpm), left to settle for around 18 h and then centrifuged for 20 min at 1700 g (Multifuge 4KR, Heraeus GmbH, Germany). This centrifugation step was necessary to remove excess soil particles from the liquid phase, which prevented effective filtration. After centrifugation, the overlying octanol phase was removed using a Pasteur pipette and vacuum-filtered with a 12 µm cellulose nitrate filter (Whatman AE 100, Cytiva, USA). The filters were washed with a 1:1 (v:v) ethanol–water mixture to remove residual octanol. Lastly, the water phase was decanted, the volume of the extracts was measured, and their radioactivity was determined.

Additionally, the soil and filters were air-dried for combustion and radioactivity determination.

The second extraction experiment (II, Table 1), a density extraction was performed as alternative second extraction step. For this, an 8.8 M $ZnCl_2$ solution (made from anhydrous $ZnCl_2$, 98%, Thermo Fisher Scientific, USA) with a density of 1.57 g/cm^3 was utilised. 100 mL $ZnCl_2$ solution were applied to the soil samples spiked with PUA MPs following the first extraction step using KOH. The samples were shaken on a horizontal shaker at 200 rpm for 45 min and then centrifuged at 1700 g for 20 min. The supernatant was vacuum-filtered through a cellulose nitrate filter (Whatman AE 100, Cytiva, USA) with a pore size of 12 µm and the filters were rinsed with UHQ water to remove most of the $ZnCl_2$. Thereafter, the soil was washed with 100 mL UHQ water, shaken, and centrifuged again. The supernatant was decanted and vacuum-filtered. The soil and filters were air-dried and combusted for radioactivity analysis. Moreover, the volume of the extracts was measured, and radioactivity was determined.

For the third extraction experiment (III, Table 1), the first extraction step involving KOH application was performed twice.

In a separate experiment, a pH correlation test was conducted to investigate the effect of pH on the extraction efficiency in the first extraction step. For this purpose, replicates of 25 g of reference soil (RefeSol 03-G) were treated with four solutions at different pH levels: hydrochloric acid (pH = 3), UHQ water (pH = 6), and two sodium hydroxide solutions (pH = 11 and pH = 14), prepared from a 2 M NaOH stock (Grüssing GmbH, Germany). Each treatment was done in triplicates.

Radioactivity analysis

The amount of ^{14}C radioactivity was determined and extrapolated to the amount of MP, in contrast to other MP quantification methods, such as pyrolysis – gas chromatography – mass spectrometry (Py – GC – MS), where the mass of the actual material is directly quantified. Hence, possible fragments or transformation products from the ^{14}C-MPs that might have additionally been extracted must be considered. The quantification of radioactivity and the corresponding mass balance in the extraction experiments across the various fractions—namely, the extracts, filters, and the soil—was conducted using liquid scintillation counting (LSC; HIDEX 600 SL, HIDEX GmbH, Germany). Solid samples such as filters and the soil were air-dried prior to combustion in an oxidizer (HIDEX 600 OX, HIDEX GmbH, Germany). The $^{14}CO_2$ formed due to combustion of the samples was trapped in a suitable LSC-cocktail (Oxysolve C-400, Zinsser Analytic GmbH, Germany) and the radioactivity was quantified by LSC-analysis.

The recovered amount of applied radioactivity ($\%_{AR}$) was calculated and assigned to each extraction fraction (soil, KOH, octanol phase *vs.* $ZnCl_2$ phase, and water phase) to establish a mass balance and derive extraction efficiencies. In this context, the total amount of the recovered AR is the sum of radioactivity found in all phases and fractions and is referred to as "total recovery". Opposed to this, "extraction efficiency" refers to the sum of the total recovered amount of applied radioactivity excluding the radioactivity remaining in the soil. Moreover, to facilitate comparison between the performed extraction experiments, the radioactivity of each extraction fraction was normalized by the "total recovery", calculated as the "proportion of the total recovered radioactivity" ($\%_{TRR}$) and can be found in the SI—Table S3. For example, when two experiments yield differing extraction efficiencies, analysing the radioactivity distribution relative to the total recovery provides a clearer basis for comparing the levels of radioactivity detected in each fraction.

Data evaluation

Data curation and evaluation were performed with Microsoft Excel (Microsoft Office Professional Plus 2019), data visualisation was performed with Graphpad Prism 6 (Version 6.07 of June 2015) and the illustration of the graphical abstract as well as Fig. 1 was created with BioRender.com.

Results and discussion

Extraction efficiencies of the different extraction experiments

The efficiency of extraction experiment (I), the modified oil extraction method using octanol, was compared with that of extraction experiment (II), the density extraction (Table 1). The investigated types of MP particles in the first experiment differed in their size, shape, polymer chemistry and density, in addition to their diverse composition, since the PUA microcapsules consisted mainly (up to 94 weight-%) of oil. Depending on its synthesis, PUA can have hydrophilic characteristics depending on ionic groups and/or non-ionic hydrophilic segments inserted in the polymer structure and thus develop H-bonds with water. However, the used PUA was synthesised to form a crosslinked polymer structure and H-bonding was developed predominantly as intermolecular bonds within the PUA structure, limiting the ability to bind to water. Jiang et al. [32] determined that intermolecular H-bonding and branched urea groups were responsible for crosslinked PUA to be insoluble. As a result, with increasing insolubility the hydrophilicity generally decreased [27]. LLDPE

Table 2 Overview of the total extraction recoveries (referring to the total applied radioactivity) and efficiencies (referring to the total applied radioactivity except for the radioactivity in the soil) of all performed extraction experiments, given as percentage of the applied radioactivity (AR)

Extraction Experiment	Spiked MPs		Reference Soil	Total extraction recovery		Extraction efficiency	
	Pristine	Light-exposed		AR Mean [%] ($n=3$)	AR SD [%] ($n=3$)	AR Mean [%] ($n=3$)	AR SD [%] ($n=3$)
Modified oil extraction using octanol (I)	PUA	no	01-A	84.6	4.92	74.6	1.33
	PUA	no	03-G	84.2	8.13	70.5	5.09
	LLDPE	no	01-A	50.6	9.61	50.3	9.49
	LLDPE	no	03-G	114	31.7	114	31.4
	PUA	yes	01-A	51.7*	9.23*	50.5*	9.09*
	PUA	yes	03-G	47.0	0.41	44.2	0.55
	LLDPE	yes	01-A	55.1	17.6	53.3	15.5
	LLDPE	yes	03-G	76.4	30.1	76.1	30.0
Density extraction using $ZnCl_2$ (II)	PUA	no	01-A	89.8	4.16	59.9	2.61
	PUA	no	03-G	88.1	6.17	62.0	4.89
Repeated first extraction step using KOH (III)	PUA	no	03-G	82.3	2.75	55.6	4.20

SD Standard deviation

* ($n=2$, due to a high deviation of the first replicate)

is generally non-polar and remains hydrophobic [70]. Thus, both used particles were predominantly hydrophobic and were efficiently extracted with the optimised oil extraction method using octanol. The use of the two reference soils enabled to compare MP extraction efficiencies of two soils with largely diverging characteristics commonly found in agricultural areas to which PUA microcapsules for pesticide application or LLDPE mulching films are applied. An overview of the total recoveries (extracts and radioactivity remaining in soil) and the extraction efficiencies of all performed extraction experiments are provided in Table 2.

The highest extraction efficiency of the pristine ^{14}C-PUA microcapsules was achieved by applying extraction experiment (I), combining the first extraction step (KOH treatment) and second extraction step using octanol with $70.4 \pm 5.1\%_{AR}$ (RefeSol 03-G) to $74.6 \pm 1.3\%_{AR}$ (RefeSol 01-A). Since the amount of applied AR was determined before, radioactivity mass balancing not only facilitated the calculation of efficiencies but also enabled to determine whether all applied MP particles were recovered or if a fraction of MP was lost during extraction. Therefore, by balancing the radioactivity, a loss of AR was seen for the ^{14}C-PUA microcapsules (light-exposed) and the ^{14}C-LLDPE MP (both pristine and light-exposed). Regarding the light-exposed ^{14}C-PUA microcapsules the total recovery of radioactivity was lower, amounting to $51.7\%_{AR}$ (RefeSol 01-A) and $47.0\%_{AR}$ (RefeSol 03-G). It was suspected that a part might have become bioavailable due to the preceding light exposure and/or might have been mineralised to $^{14}CO_2$ during the one-hour incubation time in soil. This latter presumption could be confirmed by the results of a parallel study on the performance of a transformation test in soil similar to the OECD TG 307 (to be published separately). With regard to the ^{14}C-LLDPE, the high deviations from the AR were assumed to be caused by the inhomogeneity of the MP suspension resulting in inhomogeneous MP application (Table 2).

As mentioned above, performing the first extraction, experiment (I), the modified oil extraction using octanol led to the highest extraction efficiencies (Table 2) for the pristine ^{14}C-PUA microcapsules. The density extraction using $ZnCl_2$, extraction experiment (II), resulted in extraction efficiencies that were 10 to $15\%_{AR}$ lower than those of extraction experiment (I) ($59.8 \pm 2.6\%_{AR}$ RefeSol 01-A; $62.0 \pm 4.9\%_{AR}$ RefeSol 03-G, Table 2).

Generally, the majority of the extracted radioactivity of pristine ^{14}C-PUA microcapsules was found in the KOH solution. In a preliminary test the KOH solution did not cause any visual damage to the microcapsules according to an examination by light microscopy after incubating the suspension in KOH (pH 14) for up to 5 d (SI – Figure S3). However, such optical analysis is a vague measure of visual morphological changes such as the shape of the capsules, and thus physical changes of the surface or chemical alterations due to the KOH treatment cannot be excluded. Furthermore, the possibility that the mechanical impact of centrifugation may cause the disintegration of MPs cannot be excluded. However, a study

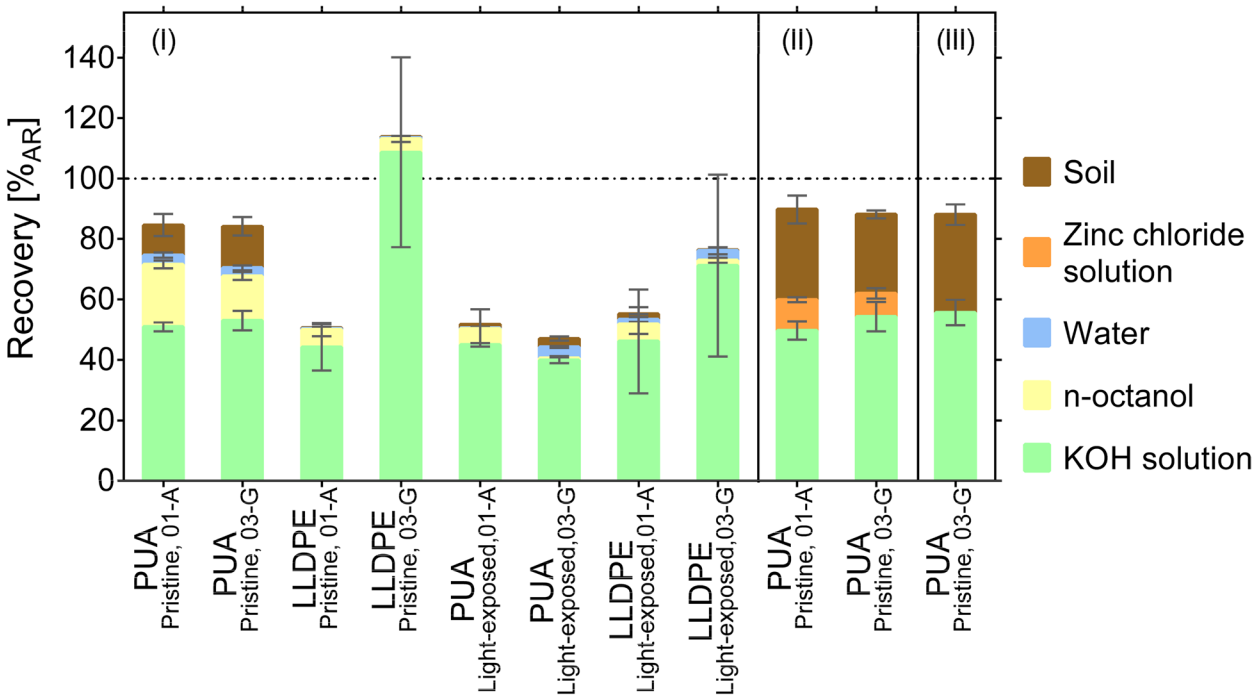

Fig. 2 Percentage of the applied radioactivity ($\%_{AR}$) recovered by the different extraction experiments (I, II, III, Table 1). Extraction experiments were performed with spiked pristine or light-exposed ^{14}C-polyurea microcapsules (PUA) and ^{14}C-LLDPE microparticles (LLDPE) and investigated on two diverse reference soils: RefeSol 01-A and 03-G. Means of $n = 3$ with SD; except for the pristine PUA on RefeSol 01-A, means of $n = 2$ with SD

of Pfohl et al. [47] found that the size of MP particles remained similar to that of the pristine particles after centrifugation at even higher centrifugal forces than in our study. Nevertheless, the MP microcapsules applied in this study might be more sensitive due to their thin polymeric shells. The inclusion of the first extraction step using KOH (Fig. 1) resulted in higher extraction efficiencies than experiments without performing this first step. (Results obtained without performing the first extraction step using KOH are displayed in the SI-Table S4.).

Consistent with our observations, Radford et al. [51] reported higher extraction efficiencies when removing SOM prior to the oil extraction procedure. By the implementation of the first extraction step, a substantial fraction of the pristine ^{14}C-PUA microcapsules was removed from the soil (RefeSol 01- A: $50.3 \pm 2.2\%_{AR}$,RefeSol 03-G: $53.6 \pm 3.7\%_{AR}$, within experiment (I) and (II), $n = 6$). In a study of Nava and Leonie (2021), a similar fraction of 60–67% polyethylene terephthalate (PET) and nylon particles, respectively, was recovered using KOH in the lowest particle size range (250 to 500 µm). However, in literature the MP extraction efficiencies by the SOM removal reagents are often not described separately, or the SOM removal is performed after the main extraction procedure [52]. Repeating the first extraction step using KOH (RefeSol 03-G only) yielded a combined extraction efficiency of $55.6 \pm 4.2\%_{AR}$ for PUA microcapsules (Table 2, Fig. 2 (III)). Hence, the repetition did not substantially enhance the extraction efficiency.

By implementing a second extraction step (either octanol, experiment (I) or $ZnCl_2$, experiment (II)), an additional amount of the remaining ^{14}C-PUA microcapsules was mobilised. Thus, the total extraction efficiency could be further improved by up to $14.9\%_{AR}$ (Table 2, (I) *vs.* (III), Refesol 03-G) by the implementation of the octanol extraction compared to experiment (III) with a repeated first extraction step. Notably, when the first extraction step was omitted a similar amount of pristine PUA microcapsules was extracted by the octanol procedure $19.0\%_{AR}$ (RefeSol 01-A) to $23\%_{AR}$ (RefeSol 03-G) (SI—Table S4, Octanol, "Modified oil extraction using octanol (I) w/o Step 1"). The density extraction experiment (II) resulted in a maximum increase of $6.4\%_{AR}$ in extraction efficiency from soil (Table 2, (II) *vs.* (III), Refesol 03-G) compared to experiment (III). Presumably, the microcapsules extracted by the octanol or $ZnCl_2$ method were not bound to SOM, but rather to other soil components, such as mineral components.

In previous studies, both density [49, 51, 65] and oil-based extraction methods [9, 38, 49, 51, 57] achieved higher MP recoveries than observed here. However,

those studies used larger MPs which are easier to extract, as discussed above. For example, Radford et al. [51] applied a $ZnCl_2$-based density extraction on MPs (PET, HDPE, PVC, LDPE, PP and PS; 0.5–5 mm) in soil, reaching 80% efficiency. This study noted a decline in extraction efficiency as MP size decreased, however, their smallest MPs were still larger than those used in this study. The used ^{14}C-PUA microcapsules had a median size of 22.9 µm and were significantly smaller than the MPs examined in most previous studies. This smaller size, along with the unique oil-filled polymer shell composition, may explain the lower recoveries observed in our study. Additionally, some microcapsules may disintegrate, making partially broken shells more difficult to extract.

The applied amount of ^{14}C-LLDPE showed high variations (4.66 ± 1.96 kBq/mL) leading to substantial variations of AR across all replicates. Calculated total recoveries of 50.6 ± 9.6%$_{AR}$ (RefeSol 01-A) and 114 ± 31.6%$_{AR}$ (RefeSol 03-G) should be regarded as compromised since no reliable values for the initially applied radioactivity were obtained due to the inhomogeneity of the suspension. To be more precise, the high deviation occurred because, unlike a dissolved substance, suspended particles were applied, making the distribution in the applied volume less uniform. This also means that recoveries can be higher than 100% of the calculated AR. Nevertheless, since only 0.3 ± 0.2%$_{AR}$ (RefeSol 01-A, RefeSol 03-G) remained unextracted in soil (Fig. 2 (I)), we conclude that ^{14}C-LLDPE MPs were overall recovered almost entirely.

As with the ^{14}C-PUA microcapsules, a large majority of the ^{14}C-LLDPE MPs were already extracted with the first KOH extraction step (RefeSol 01-A: 44.1 ± 7.6%$_{AR}$; RefeSol 03-G: 109 ± 31.4%$_{AR}$) and only a minor fraction was extracted in the second step by octanol. The improved extraction results, with less radioactivity remaining in soil compared to the pristine ^{14}C-PUA microcapsules, were presumably due to different characteristics and the larger size of the ^{14}C-LLDPE MPs.

Impact of soil types on the extraction efficiency

A difference in extraction efficiencies between the two soil materials was expected due to their largely diverging characteristics (Table S1). Considering that organic materials can adsorb and retain MPs, and vice versa, we hypothesised that a higher organic matter content would result in a stronger MP retention, consequently affecting the extraction efficiency negatively. However, despite the higher organic matter content of RefeSol 03-G (6.7% SOM content opposed to 1.8% SOM content for 01-A, acc. DIN EN 15936, SI—Table S1), no clear differences were observed between the extraction efficiencies from the two soil types, regardless of the extraction procedure (Fig. 2, SI—Table S3, S4), which contrasts with findings from other studies, such as Corradini et al. [8]. Similar to our outcome, in the studies conducted by Radford et al. [51] and Prosenc et al. [49] no significant correlation between the proportion of SOM and the MP extraction efficiency was observed when applying the density extraction.

Impact of sunlight irradiation on the extraction efficiency

Regarding the light-exposed ^{14}C-PUA microcapsules, generally lower total recoveries of 51.7 ± 9.2%$_{AR}$ (RefeSol 01-A) and 47.0 ± 0.4%$_{AR}$ (RefeSol 03-G) were achieved. By performing a biodegradation test in soil similar to the OECD TG 307 we could show that 23.2 ± 7.3%$_{AR}$ (RefeSol 01-A) to 33.1 ± 2.1%$_{AR}$ (RefeSol 03-G) of the applied radioactivity appeared to have been mineralised to $^{14}CO_2$ within one hour (details to be published separately). However, despite the low total recoveries, apparently due to biodegradation processes, the remaining radioactivity in soil (RefeSol 01-A: 50.5 ± 9.1%$_{AR}$; RefeSol 03-G: 44.2 ± 0.6%$_{AR}$) could be extracted almost completely. Only 1.2 ± 0.0% to 2.8 ± 0.7% of the AR remained in the soil (RefeSol 01-A and RefeSol 03-G respectively), indicating an overall high extraction efficiency. Again, most of the recovered radioactivity was extracted in the first extraction step using KOH (RefeSol 01-A: 44.9 ± 0.6%$_{AR}$; RefeSol 03-G: 39.9 ± 1.0%$_{AR}$; Fig. 2 (I)). A small fraction of the ^{14}C-PUA microcapsules was extracted by octanol from the reference soil RefeSol 03-G (0.7 ± 0.6%$_{AR}$, $n = 3$). However, a major difference in the recovery was observed among the three replicates of RefeSol 01-A. In replicate one, 37.5%$_{AR}$ of the ^{14}C-PUA microcapsules were found in the octanol phase, whereas in replicates two and three, considerably less was extracted in that step (9.9%$_{AR}$ vs. 0.8%$_{AR}$). Likewise, the total recovery of ^{14}C-PUA microcapsules exhibited a marked disparity, with replicate one achieving a considerably higher recovery (87.2%$_{AR}$) than replicates two and three (58.2%$_{AR}$ vs. 45.2%$_{AR}$). Thus, for the visualization in Fig. 2 (I), for the above-mentioned extraction results and for Table 2 and SI-Table S3 and S4, the first replicate was excluded.

Presumably, due to a higher extractability of ^{14}C-PUA microcapsules by the first extraction step using KOH after light exposure, less radioactivity was found in the octanol phase, in contrast to the pristine ^{14}C-PUA microcapsules (pristine PUA microcapsules in octanol: RefeSol 01-A: 20.7 ± 1.3%$_{AR}$; RefeSol 03-G: 14.8 ± 1.3%$_{AR}$; light-exposed PUA microcapsules in octanol: RefeSol 01-A: 5.3 ± 6.5%$_{AR}$; RefeSol 03-G: 0.7 ± 0.6%$_{AR}$); this also applied for the normalised TRR values (given in the percentage of the total recovered radioactivity for better comparison regarding the

highly deviating recoveries, SI – Table S3). Studies have revealed that light exposure can lead to decreased molecular mass and gravimetric weight and increased hydrophilicity, which makes the polymers more susceptible for degrading microorganisms [15, 22, 60, 61, 69]. Following this assumption, due to an increased hydrophilicity, a higher extraction efficiency of PUA microcapsules may have been achieved already with the first extraction step using KOH. Exposure to artificial sunlight may have led to the fragmentation of microcapsules, potentially releasing transformation products. These products could have facilitated mineralisation during the period between the application of the MP suspension to the soil and the execution of the extraction procedure. In a study conducted by Mani et al. [38] the oil extraction efficiencies of MPs were compared between spiked sediments containing pristine MPs and environmental samples that likely contained weathered MPs. The extraction efficiency for environmental samples, which presumably contained weathered MP particles, was 74 ± 13% relative to the total amount quantified by stereomicroscopic analysis. In contrast, spiked samples with pristine MPs achieved a significantly higher extraction efficiency of 99 ± 4%. The authors suggested that the weathering state of MPs might have contributed to the lower extraction efficiency. However, since the weathered MPs were obtained directly from the environment, it is likely that other factors, such as different solid environmental matrix components and properties, also influenced the extraction.

Similar to the pristine LLDPE, the light-exposed LLDPE MPs were almost entirely extracted from soil, as indicated by the minimal residual radioactivity detected in soil (Fig. 2 (I), SI—Tables S3, S4). This suggests that any changes induced by light exposure did not impact the extractability of LLDPE MPs. However, the overall extraction efficiency remained comparable between pristine and light-exposed MPs, with values ranging from $53.3 \pm 15.5\%_{AR}$ (RefeSol 01-A) to $76.1 \pm 30.0\%_{AR}$ (RefeSol 03-G). This similarity is likely due to the relatively low recovered radioactivity and high variability observed across both extraction steps ($55.1 \pm 17.6\%_{AR}$ and $76.4 \pm 30.1\%_{AR}$, SI—Tables S3, S4).

It is important to note that the simulated sunlight irradiation applied in this study followed a standardized laboratory approach, which does not fully replicate realistic environmental sunlight exposure. In natural settings, MPs are subjected to a range of physico-chemical and biological processes that contribute to their ageing and weathering, which could make them more reactive than MPs exposed to controlled laboratory conditions. Therefore, to fully assess the effectiveness of the extraction method, further investigations should consider environmentally aged MPs, which may exhibit different extraction behaviours due to their altered physicochemical properties. Moreover, in this study, the polymers were suspended in water during exposure to artificial sunlight and subjected to hydrolysis. In contrast, under realistic environmental conditions, MPs would typically deposit on soil following their application in the field. This difference in exposure conditions may influence the weathering processes and, consequently, the extractability of MPs from environmental matrices.

Impact of the pH of the KOH solutions used in the first extraction step

The pH correlation experiment showed that by gradually increasing the pH of the aqueous solution from pH 3 to pH 14, a higher extraction efficiency of ^{14}C-PUA microcapsules was achieved, with an optimal pH of 14 (SI—Figure S4). We observed that the extract gradually darkened with increasing pH, indicating a higher SOM extraction efficiency (SI—Figure S5). Generally, with increasing pH the solubility of SOM, particularly its humic substances, is increased due to their destruction induced, e.g., by the deprotonation of their charged functional groups, such as carboxylic acids and phenolic groups [48, 68]. Consequently, the high extraction efficiency of ^{14}C-PUA microcapsules with highly alkaline solutions is likely attributable to the extraction of humic and fulvic acids from the soil, to which the ^{14}C-PUA microcapsules presumably adhere, resulting in their release to the aqueous phase. Since lowering in pH leads to a precipitation of humic acids, the extraction efficiency of organic matter and the microcapsules was also decreased at lower pH. However, although the pH plays a significant role, different alkaline solutions at the same pH could potentially yield different results due to their varying ionic compositions. This experiment was performed with NaOH and since Na^+ is a smaller ion with different binding affinities, differences could also occur due to different solution types used. As a matter of fact, K^+ and Na^+ ions differ in their impact of soil aggregate stability [36]. In our experiment using NaOH, the results showed similar extraction efficiencies to those observed with KOH (KOH with $63.0 \pm 2.25\%_{AR}$; experiment (I), Refesol 03-G, Table S4 and NaOH with $72.2 \pm 11.2\%_{AR;}$ Refesol 03-G) at comparable solution molarity (2 M *vs.* approx. 1.8 M, respectively), however minor variations may be introduced by the used solution type.

Conclusion

The first extraction experiment (I) efficiently extracted ^{14}C-PUA microcapsules and ^{14}C-LLDPE MPs, in both their pristine and light-exposed forms (irradiated with simulated sunlight) from two soil types with distinct pedological characteristics. The method has good potential to be applicable for diverse hydrophobic polymers and, notably, might be especially suitable for the most challenging small MP sizes (< 500 µm), but further testing is needed. Artificial sunlight irradiation was shown to induce polymer weathering that not only changed extractability but might also facilitate (bio)degradation in soil. Nevertheless, there is only limited data available regarding the degradation of MPs in soil. Therefore, further studies are imperative to gain in-depth understanding of the fate of MPs in soils, particularly for weathered MPs. Overall, further research is needed for better understanding the interactions of MPs and soil materials for identifying key factors that influence the efficiency of current extraction methods from soil. Consideration should be given to the resistance of MP – especially smaller and weathered particles – when using organic solvents such as octanol. Given that several polymers have low resistance to organic solvents, such as hexane [6, 53], there is a potential risk of partial or complete dissolution of the MPs during extraction, which could affect the accuracy of results and recovery rates.

To the best of the authors' knowledge, this study was the first to investigate the extraction of small MPs including ^{14}C-PUA microcapsules of 22.9 µm filled with oil from soil. Radioactive labelling of the polymers enabled exact mass balancing during the performed extraction tests and identification of losses, e.g., due to volatilisation (mineralisation) of the light-exposed microcapsules. Additionally, the methodological approach of ^{14}C-labelling allows to control any bias due to background contamination which frequently hampers reliable MP quantification. Furthermore, even though achievement of a homogeneous distribution of MPs in the soil matrix is challenging, robust results can be obtained by determining the remaining radioactivity in soil. For these reasons, radioactive labelling can be recommended for verification or validation purposes of MP extraction methods.

Abbreviations

MP	Microplastic
PE	Polyethylene
PUA	Polyurea
KOH	Potassium hydroxide
TG	Test guideline
SOM	Soil organic matter
PET	Polyethylene terephthalate
FTIR	Fourier-transform infrared spectroscopy
LLDPE	Linear low-density polyethylene
AR	Applied radioactivity
PSA	Particle size analysis
UHQ	Ultra-high quality
OC	Organic carbon
WHC	Water-holding capacity
$ZnCl_2$	Zinc chloride
TRR	Total recovered radioactivity

Supplementary Information

The online version contains supplementary material available at https://doi.org/10.1186/s43591-025-00121-0.

Supplementary Material 1.

Acknowledgements

We gratefully acknowledge the laboratory technicians Christoph Eggenstein-Deimel, Thomas Hennecke and Joana Bräutigam of the Fraunhofer IME Schmallenberg for their skilled technical assistance and support throughout this project. Their expertise and dedication have been invaluable.

Authors' contributions

EMT: Conceptualisation, visualisation, methodology, data curation and formal analysis, writing—original draft preparation. SH: Investigation, methodology, data curation, writing—original draft. AJ, AS, BM, DH: writing—review & editing. AJ, AS, BM, DH, MS,RH, PD, HE: Supervision, project administration. AS, BM, DH, MS, RH,PD, HE: funding acquisition. All authors revised and edited the manuscript and approved the final version before submission.

Funding

Open Access funding enabled and organized by Projekt DEAL. This project was funded by Bayer AG, Crop Science Division.

Data availability

Data are provided within the manuscript or supplementary information files.

Declarations

Ethics approval and consent to participate

Not applicable.

Consent for publication

Not applicable.

Competing interests

Philipp Dalkmann and Holger Egger are employees of the Bayer AG Division Crop Science, a leading manufacturer of agricultural chemicals. Roman Heumann and Eva-Maria Teggers are employed at INVITE GmbH, Germany, a cross-industry company with 50% business shares belonging to Bayer AG and 50% business shares belonging to universities (Technical University of Dortmund, Germany and Heinrich Heine University Düsseldorf, Germany).

Author details

[1]INVITE GmbH, Otto-Bayer-Straße 32, Cologne 51061, Germany. [2]Fraunhofer Institute for Molecular Biology and Applied Ecology IME, Auf dem Aberg 1, Schmallenberg 57392, Germany. [3]Department of Exposure Science, Helmholtz Centre for Environmental Research - UFZ, Permoserstraße 15, Leipzig 04318, Germany. [4]Bayer AG, Research & Development, Alfred-Nobel-Straße 50, Monheim 40789, Germany. [5]Institute for Environmental Research, RWTH Aachen University, Worringerweg 1, Aachen 52074, Germany. [6]State Key Laboratory of Pollution Control and Resource Reuse, School of the Environment, 163 Xianling Road, Nanjing 210023, China. [7]Key Laboratory of the Three Gorges Reservoir Region's Eco-Environment, Chongqing University, 174 Shazheng Street Shapingba, Chongqing 400045, China.

Received: 29 October 2024 Accepted: 31 March 2025
Published online: 19 May 2025

References

1. Alimi OS, Claveau-Mallet D, Kurusu RS, Lapointe M, Bayen S, Tufenkji N. Weathering pathways and protocols for environmentally relevant microplastics and nanoplastics: What are we missing? J Hazard Mater. 2022;423:126955. https://doi.org/10.1016/j.jhazmat.2021.126955.
2. Anbumani S, Kakkar P. Ecotoxicological effects of microplastics on biota: a review. Environ Sci Pollut Res. 2018;25:14373–96. https://doi.org/10.1007/s11356-018-1999-x.
3. Bläsing M, Amelung W. Plastics in soil: Analytical methods and possible sources. Sci Total Environ. 2018;612:422–35. https://doi.org/10.1016/j.scitotenv.2017.08.086.
4. Boucher J, Friot D. Primary microplastics in the oceans: A global evaluation of sources. IUCN Int Union Conserv Nat. 2017. https://doi.org/10.2305/IUCN.CH.2017.01.en.
5. Bravo Rebolledo EL, Van Franeker JA, Jansen OE, Brasseur SMJM. Plastic ingestion by harbour seals (Phoca vitulina) in The Netherlands. Mar Pollut Bull. 2013;67:200–2. https://doi.org/10.1016/j.marpolbul.2012.11.035.
6. Cavazzoli S, Ferrentino R, Scopetani C, Monperrus M, Andreottola G. Analysis of micro- and nanoplastics in wastewater treatment plants: key steps and environmental risk considerations. Environ Monit Assess. 2023;195:1483. https://doi.org/10.1007/s10661-023-12030-x.
7. Cole M, Webb H, Lindeque PK, Fileman ES, Halsband C, Galloway TS. Isolation of microplastics in biota-rich seawater samples and marine organisms. Sci Rep. 2014;4:4528. https://doi.org/10.1038/srep04528.
8. Corradini F, Meza P, Eguiluz R, Casado F, Huerta-Lwanga E, Geissen V. Evidence of microplastic accumulation in agricultural soils from sewage sludge disposal. Sci Total Environ. 2019;671:411–20. https://doi.org/10.1016/j.scitotenv.2019.03.368.
9. Crichton EM, Noël M, Gies EA, Ross PS. A novel, density-independent and FTIR-compatible approach for the rapid extraction of microplastics from aquatic sediments. Anal Methods. 2017;9:1419–28. https://doi.org/10.1039/C6AY02733D.
10. Cui W, Gao P, Zhang M, Wang L, Sun H, Liu C. Adverse effects of microplastics on earthworms: A critical review. Sci Total Environ. 2022;850:158041. https://doi.org/10.1016/j.scitotenv.2022.158041.
11. da Costa JP, Duarte AC. 2022. Introduction to the Analytical Methodologies for the Analysis of Microplastics, in: Rocha-Santos, T., Costa, M.F., Mouneyrac, C. (Eds.), Handbook of Microplastics in the Environment. Springer International Publishing, Cham, pp. 3–32. https://doi.org/10.1007/978-3-030-39041-9_1
12. Dehaut A, Cassone A-L, Frère L, Hermabessiere L, Himber C, Rinnert E, Rivière G, Lambert C, Soudant P, Huvet A, Duflos G, Paul-Pont I. Microplastics in seafood: Benchmark protocol for their extraction and characterization. Environ Pollut. 2016;215:223–33. https://doi.org/10.1016/j.envpol.2016.05.018.
13. Dissanayake PD, Kim S, Sarkar B, Oleszczuk P, Sang MK, Haque MN, Ahn JH, Bank MS, Ok YS. Effects of microplastics on the terrestrial environment: A critical review. Environ Res. 2022;209:112734. https://doi.org/10.1016/j.envres.2022.112734.
14. Du J, Ibaseta N, Guichardon P. Characterization of polyurea microcapsules synthesized with an isocyanate of low toxicity and eco-friendly esters via microfluidics: Shape, shell thickness, morphology and encapsulation efficiency. Chem Eng Res Des. 2022;182:256–72. https://doi.org/10.1016/j.cherd.2022.03.026.
15. Duan J, Bolan N, Li Y, Ding S, Atugoda T, Vithanage M, Sarkar B, Tsang DCW, Kirkham MB. Weathering of microplastics and interaction with other coexisting constituents in terrestrial and aquatic environments. Water Res. 2021;196:117011. https://doi.org/10.1016/j.watres.2021.117011.
16. ECHA ECA. Microplastics. Hot- Top. 2021. URL https://echa.europa.eu/de/hot-topics/microplastics. Accessed 3.7.24.
17. European Commission, 2023. Commission Regulation (EU) 2023/2055 of 25 September 2023 amending Annex XVII to Regulation (EC) No 1907/2006 of the European Parliament and of the Council concerning the Registration, Evaluation, Authorisation and Restriction of Chemicals (REACH) as regards synthetic polymer microparticles. Official Journal of the European Union. https://eur-lex.europa.eu/legal-content/EN/TXT/HTML/?uri=CELEX:32023R2055.
18. Galafassi S, Nizzetto L, Volta P. Plastic sources: A survey across scientific and grey literature for their inventory and relative contribution to microplastics pollution in natural environments, with an emphasis on surface water. Sci Total Environ. 2019;693:133499. https://doi.org/10.1016/j.scitotenv.2019.07.305.
19. Gigault J, Halle AT, Baudrimont M, Pascal P-Y, Gauffre F, Phi T-L, El Hadri H, Grassl B, Reynaud S. Current opinion: What is a nanoplastic? Environ Pollut. 2018;235:1030–4. https://doi.org/10.1016/j.envpol.2018.01.024.
20. Grause G, Kuniyasu Y, Chien M-F, Inoue C. Separation of microplastic from soil by centrifugation and its application to agricultural soil. Chemosphere. 2022;288:132654. https://doi.org/10.1016/j.chemosphere.2021.132654.
21. Gregory MR. Environmental implications of plastic debris in marine settings—entanglement, ingestion, smothering, hangers-on, hitch-hiking and alien invasions. Philos Trans R Soc B Biol Sci. 2009;364:2013–25. https://doi.org/10.1098/rstb.2008.0265.
22. Gu J-D. Microbiological deterioration and degradation of synthetic polymeric materials: recent research advances. Int Biodeterior Biodegrad. 2003;52:69–91. https://doi.org/10.1016/S0964-8305(02)00177-4.
23. Han X, Lu X, Vogt RD. An optimized density-based approach for extracting microplastics from soil and sediment samples. Environ Pollut. 2019;254:113009. https://doi.org/10.1016/j.envpol.2019.113009.
24. Hann S, Sherrington C, Jamieson O, Hickman M, Kershaw P, Bapasola A, et al. Investigating options for reducing releases in the aquatic environment of microplastics emitted by (but not intentionally added in) products. Report for DG Environment of the European Commission, 335, 2018-04. 2018.
25. Hartmann NB, Hüffer T, Thompson RC, Hassellöv M, Verschoor A, Daugaard AE, Rist S, Karlsson T, Brennholt N, Cole M, Herrling MP, Hess MC, Ivleva NP, Lusher AL, Wagner M. Are We Speaking the Same Language? Recommendations for a Definition and Categorization Framework for Plastic Debris. Environ Sci Technol. 2019;53:1039–47. https://doi.org/10.1021/acs.est.8b05297.
26. He D, Zhang X, Hu J. Methods for separating microplastics from complex solid matrices: Comparative analysis. J Hazard Mater. 2021;409:124640. https://doi.org/10.1016/j.jhazmat.2020.124640.
27. Hill AP, Young RJ. Getting physical in drug discovery: a contemporary perspective on solubility and hydrophobicity. Drug Discov Today. 2010;15:648–55. https://doi.org/10.1016/j.drudis.2010.05.016.
28. Hoang V-H, Nguyen M-K, Hoang T-D, Ha MC, Huyen NTT, Bui VKH, Pham M-T, Nguyen C-M, Chang SW, Nguyen DD. Sources, environmental fate, and impacts of microplastic contamination in agricultural soils: A comprehensive review. Sci Total Environ. 2024;950:175276. https://doi.org/10.1016/j.scitotenv.2024.175276.
29. Hurley RR, Lusher AL, Olsen M, Nizzetto L. Validation of a Method for Extracting Microplastics from Complex, Organic-Rich, Environmental Matrices. Environ Sci Technol. 2018;52:7409–17. https://doi.org/10.1021/acs.est.8b01517.
30. Imhof HK, Ivleva NP, Schmid J, Niessner R, Laforsch C. Contamination of beach sediments of a subalpine lake with microplastic particles. Curr Biol. 2013;23:R867–8. https://doi.org/10.1016/j.cub.2013.09.001.
31. ISO. Principles for the Analysis of Microplastics Present in the Environment (ISO 24187:2023). Geneva: International Organization for Standardization; 2023.
32. Jiang X, Zhu X, Arnold AA, Kong XZ, Claverie JP. Polyurea Structure Characterization by HR-MAS NMR Spectroscopy. Ind Eng Chem Res. 2017;56:2993–8. https://doi.org/10.1021/acs.iecr.7b00192.
33. Kershaw PJ, Rochman CM. Sources, fate and effects of microplastics in the marine environment: part 2 of a global assessment. Reports and studies-IMO/FAO/Unesco-IOC/WMO/IAEA/UN/UNEP joint group of experts on the scientific aspects of marine environmental protection (GESAMP) Eng No. 93. 2015.
34. Krause J, Egger H. Aqueous Capsule Suspension Concentrates Based on Polyurea Shell Material Containing Polyfunctional Aminocarboxylic Esters. WO 2021/136758 A1. World Intellectual Property Organization (WIPO). Patent Publication of 2021.
35. Kühn S, Van Werven B, Van Oyen A, Meijboom A, Bravo Rebolledo EL, Van Franeker JA. The use of potassium hydroxide (KOH) solution as a suitable approach to isolate plastics ingested by marine organisms. Mar Pollut Bull. 2017;115:86–90. https://doi.org/10.1016/j.marpolbul.2016.11.034.
36. Li S, Wang B, Zhang X, Wang H, Yi Y, Huang X, Gao X, Zhu P, Han W. Soil particle aggregation and aggregate stability associated with ion specificity and organic matter content. Geoderma. 2023;429:116285. https://doi.org/10.1016/j.geoderma.2022.116285.

37. Lusher AL, McHugh M, Thompson RC. Occurrence of microplastics in the gastrointestinal tract of pelagic and demersal fish from the English Channel. Mar Pollut Bull. 2013;67:94–9. https://doi.org/10.1016/j.marpolbul.2012.11.028.
38. Mani T, Frehland S, Kalberer A, Burkhardt-Holm P. Using castor oil to separate microplastics from four different environmental matrices. Anal Methods. 2019;11:1788–94. https://doi.org/10.1039/C8AY02559B.
39. Manshoven S, Smeets A, Malarciuc C, Tenhunen-Lunkka A, Mortensen LF. Microplastic pollution from textile consumption in Europe (No. ETC/CE 2022/1), Eionet Report. European Topic Centre Circular Economy and Resource Use. 2022. https://www.eionet.europa.eu/etcs/etc-ce/products/etc-ce-products/etc-ce-report-1-2022-microplastic-pollution-from-textile-consumption-in-europe.
40. Mattsson K, Ekstrand E, Granberg M, Hassellöv M, Magnusson K. Comparison of pre-treatment methods and heavy density liquids to optimize microplastic extraction from natural marine sediments. Sci Rep. 2022;12:15459. https://doi.org/10.1038/s41598-022-19623-5.
41. Mock W, Bartyczak S, Lee G, Fedderly J, Jordan K, Elert M, Furnish MD, Anderson WW, Proud WG, Butler WT. DYNAMIC PROPERTIES OF POLYUREA 1000. Presented at the SHOCK COMPRESSION OF CONDENSED MATTER 2009: Proceedings of the American Physical Society Topical Group on Shock Compression of Condensed Matter, Nashville (Tennessee), 2009:pp. 1241–1244. https://doi.org/10.1063/1.3295029
42. Möller JN, Löder MGJ, Laforsch C. Finding Microplastics in Soils: A Review of Analytical Methods. Environ Sci Technol. 2020;54:2078–90. https://doi.org/10.1021/acs.est.9b04618.
43. Nava V, Leoni B. Comparison of Different Procedures for Separating Microplastics from Sediments. Water. 2021;13:2854. https://doi.org/10.3390/w13202854.
44. Nuelle M-T, Dekiff JH, Remy D, Fries E. A new analytical approach for monitoring microplastics in marine sediments. Environ Pollut. 2014;184:161–9. https://doi.org/10.1016/j.envpol.2013.07.027.
45. OECD draft TG. OECD Guideline for the Testing of Chemicals - Proposal for a new guideline – Phototransformation of chemicals on soil surface (Draft Test Guideline). Organisation for Economic Co-operation and Development. 2002. https://www.eppltd.com/wp-content/uploads/2018/08/OECD-Guideline-for-the-Testing-of-Chemicals-Draft-Document-Phototransformation-of-Chemicals-on-Soil-Surfaces.pdf. Accessed 7 Apr 2025.
46. OECD TG 316. OECD Guideline for the Testing of Chemicals - Phototransformation of chemicals in Water - Direct Photolysis (Test No. 316). Organisation for Economic Co-operation and Development. 2008. https://www.oecd-ilibrary.org/environment/test-no-316-phototransformation-of-chemicals-in-water-direct-photolysis_9789264067521-en.
47. Pfohl P, Roth C, Wohlleben W. The power of centrifugation: How to extract microplastics from soil with high recovery and matrix removal efficiency. MethodsX. 2024;12:102598. https://doi.org/10.1016/j.mex.2024.102598.
48. Powell HKJ, Fenton E. Size fractionation of humic substances: Effect on protonation and metal binding properties. Anal Chim Acta. 1996;334:27–38. https://doi.org/10.1016/S0003-2670(96)00324-8.
49. Prosenc F, Leban P, Šunta U, Bavcon Kralj M. Extraction and Identification of a Wide Range of Microplastic Polymers in Soil and Compost. Polymers. 2021;13:4069. https://doi.org/10.3390/polym13234069.
50. Quijada R, Narváez A, Rojas R, Rabagliati FM, Barrera Galland G, Santos Mauler R, Benavente R, Pérez E, Pereña JM, Bello A. Synthesis and characterization of copolymers of ethylene and 1-octadecene using the rac-Et (Ind) 2ZrCl2/MAO catalyst system. Macromol Chem Phys. 1999;200:1306–10.
51. Radford F, Zapata-Restrepo LM, Horton AA, Hudson MD, Shaw PJ, Williams ID. Developing a systematic method for extraction of microplastics in soils. Anal Methods. 2021;13:1695–705. https://doi.org/10.1039/D0AY02086A.
52. Rani M, Ducoli S, Depero LE, Prica M, Tubić A, Ademovic Z, Morrison L, Federici S. A Complete Guide to Extraction Methods of Microplastics from Complex Environmental Matrices. Molecules. 2023;28:5710. https://doi.org/10.3390/molecules28155710.
53. Roscher L, Halbach M, Nguyen MT, Hebeler M, Luschtinetz F, Scholz-Böttcher BM, Primpke S, Gerdts G. Microplastics in two German wastewater treatment plants: Year-long effluent analysis with FTIR and Py-GC/MS. Sci Total Environ. 2022;817:152619. https://doi.org/10.1016/j.scitotenv.2021.152619.
54. Sa'adu I, Farsang A. Plastic contamination in agricultural soils: a review. Environ Sci Eur. 2023;35:13. https://doi.org/10.1186/s12302-023-00720-9
55. Scheurer M, Bigalke M. Microplastics in Swiss Floodplain Soils. Environ Sci Technol. 2018;52:3591–8. https://doi.org/10.1021/acs.est.7b06003.
56. Schwaferts C, Niessner R, Elsner M, Ivleva NP. Methods for the analysis of submicrometer- and nanoplastic particles in the environment. TrAC Trends Anal Chem. 2019;112:52–65. https://doi.org/10.1016/j.trac.2018.12.014.
57. Scopetani C, Chelazzi D, Mikola J, Leiniö V, Heikkinen R, Cincinelli A, Pellinen J. Olive oil-based method for the extraction, quantification and identification of microplastics in soil and compost samples. Sci Total Environ. 2020;733:139338. https://doi.org/10.1016/j.scitotenv.2020.139338.
58. Seo Y, Zhou Z, Lai Y, Chen G, Pembleton K, Wang S, He J, Song P. Micro- and nanoplastics in agricultural soils: Assessing impacts and navigating mitigation. Sci Total Environ. 2024;931:172951. https://doi.org/10.1016/j.scitotenv.2024.172951.
59. Sinn H, Kaminsky W, Vollmer H, Woldt R. "Living Polymers" on Polymerization with Extremely Productive Ziegler Catalysts. Angew Chem Int Ed Engl. 1980;19:390–2. https://doi.org/10.1002/anie.198003901.
60. Sivan A. New perspectives in plastic biodegradation. Curr Opin Biotechnol. 2011;22:422–6. https://doi.org/10.1016/j.copbio.2011.01.013.
61. Sun Y, Yuan J, Zhou T, Zhao Y, Yu F, Ma J. Laboratory simulation of microplastics weathering and its adsorption behaviors in an aqueous environment: A systematic review. Environ Pollut. 2020;265:114864. https://doi.org/10.1016/j.envpol.2020.114864.
62. Surendran U, Jayakumar M, Raja P, Gopinath G, Chellam PV. Microplastics in terrestrial ecosystem: Sources and migration in soil environment. Chemosphere. 2023;318:137946. https://doi.org/10.1016/j.chemosphere.2023.137946.
63. Teggers EM, Hardebusch J, Meisterjahn B, Simon M, Hennecke D, Heumann R, u. a. Diversifying endpoints in biodegradation testing of microplastics. Environ Sci Eur. 2025;37(1):65. https://doi.org/10.1186/s12302-025-01096-8.
64. Thomas D, Schütze B, Heinze WM, Steinmetz Z. Sample Preparation Techniques for the Analysis of Microplastics in Soil—A Review. Sustainability. 2020;12:9074. https://doi.org/10.3390/su12219074.
65. Vermeiren P, Muñoz C, Ikejima K. Microplastic identification and quantification from organic rich sediments: A validated laboratory protocol. Environ Pollut. 2020;262:114298. https://doi.org/10.1016/j.envpol.2020.114298.
66. Wagner M, Lambert S. (Eds.) Freshwater Microplastics: Emerging Environmental Contaminants?, The Handbook of Environmental Chemistry. Springer International Publishing, Cham. 2018. https://doi.org/10.1007/978-3-319-61615-5
67. Wenzel M, Fischer B, Renner G, Schoettl J, Wolf C, Schram J, Schmidt TC, Tuerk J. Efficient and sustainable microplastics analysis for environmental samples using flotation for sample pre-treatment. Green Anal Chem. 2022;3:100044. https://doi.org/10.1016/j.greeac.2022.100044.
68. You S-J, Thakali S, Allen HE. Characteristics of soil organic matter (SOM) extracted using base with subsequent pH lowering and sequential pH extraction. Environ Int. 2006;32:101–5. https://doi.org/10.1016/j.envint.2005.07.003.
69. Yuan J, Ma J, Sun Y, Zhou T, Zhao Y, Yu F. Microbial degradation and other environmental aspects of microplastics/plastics. Sci Total Environ. 2020;715:136968. https://doi.org/10.1016/j.scitotenv.2020.136968.
70. Yuan Z, Chen H, Zhang J, Zhao D, Liu Y, Zhou X, Li S, Shi P, Tang J, Chen X. Preparation and characterization of self-cleaning stable superhydrophobic linear low-density polyethylene. Sci Technol Adv Mater. 2008;9:045007. https://doi.org/10.1088/1468-6996/9/4/045007.

Publisher's Note